VOLUME 12 NUMBER 1 2019 ISSN 2218-7979
eISSN 2409-370X

International Journal of Biology and Chemistry

Al-Farabi Kazakh National University

International Journal of Biology and Chemistry is published twice a year by
al-Farabi Kazakh National University, al-Farabi ave., 71, 050040, Almaty, Republic of Kazakhstan
website: http://ijbch.kaznu.kz/

Any inquiry for subscriptions should be sent to:
Prof. Mukhambetkali Burkitbayev, al-Farabi Kazakh National University
al-Farabi ave., 71, 050040, Almaty, Republic of Kazakhstan
e-mail: Mukhambetkali Burkitbayev@kaznu.kz

EDITORIAL

The most significant achievements in the field of natural sciences are reached in joint collaboration, where important roles are taken by biology and chemistry. Therefore publication of a Journal, displaying results of current studies in the field of biology and chemistry, facilitates highlighting of theoretical and practical issues and distribution of scientific discoveries.

One of the basic goals of the Journal is to promote the extensive exchange of information between the scientists from all over the world. We welcome publishing original papers and materials of biological and chemical conferences, held in different countries (by prior agreement, after the process of their subsequent selection).

Creation of special International Journal of Biology and Chemistry is of great importance, since scientists worldwide, including other continents, might publish their articles, which will help to widen the geography of future collaboration.

The Journal aims to publish the results of the experimental and theoretical studies in the field of biology, biotechnology, chemistry and chemical technology. Among the emphasized subjects are: modern issues of technologies for organic synthesis; scientific basis of the production of physiologically active preparations; modern issues of technologies for processing of raw materials; production of new materials and technologies; study on chemical and physical properties and structure of oil and coal; theoretical and practical issues in processing of hydrocarbons; modern achievements in the field of nanotechnology; results of studies in various branches of biology, biotechnology, genetics, nanotechnology, etc.

We hope to receive papers from the leading scientific centers, which are involved in the application of the scientific principles of biological and chemical sciences on practice and carrying out research on the subject, related to production of new materials, technologies and ecological issues.

IRSTI 62.13.99

[1*]A. Akindykova, [2]C. Cakir-Kiefer, [1]A. Baubekova, [2]S. Jurjanz

[1]Al-Farabi Kazakh National University, Almaty, Kazakhstan
[2]University of Lorraine, Vandoeuvre-lès-Nancy, France
[*]e-mail: akindykova@gmail.com

Isolation and characterization of camel milk proteins

Abstract: Camel milk is an important constituent of Kazakh diet. Populaces of several regions of the country used camels as one of the basic sources of nutrients for many centuries. Camel milk contains high amounts of the immune-active proteins – lysozyme, lactoferrin, lactoperoxidase, immunoglobulins. It is also rich in vitamin C. Like any other, camel milk is highly perishable, with losses occurring during work at farm and under industrial conditions. These losses can be associated with challenges in preservation of the camel milk caused by the inability to process it into the shelf-stable products. The process of freeze-drying may be applied in order to retain the nutritional properties as well as technical and functional characteristics of the camel milk. Assessment of the effects of the isolation procedure and following freeze-drying on the mass yield of dry camel milk caseins and whey proteins could be interesting in order to get consolidated processes, which may further be transferred to an industrial level. These findings will play a central role in future freeze-drying operations since the retention of important nutritional components is an important part of food processing. In order to reveal the possible hurdles and to get a consolidated procedure to produce functional foods for different purposes, it is important to study the preceding data on isolation and preservation of camel milk proteins, as well as study their characteristics.
Key words: camel milk, caseins, freeze-drying, acid precipitation, SDS-PAGE, whey proteins.

Introduction

Kazakh population consumes large amounts of animal-originated food, with 237.7 kg of milk and dairy products (from cow, camel, mare) per person in 2018 [1]. In arid areas of South and West Kazakhstan, camel milk is an important part of nutrition of the local population [2], as habitants of these regions use camels as one of the basic sources of nutrients for many centuries. The number of camels in Kazakhstan is growing; reached approximately 230,000 heads to this moment [1].

Camel milk differs from cow milk in composition, protein content and structure [3]. The main groups of milk proteins are caseins and whey proteins. According to the literature data, caseins are the most common protein fraction, varying from 61.8 to 88.5% of the total milk protein. The components of camel milk (CN) casein are homologous to cow milk casein: aS1-CN, aS2-CN, b-CN and k-CN. The proportion of each casein component as follows: aS1-CN 22%, aS2-CN 9.5%, b-CN 65% and k-CN 3.5% (w/w). Casein fractions in camel milk are quite similar to bovine casein. At the same time the total amount of casein in camel milk can be lower (52-87%) than in cow milk (80%) [4]. Whey proteins of camel milk make up to 20-25% of all proteins and mainly consist of β-lactalbumin, lactoforin (also called GlyCAM-1), IgG, lactoferrin and serum albumin. Accordingly, the ratio of whey protein fraction to casein fraction in camel milk is higher than in bovine milk, but lower than in breast milk [5]. Camel milk is characterized by the absence of β-lactoglobulin, one of the major allergens in bovine milk [6]. Finally, this milk contains high concentrations of various minerals, large amount of immune-active proteins, and is three times richer in vitamin C than bovine milk. All these components play an important role in the mechanisms of protection against diseases and are beneficial to the healing properties of camel milk [7].

The Food and Agriculture Organization (FAO) forecasts that global population will increase by third by 2050 [8]. The projections are such that with increase in population size, the demand for food products rich in protein will grow, and this in turn will stimulate high demand for milk protein. Consequently, the global dairy protein market should grow by an average of 7.8% over the next decade, reaching

about $ 18.25 billion by 2025 [9]. Since prevailing part of the population of West, East African and Central Asian countries have access to camel milk (60% of the dromedary population is concentrated in the countries of North-East Africa) [7], demand for camel milk proteins will increase in these regions.

Camel milk, like any other milk, is highly perishable, with losses occurring during work at farm and under industrial conditions. These losses can be associated with challenges in preservation of the camel milk caused by inability to process it into the shelf-stable dairy products. The process of freeze-drying minimizes reactions of decomposition and supports physical, chemical and biological stability of the product for a long time storage at ambient temperature [10].

Freeze-drying or lyophilization is a technological process used for soft drying of substances, during which dried product is frozen, and then placed in a vacuum chamber for sublimation of the solvent. Being a cold process, freeze-drying is especially useful for drying heat sensitive foods. Freeze-drying is recognized as the best method of water removal with final production of a highest quality dry materials compared to other methods of food drying. This process can be used in order to retain the nutritional properties and techno-functional characteristics of the milk [11]. Disadvantage of freeze-drying is its expensiveness and time consumption. Nevertheless, it is an important drying procedure for milk, which allows preserving its taste, good flavour appearance, and nutritive properties [12; 13].

Assessment of the effects of the isolation procedure and following freeze-drying on the mass yield of dry camel milk caseins and whey proteins could be interesting in order to get consolidated processes, which may further be transferred to an industrial level. These findings will play central role in future freeze-drying operations since the retention of important nutritional components is an important part of food processing [14; 15].

Materials and methods

Collection of milk samples. For the high representativeness of the method of random selection three multiparous 10-year-old camels were selected from a commercial farm in Almaty region. Camels were placed on pasture keeping with the provision of additional feeding in the cold period of the year. The main source of food for camels were natural plants growing in places of grazing. Camel milk was obtained by manual milking in accordance with generally accepted camel milking standards. During sampling period, on average from February to December, camels were milked thrice a day (at 6 a.m., 2 and 6 p.m.). Milk was collected jointly from the evening of the first day and from the morning of the next day. 2 L of milk were collected from each animal. For conservation, sodium azide, which does not affect the structure of milk proteins, was added at 0.02%, immediately to the sampled milk before its transport to the laboratory in a cooler bag. All sampled milk has been transported in 5 hours after milking, kept at 4°C until they reached the laboratory, then frozen and stored at 4°C until the analysis.

Preparation of camel milk proteins. Camel milk was defatted by centrifugation at 5,000 g at 4°C for 30 min. After precipitation of skimmed milk by slowly adding 1M HCl to pH 4.4, the casein pellet was separated from the whey proteins by centrifuging at 5,000 g at 20°C for 30 min. Then, both separated protein fractions were neutralized with 1M NaOH and dialyzed against ultrapure water for 96 hours. Dialyzed proteins were freeze-dried (Martin Christ Alpha 1-4 LSC plus, Osterode am Harz, Germany) and stored at 4°C until the analysis.

Estimation of protein concentration. Thermo Scientific Pierce BCA Protein Assay Kit was used to check the protein concentrations. The Protein Assay was carried out with 1:2 and 1:10 times dilution of proteins in dH_2O on the 96-well microplate by keeping the microplate in an incubator at 37°C for 30 min. The absorption was read at 570 nm by BMG FLUOstar Galaxy – Multi-functional Microplate Reader (MTX Lab Systems, USA) for 96-well (217×85 mm) microplates.

Estimation of yield after freeze-drying. In the absence of data on protein fractions in the milk of the Kazakh breeds of dromedary (*Camelus dromedarius*), the obtained dry masses of each fraction were compared to reported concentrations of caseins and whey proteins in camel milk of dromedaries from Saudi Arabia, United Arab Emirates and Pakistan. In data, reported by Al-Alawi et al. [16], the mean value for protein content in the camel milk was 1.9% of caseins and 0.7% of whey proteins. However, this was slightly lower than the contents (2.1 and 0.8%, respectively) reported by Rafiq et al. [17]. According to Khaskheli et al. [18], the casein content was slightly higher (2.21 g per 100 g). In this regard, for further calculations, the average concentrations of proteins obtained from these three studies was used as a theoretically expected protein mass, namely 20.6 g for casein and 7.5 g for whey protein per 100 g of camel milk. This ratio was expressed as follows:

Yield (%) = (obtained dry mass of a considered protein fraction / Theoretical expected concentration)*100

Characterization of camel milk proteins by SDS-PAGE. The purity and electrophoretic profiles of all proteins were checked by Bio-Rad's SDS-PAGE System, following the method described by Laemmli, 1973 [17], with slight modification under reducing conditions on a 15% separation gel and 5% concentration gel. For preparing the separation gel for 2 mini-gels 3.75 mL of acrylamide/bis-acrylamide (1:29) solution was mixed with 2.5 mL of Tris buffer pH 8.8 for separation gel with 2.5 mL of dH_2O water, 100 µL of 10% SDS, 5 µL of tetramethylethylenediamine (TEMED) and 100 µL of solution of 100 mg/mL ammonium persulfate in a tube and thoroughly mixed. The solution was poured between the spacer and short plates and then gel was isolated from the air by using distilled water on the surface. When the gel solidified well, the distilled water was poured off. The top of the gel was dried using the filter paper. Then, 0.65 mL of acrylamide/bis-acrylamide (1:29) solution was mixed with 1.25 mL of Tris buffer pH 6.8 for separation gel with 3.15 mL of distilled water, 50 µL of 10% SDS, 10 µL of TEMED and 50 µL of 100 mg/mL ammonium persulfate to compound the concentration gel. The mixture was then poured between the plates on the separation gel. When the concentration gel became solidified, it was washed with distilled water. The gel cassettes were loaded into electrophoresis tank, where 700 mL of electrode buffer (70 mL of 10x electrode buffer mixed with 630 mL of dH_2O) was poured. For sample preparation, 100 µg of each protein sample were incubated with the sample buffer at 1:1 ratio (50% glycerol, 10% SDS, 2-mercaptoethanol, bromophenol blue) at 100°C for 5 min and then loaded into the gel. Run time was approx. 35 min at 200 V. The gels were taken out carefully and put for 1 hour in 12% trichloroacetic acid for fixation. Then, the gels stained overnight with Sigma's Coomassie brilliant blue R250 (0.1% w/v). After discoloration, the gels were visualized, and images were captured under the visible light.

Results and discussion

The results of obtaining a mass of camel milk proteins from three camels were studied according to the methods described above. As can be seen from the obtained data, the pH of raw camel milk ranges from 6.4 to 6.5 and it is in line with the pH values reported by other studies on the camel milk [18-20].

The resulting weight of caseins fraction and the volume of whey proteins fraction were measured after the protein isolation before dialysis (Tables 1 and 2).

Table 1 – Results of casein separation

	Camel 1	Camel 2	Camel 3
Quantity (L)	2		
pH of raw milk	6.47 – 6.54	6.45 – 6.50	6.46 – 6.48
Weight (g) of wet proteins after separation	--	403 g	278 g

Table 2 – Results of whey separation

	Camel 1	Camel 2	Camel 3
Quantity (L)	2		
pH of raw milk	6.47 – 6.54	6.45 – 6.50	6.46 – 6.48
Volume (L) of wet proteins after separation	1.6	1.4	1.4

Due to the losses linked to a laboratory accident, the casein yield of Camel 1 has been excluded from the data analysis. In the case of whey proteins, the results obtained from the milk of three camels will be taken into account.

After obtaining separate protein fractions, to eliminate low molecular weight impurities and reduce the salt concentration, dialysis was carried out. The results obtained for dried caseins and whey proteins of camel milk are presented in Table 3.

Table 3 shows the mass of dried proteins obtained from 1L of the camel milk. From 1L of the camel milk 10.9 g of dry caseins and 3.1 g of dry whey proteins were obtained on average (Table 3). These quantifications would correspond to a yield between 32 and 66% of theoretically expected proteins in camel milk. From the literature data, it follows that from the mass of total protein (33.5 g/L of camel milk) the proportion of caseins was 61.8-88.5%, which is in terms of mass from 20.6 g to 29.6 g, and the proportion of whey proteins in turn, ranged from 11.49 to 38.82%, i.e. from 3.8 g to 13.0 g [5; 18]. The mass of pure caseins obtained in this study (on average 10.9 g of dry caseins) was lower than the values from the literature data, while the obtained mass of whey proteins (on average 3.1 g of dry whey proteins) is comparable to the results shown by other researchers.

Table 3 – Yield of camel milk proteins

	Camel 1	Camel 2		Camel 3	
Protein fraction	whey proteins	caseins	whey proteins	caseins	whey proteins
Mass of freeze-dried protein fraction (g)	6.6	22.8	5.3	14.7	5.2
Proportion of pure protein (%) (BCA-Pierce Dosage)	56.5	60.2	59.9	55.5	45.6
Dry weight of purified protein (g)	3.7	13.7	3.1	8.1	2.4
Yield[a] (%)	49.3	66.5	41.3	39.3	32.0
Note: [a] Yield (%) = (Obtained dry mass / Theoretically expected dry mass)*100					

Nevertheless, our reference values have been taken from the same camel breeds – *Camelus dromedarius* of Saudi Arabia and United Arab Emirates, reviewed by Al-Alawi et al. [16] and Pakistani breeds, reviewed by Khaskheli et al. [18], what allows us to suppose differences in protein contents in comparison to the camel milk of the local breeds. According to Konuspayeva et al. [23], the variability of camel milk composition is clearly dependent on geographical origin. In addition, such factors as dairy performance, feeding conditions or the physiological stage of the animals can increase variations in milk protein content. As the growing conditions may affect the rate of the protein synthesis in a notable manner, revealed differences to theoretical values have to be taken with cautions. To increase the statistical reliability, all experiments were performed in triplicate, after which the average values were taken.

Unfortunately, no specific Protein Assay Kit for camel milk proteins is available on the market. The colorimetric detection and quantitation of total proteins content, i.e. to determine the pure protein concentration in the obtained fractions colorimetric method performed with bovine serum albumin (SAB) is usually used as standard provided by the Pierce BCA Protein Assay Kit. The results of the colorimetric analysis (Figure 1) show that the obtained casein fractions contain from 48.5 to 60.2 (in average of 55%) of pure proteins.

The question can be asked if this BCA-Pierce Assay kit would allow the quantification of fully camel caseins. Our results show clear variations in protein yields between different individuals as well as possibility of non-negligible losses. Nevertheless, yield of approximately 50% of initially contained proteins can be expected for both major protein fractions.

To determine the purity and homogeneity of each individual protein fraction (camel milk caseins and whey proteins) Bio-Rad's SDS-PAGE was carried out. In the lines CMWP-A, CMWP-S and CMWP-U (whey protein fractions), shown on the Figure 2, the protein bands can be observed with an apparent molecular weight (MW) of 14,000; 30,000 and 65,000 Da, which are identified as α-lactalbumin, IgGs1 and serum albumin.

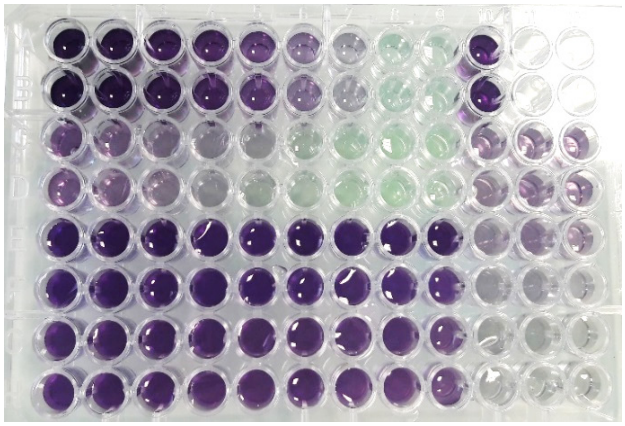

Figure 1 – The results of colorimetric analysis with caseins and whey proteins from all camel milk samples

These results are consistent with the data provided by Mati et al. [6], which showed that camel α-lactalbumin has a molecular weight of 14.4 kDa, while the molecular weight of IgGs1 and serum albumin is 30 and 67 kDa, respectively.

In addition, in these lines protein bands were observed with an apparent Molecular Weight (MW) 12,000 and 19,000 Da, which were identified as whey acidic protein (WAP) and peptidoglycan recognition protein-1 (PGRP-1). These results were comparable with the literature data reported by Beg et al. [24] and Kappeler et al. [25], who found that the MW of WAP and PGRP-1 are 12,534 Da and 19,143 Da, respectively. In the lines CMC-A, CMC-S and CMC-U (casein fractions), protein bands were observed with an apparent MW of 21,000 and 24,000 Da, which

are identified as β-CN and α-S2-CN with MW of 24,650.76 Da and 21,265.90 Da, respectively, matching the data provided by Mati et al. [7]. After the performed electrophoresis, we were convinced that caseins and whey proteins from the camel milk were isolated correctly.

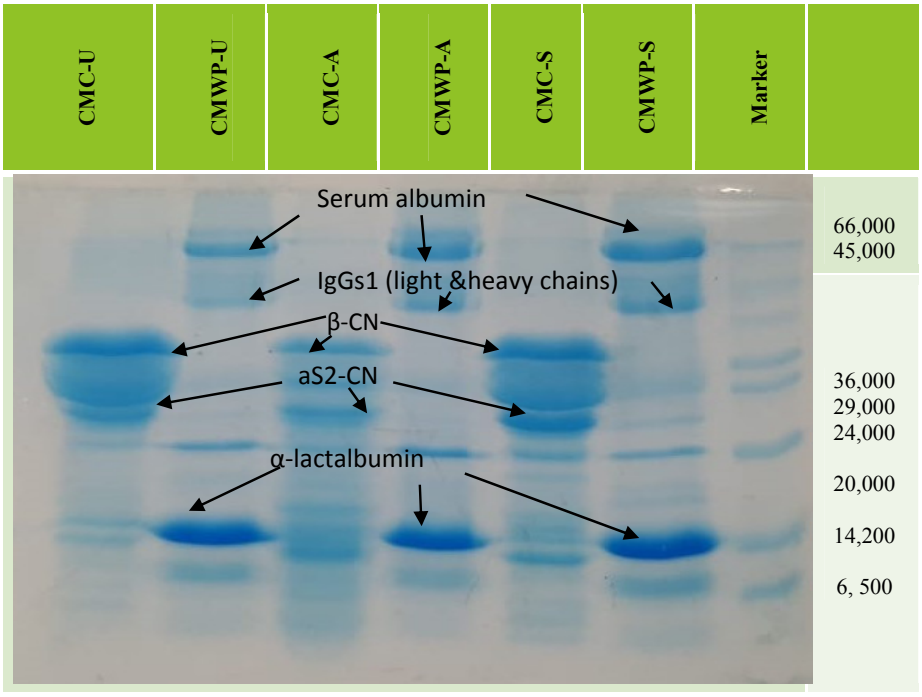

Sample	Type of protein	Origin	Name of animal
CMWP-S	Whey protein	Camel	Saltanat (C-2)
CMC-S	Casein	Camel	Saltanat (C-2)
CMWP-A	Whey protein	Camel	Aktilek (C-1)
CMC-A	Casein	Camel	Aktilek (C-1)
CMWP-U	Whey protein	Camel	Ushinshi (C-3)
CMC-U	Casein	Camel	Ushinshi (C-3)
Marker	Sigma-Aldrich Catalog Number M3913		

Figure 2 – Gel after SDS-PAGE with caseins and whey proteins from all camel milk samples

Conclusion

This work demonstrated that from 1L of camel milk it is possible to get 8.1-13.7 g (10.9 g/L in average) of pure caseins and 2.4-3.7 g (3.1 g/L in average) of pure whey proteins. The wide variability between the masses of the obtained protein fractions can be explained by the individual characteristics of each camel (geographical location, seasonality factor, physiological conditions, and health status). Separation of protein fractions by acid coagulation, classically used for cow milk, will work also in camel milk although an apparent yield of only around 50% has been achieved. Improvements in quality are possible on the stages of re-solubilization of the fractions after separation as well as quality of dialysis, where the ratio between expected the protein mass and water volume should be especially re-considered. Moreover, a specific identification of caseins and whey proteins from *Camelus dromedarius* can improve the calculated yields.

Results of the present study are valuable for further evaluation of the properties of proteins and peptides of the camel milk, which have been studied for much less extent than such of the cow milk [15; 17]. Some studies were performed to study the properties of milk proteins of camels from the other countries [4-7]. However, since the geographic location plays an important role, the study of the properties of the camel milk proteins in Kazakhstani breeds is of par-

ticular interest, since this issue has not been studied in our country yet. Therefore, new research in this direction is of interest to the international scientific community, which increases the significance of this work. The results of this current study will form the basis for further research on the peptides and milk proteins of camels habituating on the territory of Kazakhstan.

References

1. Committee on statistics of the Republic of Kazakhstan. Last modified April 28, 2019. http://stat.gov.kz

2. Petrlik J., Kalmykov D., Zatloukalova K. (2016) Toxic pollutants in camel milk from the Mangystau region of Kazakhstan, Results of sampling conducted in 2015-2016, 50 p.

3. Al-Shamsi K.A, Mudgil P., Hassan H.M., Maqsood S. (2018) Camel milk protein hydrolysates with improved technofunctional properties and enhanced antioxidant potential in in vitro and in food model systems. *J Dairy Sci.*, vol. 101, no. 1, pp. 47-60. https://doi.org/10.3168/jds.2017-13194

4. Khalesi M., Salami M., Moslehishad M., Winterburn J., Moosavi-Movahedi A.A. (2017) Biomolecular content of camel milk: a traditional superfood towards future healthcare industry. *Trends Food Sci Tech.*, no. 62, pp. 49-58. https://doi.org/10.1016/j.tifs.2017.02.004

5. El-Agamy E.I. (2009). Bioactive components in camel milk, pp. 159-192. In: Bioactive components in milk and dairy products, ed. by Park Y.W., Wiley-Blackwell Publishers, Ames, Iowa and Oxford, England.

6. El-Agamy E.I., Nawar M.A. (2000) Nutritive and immunological values of camel milk: a comparative study with milk of other species. In: 2nd International Camelid Conference Agroeconomics of Camelid Farming, Almaty, Kazakhstan.

7. Mati A., Senoussi-Ghezali C., Zennia S.A., Almi-Sebbane D., El-Hatmi H., Girardet J-M. (2017) Dromedary camel milk proteins, a source of peptides having biological activities a review. *Int Dairy J.*, no. 73, pp. 25-37. https://doi.org/10.1016/j.idairyj.2016.12.001

8. Food and Agriculture Organization of United Nations (2009). How to feed the world 2050, high-level expert forum, Global agriculture towards 2050. FAO, Rome, 4 p.

9. Research and Markets. The world's largest market research store. Global Milk Protein Market Analysis & Trends – Industry Forecast to 2025. Last modified April 19, 2019 https://www.researchandmarkets.com/reports/4115294/global-milk-protein-market-analysis-and-trends

10. Fonseca F., Passot S., Cunin O., Marin M. (2008) Collapse temperature of freeze-dried Lactobacillus bulgaricus suspensions and protective media. *Biotechnol Prog.*, vol. 20, no. 1, pp. 229-238 https://doi.org/10.1021/bp034136n

11. Ibrahim A.H., Khalifa S.A. (2015) Effect of freeze-drying on camel's milk nutritional properties. *Int Food Res J.*, vol. 22, no. 4, pp. 1438-1445.

12. Ratti C. (2001) Hot air and freeze-drying of high-value foods: a review. *J Food Eng.*, no. 49, pp. 311-319. https://doi.org/10.1016/S0260-8774(00)00228-4

13. Yao Y., Zhao G., Yan Y., Chen C., Sun C., Zou X., Jin Q. and Wang X. (2016) Effects of freeze drying and spray drying on the microstructure and composition of milk fat globules. *RSC Advances*, vol. 6, no. 4, pp. 2520-2529. https://doi.org/10.1039/C5RA22323G

14. Munro P.A. (2002) Caseins, functional properties and food uses, pp. 1909-1915. In: Encyclopedia of Dairy Sciences, ed. by Fuquay J., Fox P.,. San Diego: Academic Press

15. Moughan P.J. (2009) Milk proteins: a cornucopia for developing functional foods, pp. 483-499. In: Milk proteins from expression to food, ed. by Thompson A., Boland M. San Diego: Academic Press. https://doi.org/10.1016/B978-0-12-374039-7.00017-9

16. Al-Alawi A.A., Laleye L.C. (2008) Characterization of camel milk protein isolates as nutraceutical and functional ingredients. Collaborative Research Project SQU/UAEU.

17. Rafiq S., Huma N., Pasha I., Sameen A., Mukhtar O., Khan M.I. (2016) Chemical composition, nitrogen fractions and amino acids profile of milk from different animal species. *Asian-Australas J Anim Sci.*, vol. 29, no. 7, pp. 1022-1028. http://dx.doi.org/10.5713/ajas.15.0452

18. Khaskheli M., Arain M.A., Chaudhry S., Soomro A.H., Qureshi T.A. (2005) Physico-chemical quality of camel milk. *J Agric Soc Sci.*, no. 2, pp. 164-166.

19. Laemmli U.K., Favre M. (1973) Maturation of the head of bacteriophage T4: I. DNA packaging events. *J Mol Biol.*, vol. 80, no. 4, pp. 575-599. https://doi.org/10.1016/0022-2836(73)90198-8

20. Mal G., Dande S.S., Sahani M.S. (2006) Milk production potential and keeping quality of camel milk. *J Camel Pract Res.*, vol. 13, no. 2, pp. 175-178.

21. Mal G., Dande S.S., Sahani M.S. (2007) Changes in chemical and macro-minerals content of dromedary milk during lactation. *J Camel Pract Res.*, vol. 14, no. 2, pp. 195-197.

22. Singh R., Mal G., Kumar D., Patil N.V., Pathak K. (2017) Camel milk: an important natural adjuvant. *Agric Res.*, vol. 6, no. 4, pp. 327-340.

23. Konuspayeva G., Faye B., Loiseau G. (2009) The composition of camel milk: a meta-analysis of the literature data. *J Food Compos Anal.*, vol. 22, no. 2, pp. 95-101. https://doi.org/10.1016/j.jfca.2008.09.008

24. Beg O.U., von Bahr-Lindström H., Zaidi Z.H., Jörnval H. (1984) A small camel-milk protein rich in cysteine/half-cystine. *Bioscience Rep.*, vol. 4, no. 12, pp. 1065-1070. https://doi.org/10.1016/0014-5793(87)80704-4

25. Kappeler S.R., Heuberger C., Farah Z., Puhan Z. (2004) Expression of the peptidoglycan recognition protein, PGRP, in the lactating mammary gland. *J Dairy Sci.*, vol. 87, no. 8, pp. 2660-2668.

26. Konuspayeva G., Faye B., Loiseau G., Levieux D. (2007) Lactoferrin and immunoglobulin contents in camel's milk (*Camelus bactrianus, Camelus dromedarius*, and hybrids) from Kazakhstan. *J Dairy Sci.*, vol. 90, no. 1, pp. 38-46. https://doi.org/10.3168/jds.S0022-0302(07)72606-1

IRSTI 34.23.41; 34.35.17; 68.03.03

[1*]A.Y. Amalova, [1,2]K.A. Yermekbayev,
[2]S. Griffiths, [1]S.I. Abugalieva, [1]Y.K. Turuspekov

[1]Institute of Plant Biology and Biotechnology, Almaty, Kazakhstan
[2]John Innes Centre, Norwich, United Kingdom
*e-mail: akerke.amalova@gmail.com

Phenotypic variation of common wheat mapping population Pamyati Azieva x Paragon in south-east of Kazakhstan

Abstract: Development of mapping populations (MP) of any crop, including wheat, with its high-density genetics map is a crucial initial step in breeding programs aimed towards identification of quantitative trait loci for complex traits, such as yield. Current study is related to the field observations of hexaploid common wheat MP derived from a cross between the cultivars Pamyati Azieva (Russian Federation) and Paragon (UK). MP consisted of 98 recombinant inbred lines (RILs). It is the first mapping population to be constructed using one of the registered commercial cultivars in Kazakhstan. All 98 RILs were tested for four consecutive years (2015-2018) in the field conditions of the Kazakh Research Institute of Agriculture and Plant growing (KAZNIIZR). Field study suggests that the MP is a highly suitable genetic resource for wheat breeding projects, as the developed RILs showed a wide range of variation in yield related traits, including plant height (PH), number of fertile spikes (NFS), number of kernels per spike (NKS), and thousand kernel weight (TKW). The analysis of weight of kernels per plant (WKP) indicated that in total 40 RILs, including these five RILs: RIL48, RIL36, RIL83, RIL01, and RIL46, outperformed the local parent cultivar Pamyati Azieva. They showed averaged best yield values over the indicated period, which is highly correlated with PH, NFS, NKS, and TKW, as indicated by the Pearson correlation index. Individuals with favorable values for all yield-related traits were identified for their incorporation into the breeding studies. The GGE Biplot analysis allowed the separation of four trials to two mega-environments, possibly reflecting the amount of precipitation around flowering time and seed maturation time, which are crucial phases of wheat plant growth and development. These observations will be used to inform further studies related to genetic mapping of quantitative trait loci of yield components in common wheat.

Key words: wheat, recombinant inbred lines, mapping population, yield components, genotype-environment interaction.

Introduction

Wheat (*Triticum aestivum* L.) is a member of the *Poaceae* family, comprised of the major cereal grains, including maize and rice [1]. Among the food crops, wheat is one of the most abundant sources of energy and proteins for the world population and its increased production is essential for food security of our country as well as on the global range. Wheat occupies about 17% of the total cropland and contributes around 35% of the common staple food in many countries [2].

Increased demand for wheat at the international as well as internal market is requiring improvements in Kazakhstani wheat breeding programs. The global food market incentivizes Kazakhstan as an important producer and exporter of wheat, strengthening its position and promoting wheat production [3]. However, Kazakh wheat production is conducted under adverse weather conditions, and therefore, yields are lower than in other major wheat producing countries [4]. In addition, producers seem to face other constraints, such as weak infrastructure, remoteness from principal markets and a restrictive institutional environment [5]. Relative wheat production has been declining in the last fifty years, conveying that Kazakh wheat share has not been keeping pace with the global wheat production rates. Encouragingly, in the last decade, the rate of decline is slowing down, suggesting improvements in the Kazakh wheat production [6].

According to the data presented by the Ministry of Agriculture of the Republic of Kazakhstan, from the 2018 harvest, the total weight was 22.8 million

tons, and average yield was 15.1 t/ha. In general, the gross harvest of grain exceeds the last year's level by 760 thousand tons, or 3%, and the yield has inceased by 0.6 t/ha or 4% [7].

The success of wheat growth is also largely dependent on the local breeding projects that focus on development of highly productive local cultivars. As agronomic traits of new cultivars, such as grain yield components, show continuous variation and are controlled by quantitative genes, the analysis of quantitative trait loci (QTL) is of great importance for plant breeders. The progress in genetic improvement of cereals over the last century was based mainly on the use of single genes with relatively clear-cut effects on the phenotype. Predicting genetic variances of biparental populations has been a long-standing goal for plant breeders. The ability to discriminate among crosses with similarly predicted high means, but different levels of genetic variance should improve the effectiveness of breeding [8]. Although it is possible to start breeding programs using only phenotypic selection, understanding the number and genomic location of genes controlling agronomically important traits can enhance the efficiency of selection [9]. The most widely used methods for identifying the marker-trait associations (QTL analysis) are genetic map construction, phenotyping and genotyping with the molecular markers, and use of differentiation populations [10; 11]. Experimental populations used for identifying the QTL in crops are F_2, backcrossed (BC1F1), recombinant inbred lines (RILs), and doubled haploid (DH) populations. DH populations are quicker to produce than RILs when methods to produce DH are available [12]. However, major disadvantage of DH is that recombination rate is less than that of RILs [13].

In breeding programs designed to increase grain yield, it is particularly important to make selections based on components and traits affecting yield. The yield components, which develop during ontogenesis, are the factors that determine the productivity of a wheat crop [14]. The contribution of each of these components in estimating the grain yield, though influenced by the genetic properties of a particular cultivar, can change depending on growth and development conditions, in particular under the influence of habitat and agronomic factors [15]. The individual yield components developed at different growth stages and the conditions prevailing during these stages are directly translated into the quantitative parameters of these traits.

Large number of quantitative traits in wheat, including kernel yield, flowering time, and resistance to various diseases, demonstrate significant variability in the manifestation of the genotype – environment interaction (GEI) [16]. Determining the nature of the ecological-genetic interaction or "genotype-environment" is one of the key tasks, the resolution of which is possible through the establishment of the mechanisms of inheritance of the genetic components of this system. Obviously, the phenotypic manifestation of quantitative traits depends on both genetic and non-genetic components that influence the formation of an individual or population genotype. Classical studies of quantitative traits assess the genotype-environment interaction, averaged, taking the action of the entire genome into account to a greater extent than the genome's individual loci or QTL [17].

As stated above, the development of bi-parental mapping populations is essential for the development of regional wheat breeding projects. Therefore, as part of the international project "ADAPTAWHEAT" [18], the genetic map from the cross of Pamyati Azieva (Russian cultivar registered in Kazakhstan) x Paragon (UK cultivar) was developed. The mapping population (MP) consisted of 98 recombinant inbred lines (RILs) [19]. As GEI is enormously influential to the yield and yield components, it was important to test the MP in Kazakhstani field conditions. The aim of the study was to evaluate the morphological variability of RILs in the southeast of the country.

Materials and methods

The subject of the study is a common wheat biparental mapping population (MP) from the cross of cultivars Pamyati Azieva (Russian Federation, registered in Kazakhstan) and Paragon (UK), hereafter referred to as Pam x Par. The Pam x Par MP consisted of 98 recombinant inbred lines (RILs) developed from F_2 generation by single seed descent method in greenhouse conditions by using facilities of the John Innes Centre (Norwich, UK) from the period of 2011-2015 yy. By 2015, 98 RILs were available at F_8 generation for field trials in Kazakhstan. MP along with the parent plants have been grown in the experimental station of the Kazakh Research Institute of Agriculture and Plant growing (KAZNIIZR, southeast of Kazakhstan). The station's GPS coordinates are N 43°13'09" E 76°41'17", altitude 740 m. The cultivar Pamyati Azieva provides a combination of drought resistance, resistance to powdery mildew, and contains a large number of kernels per spike, which ensures high productivity per spike. Paragon served both conventional and organic growers well, and is recognized as a high bread making cultivar. In

addition, Paragon has broad-spectrum disease resistance and good straw characteristics. The MP was developed under the project "ADAPTAWHEAT" [18].

Ninety-eight RILs (F_8 generation) have been planted on the field of the KAZNIIZR in two randomized replications in 2015-2018 yy. The rows were spaced 15 cm apart and the distance between plants within a row was 5 cm. In total, the data for mean values of eight agronomic traits of the 98 RILs harvested in four-year trials was analysed. The studied traits included plant height (PH), peduncle length (PL), number of fertile spikes (NFS), spikes length (SL), number of kernels per spike (NKS), thousand kernels weight (TKW), weight of kernels per main spike (WKS), and weight of kernels per plant (WKP). Soil in the experimental field is light chestnut (humus 2.0-2.5%). Annual precipitation at the experimental site ranged from 51 to 103 mm during the experiment, while the average temperature varied from 23 to 27°C (Figure 1).

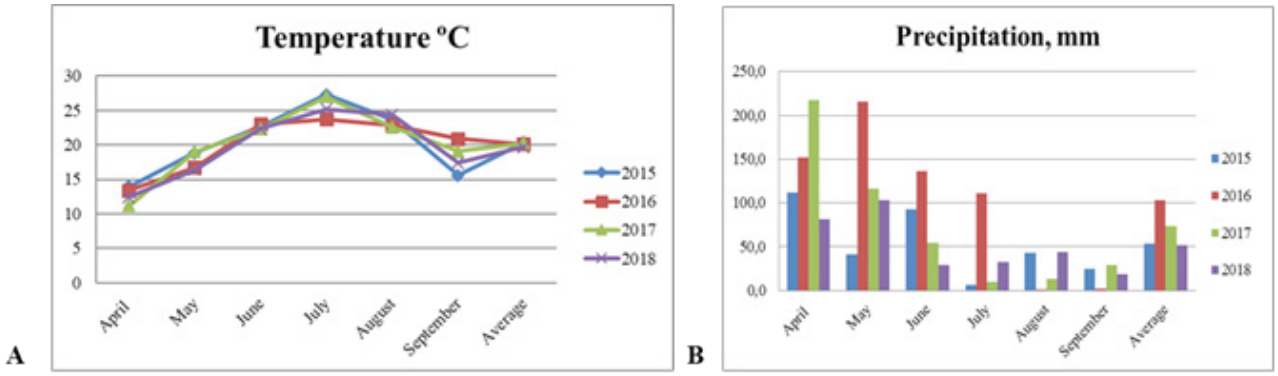

Figure 1 – Temperature (A) and Precipitation (B) data over the four years (2015-2018 yy.) at the KAZNIIZR breeding station

Statistical data analysis. Variability of key yield traits was assessed using Statistical Package for the Social Sciences Version 16.0 (SPSS software; International Business Machines: New York, USA, https://www.ibm.com/products/software). The descriptive statistics of all traits was measured during the experiment. The correlation analysis was calculated using GraphPad Prism Version 8.0 (GraphPad Software; La Jolla California, USA, https://www.graphpad.com/). The genotype-environment interaction (GEI) analysis was calculated using GenStat software Version 19.1 (VSN International, Hemel Hempstead: UK, www.vsni.co.uk).

Results and discussion

Yield performance of the MP. The value of WKP ranged from 2.3 g (RIL51) to 5.6 g (RIL48). The average WKP for the MP over the four years was 3.9±0.7 g and it was slightly less than WKP for Pamyati Azieva (4.1 g). In total, 40 out of tested 98 RILs exceeded the WKP in comparison with the parent cultivar Pamyati Azieva (Figure 2).

Results suggest that developed MP Pam x Par is well adapted to the local environmental conditions. RILs with the best yield performance are listed in Table 1. The list suggests that those RILs can be successfully introduced to further breeding studies in south-east of Kazakhstan.

The WKP data from the Table 1 suggests that lines RIL48, RIL36, RIL83, RIL01, and RIL46 should be selected for extended field trials with larger field plots.

The Pearson correlation analysis indicates that WKP significantly correlated with PH, NFS, NKS, and TKW (Table 2).

As can be seen from the Table 2, the correlation indices were positive for all four traits, the analysis suggests that most high yielding accessions should be tall, with greater NFS, NKS and TKW numbers. Since the productivity of the studied population is largely dependent on weather conditions, which differed by year, the yield components were studied separately in all four years (2015-2018 yy.). The highest average WKP values were registered in 2016 and 2018. The average yield in 2016 was 4.6 ± 0.13 grams per spike and 4.3 ± 0.11 grams per plant in 2018. These results correlate with the amount of precipitation in July (Figure 1). Since wheat flowering and seed maturation occurs in July in south-east of Kazakhstan, precipitation in this month plays a crucial role in the final grain yield.

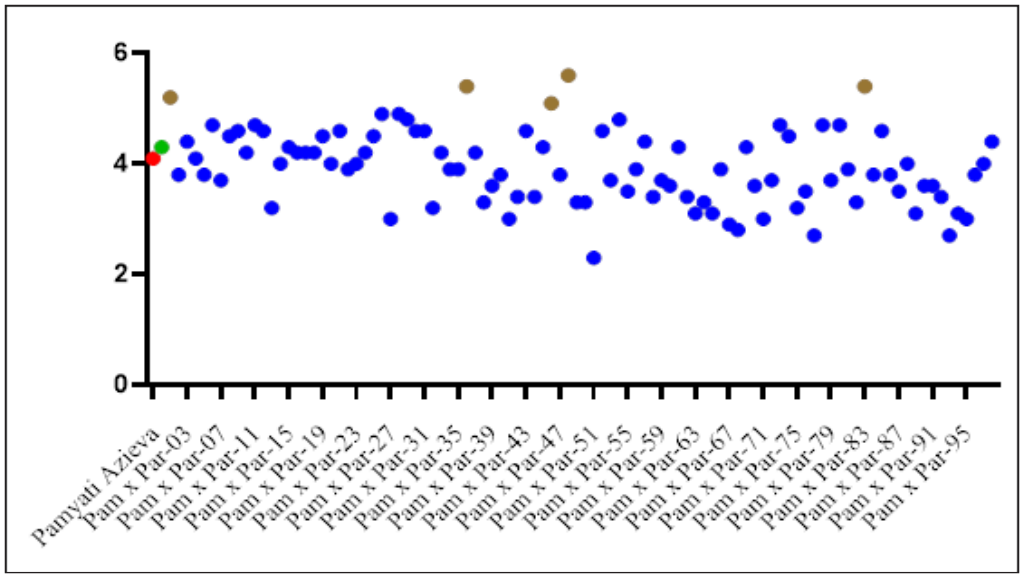

Figure 2 – The range of averaged WKP over the four years (2015-2018 yy.) in Pam x Par MP.
Note: Pamyati Azieva – red colour, Paragon – green colour, RILs – blue colour.
Brown colour designates RILs with the highest WKP values

Table 1 – List of RILs that showed best average values over four years (2015-2018) for three studied yield components, WKS, WKP, and TKW

RILs	WKS (g)	RILs	WKP (g)	RILs	TKW (g)
RIL83	1.8	RIL46	5.1	RIL98	33.3
RIL88	1.8	RIL01	5.2	RIL54	34.4
RIL25	1.9	RIL83	5.4	RIL57	34.6
RIL26	1.9	RIL36	5.4	RIL52	34.7
RIL52	1.9	RIL 48	5.6	RIL29	35.4
Pam	1.3	Pam	4.1	Pam	30.6
Paragon	1.7	Paragon	4.3	Paragon	25.7
Max*	1.93	Max*	5.6	Max*	35.4
Min*	0.97	Min*	2.3	Min*	19.6
Mean*	1.47 ± 0.02	Mean*	3.9±0.07	Mean*	28.6 ± 0.29
*Averaged data on bi-parental mapping population					

Table 2 – Pearson correlation index for major yield-related traits in 98 RILs of Pam x Par MP

Trait	PH	NFS	NKS	WKS	WKP	TKW
NKS	0.35***	0.12ns	1.00***	0.68***	0.47***	-0.14 ns
WKS	0.60***	0.03 ns	0.68***	1.00***	0.66***	0.49***
WKP	0.37***	0.54***	0.47 ***	0.66***	1.00***	0.40***
TKW	0.40***	-0.06 ns	-0.14 ns	0.49***	0.40***	1.00***
Note: P – values are provided with significance level indicated by the asterisks; * P < 0.05, ** P < 0.001, *** P < 0.0001, ns – not significant						

Despite the fact that yield in 2015 and 2018 was highest for the MP in the four subsequent years, the WKP was not interrelated (0.133). However, in all other cases the WKP significantly correlated with other trials. This result matches the GGE biplot analysis that graphically shows the relationship between genotypes and environments (Figure 3).

The genotype main effect and genotype x environment interaction (GGE) Biplot analysis suggests that environmental conditions in 2015 and 2016 were similar and combined in the first mega-environment (ME), and conditions in 2017 and 2018 were pooled in the second ME. In addition, the separation of four years trials into two mega-environments reflects the amount of precipitation in June (Figure 1), which is the key month for heading time in the southeast of the country.

The GGE Biplot graph (Figure 3) also suggests that the most suitable accessions for the first ME were RIL11, RIL25, and RIL46, while in the second ME – RIL25, RIL36, and RIL26, which match the data in the Table 1 well.

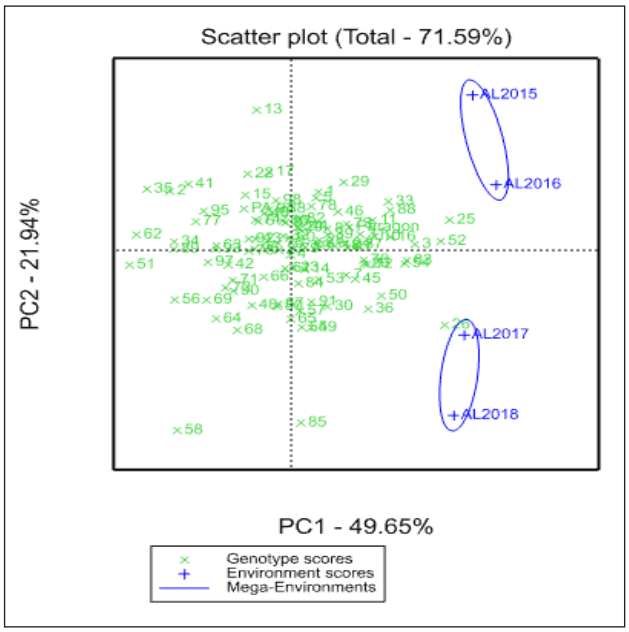

Figure 3 – The scatter plot of the GGE Biplot graph for 98 RILs of Pam x Par MP

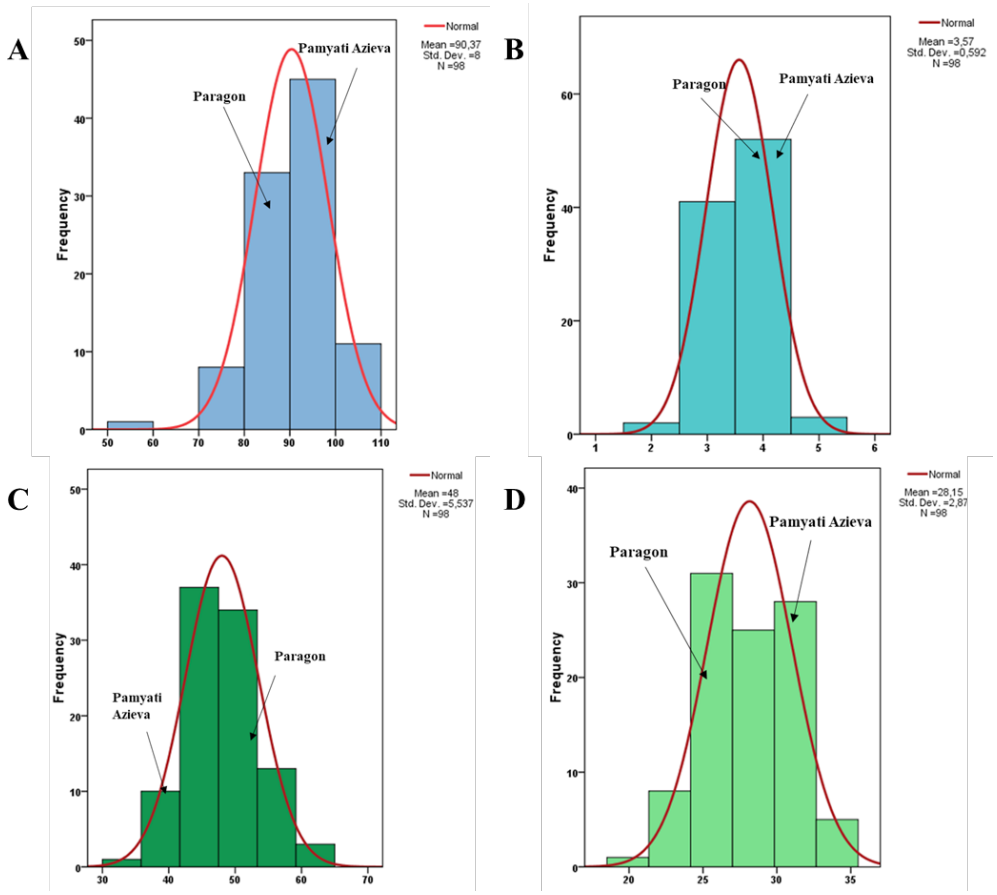

Figure 4 – The binomial distributions of major yield-related traits averaged over the four years (2015-2018 yy.) in Pam x Par MP. Note: A – plant height, B – number of fertile spikes, C – number of kernels per spike, D – thousand kernels weight

Variability in the main yield components. The Pearson correlation indices suggest that PH, NFS, NKS and TKW are major yield components for the studied region (Table 2), variation of these four traits was observed in the Pam x Par MP. It was found that PH ranged from 58.9 cm in RIL51 to 105.5 cm in RIL 49 (Figure 4.A). The PH of Pamyati Azieva was higher than in Paragon, and most of the RILs were in the range of 85 cm to 95 cm (Figure 4, A). The NFS ranged from 2.0 in RIL58 to 6.0 in RIL01, and the parents of the MP were similar in PH (Figure 4, B). However, when the parents were compared for NKS, Paragon (59.0) significantly outperformed Pamyati Azieva (42.0, $P<0.0001$) (Figure 4, C), which suggests that UK standard is well suited to use in breeding for PH, one of the important yield components. The TKW, another important yield trait, ranged from 19.6 g in RIL22 to 35.4 g in RIL29 (Figure 4, D). In contrast with NKS, in study of TKW, the cultivar Pamyati Azieva (30.6 g) showed significantly higher value ($P<0.0001$) than Paragon (25.7 g).

In overall, the assessment of the range of all four yield related components allowed the selection of valuable RILs that may play an important role in future wheat breeding studies in the region. The study allowed the identification of high yield RILs that may significantly contribute to the improvement of yield in southeast of the country. In addition, the variation of the field data can be successfully used in further studies related to the identification and genetic mapping of quantitative trait loci of yield related traits.

Conclusion

This study reports the field evaluation of the MP (98 RILs of Pam x Par) of common hexaploid wheat generated from the collaboration between Kazakh and British scientists. This is the first MP to be constructed by using one of the registered commercial cultivars in Kazakhstan. All 98 RILs were tested over the four consecutive years (2015-2018 yy.) at the KAZNIIZR breeding station. The field study suggests that the MP is a highly suitable genetic resource for wheat breeding projects, as developed RILs show a wide range of variation in yield related traits, including PH, NFS, NKS and TKW. The analysis of WKP indicated that in total 40 RILs outperformed the local parent cultivar Pamyati Azieva, including those five RILs (RIL48, RIL36, RIL83, RIL01, and RIL46) that showed averaged best yield values over the four years (2015-2018 yy.). The Pearson correlation index indicated that the average yield over all the four years was highly correlated with PH, NFS, NKS, and TKW. Individuals with favorable values for all yield-related traits were identified for their incorporation into the breeding studies. The GGE Biplot analysis allowed the separation of four trials to two mega-environments. It was hypothesized that the separation reflects the amount of precipitation in flowering and seed maturation times, which are crucial phases of wheat plant growth. Finally, all obtained observations will be used for further studies related to genetic mapping of quantitative trait loci of yield components in common wheat.

Acknowledgment

This study was supported by "ADAPTAWHEAT" project funded by the 7TH EU FP and the project "Creation of new DNA markers of drought resistance of spring wheat grown in the conditions of Northern Kazakhstan" (state registration number of the project 0118PK01352) under the budget program 0.0888 "Selection and seed production of drought-resistant, productive, high-quality varieties of spring wheat on the basis of classical methods of selection and modern approaches of biotechnology for the conditions of Northern Kazakhstan" (BR06249219) for 2018-2020 yy.

References

1 Michael J. (2009) The Wheat Crop. Wheat: Chemistry and Technology, Elsevier, 4th ed., Ch.2, pp. 19-49, ISBN: 978-1-891127-55-7.

2 Mitikul A., Regassa T. (2019) Participatory evaluation of bread wheat (Triticum aestivum L.) varieties for its yield performance at Madda Wlabu district of Bale Zone, South Eastern Ethiopia. *J Eq. Sci. Sustain. Dev.*, vol. 3, no. 1, pp. 84-89.

3 Fellmann T., Hélaine S., Nekhay O. (2014) Harvest failures, temporary export restrictions and global food security: the example of limited grain exports from Russia, Ukraine and Kazakhstan. *Food Sec.*, vol. 6, no. 5, pp. 727-742.

4 Gupta R., Kienzler K., Martius C., Mirzabaev A., Oweis T., de Pauw E., Qadir M., Shideed K., Sommer R., Thomas R., Sayre K., Carli C., Saparov A., Bekenov M., Sanginov S., Nepesov M., Ikramov R. (2009) Research Prospectus: A Vision For Sustainable Land Management Research In Central Asia. ICARDA Central Asia and Caucasus Program. Sustainable Agriculture in Central Asia and the Caucasus Series, no.1, p. 84.

5 Edinaldo T. (2018) The Impacts of El Niño and La Niña on Large Grain Producing Countries in

ECA: Yield, Poverty and Policy Response. Economics Faculty Journal Articles, pp. 1-78.

6 Report prepared under the FAO/EBRD cooperation (2012) Challenges in enhancing agricultural and food production, 182 p.

7 FAS staff (2018) Kazakhstan grain and feed update report, 11 p.

8 Mohammadia M., Tiedebc T., Smith K. (2015) PopVar: A Genome-Wide Procedure for Predicting Genetic Variance and Correlated Response in Biparental Breeding Populations. *Crop Sci.*, vol. 55, no. 5, pp. 2068-2077. doi: 10.2135/cropsci2015.01.0030

9 Heidari B., Sayed-Tabatabaei B., Saeidi G., Kearsey M., Suenaga K. (2011) Mapping QTL for grain yield, yield components, and spike features in a doubled haploid population of bread wheat. *Genome*, vol. 54, no. 6, pp. 517-527. doi: 10.1139/g11-017.

10 Lörz H., Wenzel G. (ed.) (2004). Molecular marker systems in plant breeding and crop improvement. Biotechnol. Agric. For., Springer-Verlag, Ch. 55, 476 p.

11 van Eeuwijk F.A., Bink M.C., Chenu K., Chapman S.C. (2010) Detection and use of QTL for complex traits in multiple environments. Curr. Opin. Plant Biol., vol. 13, no. 2, pp. 193-205. doi: 10.1016/j.pbi.2010.01.001

12 Newbury H.J. (2003). Plant molecular breeding, Biological sciences series, Blackwell, Ch.12, 265 p., ISBN 1-84127-321-X.

13 Guan H., Farhan A., Qingchun P. (2017) Dissection of recombination attributes for multiple maize populations using a common SNP assay. Front Plant Sci., vol. 8, p. 2063. doi: 10.3389/fpls.2017.02063

14 Singh S.P., Diwivedi V.K. (2002) Character association and path analysis in wheat (Triticum aestivum L.). *Agric. Sci. Dig.*, vol. 22, no. 4, pp. 255-257.

15 Sainis J.K., Shouche S.P., Bhagwat S.G. (2006) Image analysis of wheat grains developed in different environments and its implications for identification. *J. Agric. Sci.*, vol. 144, pp. 221-227. doi: 10.1017/S0021859606006010

16 Bariana H.S., Bansal U.K., Schmidt A., Lehmensiek A., Kaur J., Miah H, Howes N., McIntyre C.L. (2010). Molecular mapping of adult plant stripe rust resistance in wheat and identification of pyramided QTL genotypes. *Euphytica*, vol. 176, no. 2, pp. 251-260. doi: 10.1007/s10681-010-0240-x

17 Börner A., Schumann E., Fürste A., Cöster H., Leithold B., Röder S., Weber E. (2002) Mapping of quantitative trait loci determining agronomic important characters in hexaploid wheat (Triticum aestivum L.). *Theor. Appl. Genet.*, vol. 105, pp. 921-936. doi: 10.1007/s00122-002-0994-1

18 European Commission (2012-2015). Genetics and physiology of wheat development to flowering: tools to breed for improved adaptation and yield potential. URL: https://cordis.europa.eu/project/rcn/101673/factsheet/en.

19 Yermekbayev K., Turuspekov Y., Ganal M., Plieske J., Griffiths S. (2017) Construction and utilization of the hexaploid map Pamyati Azieva x Paragon Plant Genetics, Genomics, Bioinformatics and Biotechnology. p. 119. In: Proceedings of the 4th International conference "Plant Genetics, Genomics, Bioinformatics and Biotechnology" (PlantGen2017), Turuspekov Y. & Abugalieva S. (eds.). Almaty, Kazakhstan.

IRSTI 34.43.35; 61.45.31

[1*]L.K. Baktybayeva, [1]M.K. Tauassarova, [1]B.K. Kairat, [2]B.K. Darrell,
[1]N.B. Baktybay, [3] V.K. Yu, [3]A.G. Zazybin, [3]A.E. Malmakova

[1]Laboratory of ecological physiology, Almaty, Kazakhstan
[2]Oklahoma State University, Center for Health Sciences, Stillwater, Oklahoma City, USA
[3]A.B. Bekturov Institute of Chemical Sciences, Laboratory of chemistry of synthetic and natural drugs;
Kazakh-British Technical University, School of Chemical Engineering, Almaty, Kazakhstan
*e-mail: Layilia.Baktybaeva@kaznu.kz

Myeloid poiesis stimulating activity of azaheterocycles compound of the dimethyl ether of P-(4-methoxyphenyl)-1-(4-phenylpiperazine) methyl] phosphonic acid

Abstract: Development of new effective drugs with myeloid poiesis stimulating activity is highly relevant due to the increase in the number of patients with hematological disorders. Acquired hematological diseases are associated with unbalanced and inadequate nutrition, chronic blood loss, living in ecologically disadvantaged areas, extreme physical activity, use of cytostatic and cytotoxic drugs, chronic stress, and other. Azaheterocyclic compounds are perspective for search of new effective myeloid poiesis stimulating drugs. The incentive for this search was the manifestation of myeloid poiesis stimulating activity by azaheterocycles drug Prosidol (Propionylphenylethoxyethylpyperidine) in clinical practice. On the model cyclophosphamide myeloid depression high myeloid poiesis stimulating activity showed that compound of the dimethyl ether of P-(4-methoxyphenyl)-1-(4-phenylpiperazine) methyl] - phosphonic acid in laboratory coding of BIV-95. In a series of experiments showed myeloid poiesis stimulating activity at the level of comparison compound (2, 3, 5, 6-tetrahydro-6-phenylimidazo [2, 1-b] thiazole hydrochloride (Levamizol drug). The erythropoiesis stimulating activity exceeded the activity of the comparison compounds. The thrombocytopoiesis stimulating activity was at the level of the comparison compounds. Leukopoiesis stimulating activity also was slightly higher than the activity of Levamizol drug. Recovery of granulocytic and agranulocytic leukocyte were no violations of immunoregulatory index in leukogram blood. The test compound is the dimethyl ether of P-(4-methoxyphenyl)-1-(4-phenylpiperazine) methyl]-phosphinic acid compound under the laboratory coding BIV-95 had low toxicity.
Key words: azaheterocyclic compound, erythropoiesis-stimulating activity, thrombocytopoiesis stimulating activity, leukopoiesis stimulating activity.

Introduction

Humans and animals' immune system performs an important function to maintain the constancy of the body internal environment, carried out by recognizing and eliminating alien substances of antigenic nature from the body. This function of immune system is carried out with the congenital and acquired immunity factors. Different types of radiation, heavy metal salts, vitamin and micronutrient deficiency, stressful situations, age-related changes in the lymph myeloid complex, therapy with anti-tuberculosis, antibacterial, hormonal, cytostatic drugs and a number of other factors lead to the development of immune diseases. These diseases treated with a set of immunotherapy methods, the use of immunostimulants is one of them. Today, immunostimulants distinguish such of microbial, thymus, bone marrow, cytokines, nucleic acids, vegetable and synthetic origin. Many immunostimulants have a wide range of side effects [1; 2]. Preparations from thymus cause severe allergic reactions [3; 4]. Preparations based on nucleic acids cause uncontrolled division of all cells of the body: benign, malignant, bacterial microflora [5; 6]. Preparations of plant origin require long-term systemic use [7]. With introduction of medicinal interleukins it is difficult to control the reaction of the body, which in a negative case can result in septic shock [5].

In the Republic of Kazakhstan monitoring and synthesis of new synthetic myeloid poiesis stimulating and immunostimulants preparations is carried out in the laboratory of chemistry of synthetic and natural drugs of the JSC A.B. Bekturov Institute of Chemical Sciences [3]. Staff of chemistry of synthetic and natural drugs laboratory has accumulated vast experience in the field of synthesis and chemical transformations of 4-oxipiperidines, obtained new data, which allows making important conclusions about the relationship between the fine chemical structure of synthesized compounds and their reactivity, spectral characteristics and biological activity. Drugs with high anesthetic, antiarrhythmic, anti-allergic, immunostimulatory and other types of activity were discovered having substantial advantages over the conventional medicines. The stimulus for the search among piperidine derivatives was the manifestation of immunostimulating activity by the preparation Prosidol (propionylphenylethoxyethylpyperidine), obtained in this laboratory [8]. The aim of the current study was to examine the myeloid stimulating activity and acute toxicity of dimethyl ester of P-[(4-methoxyphenyl)-1-(4-phenylpiperazine) methyl] phosphinic acid compound under the laboratory coding BIV-95.

Materials and methods

Dimethyl ester of P- [(4-methoxyphenyl)-1-(4-phenylpiperazine) methyl] phosphonic acid compound under the laboratory coding BIV-95 (chemical formula shown on Figure 1) was studied for leukopoiesis stimulating action and acute toxicity.

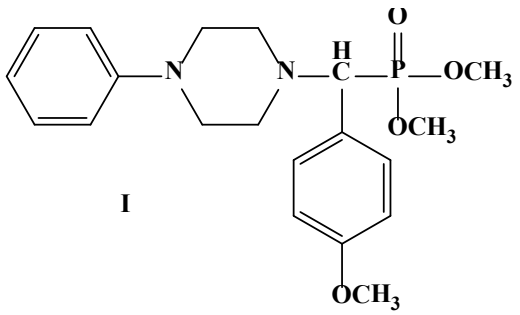

I

Figure 1 – Chemical formula of BIV-95

In the experiment 30 healthy 16-18 weeks old, 210-280 g albino laboratory female rats were used. The scatter in the groups according to the initial body weight did not exceed ± 10%. Animals were taken from the nursery of the biological clinic of the Faculty of Biology and Biotechnology of the al-Farabi Kazakh National University. Before the experiment and during it, control and experimental animals were kept in the same standard conditions, on a standard diet, with six animals in each cage. Investigations were carried out in accordance with the "Rules for the pre-clinical (non-clinical) studies of biologically active substances" and "Ethical principles and guidelines for scientific experiments on animals" [9]. Animals were divided into 5 groups of 6 animals. Group 1 was intact. Animals did not receive cytostatic and test compounds. On the 1st, 3rd, 5th day of the experiment, all other groups received a cytostatic drug doxorubicin hydrochloride at a dose of 10 mg/kg of animal weight in a volume of 0.2 ml [10]. On the 8th day of the experiment, the number of cells in the peripheral blood was counted. On the 8th, 10th, 12th day of the experiment the animals of the second group were injected with BIV-95 at a dose of 5 mg/kg intraperitoneally in a volume of 0.2 ml, saline used as solvent. On the 18th day of the experiment the number of cells in the peripheral blood was counted. Third group of animals was given as placebo, i.e. saline in a volume of 0.2 ml. Fourth group was used as control. The animals of this group were injected with (2, 3, 5, 6-tetrahydro-6-phenylimidazo [2, 1-b] thiazole hydrochloride (Levamizole drug) at a dose of 1 mg/kg intraperitoneally in a volume of 0.2 ml, saline used as solvent [11]. Fifth group after intoxication was not administered any compounds, which controlled the physiological rate of blood cell recovery. Blood sampling was performed at 09:00 am from the orbital vein of rats in sterile hematologic tubes VF-052SDK with 2 mL of EDTA (K2) under the mild anesthesia with ether. Blood tests were carried out on a hematology analyzer for animal blood **Abacus junior VET** (Diatron, Denmark). Following parameters were analyzed: WBC – white blood cell count, LY – absolute lymphocyte count; MID – absolute monocyte-eosinophil value; GRA – absolute granulocytic value; LY – comparative lymphocytic value; MI – comparative monocyte-eosinophil value; GR – comparative granulocytic value; RBC – red blood cell count; HGB – hemoglobin; HCT – hematocrit; MCV – mean corpuscular volume; MCH – mean corpuscular hemoglobin; MCHC – mean corpuscular hemoglobin concentration; RDWC – red blood cell distribution width; PLT – total platelets volume; PCT – plateletcrit; MPV – mean platelet volume; PDWC – platelet distribution width.

For the dual cytological control, in order to count blood leukogram, blood smears were produced by Gi-

emsa stain method, and counted under a microscope SA3300S immersion (magnification x100) with 100 cells per each smear sample, afterwards the relative amount of each type of the cells converted into the absolute value [12]. Statistical data processing was carried out with the reduction of the Student's confidence factor.

For the study of acute toxicity, groups of animals (by 6 in each) were injected intraperitoneally with the test compound in various doses and observed for 5 days. External signs of intoxication, duration of toxic action and time of death were recorded. For the quantitative assessment of acute toxicity, the LD_{50} index was calculated (the dose that caused the death of 50% of the test animals). The comparison compound was the (2, 3, 5, 6-tetrahydro-6-phenylimidazo [2, 1-b] thiazole hydrochloride (Levamizole drug) [11]. The toxicity grade of the drug was judged by LD_{50} in the experimental and control groups of animals.

Results and discussion

Data on myeloid poiesis stimulating activity. Control values obtained from intact animals enrolled in the experiment maintained within the physiological norm. Leukocyte indicator (11.1 ± 2.51) $\cdot 10^9$/L of blood, with lymphocytic indicator (5.96 ± 1.44) $\cdot 10^9$/L of blood, which was (53.72 ± 0.7) %. Granulocyte leukocytes had a value (4.44 ± 0.9) $\cdot 10^9$/L of blood with a percentage ratio in leukogram (40.0 ± 1.4) %. The lowest was a monocytic-eosinophilic index (07.0 ± 0.0) $\cdot 10^9$/L of blood, which in relative value was (6.28 ± 0.4) %. Erythrocyte and platelet counts were normal. The erythrocyte index was (6.5 ± 1.2) $\cdot 10^{12}$/L of blood with hemoglobin content (140.7 ± 1.9) g/L of blood and hematocrit (39.8 ± 1.5). The platelet count was also normal (660.0 ± 122.2) $\cdot 10^9$/L of blood, as well as thrombocrit was (0.44 ± 0.021). In overall, the main blood parameters were normal (Table 1).

Table 1 – Hemogram of blood after administration of doxorubicin hydrochloride

Complete blood count	Control group		Intoxication group		Intact group		Placebo group	
	$X_{avi.}$	$d_{avi.}$	$X_{avi.}$	$d_{avi.}$	$X_{avi.}$	$d_{avi.}$	$X_{avi.}$	$d_{avi.}$
WBC, $\cdot 10^9$/L	4.15	1.2	2.37	0.16	11.1	2.51	2.79	0.93
LY, $\cdot 10^9$/L	2.57	0.83	1.12	0.2	5.96	1.1	1.41	0.9
MID, $\cdot 10^9$/L	0.22	0.17	0.12	0.1	0.70	0	0.17	0.1
GRA, $\cdot 10^9$/L	1.36	0.14	0.62	0.3	4.44	0.9	0.93	0.13
LY, %	62.04	3.93	47.2	1.8	53.72	0.7	50.65	1.65
MI, %	5.28	2.4	4.9	1.3	6.28	0.4	6.0	5.3
GR, %	32.68	4.6	26.18	4.5	40	1.4	43.35	9.3
RBC, $\cdot 10^{12}$/L	4.69	1.36	3.8	0.5	6.5	1.2	4.67	0.1
HGB, g/L	86.0	12.0	90.75	12	140.7	1.9	96.0	1.0
HCT, %	24.69	2.7	21.21	7.79	39.8	1.5	28.1	0.84
MCV, fl	52.5	1.5	52.75	1.25	55.0	1.3	50.0	11.3
MCH, pg	18.45	0.55	17.45	1.15	19.0	3.6	17.0	0.3
MCHC, g/L	349.25	4.0	347.25	3.0	350.6	2.8	342.5	6.5
RDWC	12.7	0.4	13.68	0.5	14.0	0.8	13.55	0.22
PLT, $\cdot 10^9$/L	318.25	99.0	70.5	23.33	660.0	122.2	447.0	51.0
PCT, %	0.21	0.06	0.05	0.03	0.44	0.021	0.32	0.04
MPV, FL	6.63	0.3	5.28	2.0	7.9	0.8	7.1	0.0
PDWC	30.95	0.25	23.1	8.6	46	0.8	32.35	1.3

The directed myeloid depressive effect of the administered doxorubicin hydrochloride led to the myeloid depressive syndrome with a drop in blood counts on the 14th day after the last injection. The overall leukocyte index was (4.15 ± 1.2) · 10^9/L of blood, i.e. with a decrease of 2.67 times ($p \leq 0.05$) and on the 14th day after the injection, the level of leukocytes was (2.69 ± 0.54) · 10^9/L of blood, which

amounted to 4.12-fold drop compared to with intact animals ($p \leq 0.01$). According to the blood leukogram, significant negative changes in the cell pools of lymphocytes, granulocytes, monocyte-eosinophil indicator can be noted. Indicators of immunocompetent cells – lymphocytes from the control value (5.96 ± 1.1) · 10^9/L of blood decreased on the 3rd day to (2.46 ± 0.75) · 10^9/L of blood and reached (1.99 ± 0.18) · 10^9/L of blood, i.e. 2.99 times less ($p \leq 0.05$) on the 14th day. Changes that are even more significant occurred in the cell populations of granulocytes: the value of (4.44 ± 0.9) · 10^9/L of blood decreased by the 3rd day to (1.33 ± 0.18) · 10^9/L of blood, i.e. 3.34 times less ($p \leq 0.01$). A significant decrease in the absolute index of granulocytes can be explained by a significant drop in the total leukocyte index, which affected the absolute indicators of blood cells (Table 1).

On the 1st day after injection of doxorubicin hydrochloride increase in monocytes index was observed, which can be explained by mass cell death and an increase in the functional load on monocytes. The monocyte index (6.0 ± 0.7) % by the 1st day after the injection of doxorubicin hydrochloride became (7.05 ± 1.6) %, but already on the 3rd day after the injection, it fell down to (0.6 ± 0.0) %, however, on the 14th day it was (16.6 ± 0.0) % ($p \leq 0.01$).

Myeloid depressive syndrome was recorded in red blood cells. Reduction of erythrocyte cells from (6.5 ± 1.2) · 10^{12}/L of blood with a decrease on the 1st day to (4.71 ± 1.37) · 10^{12}/L by 1.38 times and a slight increase to (5.80 ± 0.27) · 10^{12}/L on the 3rd day after the injection of doxorubicin hydrochloride. The trend in fluctuations of indicators on the first day and third day after injection of doxorubicin hydrochloride was observed in hemoglobin, hematocrit, mean red blood cell volume, average hemoglobin content in red blood cells, and the width of red blood cell distribution. The decline was observed on the 1st day of 1.2-1.6 times and then with a slight increase on the 3rd day and a further drop in all erythrocyte values of more than 1.7 times. Significant changes were recorded in platelet indices, which naturally affected the values of trombocrit, average platelet volume and platelet distribution. On the 1st day after injection of doxorubicin hydrochloride, the level of platelets immediately fell down to (345.0 ± 126.0) · 10^9/L blood with the value in intact animals equal to (660.0 ± 122.0) · 10^9/L blood, i.e. 1.91 times less ($p \leq 0.05$). By the 14th day after injection, the platelet level decreased to (74.5 ± 39.5) · 10^9/L of blood from the baseline value (660.0 ± 122.0) · 10^9/L of blood, i.e. 8.85 times ($p \leq 0.01$) (Table 1). This indicator is considered critical and is characterized by spontaneous intracavitary hemorrhage and other hemophilic disorders.

It can be concluded that doxorubicin hydrochloride caused myeloid suppression syndrome and the most sensitive cells were leukocyte cells and platelets. Among leukocyte cells, lymphocytes, granulocytes, and then monocytes died first. Then, on the background of myeloid depressive syndrome, animals were injected with BIV-95. For myelostimulating activity, the following results were obtained.

Compound BIV-95 differed in average leukopoiesis stimulating activity. It stimulated leukopoiesis and the release of leukocytes from peripheral immune organs. The common leukocyte index was (5.35 ± 0.8) · 10^9/L of blood, exceeding the indicators of the placebo group (2.79 ± 0.92) · 10^9/L of blood by 1.92 times and the control group (4.15 ± 1.2) 10^9/L of blood by 1.29 times (Table 2).

The relative indicators of blood leukogram were presented in the following form: the lymphocytic values in the group with injection of BIV-95 and the control group differed slightly and varied within the error range from (57.22 ± 0.9) % to (62.04 ± 3.93) %; granulocytic values were also similar to each other and ranged from (31.15 ± 0.2) % to (32.68 ± 4.6) %; monocytic-eosinophilic index was higher BIV-95 group equal to (11.63 ± 0.1) %, which was 2.2 times higher than the value in control group (5.28 ± 2.4) %. The absolute and relative indicators of lymphocytes and granulocytes were at the level of the control group or slightly exceeded. The erythrocyte and platelet indices in the injection group of the compound BIV-95 were higher than in the injection group of the comparison drug. Erythrocyte indices in BIV-95 group were (5.4 ± 0.1) · 10^{12}/L against the same indicator of the control group (4.69 ± 1.36) · 10^{12}/L, which amounted to 1.15 times the difference. A significant difference was recorded in hemoglobin values of (105.0 ± 5.6) g/L versus the value of the control group of (86.0 ± 12.0) g/L. The average volume of erythrocytes differed slightly in the experimental and control groups: (48.2 ± 0.6) vs. (42.5 ± 1.5). The average hemoglobin content in the erythrocytes of the experimental group was significantly different from the values of the control group: (17.2 ± 0.1) pg. vs. (8.45 ± 0.55) pg., i.e. 2.04 times higher.

Platelet indices in BIV-95 group and the control group were within an **accepted error rate**: (315.0 ± 9.6) · 10^9/L against (318.25 ± 99.0) · 10^9/L. The number of platelets, the average volume of platelets and the width of the distribution of platelets in the control and experimental group did not differ much.

Table 2 – Blood hemogram after administration of the test compounds

Indicators	Intact group	Toxic group	BIV-95	Placebo group	Control group
WBC, $\cdot 10^9$/L	11.1±2.51	2.69±0.54	5.35±0.8	2.79±0.93	4.15±1.2
LY, $\cdot 10^9$/L	5.96±1.1	1.44±0.18	2.98±0.1	1.41±0.87	2.57±0.83
MID, $\cdot 10^9$/L	0.70±0.0	0.61±0.01	0.65±0.01	0.17±0.1	0.22±0.17
GRA, $\cdot 10^9$/L	4.44±0.9	0.90±0.36	1.74±0.1	1.21±0.13	1.36±0.14
LY, %	53.72±0.7	49.65±8.6	57.22±0.9	50.65±14.65	62.04±3.93
MI, %	6.28±0.4	16.6±0.0	11.63±0.1	6.0±5.3	5.28±2.4
GR, %	40.0±1.4	33.75±8.6	31.15±0.2	43.35±9.3	32.68±4.6
RBC, $\cdot 10^{12}$/L	6.5±1.2	3.80±0.27	5.4±0.1	4.67±2.58	4.69±1.36
HGB, g/L	140.7±1.9	77.0±4.0	105.0± 5.6	86.0±1.0	86.0±12.0
HCT, %	39.8±1.5	30.85±0.9	45.2±0.5	28.10±0.84	24.69±2.7
MCV, fl	55.0±1.3	43.0±1.0	48.2±0.6	40.0±0.0	42.5±1.5
MCH, pg	19.0±3.6	18.45±0.2	17.2±0.1	17.0±0.3	8.45±0.55
MCHC, g/L	350.6±2.8	306.5±2.5	321.0±8.5	312.5±6.5	319.25±4.0
RDWC	14.0±0.8	13.85±0.1	14.5±0.5	13.55±0.25	12.7±0.4
PLT, $\cdot 10^9$/L	660.0±122.2	74.5±39.5	315.0±9.6	107.0±51.0	318.25±99.0
PCT, %	0.44±0.021	0.05±0.07	0.34±0.01	0.032±0.04	0.31±0.06
MPV, fl	7.9±0.8	5.9±0.15	7.4±0.1	4.1±0.0	6.63±0.3
PDWC	46.0±0.8	29.5±29.5	36.2±0.9	22.35±0.65	30.95±0.25

As a result of studies, it was found that BIV-95 compound showed leucopoiesis stimulating activity higher than the comparison compound (Levamizole drug).

Toxicity results. For the study of acute toxicity, groups of animals (by 6 animals each) were injected intraperitoneally with the test compound in various doses and observed for 5 days. In mice, external signs of intoxication, the duration of toxic action and the time of animals' death were recorded. For the quantitative assessment of acute toxicity, the LD_{50} index was calculated (the dose that caused the death of 50% of the test animals). The reference drug was the pharmaceutical drug (2, 3, 5, 6-tetrahydro-6-phenylimidazo [2, 1-b] thiazole hydrochloride (Levamizole drug). The degree of toxicity of the drug was judged by LD_{50} in the experimental and control groups of animals. The LD_{50} of dimethyl ester of P-[(4-methoxyphenyl)-1-(4-phenylpiperazine) methyl] phosphonic acid compound under the laboratory coding BIV-95 was 721.7 mg/kg, which is 3.6 times lower than the toxicity of the reference compound (Levamizole drug).

Conclusion

The newly obtained compound dimethyl ether of P-(4-methoxyphenyl)-1-(4-phenylpiperazine) methyl]-phosphonic acid in laboratory coding BIV-95 is promising for developing it as a new myeloid stimulating preparation. It shows high myeloid stimulating activity on the model cyclophosphamide myeloid depression. Restoration of leukocyte, erythrocyte, platelet values is more effective than with the comparison compound (2, 3, 5, 6-tetrahydro-6-phenylimidazo [2, 1-b] thiazole hydrochloride (Levamizole drug). It effectively stimulates the regeneration of the leukocyte populations without disturbing the immunoregulatory blood indexes. The test compound had low level of toxicity 721.7 mg/kg, which is 3.6 times lower than the toxicity of reference compound. Test compound dimethyl ether of P-(4-methoxyphenyl)-1-(4-phenylpiperazine) methyl]-phosphonic acid in laboratory coding of BIV-95 needs further studies of its pharmacodynamic and pharmacokinetic properties.

References

1 Khaitov R.M., Pinegin B.V. (2003) Immunomodulators: the mechanism of action and clinical application. *Immunology*, vol. 24, no. 4, pp.196-203.

2 Khaitov R.M., Pinegin B.V. (2000) Modern immunomodulators: the basic principles of their use. *Immunology*, no. 5, pp. 4-7.

3 Hutzschenreuter F., Monsef I., Kreuzer K.A., Engert A., Skoetz N. (2016) Granulocyte and granulocyte-macrophage colony-stimulating factors for newly diagnosed patients with myelodysplastic syndromes. Cochrane Database Syst Rev., vol.16, no.2, pp. 22-28. CD009310. doi: 10.1002/14651858. Review. PMID: 26880256.

4 Novoseletskaya A.V., Kiseleva N.M., Zimina I.V., Bystrova O.V., Belova O.V., Inozemtsev A.N., Arion V.Y., Sergienko V.I. (2015) Thymus polypeptide preparation Tactivin restores learning and memory in thymectomied rats. *Bull Exp Biol Med.*, vol. 159, no. 5, pp. 623-625. doi: 10.1007/s10517-015-3030-6.

5 Ran Y., Xu B., Wang R., Gao Q., Jia Q., Hasan M., Shan S., Ma H., Dai R., Deng Y., Qing H. (2016) Dragon's blood extracts reduce radiation-induced peripheral blood injury and protects human megakaryocyte cells from GM-CSF withdraw-induced apoptosis. *Phys Med.*, vol. 32, no. 1, pp. 84-93. doi: 10.1016/j.ejmp.2015.09.010.

6 Craig M., Humphries A.R., Nekka F., Bélair J., Li J., Mackey M.C. (2015) Neutrophil dynamics during concurrent chemotherapy and G-CSF administration: Mathematical modelling guides dose optimization to minimise neutropenia. *J Theor Biol.*, vol.21, no. 385, pp.77-89. doi: 10.1016/j.jtbi. 2015.08.015. Epub 2015 Sep 3.

7 Praliev K.D., Yu V.K., Fomicheva E.E., Baktybayeva L.K., Svambaev E.A., Tuleukhanov S.T. (2007) Immunostimulants of the N-alkoxyalkyl piperidine series. *Chemical Journal of Kazakhstan*, no. 2, pp. 180-187.

8 Yu V.K., Praliev K.D., Fomicheva E.E., Baktybayeva L.K., Svambayev E.A., Tuleukhanov S.T. (2007) Immunostimulants based on N-alkoxypiperidines. *Chemical Journal of Kazakhstan*, no. 2, pp. 180-187.

9 Order of the Minister of Health of the Republic of Kazakhstan dated from November 19, 2009, No. 745 "On approval of the Rules for preclinical (non-clinical) studies of biologically active substances". https://aipm.kz/en/2016-07-11-17-52-27/kazakhstan-legislation/424-order-of-the-minister-of-health-and-social-protection-of-the-republic-of-kazakhstan-no-10-dated-january-14-2015.html

10 Doxorubicin hydrochloride. In: European Pharmacopoeia (2005) 6th ed., monograph, pp. 1389-1413.

11 Khaitov R.M., Pinegin B.V., Latysheva T.V. (2002) Methodical instructions for testing new immunomodulating medications. Vedomosti, scientific center of expertise and state control of medicines, no.1, pp. 11-21.

12 Giemsa G. (1904) Eine Vereinfachung und Vervollkommnung meiner Methylenazur-Methylenblau-Eosin-Färbemethode zur Erzielung der Romanowsky-Nochtschen Chromatinfärbung. Centralbl f Bakt etc., no. 37, pp. 308-311. 90.

13 Yu V.K., Praliyev K.D. (1997) 1-(2-Ethoxyethyl)-4-(dimethylphosphoryl)-4-hydroxypiperidine possess plant growth-stimulating activity. Provisional Patent, no. 5011. Bulletin RK, no. 3, pp. 8-15.

14 Praliyev K.D., Yu V.K., Zhaxibaeva Zh.M., Togyzbaeva N.A., Kemelbekov U.S., Baktybayeva L.K., Svambayev E.A. (2008) Complex of 3-(3-i-propoxypropyl)-7-(2-morpholinoethyl)-3,7-diazabicyclo [3.3.1] nonan with β-cyclodextrin and its precursors synthesis. Provisional Patent, no. 19832. Bulletin RK, no. 8, pp. 6-12.

15 Zimin Yu.S., Borisova N.S., Timerbaeva G.R., Gimadieva A.R., Mustafin A.G. (2016) Obtaining, toxicity and anti-inflammatory activity of complex compounds of uracil derivatives with polyfunctional acids. *Chemical-pharm J.*, vol. 50, no. 10, pp.16-24.

16 Khaitov R.M., Pinegin B.V. (1996) Immunomodulators and some aspects of their clinical use. *Clinical medicine*, vol. 74, no. 8, pp. 7-12.

17 Kharkevich D.A. Pharmacology. Textbook for high schools. M.: GEOTAR – MED, 2002, 672 p.

18 Hadden, J.W. (1993) Immunostimulants. *Immunology Today*, vol. 14, pp. 275-280.

19 Werner G.H., Jolles P. (1996) Immunostimulating agents: what next? A review of their present and potential medical applications. *European Journal of Immunology*, vol. 242, pp. 1-19.

20 Mikhailova A.A. (1996) Individual myelopeptides are "new generation" drugs used for immunorehabilitation. *International Journal of Immunoreability*, no. 2, pp. 27-31.

21 Petrov R.V., Khaitov R.M., Nekrasov A.V. (1999) Polyoxidonium – immunomodulator of the last generation: results of a three-year clinical application. *Allergy, asthma and clinical immunology*, no. 3, pp. 3-6.

22 Petrov R.V. (1994) Immunorehabilitation and strategy of medicine. *International Journal of Immunoreability*, suppl.1, pp. 5-6.

23 Gaetke L.M., Chow C.K. (2003) Copper toxicity, oxidative stress and antioxidant nutrients. *Toxicology*, vol. 189, pp. 147-163.

IRSTI 34.15.51

[1, 2*]S.K. Davletova

[1]Present address: Department of Biology and Biotechnology,
al-Farabi Kazakh National University, Almaty, Kazakhstan
[2] Department of Otolaryngology-Head and Neck Surgery, Ohio State University, Columbus, Ohio, USA.
*e-mail: davlets@gmail.com

Merlin tumor suppressor signaling in the neurofibromatosis type 2 tumorigenesis

Abstract: In this review a complex signaling in human neurofibromatosis type 2 (NF2) in nervous system and other tissues is discussed. The *neurofibromatosis type 2* (*Nf2)* gene, known as a tumor suppressor, encodes a protein Merlin, which is closely related to the ezrin, radixin, and moesin (ERM) proteins of the band 4.1 protein superfamily. Mutations of the *NF2* gene cause an autosomal dominant disorder neurofibromatosis type 2 (NF2). Merlin's function as a growth suppressor depends on its structural conversion from an inactive to an active form caused by changes in its phosphorylation status. Depending on its structural conformation Merlin binds to numerous interacting proteins, which are either required for Merlin's tumour suppressor function or impair Merlin's growth suppressor activity contributing to tumorigenesis.

Despite significant progress made in the NF2 study for the last two decade, the molecular mechanisms of the tumor suppressor function of Merlin are still little understood. Loss of the *Nf2* function leads to aberrant activation of receptor tyrosine kinases (RTK) and the downstream mitogenic signaling pathways. Overexpression of ErbB receptors has been reported in NF2-related and sporadic vestibular schwannomas (VS) and many other human cancers. Studies have shown that inhibition of the ErbB family RTKs can serve as an alternative approach for the treatment of sporadic and NF2-related VS through inhibition of ERK1/2 and PI3K/AKT signaling pathways. Preclinical and clinical studies of the potential therapeutic targets for the treatment of VS, and other brain tumors are underway. A better understanding of Merlin's deregulated signaling in NF2 can provide useful therapeutic strategies for treatment of human VS and other brain tug mors.

Key words: Neurofibromatosis type 2, NF2, Merlin, vestibular schwannoma, receptor tyrosine kinases.

Introduction

Neurofibromatosis type 2 (NF2) is bilateral acoustic neurofibromatosis, a dominantly inherited autosomal disorder associated with the development of nervous system tumors [1]. The *Nf2* gene encodes for Merlin (for moesin, ezrin, radixin-like protein), a member of the band 4.1 superfamily of membrane-associated proteins [2]. Merlin is implicated in diverse processes at different stages of development and is critical for embryonic development of different cell types [3]. Loss of *Nf2* function was lethal for embryonic mice, while heterozygous *Nf2*-mutant mice developed metastatic tumors [4]. The *Nf2* disfunction in the liver resulted in an expansion of progenitor cells, suggesting that Merlin is involved in regulation of stem-cell renewal [5; 6]. Numberous studies have shown that Merlin functions as a negative regulator of cell growth and proliferation [7; 8]. Mutation in the *Nf2* leads to the development of the nervous system tumors, such as schwannomas, meningiomas, and ependymomas [4; 9], as well as cancers of non-nervous system, mainly mesotheliomas [10], glioblastomas [11] and in rare cases to other solid tumors [12]. In addition, sporadic non-germline loss of *NF2* function has been observed nearly in all vestibular schwannomas, meningiomas, and to a lesser extends in ependymomas.

The band 4.1 superfamily proteins are cytoskeletal linker proteins, which are involved in the cytoskeleton organization. Merlin has high homology with the ERM (for ezrin, radixin, moesin) family proteins and shares a common structural organization: the global N-terminal FERM (fourpoint-one, ERM) domain (NTD), the central α-helical domain and the C-terminal domain (CTD) (Figure 1). In contrast to other ERM family proteins, Merlin lacks the actin-binding motif at the CTD region. Despite the struc-

tural similarities, Merlin is the only protein of this family, which possesses growth-suppressive activity. The *Nf2* gene encodes two isoforms such as Merlin (or Merlin-1), which has the CTD, and Merlin-2, which lacks the CTD. The isoform 1 contains exon 17 and lacks exon 16, while the isoform 2 contains exon 16, followed by a termination codon that prevents the translation of exon 17. It has been generally accepted that the isoform 2 does not possess the tumor suppressor activity. Nevetheless, studies have shown that both isoforms possess the tumor suppressor activity [13]. Most of mutations within the FERM domain lead to cell proliferation and tumorigenesis. This indicates that the FERM domain in Merlin is crucial for contact inhibition and tumor suppression. It was believed that Merlin acquired tumor suppressive activity, by adopting a closed growth-suppressive conformation through the intramolecular association of its NTD and the CTD [14]. However, subsequent studies have revealed a more complex regulation of Merlin's growth suppressive function, which will be discussed in this review.

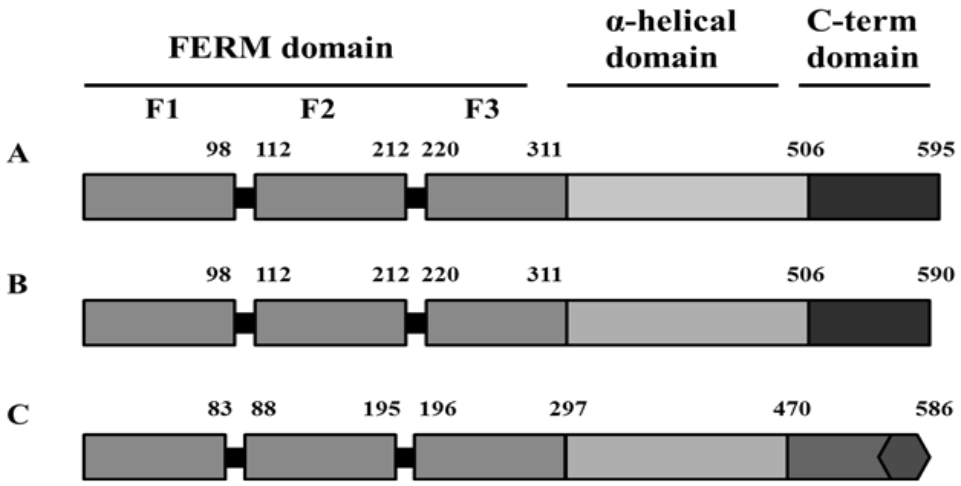

Figure 1 – The structure of the ERM family is composed of three structural regions an amino terminal domain (FERM), an α-helix domain, and a carboxyl terminal domain (CTD). The FERM domain consists of the three sub-domains F1, F2 and F3. The two Merlin isoforms. A - Isoform 1 (Merlin or Merlin-1), and B - Isoform 2 (Merlin-2). C – The ERM family proteins share high homology with Merlin and contain F-actin region at the end of the CTD, which is absent in Merlin.

Merlin is localized at the cortex and contact-dependent membrane domains to organize cell junctions [7]. The "Blue box motif", the conserved region corresponding to residues 177-183 in the F2 subdomain of the FERM domain has been shown to be critical for Merlin growth suppressive function. Merlin's association with actin is not required for growth inhibition, but is necessary for its localization at the plasma membrane in the phosphorylated, so-called dormant state. Loss of Merlin's growth suppressive function results in an impairment of contact-dependent inhibition of proliferation and formation of stable adherens junctions (AJs). It has been shown that Merlin forms an association with adhesion proteins and other AJ components and controls the cadherin-mediated formation of cell-cell adhesions. Cadherins maintain AJs between adjacent cells via interaction with intracellular proteins such as catenins and the actin cytoskeleton. Thus, the main functions of Merlin include contact inhibition of proliferation and tumor suppression.

Merlin's tumor suppressor activity is regulated by phosphorylation

The structural transformation of Merlin from an inactive to an active state is regulated by changes in its phosphorylation status. Recent studies have resolved the contradiction between the structure and function of Merlin. Classical studies considered that dephosphorylated Merlin functions as a tumor suppressor in a closed conformation. However, recent studies have shown that phosphorylated or mutated Merlin has a more closed form, leading to impaired growth inhibition, while more open forms have active growth inhibiting activity [13; 15]. Merlin can be inacti-

vated by phosphorylation at serine 518 by the p21-activated protein kinases (PAKs) or by the cAMP-dependent protein kinase A (PKA). PAKs belong to a serine/threonine protein kinase family, which are involved in the Rac/Cdc42 signaling pathway. It has been shown that PAK1 phosphorylates Merlin on serine 518 and abolishes its growth suppressor activity [16]. In turn, Merlin can inhibit PAK1 in a contact-independent manner preventing its activation by Rac [17]. In addition, it was shown that cadherin inactivates PAK, which implies contact-independent activation of PAK [18]. Phosphorylation on serine 518 disrupts Merlin association with the actin cytoskeleton, resulting in Merlin intracellular relocalization from the plasma membrane to the cytoplasm [19]. In addition, phosphorylation of Merlin at serine 518 disrupts its interaction with the integral membrane hyaluronan receptor CD44 [20] and hepatocyte growth factor-regulated tyrosine kinase substrate HRS [21], which impairs Merlin's growth suppressive activity. The binding of Merlin to CD44 is associated with hypophosphorylation of Merlin and growth inhibition, while the ERM proteins, competing with Merlin for CD44 binding, prevent the growth suppressive activity of Merlin and contribute to tumorigenesis.

PKA has been shown to phosphorylate Merlin at serine 518 [22]. It has been suggested that phosphorylation of Merlin at serine 518 can convert Merlin into a growth-permissive form through heterodimerization between Merlin and ezrin, while serine 10 phosphorylation plays a role in the cytoskeletal organization and cell motility. Activation of cAMP/PKA signaling leads to growth proliferation and cell cycle progression in Schwann cells. Conversely, dephosphorylation of serine 518 by MYPT-1-PP1δ restores Merlin tumor suppressive function [20; 23].

The serine/threonine kinase AKT, also known as protein kinase B (PKB), is regulated by phosphorylation at threonine 308 by phosphoinositide-dependent kinase 1 (PDK-1) and is fully activated by additional phosphorylation at serine 473 [24]. AKT has been shown to phosphorylate Merlin at threonine 230 and serine 315, which abolishes Merlin tumor suppressor activity leading to the degradation of Merlin through polyubiquitination [25]. In turn, Merlin suppresses PI3K/AKT signaling through direct binding to PIKE-L. Studies have demonstrated that phosphorylation of Merlin on serine 10 by AKT leads to Merlin targeting for ubiquitination by the E3 ubiquitin-protein ligase complex and subsequent proteasome-mediated degradation [26]. This requires multistep phosphorylation of Merlin on serine 318 by PAK or PKA and subsequent phosphorylation on serine 10 by PKA that leads to a fully open conformation of Merlin resulting in its degradation and ubiquitination. It has been suggested that Merlin phosphorylation on serine 10 by hyperactivated AKT occurs in malignant cells, which leads to Merlin degradation and consequent activation of the PI3K/AKT signaling pathway. Jacob and co-workers have shown that AKT phosphorylation at the serine 308 and threonine 473 sites promoted cell growth and proliferation, indicating activation of the PI3K/AKT signaling pathway in HMS-97 cells and Schwannoma vestibular cells [27]. Although Merlin's tumor suppressor function has been shown to depend on its conformation and phosphorylation status, it is possible that multiple mechanisms may modulate Merlin's growth suppressive activity.

Receptor tyrosine kinases in NF2 signaling

Receptor tyrosine kinases (RTKs) are implicated in regulation of the Ras/Raf/MEK/ERK and PI3K/AKT signaling pathways. The ErbB family of receptor tyrosine kinases (RTKs) is a family of transmembrane RTKs, including epidermal growth factor receptor (EGFR), ErbB2/HER2, ErbB3, and ErbB4. RKTs are implicated in cell differentiation and proliferation in Schwann cells and expressed in both vestibular nerve and VS. The EGFR activation starts by binding its specific ligands, such as epidermal growth factor (EGF) and transforming growth factor α (TGF α) to activate Ras/MAPK signaling pathway. Upon ligand binding, RTK inactive monomers activate their cytoplasmic tyrosine kinase domain by dimerization. Merlin inhibits Src binding to ErbB2 and consequently ErbB2-mediated phosphorylation, which prevents downstream mitogenic signaling [28].

Merlin regulates cell-to-cell contact inhibition of proliferation by regulating the accumulation of EGFR, ErbB2, ErbB3, PDGFR and IGF1R growth factors at the plasma membrane in Schwann cells [8; 29]. Activation of ErbB receptors has been linked to increased proliferation, and consequently to the downstream mitogenic signaling [29]. Overexpression of ErbB receptors has been reported in many other human cancers such as human breast and ovarian cancers, as well as transitional cell carcinoma of the bladder [30; 31].

Current study has shown activation of ErbB receptors in human VS and paired normal vestibular nerves using phospho-RTK arrays [32]. Activation and aberrant signaling of ErbB receptors, such as ErbB3 and to a lesser extend activation of EGFR, ErbB2 and ErbB4 have been observed in VS tumors compared to the normal vestibular nerve from the

same patients. High levels of EGFR phosphorylation have been observed compared to the normal Schwann cells in primary VS culture and human malignant schwannoma HMS-97 cells. In addition, fibroblast growth factor receptor-2α (FGFR-2α), insulin receptor, macrophage-stimulating protein receptor (MSPR), PDGFR-β, C-RET, and Ephrin type-A4 receptor (EphA4) were upregulated in VS compared to the paired vestibular nerve. Other studies have shown activation of EGFR and ErbB2 in VS and Schwann cells [33; 34]. Lallemand and coworkers have observed activation of ErbB2, ErbB3, insulin-like growth factor 1 receptor (IGF1R), and platelet-derived growth factor receptor-β (PDGFR-β) at the plasma membrane in Merlin-deficient confluent but not sub-confluent Schwann cells [29]. The level of EGF was elevated in all NF2-related VS, but not in the sporadic VS, while ErbB ligand was elevated in most of sporadic VS but only in few NF2-related VS [33]. Activation of FGFR and PDGFR has been linked to VS growth and progression [35]. The *NF2* gene overexpression inhibits schwannoma cell proliferation through promoting PDGFR degradation [36]. Thus, inhibition of RTK aberrant signaling can serve as a potential therapeutic strategy for the treatment of nervous system tumors and other tumors. Therapeutic approaches to the treatment of sporadic and NF2-related VS, as well as other brain tumors will be discussed in the latter part of this review.

Merlin regulates numerous signaling pathways

It was previously reported that Merlin is localized on the plasma membrane through the FERM NTD and is associated with microtubules and the cortical actin cytoskeleton [13]. Mutations in the NTD impair the interaction of Merlin with the actin-cytoskeleton, which leads to its translocation from the plasma membrane into the cytoplasm [37]. It has been generally accepted that changes in Merlin's localization at the plasma membrane disrupts Merlin's suppression of mitogenic signaling and cause the development of NF2 tumors. Later studies have shown that Merlin's tumor suppressor function does not require its association with the actin cytoskeleton [13; 37]. At the plasma membrane, integrins bind to intracellular matrix components and form a multiprotein complex consisting of RTK, growth factor receptor-bound protein 2 (Grb2), SOS, ERM-actin and Ras [38]. The ERM proteins serve as a scaffold, promoting Ras activation and signaling. Merlin suppresses a variety of signaling pathways by regulating integrins and tyrosine receptor kinases (RTKs) and the downstream mitogenic signaling of Ras/Raf/MEK/ERK [20], Rac/PAK/JNK [17; 19], PI3K-Akt [25; 26], mTORC1 [9], FAK-Src [10], Wnt/b-catenin [39] and the EGFR-Ras-ERK pathway [8].

Studies reveal interaction of Merlin with numerous proteins, which can affect Merlin growth suppressor function (Table 1). It has been reported that many putative binding partners interact with Merlin including proteins involved in translation, cell-cycle transit, cytoskeletal organization, and signaling [40]. Merlin regulates cell growth and proliferation through an interaction with proteins of focal adhesion junctions [7], actin [13], βII-spectrin [40], microtubules [41], CD44 [20], HRS [21], PIKE-L [42], eIF3c [40], paxillin [43], VprBP [44] (also known as DCAF1), angiomotin [45] and other proteins. As described above, Merlin interacts with several protein kinases, including PAK, PKA, AKT and phosphatase MYPT-1-PP1δ. The phosphatase MYPT-1-PP1δ dephosphorylates Merlin and restores Merlin's antiproliferative function by inhibiting Ras-dependent signaling pathway. The inhibition of MYPT-1-PP1δ with the oncoprotein CPI-17 can induce phosphorylation of ERM proteins and Ras activation [20; 23].

Using coimmunoprecipitation, phosphoprotein enrichment, and liquid chromatography coupled with tandem mass spectrometry (LC-MS/MS), several proteins interacting with Merlin have been identified, most of which belong to DNA and chromatin function group, DNA damage response (DDR) proteins, DNA replication and transcription (Davletova et al., unpublished data). Some of these proteins have been reported to be involved in various types of cancer and can serve as both diagnostic and prognostic biomarkers of cancer. Further research is needed to better understand the role of proteins interacting with Merlin in human VS and other types of brain tumors.

In addition to Merlin's localization at the cell cortex and the contact-dependent membrane, Merlin plays a role in the cytoplasm. In the cytoplasm, Merlin associates with actin and tubulin and regulates the dynamics of the cytoskeleton and vesicular transport [13]. Recently, Merlin's tumor suppressor activity has been shown in the nucleus [37]. The FERM domain of Merlin has been reported to be necessary for its nuclear localization. The dephosphorylated form of Merlin, which, as has been demonstrated, has an tumor suppressive activity, is preferentially localized in the nucleus. In the nucleus, Merlin directly interacts with $CRL4^{DCAF1}$E3 ubiquitin ligase leading to suppression of oncogenic signaling [37; 45]. Merlin inhibition of $CRL4^{DCAF1}$E3 ubiquitin ligase is linked

to its tumor suppressor function in contact-inhibited cells. Indeed, mutations abolishing Merlin-DCAF1 binding lead to disruption of nuclear localization and subsequently to tumorigenesis. It has been shown that Merlin's binding to the E3 ubiquitin ligase component DCAF1 has been abolished after serine 10 phosphorylation, resulting in Merlin's targeting to proteasome-mediated degradation [26]. Therefore, Merlin is involved in various signaling pathway and can play different roles during cell development and tumorigenesis. The mechanisms that regulate Merlin's function as a cell growth suppressor still need to be better understood in order to develop effective therapeutic approaches for the treatment of numerous destructive and debilitating tumors of the nervous system.

Table 1 – Proteins interacting with Merlin and the sites of interaction on Merlin extended to the NTD and/or CTD regions (see references in [40] if not shown otherwise; ND – not identified)

Protein	NTD	Protein	CTD
Protein kinases/phosphotases affecting Merlin suppressive actiivity			
PAK1 [16; 17]	1-313		
PKA [22]	ND		
MYPT-1-PP1δ [23]	312-341		
Structural proteins supporting Merlin suppressive activity			
Microtubules	122-302	βII-spectrin	469–590
Actin	178-367		
Growth activators suppressed by Merlin			
CD44	1-50	TRBP	288-595
RalGDS	1-228	HEI10	306-339
eIF3c	1-304	EG1/Magicin	340–590/595
Ezrin	1-313	Syntetin	566-595
Radixin	ND	Angiomotin [45]	ND
Moezin	1-332		
Layilin	1-332		
PIKE-L [42]	1-332		
NHERF	1-332		
N-WASP	1-332		
RhoGDI	1-341		
VprBP [44]	ND		
Growth inhibitors supporting Merlin suppressive activity			
RhoGDI	1–341	HRS [21]	453–557
NGB	1–52; 288–344		
DCC	1–341		
MAP	288–595		
Paxillin [43]	50–70; 425–450		
Proteins interacting with Merlin with unclear effect			
Myelination	1–314	RIβ	463–480
SCHIP-1	1–27; 280–323	CRM1/exportin	539–551

Therapeutic strategies for the treatment of VS and other brain tumors

Currently, there are no medical therapies available for the treatment of NF2-related and sporadic VS and other nervous system tumors. The current standard of treatment remains local tumor control by surgical excision and stereotactic radiation, which can often cause complications from damage to nervous and CNS structures [4]. Moreover, radiation treatment can lead to malignant transformation and elevated growth of tumors [46]. Merlin plays a role as a cell growth suppressor and interacts with a number of proteins involved in various signaling pathways. Deregulation of one of the components in these signaling pathways can cause tumor formation. Targeted small molecule inhibitors may serve as potent therapeutic agents for the treatment of these tumours.

The PI3K/AKT signaling pathway is deregulated in VS and other tumors. A novel celecoxib-derivative OSU-03012 (developed by Dr. C.-S. Chen at Ohio State University, also called AR-12) lacking cyclooxygenase (COX2) inhibitory activity has been tested in several types of cancer cells [24] and is currently undergoing Phase I clinical trial as an anticancer agent in patients with solid and liquid tumors. The mechanism of OSU-03012 is partly modulated via direct inhibition of 3-phosphoinositide-dependent protein kinase-1 (PDK-1) within the PI3K/AKT pathway. Another anticancer mechanism of OSU-03012 involves endoplasmic reticulum (ER) stress signaling via activation of PKR-like ER kinases (PERK), downregulation of HSP70 family chaperone GRP78/BiP/HSPA5, and a caspase-independent, cathepsin-dependent autophagy-dependent form of cell death [47]. It has been shown that activation and phosphorylation of AKT has been linked to cell proliferation and VS tumor formation [48]. A dose-dependent inhibition of cell proliferation and apoptosis induced by OSU-03012 was observed both in benign human VS and malignant schwannoma cells, as well as mouse Nf2-deficient Schwann and schwannoma cells. OSU-03012 potent anti-tumor activity was demonstrated in malignant schwannoma xenografts in SCID mice.

Current study revealed aberrant activation of ErbB family RTKs in human VS [32]. The treatment with EGFR inhibitor Erlotinib and EGFR/ErbB2 inhibitor Lapatinib inhibited cell proliferation in VS and schwannoma cells. Erlotinib treatment was more potent in growth inhibition compared to Lapatinib and resulted in a decreased level of phospho-ErbB receptors including EGFR in primary VS, as well as ErbB3, and ErbB4 in human malignant schwannoma cells. Although Lapatinib was not very potent in inhibiting cell growth, it is possible that the combined action of this inhibitor with OSU-03012 might provide a better outcome and is currently being tested. Several studies have demonstrated the application of RTK inhibitors as an effective therapeutic approach for the treatment of human VS and other nervous system tumors [33; 34]. The treatment with OSU-03012 and the inhibitor of ERBB1/2/4, Lapatinib, or the HSP90 inhibitor 17-N-Allylamino-17-demethoxygeldanamycin (17AAG) reduced expression of ERBB1/2/4 growth factor receptors in glioblastoma and medulloblastoma cells [47]. Therefore, targeting ERBB growth factor receptors could reduce cell proliferation through inhibition of ERK1/2 and PI3K/AKT signaling pathways.

Preclinical and clinical studies of the potential therapeutic targets, such as lapatinib, everolimus, erlotinib and bevacizumab have been reported for the treatment of VS, NF2 and other brain tumors [49-51]. Other potential targets for therapeutic strategies include inhibitors of small GTP binding proteins, and GTPases that can inhibit Ras, Rac, and MAPK signaling pathways and have been used for certain types of cancer. Several PAK inhibitors have been tested and may be useful for treating VS and NF2 related tumors [52; 53]. The inhibition of mTORC1 signaling had a direct inhibitory effect on VS growth. The Phase II study of mTORC1 inhibition by everolimus has shown delayed growth of NF2-schwannomas [54]. A better understanding of deregulated signal transduction pathways is crucial in exploring therapeutic options and preclinical testing of effective chemical agents for treating tumors of the nervous system.

Conclusion

Merlin negatively regulates cell growth and proliferation and is involved in multiple signaling pathways. It has been shown aberrant activation of ErbB family receptor tyrosine kinases (RTK) in human VS. Current study has shown that inhibition of receptor tyrosine kinases can serve as an alternative approach for the treatment of sporadic and NF2-related VS. Other potential targets for therapeutic strategies include chemical agents that can inhibit deregulated mitogenic pathways such as Ras, Rac, and MAPK signaling pathways. A better understanding of the mechanisms underlying VS tumorigenesis can help to develop novel potent, effective and non-toxic chemical agents to supress tumor growth and metastasis. Several preclinical and clinical trials are

underway as the potential therapeutic targets for the treatment of VS and NF2-related tumors.

Acknowledgment

I wish to express my sincere thanks to Drs. D. Bradley Welling and Long-Sheng Chang for their mentorship and financial support from the Department of Otolaryngology-Head and Neck Surgery, Ohio State University and the Center for Childhood Cancer, the Research Institute at Nationwide Children's Hospital, Columbus, Ohio, USA.

References

1. Evans D.G., Sainio M., Baser M. E. (2000) Neurofibromatosis type 2. *J. Med. Genet.*, vol. 37, pp. 897-904.

2. Rouleau G.A., Merel P., Lutchman M., Sanson M., Zucman J. et al. (1993). Alteration in a new gene encoding a putative membrane organizing protein causes neuro-fibromatosis type 2. *Nature*, vol. 363, pp. 515-521.

3. Evans D.G., Huson S.M., Donnai D., Neary W., Blair V. et al. (1992) A genetic study of type 2 neurofibromatosis in the United Kingdom. I. Prevalence, mutation rate, fitness, and confirmation of maternal transmission effect on severity. *J Med Genet.*, vol. 29, pp. 841-846.

4. Gutmann D.H., Giovannini M. (2002) Mouse models of neurofibromatosis 1 and 2. *Neoplasia*, vol. 4, no. 4, pp. 279-290.

5. Larsson J., Ohishi M., Garrison B., Aspling M., Janzen V. et al. (2008) Nf2/merlin regulates hematopoietic stem cell behavior by altering microenvironmental architecture. *Cell Stem Cell*, vol. 3, pp. 221-227.

6. Benhamouche S., Curto M., Saotome I., Gladden A.B., Liu C.-H. et al. (2010) Nf2/merlin controls progenitor homeostasis and tumorigenesis in the liver. *Genes Dev.*, vol. 24, pp. 1718-1730.

7. Lallemand D., Curto M, Saotome I., Giovannini M., McClatchey A.I. (2003) NF2-deficiency promotes tumorigenesis and metastasis by destabilizing adherens junctions. *Genes Dev.*, vol. 7, pp. 1090-1100.

8. Curto M., Cole B. K., Lallemand D., Liu C., McClatchey A. I. (2007) Contact-dependent inhibition of EGFR signaling by Nf2/merlin. *J Cell Biol.*, vol. 177, pp. 893-903.

9. James M.F., Han S., Polizzano C., Plotkin S.R., Manning B.D. et al. (2009) NF2/Merlin is a novel negative regulator of mTOR complex 1, and activation of mTORC1 is associated with meningioma and schwannoma growth. *Mol and Cell Biol.*, vol. 29, no. 15, pp. 4250-4261.

10. Poulikakos P. I., Xiao G. H., Gallagher R., Jablonski S., Jhanwar S. C. et al. (2006) Re-expression of the tumor suppressor NF2/Merlin inhibits invasiveness in mesothelioma cells and negatively regulates FAK. *Oncogene*, vol. 25, pp. 5960-5968.

11. Guerrero P.A., Yin W., Camacho L., Marchetti D. (2015) Oncogenic Role of Merlin/NF2 in Glioblastoma. *Oncogene*, vol. 34, no. 20, pp. 2621-2630.

12. Morrow K.A., Das S., Metge B.J., Ye K., Mulekar M.S. et al. (2011) Loss of tumor suppressor Merlin in advanced breast cancer is due to post-translational regulation. *J Biol Chem.*, vol. 286, pp. 40376-40385.

13. Lallemand D., Saint-Amaux A.L., Giovannini M. (2009a) Tumor-suppression functions of merlin are independent of its role as an organizer of the actin cytoskeleton in Schwann cells. *J Cell Sci.*, vol. 122, pp. 4141-4149.

14. Gutmann D.H., Geist R.T., Xu H., Kim J.S., Saporito-Irwin S. (1998) Defects in neurofibromatosis 2 protein function can arise at multiple levels. *Hum Mol Genet.*, vol. 7, no. 3, pp. 335-345.

15. Sher I., Hanemann C.O., Karplus P.A., Bretscher A. (2012) The tumor suppressor merlin controls growth in its open state, and phosphorylation converts it to a less-active more-closed state. *Dev Cell.*, vol. 22, pp. 703-705.

16. Kissil J.L., Johnson K.C., Eckman M.S., Jacks T. (2002). Merlin phosphorylation by p21-activated kinase 2 and effects of phosphorylation on merlin localization. *J Biol Chem.*, vol. 277, pp. 10394-10399.

17. Kissil J.L., Wilker E.W., Johnson K.C., Eckman M.S., Yaffe M.B. et al. (2003). Merlin, the product of the Nf2 tumor suppressor gene, is an inhibitor of the p21-activated kinase, Pak1. *Mol Cell.*, vol. 12, pp. 841-849.

18. Okada T., Lopez-Lago M., Giancotti F. G. (2005) Merlin/NF-2 mediates contact inhibition of growth by suppressing recruitment of Rac to the plasma membrane. *J Cell Biol.*, vol. 171, pp. 361-371.

19. Shaw R.J., Paez J.G., Curto M., Yaktine A., Pruitt W.M. et al. (2001) The Nf2 tumor suppressor, merlin, functions in Rac-dependent signaling. *Dev Cell.*, vol. 1, pp. 63-72.

20. Morrison H., Sherman L.S., Legg J., Banine F., Isacke C. et al. (2001) The NF2 tumor suppressor gene product, merlin, mediates contact inhibition of growth through interactions with CD44. *Genes Dev.*, vol. 15, pp. 968-980.

21. Scoles D.R., Huynh D.P., Chen M.S., Burke S.P., Gutmann D.H. et al. (2000) The neurofibromatosis 2 tumor suppressor protein interacts with hepatocyte growth factor-regulated tyrosine kinase substrate. Hum Mol Genet., vol. 9, no. 11, pp. 1567-1574.

22. Alfthan K., Heiska L., Grönholm M., Renkema G.H., Carpén O. (2004). Cyclic AMP-dependent protein kinase phosphorylates merlin at serine 518 independently of p21-activated kinase and promotes merlin-ezrin heterodimerization. J Biol Chem., vol. 279, pp. 18559-18566.

23. Jin H., Sperka T., Herrlich P., Morrison H. (2006) Tumorigenic transformation by CPI-17 through inhibition of a merlin phosphatase, Nature, vol. 442, pp. 576-579.

24. Zhu J., Huang J.W., Tseng P.H., Yang Y.T., Fowble J. et al. (2004) From the cyclooxygenase-2 inhibitor celecoxib to a novel class of 3-phosphoinositide-dependent protein kinase-1 inhibitors. Cancer Res., vol. 64, pp. 4309-4318.

25. Okada M., Wang Y., Jang S.-W., Tang X., Neri L.M. et al. (2009) Akt Phosphorylation of Merlin Enhances Its Binding to Phosphatidylinositols and Inhibits the Tumor-Suppressive Activities of Merlin. Cancer Res., vol. 69, no. 9, pp. 4043-4051.

26. Laulajainen M., Muranen T., Nyman T.A., Carpen O., Gronholm M. (2011) Multistep phosphorylation by oncogenic kinases enhances the degradation of the NF2 tumor suppressor Merlin. Neoplasia, vol. 13, pp. 643-652.

27. Jacob A., Lee T.X., Neff B.A., Miller S., Welling B. et al. (2008) Phosphatidylinositol 3-kinase/AKT pathway activation in human vestibular schwannoma. Otol Neurotol., vol. 29, pp. 58-68.

28. Houshmandi S.S., Emnett R.J., Giovannini M., Gutmann D.H. (2009) The Neurofibromatosis 2 Protein, Merlin, Regulates Glial Cell Growth in an ErbB2- and Src-Dependent Manner. Mol and Cell Biol., vol. 29, no. 6, pp. 1472-1486.

29. Lallemand D., Manent J., Couvelard A., Watilliaux A., Siena M. et al. (2009b) Merlin regulates transmembrane receptor accumulation and signaling at the plasma membrane in primary mouse Schwann cells and in human schwannomas. Oncogene, vol. 28, pp. 854-865.

30. Bieche I., Onody P., Tozlu S., Driouch K., Vidaud M. et al. (2003) Prognostic value of ERBB family mRNA expression in breast carcinomas. Int J Cancer, vol. 106, pp. 758-765.

31. Junttila T.T., Laato M., Vablberg T., Soderstrom K.O., Visacorpi T. et al. (2003) Identification of patients with transitional cell carcinoma of the bladder overexpressing ErbB2, ErbB3, or specific ErbB4 isoforms: real-time reverse transcription-PCR analysis in estimation of ErbB receptor status from cancer patients. Clin Cancer Res., vol. 9, pp. 5346-5357.

32. Bush M. L., Burns S. S., Oblinger J., Davletova S., Chang L.-S. et al. (2012) Treatment of Vestibular Schwannoma Cells with ErbB Inhibitors. Otol. Neurotol., vol. 33, no. 2, pp. 244-257.

33. Doherty J.K., Ongkeko W., Crawley B., Andalibi A., Ryan A.F. et al. (2008) ErbB and Nrg: potential molecular targets for vestibular schwannoma pharmacotherapy. Otol Neurotol., vol. 29, pp. 50-57.

34. Ammoun S., Cunliffe C.H., Allen J.C., Chiriboga L., Giancotti F.G. et al. (2010) ErbB/HER receptor activation and preclinical efficacy of lapatinib in vestibular schwannoma. Neuro Oncol., vol. 12, pp. 834-843.

35. Ammoun S., Flaiz C., Ristic N., Schuldt J., Hanemann C.O. (2008) Dissecting and targeting the growth factor-dependent and growth factor-independent extracellular signal-regulated kinase pathway in human schwannoma. Cancer Res., vol. 68, pp. 5236-5245.

36. Fraenzer J.T., Pan H., Minimo Jr. L., Smith G.M., Knauer D. et al. (2003). Overexpression of the NF2 gene inhibits schwannoma cell proliferation through promoting PDGFR degradation. Int J Oncol., vol. 23, pp. 1493-1500.

37. Cooper J., Giancotti F.G. (2014) Molecular insights into NF2/Merlin tumor suppressor function. FEBS Lett., vol. 588, no. 16, pp. 2743-52.

38. Sperka T., Geißler K.J., Merkel U., Scholl I., Rubio I. et al. (2011) Activation of Ras Requires the ERM-Dependent Link of Actin to the Plasma Membrane. PLoS One, vol. 6, no. 11, e27511.

39. Bosco E.E., Nakai Y., Hennigan R.F., Ratner N., Zheng Y. (2010) NF2-deficient cells depend on the Rac1-canonical Wnt signaling pathway to promote the loss of contact inhibition of proliferation. Oncogene, vol. 29, pp. 2540-2549.

40. Scoles D.R. (2008) The merlin interacting proteins reveal multiple targets for NF2 therapy. Biochim Biophys Acta, vol. 1785, no. 1, pp. 32-54.

41. Muranen T., Grönholm M., Lampin A., Lallemand D., Zhao F. et al. (2007) The tumor suppressor merlin interacts with microtubules and modulates Schwann cell microtubule cytoskeleton. Hum Mol Genet., vol. 16, no. 14, pp. 1742-1751.

42. Rong R., Surace E.I., Haipek C.A., Gutmann D.H., Ye K. (2004). Serine 518 phosphorylation modulates merlin intramolecular association and binding to critical effectors important for NF2 growth suppression. Oncogene, vol. 23, pp. 8447–8454.

43. Fernandez-Valle C., Tang Y., Ricard J., Rodenas-Ruano A., Taylor A. et al. (2002) Paxillin binds schwannomin and regulates its density-dependent localization and effect on cell morphology. *Nat. Genet.*, vol. 31, pp. 354–362.

44. Huang J., Chen J. (2008) VprBP targets Merlin to the Roc1-Cul4A-DDB1 E3 ligase complex for degradation. *Oncogene*, vol. 27, pp. 4056-4064.

45. Yi C., Troutman S., Fera D., Stemmer-Rachamimov A., Avila J.L. (2011) A tight junction-associated Merlin-angiomotin complex mediates Merlin's regulation of mitogenic signaling and tumor suppressive functions. *Cancer Cell*, vol. 19, pp. 527–40.

46. Balasubramaniam A., Shannon P., Hodaie M., Laperriere N., Michaels H. et al. (2007) Glioblastoma multiforme after stereotactic radiotherapy for acoustic neuroma: case report and review of the literature. *Neuro-Oncol*., vol. 9, pp. 447–453.

47. Booth L., Cazanave S.C., Hamed H.A., Yacoub A., Ogretmen B. et al. (2012b) OSU-03012 suppresses GRP78/BiP expression that causes PERK-dependent increases in tumor cell killing. *Cancer Biol Ther*., vol. 13, pp. 224-236.

48. Lee T.X., Packer M.D., Huang J., Akhmametyeva E.M., Kulp C.D. et al. (2009) Growth Inhibitory and Anti-Tumour Activities of OSU-03012, a Novel PDK-1 Inhibitor, on Vestibular Schwannoma and Malignant Schwannoma cells. *Eur J Cancer.*, vol. 45, no. 9, pp. 1709-1720.

49. Karajannis M.A., Legault G., Hagiwara M., Ballas M.S., Brown K. et al. (2012) Phase II trial of lapatinib in adult and pediatric patients with neurofibromatosis type 2 and progressive vestibular schwannomas. *Neuro Oncol.*, vol. 14, no. 9, pp. 1163-1170.

50. Karajannis M.A., Legault G., Hagiwara M., Giancotti F.G., Filatov A. et al. (2014) Phase II study of everolimus in children and adults with neurofibromatosis type 2 and progressive vestibular schwannomas. *Neuro Oncol.*, vol. 16, no. 2, pp. 292-297.

51. Ouerdani A., Goutagny S., Kalamarides M., Trocóniz I.F., Ribba B. (2016) Mechanism-based modeling of the clinical effects of bevacizumab and everolimus on vestibular schwannomas of patients with neurofibromatosis type 2. *Cancer Chem Pharmacol.*, vol. 77, no. 6, pp. 1263-1273.

52. Licciulli S., Maksimoska J., Zhou C., Troutman S., Kota S. et al. (2013) FRAX597, a Small Molecule Inhibitor of the p21-activated Kinases, Inhibits Tumorigenesis of Neurofibromatosis Type 2 (NF2)-associated Schwannomas. *J Biol Chem.*, vol. 288, no. 40, pp. 29105-29114.

53. Mercado-Pimentel M.E., Miller C., Rolph D.N., Villalobos E.F., Dunn A.M. et al. (2017) Inhibiting p21-Activated Kinase Induces Cell Death in Vestibular Schwannoma and Meningioma via Mitotic Catastrophe. *Otol Neurotol.*, vol. 38, no. 1, pp. 139-146.

54. Goutagny S., Raymond E., Esposito-Farese M., Trunet S., Mawrin C. et al. (2015) Phase II study of mTORC1 inhibition by everolimus in neurofibromatosis type 2 patients with growing vestibular schwannomas. *J Neurooncol.*, vol. 122, no. 2, pp. 313-320.

IRSTI 68.35.31

[1*]B.N. Doszhanova, [2]S.V. Didorenko, [1]A.K. Zatybekov,
[1]Y.K. Turuspekov, [1]S.I. Abugalieva

[1]Institute of Plant Biology and Biotechnology, Almaty, Kazakhstan
[2]Kazakh Research Institute of Agriculture and Plant Growing, Almalybak, Kazakhstan
*e-mail: sybanbaeva_bota@mail.ru

Analysis of soybean world collection in conditions of south-eastern Kazakhstan

Abstract: The study of the phenotypic variability of the world crop collections in various conditions is an important step for identification of genetic factors (genes, quantitative trait loci), associated with yield and its components in order to increase the effectiveness of genetic and breeding programs. Current paper presents some results from the comparative analysis of the phenotypic data from the soybean world collection (originators – Kazakhstan, Russia, Canada, France, Sweden, Switzerland, Serbia, Belarus, Poland, Ukraine, Moldavia, Bulgaria, Belgium, Czech Republic, Slovakia, USA, China, Japan, Uzbekistan, Kyrgyzstan). The collection consisted of 192 cultivars and lines grown on the experimental plots of the Kazakh Research Institute of Agriculture and Plant Growing (KAZNIIZR, Almalybak v., Almaty region, Kazakhstan) in 2017 and 2018 yy. A number of key yield-associated traits, including plant height, pod insertion height, number of branches, nodules and seeds per plant, yield per plant and thousand seed weight were studied. It was noted that the yield over the two years of trials positively correlated with the above-mentioned traits. The soybean accessions were ranked based on all the studied traits. As a result of the study of the yield components, several high-productive cultivars were identified. Cheremosh (Ukraine), Agassiz (USA), Iskra (Kazakhstan) and Evrika (Kazakhstan) showed high stable results in both years. The obtained results will be used in the genome-wide association study to identify the significant relations between DNA markers and complex quantitative traits to be applied in further genetic and breeding programs.
Key words: soybean, collection, cultivar, yield, correlation, economically valuable traits.

Introduction

Cultivated soybean (*Glycine max* (L.) Merrill) is an annual plant that belongs to the genus *Soya* (*Glycine*), family *Fabaceae*. Due to its rich biochemical composition, soybean is considered as a universal agricultural crop cultivated with the aim of producing food, technical raw materials and feed for livestock [1-3].

World soybean production over the past 10 years has increased by 65%. According to the United States Department of Agriculture (USDA), in 2017 y., 346.9 million tons of soybeans were produced worldwide [4]. The main producers of soybeans are the United States, Argentina and Brazil, whose total output makes around 87% of the world production [5].

The lands under soybean in Kazakhstan increase from year to year. The total sowing area for this crop over the past 10 years has expanded to 129,000 in 2017, compared to 50,000 hectares in 2007. Soybean is grown mostly in Almaty, Kostanay and East Kazakhstan regions with about 83% of this crop grown in Almaty region [6].

The ecological trails of cultivars from different origins have an important role for modern agriculture. A wide range of soybean genotypes with studied traits in conditions of southeastern Kazakhstan is the basis of successful breeding programs. Nowadays more research is being conducted with the aim of upbringing early-maturing and high-protein soybean cultivars for cultivation in northern and eastern regions of the country [7; 8].

For refinement of cultivars with high yield and quality, it is important to consider the variation and association of morphometric and productivity traits [9; 10]. In this regard, the actual aim of this work was to analyze the world soybean collection of local and foreign origins in the conditions of southeast Kazakhstan in 2017 and 2018.

Materials and methods

The experimental material comprised 192 cultivars and lines from different countries of Eastern and Northern Europe (France, Sweden, Switzerland, Serbia, Russia, Belarus, Poland, Ukraine, Moldavia, Bulgaria, Belgium, Czech Republic and Slovakia), North America (Canada, USA), East Asia (China, Japan), Central Asia (Kazakhstan, Uzbekistan, Kyrgyzstan) was studied in conditions of southeast Kazakhstan in 2017 and 2018 [7; 11]. The cultivar (cv.) Zhansaya bred by the Kazakh Research Institute of Agriculture and Plant growing (KAZNIIZR) was involved into the study as a standard cv. for Almaty region [11].

Field experiments were conducted on experimental sites of KAZNIIZR, located at an altitude of 740 meters above the sea level, 43°15' N, 76°54' W. This territory is characterized by the continental climatic conditions: mild and cool winters, cool spring, hot and dry summers, warm and dry fall. The soil cover is represented by light chestnut, loamy, or less often sandy soils [8].

The seeds of soybean accessions were sown in April of 2017 and 2018 according to Dospekhov [13], without any soil fertilizers. Structural analysis was conducted using the guidelines of The State Commission for Variety Testing of agricultural crops [12]. Plants were selected to record the observations during the maturation period, prior to plots harvesting. For each accession the following traits were analyzed: Plant height (PH), cm; Pod insertion height (PIH), cm; Number of branches per plant (NBP); Number of nodules per plant (NNP), No.; Number of seeds per plant (NSP), No.; Yield per plant (YP); Thousand seeds weight (TSW), g [14].

Data processing was performed using Statistical Package for the Social Sciences (SPSS 16.0; https://www.ibm.com/analytics/data-science/predictive-analytics/spss-statisticalsoftware).

Results and discussion

The world soybean collection grown in southeast Kazakhstan (KAZNIIZR) in 2017 and 2018, was analyzed by complex of morphometric and yield traits. Correlation analysis showed significant association between two years of field experience, with Pearson correlation coefficient r= 0.34, P<0.001.

Table 1 represents data showing the variability ranges of the studied traits.

Table 1 – The variability ranges of morphometric and yield-associated traits

Trait	2017			2018		
	Min	Max	Mean	Min	Max	Mean
PH	22.7	132.6	75.8±2.1	21.7	123.8	59.3±1.4
PIH	3.0	26.2	10.1±0.3	2.5	14.4	6.7±0.2
NBP	0.0	3.1	1.4±0.0	0.0	4.8	1.8±0.1
NNP	7.6	26.8	15.1±0.3	6.9	40.0	17.4±0.4
NSP	1.5	103.6	35.2±0.9	15.0	101.8	41.1±1.2
YP	2.5	19.3	10.6±0.3	3.0	30.5	13.8±0.5
TSW	90.0	218.0	159.8±1.4	124.0	268.0	179.0±1.7

Notes: PH – plant height, cm; PIH – pods insertion height, cm; NBP – number of branches per plant; NNP – number of nodules per plant; NSP – number of seeds per plant; YP – seed yield per plant, g; TSW – thousand seed weight, g

Yield per plant (YP) is one of the key components of soybean productivity, which is dependent on the weather and/or agro ecological conditions (~80%) and cultivar's genotype (~20%) [14]. In analyzed collection YP ranged as 2.5-19.3 g in 2017 and 3.0-30.5 g in 2018, with an average of 10.6 and 13.8 g, respectively (Table 1). It was found that the yield of 54% of accessions was higher than in standard cv. Zhansaya in 2017, while about 44% of the collection exceeded standard during the next year (Figure 1).

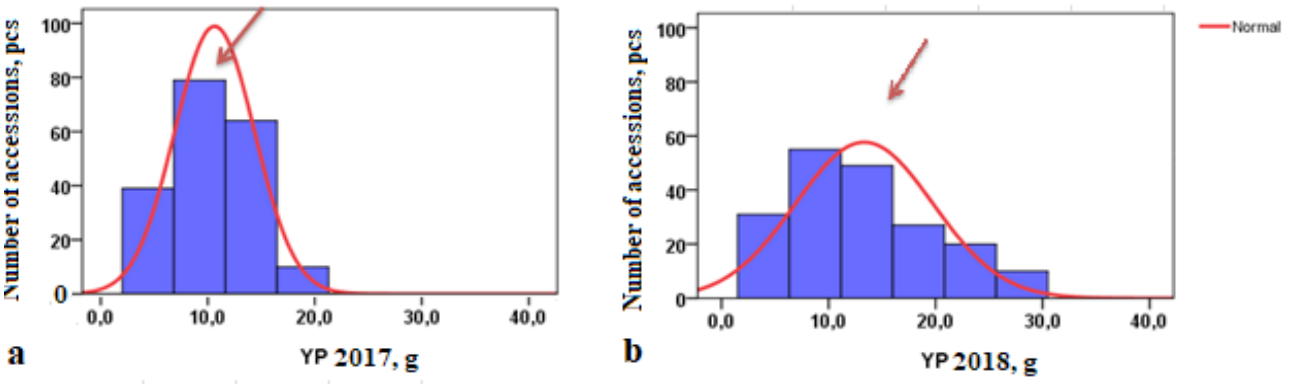

Figure 1 – Distribution of soybean world collection accessions by yield per plant in 2017 and 2018 yy. Note: YP – yield per plant. The arrow indicates the data for the standard cv. Zhansaya

Top ten soybean cultivars with the highest YP values observed in 2017 and 2018 in Almaty region are presented in Table 2. It was observed that cultivars Renta, Agassiz, Cheremosh, Iskra, Ana and Renta had a stable high YP in both years.

Correlation analysis illustrated that yield per plant had positive correlation with all studied traits, particularly with productivity components. Significant correlation with the highest coefficient between YP and the number of seeds per plant, NSP ($r=0.84$, $P<0.001$) and the number of nodules per plant, NNP ($r=0.79$, $P<0.001$) were found (Table 3).

The number of seed per plant (NSP) is also a major component of productivity. This trait is directly related to the yield of soybean [15]. In the first year of field trials, NSP varied from 10 to 103.6 seeds per plant (Table 1), for Zhansaya – 35 seeds per plant, about 46% of the collection showed higher value than standard cv., and among them were Zispida 641 (Belgium) – 103.6, Slavia (Russia) – 93.7, Agassiz (USA) – 62.7, Misula (Kazakhstan) – 61 and Ana (Serbia) – 60 seeds per plant. In the second year, 30% of collections were higher than standard (47.9), including Vesta (Russia) – 101.8, Agassiz (USA) – 96.0, Cheremosh (Ukraine) – 87.5, Vilana (Russia) – 80.2 and Bystritsa 2 (Russia) – 78.0 seeds per plant (Figure 2, a). It was noticed that cultivars Agassiz, Iskra, Zhalpaksai (Kazakhstan) and Vilana showed stable high NSP in both years.

Table 2 – Soybean cultivars with the top ten maximal ranks of yield per plant in 2017 and 2018

Culivar name	YP, g (2017)	Culivar name	YP, g (2018)
Slavia (Russia)	19.3	Evrica (Kazakhstan)	30.5
Agassiz (USA)	19.1	Vilana (Russia)	30.0
Cheremosh (Ukraine)	18.7	Agassiz (USA)	28.9
Misula (Kazakhstan)	18.3	Lira (Russia)	28.7
Iskra (Kazakhstan)	18.2	Renta (Russia)	28.5
Xinjiang D09-676 (China)	17.9	Parker (USA)	27.7
Ana (Serbia)	17.5	Xinjiang D10-130 (China)	27.7
Venera (Serbia)	17.4	Vesta (Russia)	27.6
Renta (Russia)	17.3	Lybid (Ukraine)	26.0
Runo (Russia)	17.3	Xinjiang D11-252 (China)	26.0
Standard cv. Zhansaya	10.1	Standard cv. Zhansaya	13.4

Table 3 – Correlation links between key elements of yield structure

Traits	PH	PIH	NBP	NNP	NSP	YP	TSW
PH	1						
PIH	0.63***	1					
NBP	0.17***	0.09	1				
NNP	0.46***	0.17***	0.77***	1			
NSP	0.52***	0.20***	0.59***	0.86***	1		
YP	0.45***	0.18***	0.48***	0.79***	0.84***	1	
TSW	-0.18***	-0.15***	0.08	0.04	-0.01	0.25***	1

Notes: PH – plant height,cm; PIH – pods insertion height, cm; NBP – number of branches per plant, No.; NFN – number of nodules per plant, No.; NSP – number of seeds per plant, No.; YP – seed yield per plant, g; TSW – a thousand seeds weight, g; *** – P<0.001, ** – P<0.05, * – P<0.01

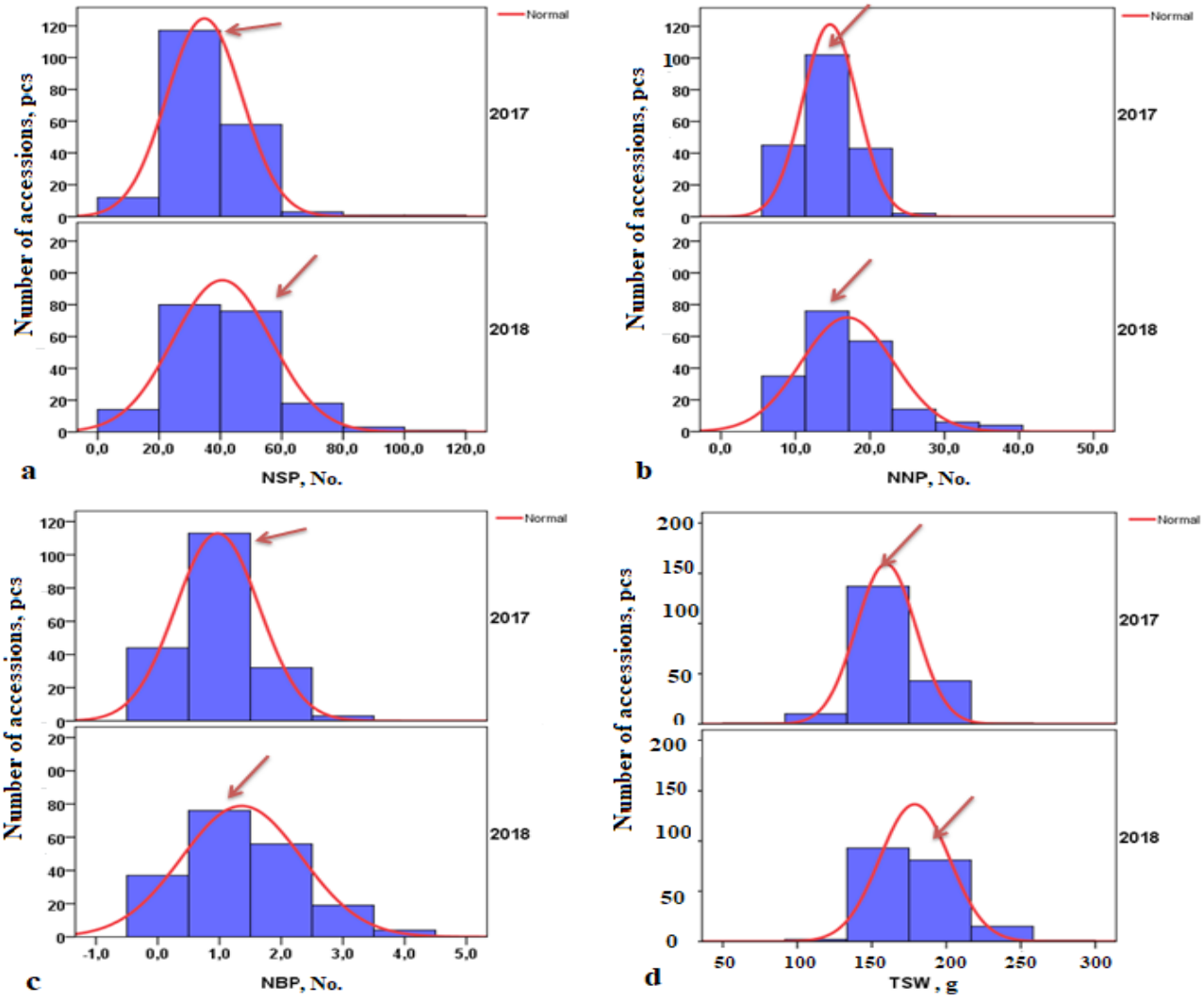

Figure 2 – Distribution of soybean accessions by number of seeds, nodules, and branches per plant and thousand seed weight in 2017 and 2018. Note: NSP – number of seeds per plant; NNP – number of nodules per plant; NBP – number of branches per plant; TSW – thousand seed weight, g. The arrow indicates the data for the standard cv. Zhansaya

The number of nodules per plant (NNP) correlated with all studied traits, except TSW (Table 3). It should be noted, that the NNP values range was higher in 2018 (from 6.9 to 40.0), than in the previous year (7.6 – 26.0), respectively (Table 1, Figure 2, b). The highest NNP values were observed for the following accessions: Evrika (Kazakhstan) – 26.0, Runo (Russia) – 26.8, 362/2 (Eastern Beauty) – 24.3, Niva 70 (Russia) – 23.1 and Misula (Kazakhstan) – 22.9 in 2017, and Agassiz (USA) – 40.0, Vesta (Russia) – 39.1, Cheremosh (Ukraine) – 36.4, Vilana (Russia) – 35.9 and Parker (USA) – 32.3 in 2018. In both years the stable high NNP showed cultivars Iskra, Cheremozh and Agassiz.

The number of branches per plant (NBP) is dependent on plant genotype and environment conditions. In our collection in the second year of field trails soybean plants NBP value increased to 4.5, comparing with 3.5 in 2017 (Figure 2, c). Some researchers, studying the number of branches, believe that the more branches on a plant, the more nodes and beans develop; therefore the higher the seed productivity is. Others consider that it is necessary to breed cultivars with a small number of branches – single-stem cultivars, the productivity of which is increased by rising of the plant density [10; 16]. The results of trails in Almaty region in both years showed that soybean plants with NBP more than one branch per plant had higher value of YP and it is similar to the first point of view. In addition, there was the high significant correlations between NBP and NNP ($r= 0.77$, $P<0.001$), NBP and NSP ($r = 0.59$, $P<0.001$), and NBP with YP ($r=0.48$, $P<0.001$) (Table 3).

The thousand seed weight (TSW) is a very important trait of seed quality, which is dependent on the seed size and fullment. According to the literature, in conditions of water deficiency, genotypes with larger seeds have advantage in high yield production due to their better absorbing ability [15; 17]. In analyzed collection TSW varied from 90.0 to 218.0 g in 2017, and from 124.0 to 268.0 g in 2018 (Table 1). TSW in the first year of field experiments were recorded for Xinjiang a don 1 (China) – 218 g, Soer 345 (Russia) – 211.3 g and Agassiz (USA) – 208 g, in the second year – Almaty (Kazakhstan) – 268 g, Nikko (Serbia) – 255 g and Lambert (USA) – 239.5 g. More than half of the collection exceeded the results of Zhansaya (148.7 and 173 g in 2017 and 2018, respectively) (Figure 2, d).

Correlation analysis of TSW indicated negative correlation with PH. $r=-0.18$, $P<0.001$) and the pod insertion height, PIH, ($r=-0.15$ ($P<0.001$). On the other hand, there was a positive correlation with the yield per plant, $r=0.25$ ($P<0.001$). In addition, correlation was found neither between TSW and NLB, nor TSW and NFN (Table 3).

Plant height (PH) is a major morphometric trait in breeding practice as it linked to the soybean lodging score [18]. PH in analysed accessions varied from 22.7 to 132.6 cm in 2017 and from 21.7 to 123.8 cm in the next year with an average equal to 75.8±2.1 and 59.3±1.4, respectively (Table 1). The standard cv. Zhansaya also showed the tendency of the stem shortening in second year in comparison with the 2017 (99.6 in 2017 vs 77.1 cm in 2018). Determinant, indeterminate and semideterminate types of soybean plant habitat were observed. As it is shown in Fig.3, in 2018 almost the entire soybean collection showed average or short PH, compared with data of 2018 (Figure 3, a).

Another morphometric characteristic used in the field trials was the pod insertion height (PIH). This trait plays an important role in the harvesting period. The higher the first pod insertion, the less likely the soybean stem is to break. Plants with especially low insertion of pod led to loses of seed at harvest. PIH varies from environmental conditions [19; 20].

The standard cv. Zhansaya showed PIH of 13.5 cm and 9.1 cm in 2017 and 2018, respectively. Just 21% and 9.1% of the soybean collection showed higher values than Zhansaya (Figure 3, b). PIH had positive and significant correlation with PH, $r=0.63$ ($P<0.001$) and negative correlation with TSW, $r= -0.18$ ($P<0.001$) (Table 3).

ANOVA analysis (analysis of variance) made it possible to identify significant affect of environmental conditions to all studied traits of soybean collection, with the highest effect on PIH (84.19%), then on TSW (74.62%), PH (41.71%) and YP (34.36%) (Table 4).

It is clear that the weather and growing conditions affect to the grain yield. According to the literature, even with the great combination of genetic resources and agronomic factors, the environmental stresses like high temperature, humidity, salinity and so on, can sharply decrease soybean yield. The stresses negatively effect on the cellular function of plant and its metabolic activity [21]. The soybean varieties and lines harvested in Almaty region in 2018 showed higher results for major productivity components (YP, NSP, NNP, TSW) comparing with 2017, which might be consequented with better environmental conditions during soybean maturation stage in 2018 (Figures 1-3).

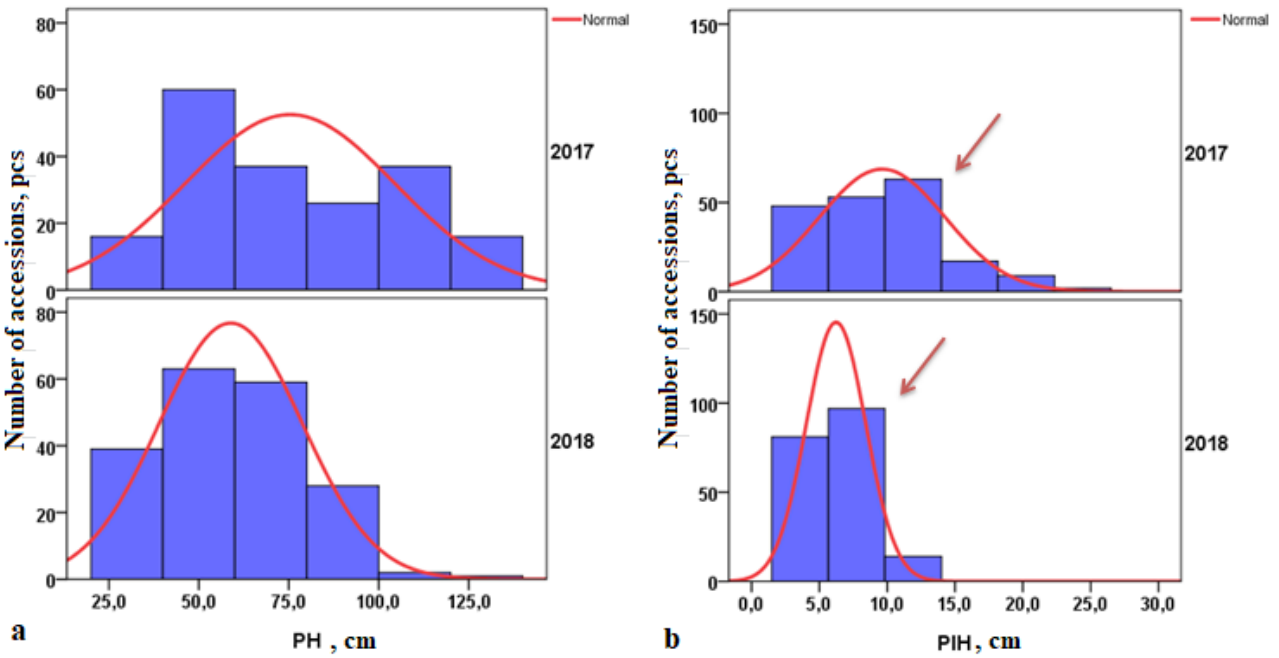

Figure 3 – Distribution of soybean collection by plant height and pod insertion height in 2017, 2018 yy. Note: PH – plant height, PIH – pod insertion height. The arrow indicates the data for the standard cv. Zhansaya

Table 4 – Analysis of variance by one factor

Traits	df	Mean square	F
Plant height (PH), cm	383	26053.5	41.71***
Pods insertion height (PIH), cm	383	1110.4	84.19***
Number of branches per plant (NBP)	383	14.6	20.88***
Number of nodules per plant (NNP)	383	511.0	19.57***
Number of seeds per plant (NSP)	383	3243.3	15.87***
Seed yield per plant (YP), g	383	943.7	34.36***
Thousand seed weight (TSW), g	383	35305.0	74.62***
Note: ***–P<0.001			

Therefore, the world collection of soybean cultivars and lines from Eastern and Northern Europe (France, Sweden, Switzerland, Serbia, Belarus, Poland, Ukraine, Moldavia, Bulgaria, Belgium, Czech Republic, Slovakia), North America (Canada, USA), East Asia (China, Japan), Central Asia (Kazakhstan, Uzbekistan, Kyrgyzstan) countries were tested in Almaty region.

The collection was ranged based on seven yield-associated traits. More valuable highly productive genotypes were revealed. The obtained data may be used in genome-wide association studies and soybean breeding programs.

Conclusion

The world soybean collection consisted of 192 cultivars and lines both local and foreign breeding were evaluated in the field conditions of southeast Kazakhstan in 2017 and 2018. It was determined that the yield per plant had positive correlation with all studied traits, particularly with productivity compo-

nents. Significant association with the highest coefficient were found between traits YP – NSP (r=0.84, P<0.001) and YP – NNP (r=0.79, P<0.001). Over a two years period Cheremosh (Ukraine), Agassiz (USA) and Iskra (Kazakhstan) showed the maximum values for three most important yield traits – yield per plant, number of seeds and nodules per plant. In addition, it was revealed that Kazakh cv. Evrika prevailed on NFN and NLB in both years; while in 2018 it was one of the best on YP. In total, 10 soybean accessions were determined as high-productivity and valuable cultivars for breeding programs.

Obtained results on the phenotypical and productivity traits variability of the world soybean collection will be used in the future genome-wide associations studies in order to identify marker-trait associations and search for reliable links between DNA markers and quantitative traits.

Acknowledgement

This study was conducted within the framework of the project AP05131592 "Genome-wide associations study of resistance to fungal diseases of soybean in Kazakhstan" supported by the Ministry of Education and Science of the Republic of Kazakhstan for 2018-2020 yy.

References

1. Zelencov S.V. (2006) Sovremennoe sostojanie sistematiki kul'turnoj soi Glycine max (L.) Merrill [The current state of systematic soybean taxonomy Glycine max (L.) Merrill]. Scientific and technical bulletin VNIIMK, vol. 1, no. 134, pp. 34-48.

2. Boiko A.T., Karyagin Y.G. (2004) Soja – vysokobelkovaja kul'tura [Soybean high protein culture]. Almaty, 22 p.

3. Chen K.I., Erh M.H., Su N.W., Liu W.H., Chou C.C., Cheng K.C. (2012) Soyfoods and soybean products: from traditional use to modern applications. *Appl Microbiol Biotechnol.*, vol. 96, no. 1, pp. 9-22.

4. Agricultural Market Information System (2019) Market Monitor., no. 66, p. 18.

5. Masuda T., Goldsmith P.D. (2009) World soybean production: area harvested, yield, and long-term projections. IFARM, vol. 12, no. 4, pp. 1-31.

6. Kazahstan ezhegodno narashhivaet ploshhadi posevov soi [online resourse]; https://kapital.kz/economic/70818/kazahstan-ezhegodno-narashivaet-plocshadi-posevov-soi.html (accessed 20.02.2019).

7. Didorenko S.V., Kudaybergenov M.S., Abugalieva S.I., Turuspekov E.K. Priznaki produktivnosti sortoobraztsov skorospeloy kollektsii soi (Glycine max) v usloviyah yugo-vostochnogo Kazahstana. XXth scientific practice conference proceedings, pp. 122-124.

8. Abugalieva S., Didorenko S., Anuarbek S., Volkova L., Gerasimova Y., Sidorik I., Turuspekov Y. (2016) Assesment of soybean flowering and seed maturation time in different latitude regions of Kazakhstan. Public library of science, vol. 11, pp. 1-12.

9. Didorenko S.V. (2014) Dostizheniya selekcionnyh rabot po soe v Kazahstane [Achievements of breeding works on soybeans in Kazakhstan]. *News of NAS RK, Agricultural series*, vol. 1, pp. 22-27.

10. Trunov M.V. (2017) Model' rannespelogo sorta soi dlja Juzhno-evropejskoj chasti Rossii [Model of early ripe soybean variety for the South European part of Russia]. *Scientific and technical bulletin VNIIMK*, vol. 2, no. 170, pp. 27-36.

11. Zatybekov A., Abugalieva S., Didorenko S., Rsaliyev A., Turuspekov Y. (2018) GWAS of a soybean breeding collection from South East and South Kazakhstan for resistance to fungal diseases. *Vavilov Journal of Genetics and Breeding*, vol. 22, no. 5, pp. 536-543.

12. Dospehov B.A. (1979) Metodika polevogo opyta [Methods of field experiments]. M.: Kolos, 416 p.

13. Kuyshenov M.M. (2014) KR Memlekettik reestr. Forma plyus, 145 p.

14. Korsakov N.I., Makashewa R.H., Adamova O.P. (1968) Metodika izuchenija kollekcii zernobobovyh kul'tur [Methods of studying the collection of leguminous crops]. L.: VIR, 175 p.

15. Mesfin, H. Habtegebriel (2018). Path analysis, genetic variability and correlation studies for soybean (Glycine max (L.) Merill) for grain yield and secondary traits at Asosa, Western Ethiopia. *Greener Journal of Plant Breeding and Crop Science*, vol. 6, no. 3, pp. 35-46.

16. Agudamua , T. Yoshihira, T. Shiraiwa. (2016) Branch development responses to planting density and yield stability in soybean cultivars. *Plant Prod Sci.*, vol. 19, no. 3, pp. 331-339.

17. Deivasigamani S., Swaminathan C. (2018) Evaluation of seed test weight on major field crops.

International journal of research studies in agricultural sciences, vol. 4, pp. 8-11.

18. Wilcox J. R., Sediyama T. (1981) Interrelationships among height, lodging and yield in determinate and indeterminate soybeans. *Euphytica*, vol. 30, no. 2, pp. 323-326.

19. Didorenko S.V., Abugalieva S.I., Zatybekov A.K. Gerasimova E.G., Sidorik I.V., Turuspekov E.K. Izuchenie skorospeloj kollekcii soi v uslovijah severnogo, vostochnogo i jugovostochnogo Kazahstana [Study of the early-ripening soybean collection in the conditions of northern, eastern and southeastern Kazakhstan]. Research and results, KazNAU, vol. 4, no. 76, pp. 294-303.

20. Galeev R.R., Vyshegurov S.K., Samarin I.S., Demshina V.S., Gumel M.A. (2018) Yield Capacity and Grain Quality of Soybeans Depending on Agrotechnical Cultivation Methods. *Journal of Pharmaceutical Sciences and Research*, vol. 10, no. 7, pp. 1668-1671.

21. Hasanuzzaman M., Nahar K., Rahman, A., Jubayer Al M., Shahadat H.Md., Masayuki F. (2016) Soybean Production and Environmental Stresses. pp. 61-102. In: Environmental stresses in soybean production. Academic Press, vol. 2.

IRSTI 76.29.29

[1]H. Teimouri, [1]M. Rezaei, [1]S. Abbaszadeh, [1*]M. Azadpour

[1]Lorestan University of Medical Sciences,
Khorramabad, Iran, *e-mail: Mojganazadpour@yahoo.com

The effects of aqueous extracts of *Cuminum cyminum* L. and *Pimpinella anisum* L. seeds on the improvement of irritable bowel syndrome compared with Loperamide in rats

Abstract: Irritable bowel syndrome (IBS) is a common disorder of the digestive system. In this study, the effects of aqueous extracts of *Cuminum* (*C.*) *cyminum* L. and *Pimpinella* (*P.*) *anisum* L. seeds in improving IBS in rats were studied in comparison with Loperamide, selective drug frequently used for the treatment of IBS in Iran. For induction of IBS, rats were anesthetized 24 hours after fasting, after which 1 ml of acetic acid was injected intrarectally at a point 8 cm from the proximal rectum, the intestine was stimulated and 1 ml of phosphate buffer was injected into the same point to dilute acetic acid. Healing process was studied in five groups: control, false control, positive control, aqueous *C. cyminum* extract-treated and aqueous *P. anisum* extract-treated. *C. cyminum* extract at 300 mg/kg reduced the movements of the gastrointestinal tract significantly, when compared to the control group. To analyze the mean differences between the groups, statistical analysis was performed by the Statistical package for the social sciences (SPSS) using continuous multivariate method. P values of less than 0.05 were regarded as statistically significant. According to the results, the most substantial improvement was observed in aqueous *C. cyminum* extract-treated group, which allows us to propose its advantage compared to other treatments. Probably one of the reasons for the beneficial effect of these plants on IBS is the presence of antioxidant substances in these plants.
Key words: irritable bowel syndrome, plant seeds, *Cuminum cyminum* L., *Pimpinella anisum* L., Loperamide.

Introduction

Gastrointestinal disease is one of the most important and common chronic noncommunicable diseases. Gastrointestinal disease imposes a heavy burden on society and healthcare system in developed and developing countries [1; 2]. Among the types of gastrointestinal disorders, recurrent abdominal pain and irritable bowel syndrome (IBS) have been more frequently addressed [1]. Small intestine is the site of the final digestion of food, absorption of nutrients and secretion of hormone. This hollow tube is composed of four layers: mucosa, submucosa, muscularis and serosa [2-4]. The bowel may develop a number of disorders, including IBS. Although the causes of IBS are not definitely known, diet, intestinal infections and psychiatric disorders are risk factors for this disorder. The frequency of depression, anxiety and other major psychiatric disorders is high in people with IBS [5]. Diagnosis of this disease is made based on symptoms such as chronic pain and changes in bowel habits in the absence of any organic cause [6]. IBS accounts for 12% of referrals to gastroenterologists in Europe [7]. The pathophysiology of this disease remains unknown. Genetic and environmental factors are likely to contribute to developing the disease [8]. Some studies have reported abnormal movements of the gastrointestinal tract, visceral irritability, psychological impairment, and emotional stress to be involved in IBS development [7; 8]. Stress, anger, intravenous injection of cholecystokinin and colonic perfusion with deoxycolic acid have also been reported to increase bowel movements in patients with IBS. Increased sensitivity of the bowel due to psychological factors, causing pain and emergency in defecation after balloon expansion in the rectum [9], and increased brain cortical activity after rectal dilation [10] are also observed in IBS. These findings reveal the relationship between the psychological factors and the sensitivity of the visceral neurotransmitters. The brain mediators that have been used include bradykinin, tachykinin, serotonin,

calcitonin gene-related peptides, and neurotrophins [11]. Most patients with IBS suffer from anxiety and depression, and patients with IBS show more severe psychosis than healthy people [12].

The prevalence of IBS in the United States is 12%, and its prevalence is between 3% and 20% in Europe and in the rest of the world with comparable prevalence rates in other parts of the world, but the actual prevalence rate is estimated to be comparatively higher, as this prevalence is reported for clients referring to health centers, while in fact, many patients do not refer to the centers [13; 14]. It has been shown that negative emotions and emotional states such as anger are associated with a decrease in intestinal motor activity in IBS patients. These patients report more stressful events in their daily lives and also throughout their lives than healthy people and may be more sensitive to stress-induced gastrointestinal function changes [15]. The approach to using plant compounds for the production of new drugs that are more effective, stronger and more compatible with the body of living beings is on the agenda of researchers in the pharmaceutical, medical and veterinary sciences, which, given the public interest in herbal drugs and the potentials of plants, such research seems essential. One of the methods that have recently been considered for treatment of IBS is the use of herbal drugs and medicine. Study showed turmeric consumption significantly improved IBS symptoms, especially abdominal pain, and improved quality of life [13].

The use of medicinal plants is common in traditional Iranian medicine. Traditionally, *Cuminum (C.) cyminum* L. and *Pimpinella (P.) anisum* L. are used to treat gastrointestinal disorders. *P. anisum* is a perennial and high plant from the *Umbeliferae* family that is very fragrant and has pink-shaped green, and small seeds. The upper part of the plant is sharp with five striking lines easily observed on it. The most important ingredient of the plant is its essential oil, which accounts for 1.5-5% of the plant. The most important compound in the essential oil is the trans-anethole (80-90% of the essential oil). Coumarins are other important compounds of *P. anisum* [19]. *P. anisum* seeds are used as an analgesic in migraine, and are traditionally used as a fragrant, disinfectant and diuretic agent, and the extract obtained from its distillation also serves these purposes. It has also antibacterial, antispasmodic, anti-inflammatory, digestive, hepatotonic, laxative, sedative, stimulant and gastrotonic properties. The pharmacological effects of *P. anisum* are more closely related to the anethole in its essential oil, whose formulation is similar to those of catecholamines (including adrenaline, adrenaline and dopamine) [20]. Green cumin, *C. cyminum* L., belongs to the *Umbeliferae* family, and is an aromatic plant. Its major ingredients include sabinene, flavonoids, polysaccharides, coumarin, cuminaldehydes, pinene and terpinene, vitamins B_1, B_2, B_3, B_9, C, E, and K, as well as various minerals such as calcium, iron, magnesium, phosphorus, potassium and sodium. Green cumin has a very warm and dry nature. In the treatment of gastrointestinal diseases, *C. cyminum* acts as an anti-inflammatory agent and facilitates digestion, and is also used in pulmonary diseases for the treatment of cough [21]. Cumin, of any kind, serves as a tonic and energizing agent for the body. These properties are enhanced when cumin is mixed with honey [22]. *C. cyminum* is effective for the treatment of gastrointestinal disorders, gastrointestinal tract weakness, bloating, and heartburn. In fact, consuming *C. cyminum* will strengthen the stomach. It is the strongest herbal carminative agent and reduces the spasm of the intestinal smooth muscles [22].

Cumin plant contains such compounds as sabine, flavonoids, polysaccharides, coumarin, cumin aldehyde, pinen and terpinene, which have antioxidant properties. *P. anisum* has flavonoids and phenols that have antioxidant properties [19-21]. Therefore, this study was conducted to investigate effects of *C. cyminum* and *P. anisum* seed aqueous extracts on the improvement of IBS in rat model.

Materials and methods

Loperamide (Eksir-danesh Co., Iran) is a type of opioid receptor agonist, used to treat symptomatic acute diarrhea (especially gastroenteritis, inflammatory bowel disease, and irritable bowel syndrome). It affects the onset of the middle cerebral nervous system of the intestine, decreasing the smooth muscle length of the intestine, thereby slowing down the intestinal activity and thus decreasing the amount of water and salt in the body.

Extraction. Plant material for study was obtained from the Agricultural Research Center of Lorestan province, Khorramabad city, southwest of Iran. The aqueous extract was prepared by maceration from plant material dried at 23±2°C. For this purpose, 100 g of seeds were weighed, put in 100 ml of water (so that the seeds were completely under the water surface), poured into a large Erlenmeyer flask and placed on a heater to boil. Then, they were boiled for 15 minutes, cleaned with a clean cloth, filtered with

filter paper, and poured into a crystallizer and dried on a Bain Marie. Due to the long drying time of the extract, exceeding 72 hours, it was stored in the refrigerator during the drying intervals. Drying continued until the weight of the extract became constant. After preparation and drying, the lid of the extract container was covered with aluminum foil and the container placed in the refrigerator until subsequent tests.

Studied animals and experiment procedure. In this study, 40 male Wistar rats weighing 220-250 g were used. They were collected from the Animal House of Razi Herbal Medicines Research Center of Lorestan University of Medical Sciences, Khorramabad city, Lorestan province, Iran. Rats were housed in the animal room under controlled conditions with respect to temperature and light, with free access to water and food as follows: 12/12 hours of light and darkness, standard food and water, 40±10 % r.h., 22±2 °C.

Induction of IBS. For induction of IBS, rats were anesthetized with ether after 24 hours fasting, after which 1 ml of 4% acetic acid was injected intrarectally at a point 8 cm from the proximal rectum, the intestine was stimulated and 1 ml of phosphate buffer was injected into the same point to dilute acetic acid. The protocol of this study fully conformed to the ethical principles regarding the use of laboratory animals in research.

Animals were randomly divided into 5 groups:

– control group: after stress induction, normal saline was intrarectally injected to rats;

– false control group: after stress induction, acetic acid was intrarectally injected to rats and distilled water (10 mg/kg) was orally administered (by gavage) for 26 days (21 days before stress induction until 4 days after);

– positive control group: Loperamide (10 mg/kg) was orally administered (by gavage) for 26 days (21 days before stress induction until 4 days after);

– *P. anisum* extract-treated group: aqueous *P. anisum* seed extract (150 and 300 mg/kg) was orally administered (by gavage) for 26 days (21 days before stress induction until 4 days after);

– *C. cyminum* extract-treated group: aqueous *C. cyminum* seed extract (150 and 300 mg/kg) was orally administered (by gavage) for 26 days (21 days before stress induction until 4 days after).

Measuring bowel movements. The rats were separately exposed to immobility stress (at certain times) and the number of stools for 1 hour was determined to be used as measure of bowel movement. Finally, the comparison was made with the corresponding results in the control group.

Measuring myeloperoxidase (MPO) activity. Myeloperoxidase activity in the intestinal tissue was measured in order to determine intestinal inflammation. 8 cm piece was removed from the distal intestine and homogenized in 1 ml of phosphate buffer (pH 6.0), containing 14 mM of hexadecyl trimethylammonium bromide. Put into freezer. Centrifuged for 2 minutes. Finally, the absorbance of the samples in all groups was read by a spectrophotometer at a wavelength of 480 nm.

Measuring lipid peroxidation. Lipid peroxidation was evaluated by determining the concentration of thiobarbituric acid reactive substances (TBARS). In order to evaluate lipid peroxidation, malondialdehyde levels in the intestinal tissue were measured by spectrophotometer at a wavelength of 532 nm.

Statistical data analysis. To analyze the mean differences between the groups, statistical analysis was performed by the Statistical Package for the Social Sciences (SPSS 16.0; https://www.ibm.com/analytics/data-science/predictive-analytics/spss-statistical-software), using continuous multivariate method. P values of less than 0.05 were regarded as statistically significant.

Results and discussion

Based on our results, regarding the movements of gastrointestinal tract, the mean (±SD) number of stools in the false control group (29±2.34) compared to the control group (8.67±3.74), indicates development of certain symptoms in comparison with the control group in which the number of stools was higher. The mean number of stools in the positive control group was 11. ±5.53, in *C. cyminum* seed extract (300 mg/kg)-treated group 18.88±5.12, and in *P. anisum* seed extract (300 mg/kg)-treated group 24±1.92, with significant changes when compared to the control group (8.67±3.74). According to our results, there was a significant improvement in rats treated with 300 mg/kg of *C. cyminum* seed extract. Comparison of the group treated with 300 mg/kg of *C. cyminum* extract and false control group showed in the group receiving the *C. cyminum* extract, the number of stools significantly decreased (P<0.01). In general, the results showed that treatment with aqueous *C. cyminum* extract (300mg/kg) for 26 days significantly reduced the symptoms of the disease (Table 1).

Table 1 – Summative analysis of effects of cumin and anise plant extracts on gastrointestinal tract

Test	Control	False control	Positive control	Cumin extract	Anise extract	ANOVA P value
Activity and movement of the colon	8.67±3.74	29±2.34	11±5.53	18.88±5.12*	24±1.92**	0.002
Peroxidation of lipids	1.05±0.12	3.36±1.08	0.47±0.04	1.16±0.28*	1.96±0.34	0.076
Measurement of mylioproxidase	15.42±1.33	45.21±1.75	25.18±1.07	19±1.52*	31.76±1.57**	0.008
* $P < 0.05$:; ** $P < 0.01$, compared to false control group						

The number of stools in the false control group at all 1 hour intervals and the total number of stools per hour in comparison with the control group, indicated the development of IBS, while in the group treated with 300 mg/kg of *C. cyminum* seed extract (P<0.01) and positive control group (P<0/05), stool numbers at all intervals were significantly lower than false control group, which can be indicative of the prevention of IBS development.

The rate of lipid peroxidation in the false control group (3.36±1.08) was higher than the control group (1.05±0.12), and in the positive control group (0.47±0.04) and the group receiving 300 mg/kg of *P. anisum* extract (1.96±0.34) was significantly lower than false control group. In the group receiving 300 mg/kg of the *C. cyminum* extract (1.616±0.28), lipid peroxidation was significantly lower than the false control group (3.36±1.08) and approximately equal to the control group (Table 1).

The MPO activity in the groups receiving *C. cyminum* extract (19±1.52) and *P. anisum* extract (31.76±1.51) significantly decreased in comparison with the false control group (45.21±1.75). The corresponding decrease in *C. cyminum* extract-treated group was also significant when compared to the control group (15.42±1.33). The results shown in the Figure indicate that the *C. cyminum* extract decreases MPO activity significantly compared to the false control group (Table 1).

The results of this study show that the *C. cyminum* extract at 300 mg/kg reduces movements of gastrointestinal tract significantly compared to the control group, which is comparable to the standard drug Loperamide, reducing the movements compared to the control group. However, the P. anisum extract did not show a significant inhibitory effect on the movements of gastrointestinal tract contents compared to the *C. cyminum*. Although the extract of the *C. cyminum* reduces the frequency of diarrhea, its antidiarrheal mechanism remains unknown. Medicinal plants are of great value and importance in providing health care to communities, in terms of both treatment and prevention of diseases. The *P. anisum* is a gastrotonic plant and therefore can be effective in preventing some gastrointestinal problems. Due to its carminative effect, the plant is also used in the formulation of some gastrointestinal antispasmodic antiflatulent drugs. From the perspective of traditional Iranian medicine, *P. anisum* seeds have anti-inflammatory and analgesic properties and can used to prevent and treat many of diseases in which inflammation is a main factor [28]. *C. cyminum* is known as helpful medicinal plant in Iran [29]. From the ancient times in traditional medicine, *C. cyminum* seeds have been used to treat diseases, such as bloating, abdominal colic, pulmonary inflammation and gastritis [31]. In addition, aqueous and oily extracts of the plant have antioxidant properties and are used as natural antioxidants to reduce oxidative stress levels and increase the levels of antioxidant agents [32]. A study has shown that essential oil, containing 26% γ-terpinene (compound of *C. cyminum* essential oil) has antioxidant and antimicrobial properties [33]. γ-terpinene also decreases the linoleic acid peroxidation [34]. Some compounds present in *C. cyminum* essential oil, such as z-ß-ocimene, limonene and carvone, have antibacterial and antifungal effects and are effective in the treatment of infections caused by various pathogenic fungi and bacteria such as *Candida albicans* [35]. In the study of Sabbaghian *et al*. [36], the effect of aqueous *Aloe vera* extract on the intestinal and brain water content and gastric acid secretion was investigated after acetic acid-induced gastric ulcer in male rats. Their results showed that the use of *Aloe vera* produced an inhibitory effect on gastric acid secretion. The inhibitory effect of *Aloe vera* is due mainly to the formulation and gastroprotective activity of the plant. Improved tissue conditions also indicated the healing properties of this plant [36].

Cruz *et al*. [37] and Ismaili *et al*. [38], found that oral intake of silymarin (a flavonoid combination derived from *Silybum marianum*) improves bowel

tissue inflammation and damage. Factors such as increased vascular permeability, long-term infiltration of neutrophils, and increased mediators of inflammation that play a role in the onset of human colitis are also associated with the formation of colitis [39]. The anti-inflammatory effects of sulfasalazine and its metabolite, 5-amino-salicylic acid, are well known [40]. The use of *Hypericum perforatum* extract has been reported as effective in improving the symptoms of IBS in rats [17]. The property of turmeric property in IBS improvement has been demonstrated [18]. Inflammatory bowel disease has been considered an important public health issue due to its impact on young people, recurring and progressive clinical course, and impact on the quality of life and social status of individuals, and the ability to work and education [41-43].

Conclusion

Although irritable bowel syndrome is a benign condition and definitely not life threatening, the duration of this illness is long and the likelihood of its recurrence is high. It is a functional gastrointestinal disease with a high population prevalence. The disorder can be debilitating in some patients, whereas others may have mild or moderate symptoms. Probably one of the reasons for the effect of aqueous extracts from *Cuminum cyminum* L. and *Pimpinella anisum* L. seeds on IBS is the presence of antioxidant substances in these plants. It has been found that these two herbs contain active substances that have antioxidant activity. In the prospective future, there is hope for a better understanding of the disease and therefore its treatment.

Acknowledgment

Research was funded within the framework of the project 33/90 from Deputy for Research and Technology, Lorestan University of Medical Sciences, Khorramabad, Iran. The Ethics Committee of Lorestan University of Medical Sciences (code 9/26/1) approved conducted animal studies (code 33/90).

References

1. Malekzadeh R., Derakhshan M.H., Malekzadeh Z. (2009). Gastric cancer in Iran: epidemiology and risk factors. *Arch Iran Med*., vol.12, no.6, pp. 576-583.

2. Lovell R.M., Ford A.C. (2012). Global prevalence of and risk factors for irritable bowel syndrome: a meta-analysis. *Clin Gastroenterol Hepatol.*, vol. 10, pp. 712-721.e4.

3. Matsui T. (2010). Draft revision of diagnostic criteria for ulcerative colitis. Annual reports of the research group of intractable inflammatory bowel disease subsidized by the Ministry of Health, Labour and Welfare of Japan, pp. 484-488.

4. Matsui T. (2013). Draft diagnostic criteria for Crohn's disease. Annual reports of the research group of intractable inflammatory bowel disease subsidized by the Ministry of Health, Labour and Welfare of Japan, pp. 43-45.

5. Olafsdottir L.B., Gudjonsson H., Jonsdottir H.H., Thjodleifsson B. (2010). Stability of the irritable bowel syndrome and subgroups as measured by three diagnostic criteria – a 10-year follow-up study. *Aliment Pharmacol Ther.*, vol. 32, pp. 670-680.

6. Gaman M., Bucur B. (2009). Therapeutic advances in function gastrointestinal disease:irritable bowel syndrome. *Therap Adv Gastroenterol*., vol. 2, no. 3, pp. 169-181.

7. Hommes D.W., van Deventer S.J. (2004). Endoscopy in inflammatory bowel diseases. *Gastroenterol.*, vol. 126, no. 6, pp.1561-1573.

8. Yarandi S.S., Nasseri-Moghaddam S., Mostajabi P., Malekzadeh R. (2010). Overlapping gastroesophageal reflux disease and irritable bowel syndrome: increased dysfunctional symptoms. *World J Gastroenterol.,* vol. 16, pp. 1232-1238.

9. Dorn S.D., Palsson O.S., Thiwan S.I., Kanazawa M., Clark W.C., van Tilburg M.A et al. (2007). Increased colonic pain sensitivity in irritable bowel syndrome is the result of an increased tendency to report pain rather than increased neurosensory sensitivity. *Gut,* vol. 56, pp. 1202-1209.

10. Lawal A., Kern M., Sidhu H., Hofmann C., Shaker R. (2006). Novel evidence for hypersensitivity of visceral sensory neural circuitry in irritable bowel syndrome patients. *Gastroenterology*, vol. 130, pp. 26-33.

11. Long M.D., Drossman D.A. (2010). Inflammatory bowel disease, irritable bowel syndrome, or what? A challenge to the functional-organic dichotomy. *Am J Gastroenterol.,* vol. 105, pp. 1796-1798.

12. Mahid S.S., Minor K.S., Soto R.E., et al. (2006). Smoking and inflammatory bowel disease: a meta-analysis. *Mayo Clin Proc.,* vol. 81, no. 11, pp. 1462-1471.

13. Lovell R.M., Ford A.C. (2012). Effect of gender on prevalence of irritable bowel syndrome in the community: systematic review and meta-analysis. *Am J Gastroenterol.*, vol. 107, pp. 991-1000.

14. Janssens K.A., Zijlema W.L., Joustra M.L., Rosmalen J.G. (2015). Mood and anxiety disorders in chronic fatigue syndrome, fibromyalgia, and irritable bowel syndrome: results from the LifeLines Cohort study. *Psychosom Med.*, vol. 77, pp. 449-457.

15. Keohane J., O'Mahony C., O'Mahony L., O'Mahony S., Quigley E.M., Shanahan F. (2010). Irritable bowel syndrome-type symptoms in patients with inflammatory bowel disease: a real association or reflection of occult inflammation? *Am J Gastroenterol.*, vol. 105, pp. 1789-1794.

16. Bundy R., Walker A., Middleton R., Booth J. (2004). Turmeric extract may improve irritable bowel syndrome symptomology in otherwise healthy adults: a pilot study. *J Altern Complement Med*., vol. 10, no. 6, pp. 1015-1018.

17. Nourani M. (2005). Encyclopedia of Islamic medicine. *Armaghan Youssef,*. vol. 1, 1st ed., p. 23

18 Mirahidar H. (1984). Medicinal education, Plant use in the prevention and treatment of diseases. *Physician Publishing*, p. 73.

19. Rojhan, M.S. (1999). Treated by Medicinal Plants. *Aban cultural center*, 2nd ed., p. 8.

20. Yazdani D., Shahnazi S., Saifi H. (2004). Planting, Planting and Harvesting of Medicinal Plants. Research Institute of Medicinal Plants, Jahad University, p. 34.

21. Tonkaboni S.M., Al-Momenin T. (2008). Tehran, Iran: Traditional Medicine & Materia Medica Research Center, Shahid Beheshti University of Medical Sciences Publication, p. 65-66.

22. Baldari A. (1992). Determination of botanical characteristics of local cumin cultures of Iran, Iran Scientific and Industrial Research Organization, *Khorasan Research Institute*, p. 42.

23. De Carvalho C.C.C.R., Da Fonseca M.M.R. (2006). Carvone: why and how should one bother to produce this terpene. *Food Chem.*, vol. 95, pp. 413-422.

24. Yu L.L., Zhou K.K., Parry J. (2005). Antioxidant properties of cold-pressed black caraway, carrot, cranberry, and hemp seed oils. *Food Chem.*, vol. 91, pp. 723-729.

25. Faleiro L., Miguel G., Gomes S., Costa L., Venâncio F., Teixeira A., et al. (2005). Antibacterial and antioxidant activities of essential oils isolated from *Thymbra capitata L.* (Cav.) and *Origanum vulgare L. J Agric Food Chem.*, vol. 53, pp. 8162-68.

26. Foti M.C., Ingold K.U. (2003). Mechanism of inhibition of lipid peroxidation by gamma-terpinene, an unusual and potentially useful hydrocarbon antioxidant. *J Agric Food Chem*., vol. 51, pp. 2758-2765.

27. Milosavljević S., Tesević V., Vucković I., Jadranin M., Vajs V., Soković M., et al. (2007). Composition and antifungal activity of the essential oil of Seseli annuum wild-growing in Serbia. *Fitoterapia*, vol. 78, pp. 319-322.

28.Sabaghian M., Keshavarzi Z., Bibak B., Vatanchian M., Mohammad Rezapour T. (2014). The effect of aqueous extract of Aloe vera leaves on gut-brain axis response following acetic acid -induced gastric ulcer in male rats, *J North Khorasan Uni Med Sci*, vol. 6, no. 3, pp. 347-357.

29. Li R., Jiang Z.T. (2004). Chemical composition of the essential oil of Cuminum cyminum L. from China. *Flavour Fragrance J.*, vol. 19, no. 4, pp. 311-313.

30. Esmaily H., Hosseini-Tabatabaei R., Reza Rahimian R., Reza Khorasani R., Baeeri M., Barazesh-Morgani A. (2009). On the benefits of silymarin in murine colitis by improving balance of destructive cytokines and reduction of toxic stress in the bowel cells. *Cent Eur J Biol*., vol. 4, no. 2, pp. 204-213.

31. Garjani A., Davaran S., Rashidi M.R., Maleki N. (2004). Protective effecs of some azoderivatives of 5-aminosalicylic acid and their pegylated prodrugs on acetic acid induced colitis. DARU, vol. 12, no. 1, pp. 24-30.

32. Levy R.L., Jones K.R., Whitehead W.E., Feld S.I., Talley N.J., Corey L.A. (2001). Irritable bowel syndrome in twins: heredity and social learning both contribute to etiology. *Gastroenterology*, vol. 121, no. 4, pp. 799-804.

33. Bradley P.R. (1992). British Herbal Compendium. Bournemouth: British Herbal Medicine Association, vol. 1, pp. 73-75.

34. Foti M.C., Ingold K.U. (2003). Mechanism of inhibition of lipid peroxidation by gamma-terpinene, an unusual and potentially useful hydrocarbon antioxidant. *J Agric Food Chem.*, vol. 51, pp. 2758-2765.

35. Milosavljević S., Tesević V., Vucković I., Jadranin M., Vajs V., Soković M., et al. (2007). Composition and antifungal activity of the essential oil of Seseli annuum wild-growing in Serbia. *Fitoterapia*, vol. 78, pp. 319-322.

36. Sabaghian M., Keshavarzi Z., Bibak B., Vatanchian M., Mohammad Rezapour T. (2014). The effect of aqueous extract of Aloe vera leaves on gut-brain axis response following acetic acid -induced gastric ulcer in male rats*, J North Khorasan Uni Med Sci*., vol. 6, no. 3, pp. 347-357.

37. Cruz T., Gµlvez J., Crespo E., Ocete M.A., Zarzuelo A. (2001). Effects of silymarin on the acute stage of the trinitrobenzenesulphonic acid model of rat colitis. *Planta Med.*, vol. 67, no. 1, pp. 94-96.

38. Esmaily H., Hosseini-Tabatabaei R., Reza Rahimian R., Reza Khorasani R., Baeeri M., Barazesh-Morgani A. (2009). On the benefits of silymarin in murine colitis by improving balance of destructive cytokines and reduction of toxic stress in the bowel cells. *Cent Eur J Biol*., vol. 4, no. 2, pp. 204-213.

39. Elson C.O., Sartor R.B., Tennyson G.S., Riddell R.H. (1995). Experimental models of inflammatory bowel disease. *Gastroentrology,* vol. 109, no. 4, pp. 1344-1367.

40. Garjani A., Davaran S., Rashidi M.R., Maleki N. (2004). Protective effecs of some azoderivatives of 5-aminosalicylic acid and their pegylated prodrugs on acetic acid induced colitis. DARU, vol.12, no. 1, pp. 24-30.

41. Jostins L., Ripke S., Weersma R.K. et al. (2012). Host-microbe interactions have shaped the genetic architecture of inflammatory bowel disease. *Nature*, vol. 491, no. 7422, pp. 119-124.

42. Sakamoto N., Kono S., Wakai K., Fukuda Y., Satomi M., Shimoyama T., Inaba Y. et al. (2005). Dietary risk factors for inflammatory bowel disease: a multicenter case-control study in Japan. *Inflamm Bowel Dis.*, vol. 11, no. 2, pp. 154-163.

43. Cornish J.A., Tan E., Simillis C., Clark S.K., Teare J., Tekkis P.P. (2008). The risk of oral contraceptives in the etiology of inflammatory bowel disease: a meta-analysis. *Am J Gastroenterol.*, vol. 103, no. 9, pp. 2394-2400.

IRSTI 68.35.31

[1]M. Hatamikia, [1*]A.H. Elhamirad, [2]R. Heydari,
[3]P. Sharayei, [3]E. Azarpazhooh

[1]Department of Food Science & Technology, Sabzevar Branch, Islamic Azad University, Sabzevar, Iran
[2]Razi Herbal Medicines Research Center, Lorestan University of Medical Sciences, Khorramabad, Iran
[3]Agricultural Engineering Research Department, Khorasan Razavi Agricultural and
Natural Resources Research and Education Center, Mashhad, Iran
*e-mail: ah.elhami@gmail.com

Investigating the effect of various methods of soaking from *Vicia ervilia* in water and alkaline, acid and salt solutions on reduction of anti-nutritional compounds

Abstract: *Vicia* (*V.*) *ervilia*, commonly termed as bitter vetch, produces grains belonging to legumes family. One of the factors limiting the usage of *V. ervilia* is the existence of large amounts of anti-nutritional factors in the grains thereof. Considering the importance of the anti-nutritional factors, the present study investigated the effect of different methods of soaking from *V. ervilia* grains on the reduction of anti-nutritional factors rates. All of the soaking methods were found considerably reducing the anti-nutritional factors rates in all treatments as compared to *V. ervilia* grain flour. It was also found out in the present study that alkaline treatment, provides for the highest reduction of hydrolysable and dense tannin, phenolic ingredients in contrast to the other methods. Moreover, considerable increase in canavanine ooze-out from *V. ervilia* was documented for aqueous and saline treatments. Among different treatments, the highest reduction in total phenolic compounds and tannins was observed in alkaline maceration, followed by acidic, aqueous and salt saline. Also the lowest amount of canavanine was observed in aqueous treatment and the highest amount in alkaline treatment. The results show that treatment method can be selected depending on the type of need to remove anti-nutritional compounds of *V. ervilia* seeds. So soaking in water and use of saline solutions is preferred to soaking in basic and acidic solutions for the latter damages to some nutrients under basic and acidic conditions.

Key words: *Vicia ervilia*, water, alkaline, anti-nutritional, tannin, phenol, canavanine.

Introduction

Legumes are plants from *Fabaceae* (*Leguminosae*) family comprised of 16 to 19 thousand species and nearly 750 genera. Legumes are enumerated amongst the most important plant sources rich in proteins and valuable nutritional biogenic compounds can be prepared from them when combined with cereals for the fact that they contain a considerable amount of high-grade protein (17-38%). The protein rate in legumes crude grains is two to three times higher than that of the cereals (10-15%). Thus, legumes can be used as rich sources of protein in the production of plant protein byproducts in the form of flour (50-65% protein), concentrates (65-90% protein) and/or protein isolates (over 90%) [1; 3]. Efforts for finding alternative and cheap sources of protein for human nourishment have led to various researches regarding the use of some such less-known legumes in developing countries. The reason for such vast studies is the abundance and cheapness of the legumes as potential protein sources for the people of these countries who have less financial affordability in supplying protein from animal sources. *V. ervilia*, commonly termed bitter vetch, belongs to legumes family and the grains of this plant look red lentil when broken [2-5]. According to the producibility of this plant in Iran and its high percentage of protein content, its flours and protein byproducts can be evaluated in terms of performance characteristics and usability in food industry. Approximate analysis of *V. ervilia* is indicative of the idea that it has a chemical composition almost similar to legumes. Investigations performed on *V. ervilia* made it clear that carbohydrates account for a large quotient of *V. ervilia* grains volume. Protein, lipid, fiber, organics

(potassium, phosphorus, copper, iron and calcium) and vitamins are other ingredients constituting *V. ervilia* grains [3-6].

The majority of the legumes grains is relatively toxic and contains proteins or lipids controlling and inhibiting digestive enzymes and the proper processing methods or varieties breeding methods should be applied to overcome such a problem [6-9]. Like the majority of legumes grains, *V. ervilia* grains contain useful nutritional ingredients plus considerable amounts of anti-nutritional biologically active ingredients amongst which phenolic compounds, tannin, canavanine, gallic acid, ellagic acid and galloyl derivatives or hexahydroxydiphenol can be pointed out [9-11]. Furthermore, *V. ervilia* grains contain such toxic amino acids as canavanine (0.035% to 0.11%), cyanogenic glycoside and trypsin inhibitor (2.14 mg/g dry matter) [12]. Annually, a large amount of *V. ervilia* grains is produced in western and northwestern regions of Iran and, unfortunately, there is made no other useful application of this natural nutritional source in our country other than its limited use for feeding livestock and poultry. One factor restricting the use of *V. ervilia* is the existence of a large amount of anti-nutritional factors in the grains thereof. Besides having adverse health effects, anti-nutritional ingredients cause a bitter and astringent taste negatively influencing its agreeability by the consumer [5-12]. The present studys objective in the first stage is the determination of the amount of anti-nutritional factors existent in *V. ervilia* grains flour and various treatments; in a second stage, four methods of soaking from *V. ervilia* grains are compared so as to make it clear which soaking method is capable of exuding a higher rate of phenolic compounds, tannin and canavanine from the *V. ervilia*. The determination of an easy and less costly method with a high efficiency for reducing anti-nutritional factors is deemed as significant a step as possible in making use of *V. ervilia* grains (Table 1).

Table 1 – Some physical processes common for the reduction or elimination of the anti-nutritional factors existent in legumes (Bravo, 1998)

Physical process	Explanations
Autoclaving, cooking under pressure, vaporing	Heating using high temperatures (over 100ºC): the efficiency of the method depends on temperature, moisture and medium pressure
Blanching	Mild boiling (75ºC-95ºC) for deactivating the internal enzymes and prevention of complete cooking
Normal cooking	Before using this method, such pretreatments as skinning, soaking, germination, fermentation and other normal home-based methods are applied.
Extrusion	In this process, high temperature is exerted within a short time (HTST). The process is a combination of high temperature and use of pressure and shear process.
Parching	Dry heating (120ºC-250ºC)
Using chemical processes along with chemical modification (addition of chemical materials)	Using such chemicals as thiols, sulfites, copper salts, ascorbic acid-chemical modification via acylation and succinylation

Materials and methods

In the present study *V. ervilia* grains were procured from Agricultural Jihad branch of Lorestan Province. The grains were grounded in a laboratory mill. To make uniform flour particles, the flour was passed through a 1mm sieve and kept in a refrigerator until the application time. Then, different solutions were used to evaluate the effect of the process of soaking from *V. ervilia* on the reduction of anti-nutritional compounds. In all treatments, 100 ml of various solutions of sodium hydroxide and acetic acid 0.5 M, sodium chloride 5% and water solvent were added to 10 g of the sample separately. The samples were soaked for 24 hours at ambient temperature in these conditions. After 24 hours, the water used, as well as acidic, alkaline, and salt solutions were discarded and the samples were washed several times with distilled water to remove any remaining soluble residue. The specimens were dried for 12 hours to constant weight at 50 ºC [13; 14].

Measuring phenolic ingredients total rates. To retrieve the crude extract, samples were firstly vacuum-dried in an oven in 50 ºC. Then, the dried samples were grounded following which 20 ml 80% methanol was poured on 0.2 g of the dried and milled

sample and the mixture was shaken thoroughly and placed for 2 hours in bain marie in 50 ºC following which the extracts were passed through filter paper and increased in volume using 80% methanol solvent in a 20-ml volumetric flask. The total phenolic ingredients rates were measured in mg/g gallic acid based on Folin-Ciocalteau reagent using spectrophotometer at 765 nm [15; 16].

Measuring the hydrolysable tannin rate. To extract the hydrolysable tannins, 5 g of the milled and dried specimen was weighed. Extraction was carried out using 80% methanol. After remaining in room temperature for 24 hours and following the complete evaporation of methanol, 50ml boiled water was poured on each of the dried specimens and the sediments were separated from the containers and each were separately poured in 100-milliliter Erlenmeyer flasks. Then, ether was added and the solution was completely stirred. Next, the etheric phase was separated using decanter and discarded and the rest of the process continued with the aqueous phase in such a manner that the aqueous solution was poured inside two 50 ml Erlenmeyer flasks to which normal soda and normal hydrochloric acid had been respectively added. The contents of the flasks were correspondingly made completely acidic and basic. Then, both of the flasks were sealed using foil and placed inside hot water bath (bain marie) in 100ºC for a period of time between 20 min to 40 min. In the end of the process, following the cooling of both solutions, normal 6 M hydrochloric acid was added to the one that had become basic and the contents of both of the flasks were eventually mixed. Twenty milliliter ether was added to the obtained mixture for two to three times, each time separating the biphasic solution using decanter. The etheric phase containing hydrolysable tannin was poured inside a previously weighed container and allowed to be vaporized. Tannin measurement was carried out using Folin-Ciocalteau reagent in a spectrophotometer at 743 nm [13-16].

Measuring dense tannin rates. To extract dense tannins, 5 g of the dried and milled specimen was poured in 100 milliliters of 70% acetone solution and the mixture was placed in a 37 ºC hot water bath (bain marie) for 24 hours. After having the solution passed through filter paper, the sediments were washed two or three times using acetone. Then, ether was poured on the obtained solution twice or thrice and the solution was each time separated using decanter. The separated etheric solution contains dense tannin. To measure the amounts of the dense tannin, the etheric solution was dried in open air and dissolved in 10 ml ether. Out of the obtained etheric extract, 0.5 ml was poured inside a vial and 3ml butanol hydrochloric acid solution (95 parts butanol + 5 parts 37% hydrochloric acid) was poured thereon along with 0.1 ml ferric reagent (2% ferric ammonium sulfate in normal 2 M hydrochloric acid). Then, the mixture was stirred and the vial was sealed following which it was boiled in bain marie for 60 minutes. Afterwards, the solution was allowed to cool down. Then, the absorption rates of the obtained solutions were measured at 550 nm [13-16].

Measuring canavanine rates: preparing sodium pentacyanoaminoferrate reagent. 10g of sodium nitroprusside was dissolved in 55ml of condensed 32% ammonia solution. The obtained solution was kept in darkness and 0ºC for 24 hours. The yellow-greenish sediment containing sodium pentacyanoaminoferrate II and III was filtered and treated using absolute ethanol so that complete sedimentation could happen. The sediment was combined with the preliminary sediment and washed in absolute ethanol till ammonia was entirely removed. After partial omission of ethanol by filtering, the sediment was dried using sulfuric acid and kept along with calcium chloride in darkness in desiccator. The mixture has to be used within 48 hours after being prepared because pentacyanoaminoferrate begins breakdown after that time hence it loses its characteristics and becomes brownish green in color.

Preparing V. ervilia specimens. 2 g of sample was subjected to extraction using 0.1 M hydrochloric acid in a sample-acid ratio of 1:25 weight-volume. The mixture was stirred on a magnetic stirrer for 6 hours and kept at room temperature for one night. The solution was subsequently centrifuged in 1000 rpm for 20 min, the unsettled part (overlying solution) was stored, and the remaining (deposited) part was exposed to a secondary extraction stage for 6 hours under conditions similar to the first stage. The mixed extracts were set at pH values and final volumes of 7 and 100 ml, respectively, using 0.1 M soda solutions.

Measuring canavanine rates. 1 ml standard canavanine solution (1 mg/ml) was diluted by 0.1 M hydrochloric acid so that concentrations in a range from 0.005 to 0.08mg/ml of canavanine could be obtained. In a 10 ml volumetric flask, 6.5 ml 0.2 M potassium phosphate buffer (pH 7), 1 ml 1% potassium persulfate and 0.5 ml 1% pentacyanoaminoferrate solution (kept in dark) were added to 1 ml diluted canavanine solution and the obtained mixture was diluted to 10 ml using distilled water. The mixing process lasted 15 min and the absorption rates were measured at 520

nm. Similarly, a good volume of the sample solution was used instead of standard canavanine solution for quantitative determinations. Using standard curves, canavanine concentration rates in samples were determined based on dry matter weight [17].

Statistical data analysis. All methods of soaking from *V. ervilia* grain and the entire experiments were replicated thrice and the results offered herein are the mean values of the three repetitions. The present study investigated the effects of various treatments of soaking from *V. ervilia* grains on the anti-nutritional factors existent in *V. ervilia* within a completely randomized statistical design in three replications. The results were analyzed using SPSS 16 software.

Results and discussion

One of the factors limiting the usage of *V. ervilia* is the existence of large amounts of anti-nutritional factors in its grains. Percent chemical composition of *V. ervilia* grain flour based on dry matter is presented in Table 2.

Table 2 – Percent chemical composition of *V. ervilia* grain flour based on dry matter in the present study

Protein	Fat	Carbohydrate	Moisture	Ash	Crude fiber
25.36±0.25	4.50±0.2	52.56±0.3	6.30±0.2	3.64±0.19	6.83±0.12

In this regards, anti-nutritional factors existent in *V. ervilia* grain flour were as shown below.

Total phenolics content. The total phenolic ingredients existent in various plant food materials are different even in various varieties belonging to a single genus and they cover a vast range (Table 3) [19]. The total phenolic compound rates of *V. ervilia* grain flour have been obtained in equivalent gallic acid, 408.46±0.33mg/100g.

Table 3 – The amount of polyphenolic ingredients in various foodstuff based on dry matter (mg/100g)

Foodstuff	Total phenolic ingredients
Legumes	34-1710
Cereals	22-102.6
Nuts (kernels)	0.04-38
Vegetables	6-2025
Fruits	2-1200
Tea	150-210

The obtained values are higher than the rates reported by Golchin-Gelehdooni et al. (2014) of *V. ervilia* grain flour (202.1 mg/100g) has found amounts equal to 34-1710 and 22-102.6mg/100g for polyphenolic compounds in legumes and cereals based on dry weight [18]. Results presented in the current research paper are consistent with the other studies [19-21] and the amounts of phenolic ingredients found herein are in a range reported for polyphenolic compounds in legumes. In the study undertaken on oak, it was made clear that the fruits contain 12.33% phenolic ingredients out of which tannin and gallic acid account, respectively, for 9.06% and 0.142% [22]. It has been reported the total phenolic ingredients of crude oak fruit of *Quercus persica* to be 2.01% [23]. In addition, it was found total phenolic ingredient equal to 1.49% in such legumes as *Canavalia cathartica* and reported the total phenolic ingredients of such cereals as sorghum and wheat in a range between 1 and 2.3% and 0.07 and 1.4%, respectively [24; 25].

Total tannin (hydrolysable and dense tannins). Content of hydrolysable and dense tannins in the studied *V. ervilia* grain flour equaled to 232.54±0.29 mg/100g and 297.51±0.2 mg/100g, respectively. Amount of anti-nutritional factors in *V. ervilia* grain flour in the present study based on dry weight (mg/100g) is presented in Table 4.

Table 4 – Phenolics in *V. ervilia* grain flour based on dry weight (mg/100g)

Total phenolic content (gallic acid)	Hydrolysable tannin	Dense/ compact tannin	Canavanine
408.46±0.33	232.54±0.29	297.51±0.2	98.72±0.22

Golchin-Gelehdooni et al. [18] acquired 188.3 mg/100g and 230.2 mg/100g values for hydrolysable and dense tannins. As can be seen from the Table 4, corresponding values were lower than that.

Furthermore, in the other studies, the amounts of dense tannin in *V. ervilia* grain have been reported as 670mg/100g; 402mg/100g and in a range from 325mg/100g to 591mg/100g [26; 27]. In all of these studies, the amounts reported for dense tannins are higher than what was obtained herein. It can be related to weather conditions of the place that plants growth.

Canavanine. In the present study, the canavanine content of *V. ervilia* grain flour was equal to 98.72±0.22mg/100g. The other studies found canavanine rates of *V. ervilia* grain in ranges between 40 and 110 mg/100g, 10 and 170mg/100g, 5 and 110mg/100g and 10 and 260mg/100g [28-30].

As it can be observed in table 5, the amount of canavanine obtained in the present research paper is in the range reported by the other researchers hence consistent therewith (Table 5).

In other studies [25; 26] values equal to 76mg/100g and 78.5mg/100g correspondingly for canavanine rates of *V. ervilia* grain were reported. Their results are lower than what has been calculated herein. Generally, the difference in the amounts of anti-nutritional factors in *V. ervilia* grains, in contrast to what has been highlighted in the other studies, can be attributed to the effects of some climatic, environmental, soil and genetic conditions. Furthermore, the amount of anti-nutritional factors removal in soaking method is subject to factors like solution type, soaking duration, type of food material, solid to liquid phase ratio, temperature and solubility of the ingredients in the applied solutions [31; 32].

Table 5 – Amount of anti-nutritional factors in *V. ervilia* grain flour in various studies based on dry weight (mg/100g)

Total phenolic content	Hydrolysable tannin	Dense tannin	Canavanine	References
202.1	188.3	230.2	78.5	[25]
-	-	670	78.5	[26]
-	-	402	76	[27]
-	-	325-591	40-110	[28]
-	-	-	70-110	[28]
-	-	-	5-110	[29]
-	-	-	10-260	[30]

The content of anti-nutritional compounds in different soaking treatments.

Total phenolics content. The analysis of the results of the present study indicated that there is a significant relationship between the method of soaking from *V. ervilia* grain and the total phenolics content extracted in a 5% level (P<0.05). Results, presented in Table 6, also demonstrate significant difference between all four soaking methods in terms of reductions in the amounts of total phenolic contents of different treatments as compared to what was scored for the evidence sample.

Table 6 – The effect of various methods of soaking from *V. ervilia* grains in water and alkaline, acid and salt solutions on the anti-nutritional factors contents (mg/100g)

Treatment	Total phenolic content/gallic acid	Hydrolysable tannins	Dense/compact tannins	Canavanine
Unprocessed *V.ervilia* grains (control)	408.46±0.33[a]	232.54±0.29[a]	297.51±0.2[a]	98.72±0.22[a]
Soaking in sodium hydroxide o.5 M	[c]48.35±0.28	[c]28.29±0.06	[c]34.58±0.24	[b]32.49±0.3
Soaking in acetic acid 0.5 M	[d]63.49±0.34	[c]35.59±0.32	[d]47.72±0.22	[c]27.55±0.26
Soaking in water	[c]97.58±0.29	[c]58.41±0.25	[c]67.41±0.2	[c]11.43±0.18
Soaking in sodium chloride 5%	[b]131.45±0.27	[b]77.51±0.16	[b]87.73±0.24	[d]19.51±0.16
Note: Numbers with at least one similar letter are not statistically significant (P<0.05), where: a, b, c, and d are statistically significant (P<0.05), so that there is a difference significant between them.				

As can be seen from the Table 6, the highest reduction in phenolic content of different soaking treatments has been obtained in basic-acidic-aqueous-salty soaking methods, respectively. Basic and acidic solutions break down the plant tissues cell walls and cause the maximal discharge of anti-nutritional factors in comparison to saline and aqueous solutions.

Alkaline soaking method. Alkaline soaking method from *V. ervilia* based on offered the lowest total phenolic content (48.35±0.28 mg/100g) in contrast to those on other methods. According to the results obtained in various investigations, the extractability of the majority of phenolic ingredients, including phenolic acids and tannins, is increased in basic pH values attribute the reduction in the amount of the phenolic ingredients in basic environments to the loss of the cell walls integrity in plant tissues under basic conditions hence increase in the solubility and dispersion speed of these ingredients into the peripheral environment. Another reason for the reduction of the amounts of the phenolic ingredients and instability of them in basic environments is the essential changes created in the phenolic compounds structures as a result of absorbing electron. These changes in the phenolic compounds structure can be related to the phenolic ingredients tendency for interacting with proteins and forming complexes with them. Under basic conditions, the electrostatic interactions between polyphenols with positive charges and proteins with negative charges is increased linearly with the increase in pH as a result of which amounts of these compounds exude in the form of soluble protein-phenol complexes from plant tissues [13; 14]. Xu and Diosady [33] showed that concentration and condensation of simple phenolic ingredients is accelerated under basic conditions. The results obtained by the other researchers in using basic solutions for removing phenols and other anti-nutritional factors confirm what has been found herein. In an investigation of the effects of soaking in water and in normal basic 0.5 and 1 M sodium hydroxide on the reduction of the phenolic ingredients in two oak varieties [34] showed that normal 1 M sodium hydroxide solvent has the highest effect on the reduction of the amounts of phenolic ingredients in both Iranian oak species. To put it differently, in this study, the reductions in total phenol content were found respectively higher in soaking with various solvents, including normal 1M sodium hydroxide, water and normal 0.5 M sodium hydroxide. In another study, Ghaderi et al. [35] investigated the effect of soaking two Iranian oak varieties in water, 1M acetic acid, 1 M soda and 5% sodium chloride for the purpose of eliminating phenolic compounds from oak fruits. The results indicated that all of the processes considerably reduce the phenolic ingredients in both of the oak varieties in respect to evidence group. The highest amounts of phenolic ingredient removal from both of the oak varieties were observed respectively for soda, acetic acid, sodium chloride and water treatments and this is in compliance with what has been documented herein. Applied various concentrations (5% and 10%) of soda for reducing anti-nutritional factors from coffee indicated that the increase in soda concentration from 5% to 10% is followed by the omission of higher amounts of phenolic and tannin ingredients [36]. In other studies, the reductions equal to 21% and 64% in polyphenolic compounds were obtained for two types of plants, namely *Vigna aconitifolia* and *Vigna sinensis*, after six hours of soaking in sodium bicarbonate solution. The reductions in the polyphenolic compounds were attributed to the instability of these ingredients in higher (basic) pH values [13; 14]. Other researchers, as well, used basic solutions for the removal of anti-nutritional factors from plant food materials and delivered similar results. To eliminate polyphenolic ingredients from black-eyed peas and increase the digestibility of protein, these grains were soaked in various basic solutions like sodium hydroxide, potassium hydroxide, sodium carbonate and sodium bicarbonate for 48 hours. The highest amounts of reductions in the soaked specimens were respectively observed for sodium hydroxide, potassium hydroxide, sodium carbonate and sodium bicarbonate. In diluted basic solutions, parts of phenolic compounds are extracted in the form of soluble sodium phenate complexes. In line with the increase in the base concentration, hydroxyl groups of phenolic compounds are ionized hence other phenolic compounds become incapable of forming complexes with proteins and sodium hydroxide [37].

Acid soaking method. In this study, the obtained amount of total phenolic ingredients of the acid soaking method from *V. ervilia* grain was 63.49±0.34mg/100g. With a significant difference in 5% level, the acid treatment contains higher amount of phenolic ingredients as compared to that alkaline treatment. It attributed the reduction in the amount of phenolic ingredients in basic and acidic solutions to the loss of plant tissues cell wall integrity under basic and acidic conditions hence increase in their solubility and dispersion speed into the peripheral environment [13; 14]. Basic and acidic solutions can break the cell walls of the plant tissues thereby to release phenolic compounds. According to the obtained results, it seems that the basic treatment, in comparison to acid-

ic treatment, acts more intensively in breaking and destroying the plant tissues cell walls and resultantly maximal releasing of the phenolic ingredients. Possibly, this is one reason for the low amount of phenolic compounds in basic treatment in comparison to that in acidic treatment. The results obtained by the other researchers in using acidic solutions for removing phenols and other anti-nutritional compounds affirm the findings of the present research paper. Towo et al. [38] indicated that 70, 28, 38, 37 and 8% following 24 hours of soaking in lactic acid (0.02%) reduce the amount of phenolic ingredients extractable from red sorghum, millet, peas, mung bean and red bean, respectively. These researchers attributed the observed reductions to anthocyanidine breakdown into simpler phenols like flavan-3-ols. The results obtained by Laurena et al. [39], as well, is suggestive of the idea that various concentrations of acidic solutions like acetic acid, hydrochloric acid, sulfuric acid and home vinegar exert a large deal of effect on the reduction of phenolic ingredients in black-eyed peas. In between, the highest reduction (61%) was obtained after 24 hours of soaking in home vinegar. Acetic acid solutions, 0.05 moles, hydrochloric acid and sulfuric acid, 0.5 moles, and vinegar, 0.005 moles, have the highest effects on the exudation of these compounds and the increase in their concentrations brings augments the percentages of these grains polyphenol residues. The researchers also asserted that disregarding the percolation of the phenolic compounds from plant tissues into the acidic solution subject to concentration gradient and acceleration of soluble tannin-protein complexes formation in lower PH values, the formation of phenolic oligomers is another factor contributing to the reduction in the amounts of phenolic compounds in acid-soaked specimens because these compounds are insoluble hence immeasurable using ordinary methods. These findings are in accordance to the results obtained in the present paper. In a few number of the studies, acidic and basic and aqueous solutions were simultaneously used for the removal of phenolic or tannin compounds. A brief summary of these studies is provided as follows: It applied various solvents (sodium hydroxide, hydrochloric acid, sodium chloride and sodium sulfite) for the removal of phenolic compounds from sunflower seed cake [40]. The results indicated that sodium hydroxides, hydrochloric acid, sodium sulfite and sodium chloride respectively reduce phenolic ingredients from 4270mg/100g to 50 mg/100g, 220 mg/100g, 1995 mg/100g and 2905mg/100g. As it can be seen in table 6, the highest reduction in phenolic ingredients has been obtained in basic-acidic-saline media, respectively. In the another study, it used sodium hydroxide, hydrochloric acid and water to reduce the amounts of anti-nutritional factors in acacia leaves [41]. The results indicated that the highest reductions in polyphenols were found caused by sodium hydroxide, acid and water solutions and that these treatments reduced polyphenols for amounts equal to 74%, 69.6% and 40.9%, respectively. In another study, Shimelis et al. [42] soaked *Phaseolus vulgaris* grains in an acidic solution (citric acid), a basic solution (sodium bicarbonate) and water. These researchers stated that the highest reductions of tannin and total polyphenolic compounds in the aforesaid grains belong to basic, acidic and aqueous environments, respectively. The results of all the explored research sources approve the findings of the present study. As it is clear from the investigation of the results of the present and the other studies, the reductions observed in the amounts of phenolic compounds and tannins are higher in basic and acidic solutions than in aqueous solution. One of the most important reasons for these results pertains to the loss of cell wall integrity in acidic and basic environments hence increase in their solubility and diffusivity from the plant tissues into the peripheral environment [13; 14]. Under acidic conditions, enzymatic oxidation of phenolic compounds occurs in a lower speed. In addition, hydrolysis of polymeric phenols as well as the discharge of the ingredients bonded to the compounds existent in the cell membrane, like hydrocinnamic acid derivatives, are accelerated under such conditions. Soaking plant tissues under acidic and even aqueous conditions is accompanied by the formation of insoluble phenol oligomers. These compounds remain inside the plant tissue and their values are not taken into account in the measurements, Table 6 [43].

Methods of soaking in water and salt solution: In the present study, the total phenolic contents in the soaking procedures in water and salt solution, were respectively found equal to 97.58±0.29 mg/100g and 131.45±0.27mg/100g. As it can be seen, salt treatment contains the highest rate of total phenolic compounds, 131.45±0.27mg/100g, in contrast to the other treatments.

In the soaking procedures in water and salt solution, the observed reduction in phenolic compound rates can be attributed to the softening of the cell walls by aqueous solvent that is usually followed by an elevation in solubility of the bonded phenolic compounds [44]. Another reason for the reduction of phenolic compounds during soaking in water is the high solubility of the phenolic compounds in water and their diffusion into the aqueous environment (sa-

line solution) subject to the effect of concentration gradient hence enhancement of the cell membranes permeability [45]. Moreover, polymerization of phenolic compounds with low molecular weights and formation of insoluble compounds hence the obstruction of their exudation from the plant cells are other reasons for the observed reductions in the amounts of phenolic compounds in saline solutions. It ascribed the reductions in phenolic compounds following soaking in water to the interaction between polyphenol ingredients and proteins, carbohydrates and the subsequent formation of insoluble complexes and their conversion into an immeasurable form [13; 14]. Furthermore, these researchers pointed to the polyphenol oxidase activation and decomposition of phenolic compounds by this enzyme as another reason for the reduction of these ingredients during soaking. The results obtained by the other researchers in using saline solutions or aqueous solvents for the removal of phenols and other anti-nutritional factors confirm the findings of the present study. In another study that was conducted by Towo et al. [46], it was pointed out that red sorghum and millet grains respectively lose 23% and 19% of their phenolic compounds after 24 hours of soaking in water. These researchers considered high solubility of phenolic compounds in water and their diffusivity in aqueous medium as the most important reasons for the reductions in phenolic compounds of the specimens during soaking. The salts efficiency in extraction of phenolic compounds depends on their abilities in interfering with the ionic bonds formed between phenolic compounds and proteins and, in between them, bivalent salts exhibited larger effects.

Tannins (hydrolysable and dense tannins). The analysis of the results of the present study indicated that there is a significant relationship in a 5% level between the type of the method used for soaking from *V. ervilia* grains and the amount of tannins ($P<0.05$). The obtained results showed with a significant difference that all four methods of soaking reduce the amounts of tannins in different treatments as compared to the evidence specimen (*V. ervilia* grain flour). As it can be observed in table 6, the highest tannin reductions in different soaking treatments, has been obtained in basic-acidic-aqueous -salty soaking methods, respectively (Table 6).

It expressed that the total tannin rates of *V. aconitifolia* and *V. sinensis* are reduced by 57 and 74%, respectively, following six hours of soaking in sodium bicarbonate basic solutions. These researchers ascribed the reduction in tannin rates to their instability in higher PH values [13; 14]. In a research paper reported that such basic solutions as sodium carbonate and sodium bicarbonate are capable of reducing tannins by 40% to 50% in sorghum. It stated that oxidative polymerization of condensed tannins is accelerated under basic conditions [33].

Acid soaking method: In this study, hydrolysable and dense tannin rates of acid treatment, were 35.59±0.32mg/100g and 47.72±0.22mg/100g, respectively. It ascribed the reductions in total tannin of the basic and acidic solutions to the loss of plant tissues cell wall integrity under basic and acidic conditions hence increase in solubility and diffusivity of them into the peripheral environment. Basic and acidic solutions can break down the plant tissues cell walls thereby to discharge tannins [13; 14]. According to the results, it seems that the basic treatment, in respect to acidic treatment, acts more intensively in breaking and destroying the plant tissues cell walls and the consequent maximal discharge of tannins. This is possibly one reason for the low amount of tannins in alkaline treatment as compared to those in acidic treatment. On the contrary, the acidic treatment contains lower amounts of tannins in comparison to the aqueous and salty treatments with a significant difference in a 5% level. As it was explained previously, basic and acidic solutions break down the plant tissues cell walls and maximally release tannins in contrast to the saline and aqueous solutions hence they are more powerful in tannin extraction while the destruction of the plant tissues cell walls, playing a major role in releasing of the phenolic compounds and tannins, has been less frequently seen in aqueous and saline solutions.

Methods of soaking in water and salt solution: In this study, the amounts of hydrolysable tannin in aqueous and saline solutions were 58.41±0.25mg/100g and 77.51±0.16mg/100g, respectively. Furthermore, the amounts of dense tannins in aqueous and saline solutions were 67.41±0.20mg/100g and 87.73±0.24mg/100g, respectively. As it is observed in table 6, saline treatment contains the highest amount of total tannins (total hydrolysable and dense tannins), 165.24mg/100g, as compared to the amounts evidenced for the other treatments. One reason for the reductions in tannins rates during soaking in water is their solubility in water and diffusivity into the aqueous environment (saline solution) subject to concentration gradient hence elevation of the plants membrane permeability [47]. It applied such solutions as sodium hydroxide, hydrochloric acid and water to reduce anti-nutritional factors in acacia leaves [48]. Their results showed that the highest tannin reductions were respectively obtained for sodium

hydroxide, acid and water and that these treatments brought about reductions by 74.9%, 70.9% and 40.9%, respectively (Table 6).

Canavanine: The analysis of the present study results indicated that there is a significant difference in a 5% level between the type of the method used for soaking from *V. ervilia* grain and the amount of canavanine ($P<0.05$). The results also showed with a significant difference that all four methods of soaking reduce canavanine rates in different treatments in contrast to the evidence specimen (*V. ervilia* grain flour). As it can be seen in table 6, the highest rates of canavanine reduction in various treatments correspondingly belong to aqueous-saline-acidic-alkaline treatments. With a significant difference in 5% level, the lowest amount of canavanine reduction, 11.43±0.18mg/100g, was observed in aqueous treatment and the highest amount of canavanine reduction, 32.49±0.3mg/100g, was evidenced for alkaline treatment. The reduction in canavanine amounts in aqueous treatment, 11.43±0.18mg/100g, and in saline treatment, 19.51±0.16mg/100g, can be ascribed to the very high solubility of canavanine in water. The higher reduction in canavanine rates in aqueous treatment as compared to saline treatment is due to the very high solubility of canavanine in water (Table 6).

It soaked (drenched) *V. ervilia* grains in 1% acetic acid solutions in 40 ºC for 24 hours. These researchers reported that the actual digestion of lysine and arginine in acetic acid-treated *V. ervilia* grains is increased due to the canavanine extraction in 1% acetic acid [49]. The results obtained in these studies affirm what has been found herein. Although one of the effective and applied methods for reducing or eliminating anti-nutritional compounds in legumes is the use of thermal processes, these methods do not enable omission or reduction of canavanine from and in legumes due to its being inherently resistant to heat. On the contrary, canavanine readily dissolves in acidic and basic, especially aqueous, solutions. Therefore, canavanine rates can be reduced or eliminated in plants (legumes) by soaking and drenching them in water and acidic and basic solvents. Due to very good solubility of canavanine in water, drenching of plants in water has been put forth as one of the most effective methods of canavanine extraction and elimination from the plants [50]. Of course, it should be noted that overheating in processes and use of concentrated basic and acidic solutions for the maximal removal of anti-nutritional factors is not recommended for the degradation of the quality of such nutrients as proteins. Thus, the proper duration and temperature for the maximal elimination of these compounds should be selected so as to reduce the damage or wastage of the nutrients to the least possible extent [51].

Conclusion

Among different treatments, the highest reduction in total phenolic compounds and tannins was observed in alkaline maceration, followed by acidic, aqueous and salt saline. The alkaline soaking yielded the lowest amount of total phenolic compounds (48.35±0.28 mg/100g) and the saline soaking did the highest total phenolic compounds (131.45±0.27 mg/100g). In our study, the lowest amount of hydrolysable (28.29±0.06 mg/100g) and compact tannins (34.58±0.24 mg/100g) was observed in alkaline treatment, and saline treatment yielded the highest amount of total (hydrolysable and compact; 165.24 mg/100g) tannins compared to other treatments. According to the results of various studies, the reduction in the amount of tannins in alkaline environments is attributed to the loss of cell wall integrity of plant tissues in alkaline conditions and, consequently, to increased solubility and release rate of these compounds into the surrounding environment. In this study, the lowest amount of canavanine was observed in aqueous treatment (11.43±0.18 mg/100g) and the highest amount in alkaline treatment (32.49±0.3 mg/100g). Reducing the amount of canavanine in aqueous treatment can be attributed to the very good solubility of canavanine in water.

Generally, common processes for the reduction or removal of anti-nutritional factors from plants are heating and drenching or soaking in diluted basic and acidic solutions, saline solutions and water. In the current research paper, all of the soaking methods were found considerably reducing anti-nutritional factors in different treatments in contrast to *V. ervilia* grain flour. It was figured out herein that alkaline treatment significantly reduces such anti-nutritional factors as phenolic compounds and dense and hydrolysable tannins in a rate higher than the other methods. Furthermore, aqueous treatment was found with a significant increase in the amount of canavanine exudation from *V. ervilia* compared to other methods. Basic and acidic solutions break down the plant tissues cell walls and cause the maximal discharge of anti-nutritional factors in comparison to saline and aqueous solutions hence they enjoy a higher extractability of anti-nutritional factors whereas the plant tissues cell wall destruction that plays a special role in releasing of the phenolic compounds and tannins was less frequently seen in aqueous and saline solu-

tions. From nutritional perspectives, soaking in water and use of saline solutions is preferred to soaking in basic and acidic solutions for the latter damages to some nutrients under basic and acidic conditions.

References

1. López Barrios L., GutiérrezUribe J. A., SernaSaldívar S.O. (2014). Bioactive peptides and hydrolysates from pulses and their potential use as functional ingredients. *J Food Sci.*, vol. 79, no. 3, pp. 273-283. doi: 10.1111/1750-3841.12365.

2. Gholamali Pouralamdari A. Karamatlou M., Bayat Kouhsar J. (2014). hydrolysis of organic ingredients in two oak varieties from north and western Iran and the effect of soaking with basic and aqueous solutions on the reduction of phenolic compounds. *J Iran Plant Ecophysiol Res.*, vol. 34, no. 2, pp. 1-10

3. Abdullah A.Y., Muwalla M. M., Qudsieh R. I., Titi, H.H. (2010). Effect of bitter vetch (Vicia ervilia) seeds as a replacement protein source of soybean meal on performance and carcass characteristics of finishing Awassi lambs. *Trop Anim Health Prod*., vol. 42, no. 2, pp. 293-300. doi: 10.1007/s11250-009-9420-x.

4. Larbi A., El-Moneim A.A., Nakkoul H., Jammal B., Hassan S. (2011). Intra-species variations in yield and quality determinants in Vicia species: 1. Bitter vetch (Vicia ervilia L.). *Anim Feed Sci Technol*., vol. 165, no. 3-4, pp. 278-287. doi: 10.1016/j.anifeedsci.2010.09.004.

5. Arabestani A., Kadivar M., Amoresano A., Illiano A., Di Pierro P., Porta R. (2016). Bitter vetch (Vicia ervilia) seed protein concentrate as possible source for production of bilayered films and biodegradable containers. *Food Hydrocoll.*, vol. 60, pp. 232-242. doi: 10.1016/j.foodhyd.2016.03.029.

6. Mejri S., Mabrouk Y., Voisin M., Delavault P., Simier P., Saidi M., Belhadj O. (2012). Variation in quantitative characters of faba bean after seed irradiation and associated molecular changes. *Afr J Biotechnol.*, vol. 11, no. 33, pp. 8383-8390. doi:10.5897/AJB11.291.

7. Ozcan H. M., Sagiroglu A. (2014). Fresh broad (Vicia faba) tissue homogenate-based biosensor for determination of phenolic compounds. *Artif. Cells Nanomed Biotechnol*., vol. 42, no. 4, pp. 256-261. doi: 10.3109/21691401.2013.764313.

8. Suresh Rajabhau B. (2014). Texturization, functional properties and utilization of proteins from plant sources in cereal products (doctoral dissertation, Punjab Agricultural University, Ludhiana). pp. 97-100.

9. Mushi J.A. (2011). Determination of physical properties of soybean, design and fabrication of improved soybean dehuller (doctoral dissertation, Sokoine University of Agriculture). pp. 15-25.

10. Mikić A. (2015). Fragmenta excerpti de thesauri leguminosarum: Three of the world's first domesticated plants in the Indo-European languages of Europe. *Ratar Povrt.*, vol. 52, no. 2, pp. 44-51. doi:10.5937/ratpov52-7634.

11. Dimovska V., Ilieva F., Gunova N., Gunova V. (2016). Correlation between climatic condition, yield and chemical compositiion in must on three grapes variety. In: Book of proceedings, VII International Scientific Agriculture Symposium "Agrosym 2016", pp. 1079-1084.

12. Bryant J.A., Hughes S. G. (2011). Vicia. In: Wild Crop Relatives: Genomic and Breeding Resources. Springer, Berlin, Heidelberg, pp. 273-289.

13. Vijayakumari K., Siddhuraju P., Pugalenthi M., Janardhanan K. (1998). Effect of soaking and heat processing on the levels of antinutrients and digestible proteins in seeds of Vigna aconitifolia and Vigna sinensis. *Food Chem.*, vol. 63, no. 2, pp. 259-264. doi: 10.1016/S0308-8146(97)00207-0.

14. Vadivel V., Janardhanan K., Vijayakumari K. (1998). Diversity in swordbean (Canavalia gladiata (Jacq.) DC.) collected from Tamil Nadu, India. *Genetic Res Crop Evol.*, vol. 45, no.1, pp. 63-68. doi: 10.1023/A:100863810.

15. Meera M. (2016). Pharmacognostic studies and evaluation of anti-inflammatory, analgesic and antioxidant potential of Manjakantha (Dracaena terniflora Roxb.) (doctoral dissertation, College of Agriculture, Vellayani). pp. 20-40.

16. Granato D., Shahidi F., Wrolstad R., Kilmartin P., Melton L.D., Hidalgo F.J., et al. (2018) Antioxidant activity, total phenolics and flavonoids contents: Should we ban in vitro screening methods? *Food Chem*., vol. 264, pp. 471-475. doi: 10.1016/j.foodchem.2018.04.012.

17. Nóbrega J.A., Sturgeon R.E., Grinberg P., Gardner G.J., Brophy C.S., Garcia EE. (2011). UV photochemical generation of volatile cadmium species. *J Anal At Spectr.*, vol. 26, no. 12, pp. 2519-2523. doi: 10.1039/C1JA10252D.

18. Golchin-Gelehdooni S., Shawrang P., Nikkhah A., Sadeghi A. A., Teimouri-Yansari A. (2014). Effect of extrusion and conventional processing methods on the levels of anti-nutrients factors and digestibility of bitter vetch (vicia ervilia) seeds in broilers. *Iran J Appl Ani Sci.*, vol. 4, no. 4, pp. 835-842.

19. Bravo L. (1998). Polyphenols: chemistry, dietary sources, metabolism, and nutritional signifi-

cance. *Nutr Rev.*, vol. 56, no. 11, pp.317-333. doi: 0.1111/j.1753-4887.1998.tb01670.x.

20. Ignat I., Volf I., Popa V.I. (2011). A critical review of methods for characterisation of polyphenolic compounds in fruits and vegetables. *Food Chem*., vol. 126, no. 4, pp. 1821-1835. doi: 10.1016/j.foodchem.2010.12.026.

21. Del Río M., Pretzsch H., Ruíz-Peinado R., Ampoorter E., Annighöfer P., Barbeito I., Fabrika M. (2017). Species interactions increase the temporal stability of community productivity in Pinus sylvestris – *Fagus sylvatica* mixtures across Europe. *J Ecol.*, vol. 105, no. 4, pp. 1032-1043. doi: 10.1111/1365-2745.12727.

22. Khattab R.Y., Arntfield S. D. (2009). Nutritional quality of legume seeds as affected by some physical treatments 2. Antinutritional factors. *LWT-Food Sci Technol.*, vol. 42, no. 6, pp. 1113-1118. doi: 10.1016/j.lwt.2009.02.004.

23. Aboutorab N., Mohammadi A. (2008). Design and analysis of wireless systems using CAC and M-QAM adaptive modulation for throughput improvement. 4th IEEE International Conference on Circuits and Systems for Communications. pp. 255-259. doi: 10.1109/ICSC.2008.60.

24. Seena S., Sridhar K. R. (2005). Physico-chemical, functional and cooking properties of under explored legumes, Canavalia of the southwest coast of India. *Food Res Int.*, vol. 38, no.7, pp. 803-814. doi: 10.1016/j.foodres.2005.02.007.

25. Santhanam R., Ramesh S., Suleria H. A. R. (2018). Biology and Ecology of Pharmaceutical Marine Plants. CRC Press. pp. 124-298.

26. Sadeghi P., Kennedy R.A., Rapajic P.B., Shams R. (2008). Finite-state Markov modeling of fading channels-a survey of principles and applications. *IEEE Signal Process Mag.*, vol. 25, no. 5, pp. 57-80. doi: 10.1109/MSP.2008.926683.

27. Johnston S., Pippen Jr, J., Pivot X., Lichinitser M., Sadeghi S., Dieras V., Press, M. F. (2009). Lapatinib combined with letrozole versus letrozole and placebo as first-line therapy for postmenopausal hormone receptor-positive metastatic breast cancer. *J. Clin Oncol.*, vol. 27, no. 33, pp. 5538-5546. doi: 10.1200/JCO.2009.23.3734.

28. Abbo S., Berger J., Turner N. C. (2003). Evolution of cultivated chickpea: four bottlenecks limit diversity andĀ constrain adaptation. *Func Plant Biol.*, vol. 30, no. 10, pp. 1081-1087.

29. Megías C., Cortés-Giraldo I., Giron-Calle J., Alaiz M., Vioque J. (2016). Free amino acids, including canavanine, in the seeds from 32 Vicia species belonging to subgenus Vicilla. *Biocatal Agric Biotechnol*., vol. 8, pp. 126-129. doi: 10.1016/j.bcab.2016.09.001.

30. Martín-Pedrosa M., Varela A., Guillamon E., Cabellos B., Burbano C., Gomez-Fernandez J., et al. (2016). Biochemical characterization of legume seeds as ingredients in animal feed. *Spanish J Agric Res.*, vol. 14, no. 1, pp. 0901. doi: 10.5424/sjar/2016141-7450.

31. Huma N., Anjum M., Sehar S., Issa Khan M., Hussain S. (2008). Effect of soaking and cooking on nutritional quality and safety of legumes. *Nutr Food Sci.*, vol. 38, no. 6, pp. 570-577. doi: 10.1108/00346650810920187.

32. Aider, M., De Halleux, D. (2009). Cryo-concentration technology in the bio-food industry: Principles and applications. *LWT-Food Sci Technol.*, vol. 42, no. 3, pp. 679-685. doi: 10.1016/j.lwt.2008.08.013.

33. Xu, L., Diosady, L. L. (2000). Interactions between canola proteins and phenolic compounds in aqueous media. *Food Res Int.*, vol. 33, no. 9, pp. 725-731. doi: 10.1016/S0963-9969(00)00062-4.

34. Gholamalipour A. E., Keramatloo M., Byat K. J. (2014). Analysis of organic compounds of two species of oak fruit (Quercus castaneifolia Ca Mey. and Quercus persica Jaub Spach.) in two regions of north and west of iran and studying the decreasing effect of soaking methods with alkaline solutions and water on phenolic compound contents. *J Plant Environ Physiol.*, vol. 9, no. 2, pp. 1-10.

35. Ghaderi G. M., Mamashloo S., Sadeghi M. A., Alami M. (2011). Evaluation of antioxidant activity, reducing power and free radical scavenging of different extract of *Artemisia annua* L. *J Plant Environ Physiol.*, vol. 6, no. 1, pp. 46-57.

36. Rojas J. U., Verreth J. A. J., Van Weerd J. H., Huisman E. A. (2002). Effect of different chemical treatments on nutritional and antinutritional properties of coffee pulp. Anim. *Feed Sci Technol.*, vol. 99, no.1-4, pp. 195-204. doi: 10.1016/S0377-8401(02)00050-0.

37. Towo, E., Kamala, A. (2003). Phenolic compounds, phytate, citric acid and the in-vitro iron accessibility of cowpeas, mung beans and four varieties of kidney beans. *Afr J Food Agric Nutr Dev.*, vol. 3, no. 1, pp. 53-59.

38. Ibrahim S., Habiba R., Shatta A., Embaby H. (2002). Effect of soaking, germination, cooking and fermentation on antinutritional factors in cowpeas. *Food*, vol. 46, no. 2, pp. 92-95.

39. Gandhi N.S., Mancera R.L. (2008). The structure of glycosaminoglycans and their interac-

tions with proteins. *Chem Boil Drug Des.*, vol. 72, no. 6, pp. 455-482.

40. Maloney J. H., Peppler K., Kafai Y., Resnick M., Rusk N. (2008). Programming by choice: urban youth learning programming with scratch. Presented at SIGCSE Annual Meeting. pp. 367-371.

41. Shimelis E. A., Rakshit S. K. (2007). Effect of processing on antinutrients and in vitro protein digestibility of kidney bean (*Phaseolus vulgaris* L.) varieties grown in East Africa. *Food Chem.*, vol.103, no.1, pp. 161-172. doi: 10.1016/j.foodchem.2006.08.005.

42. Egounlety M., Aworh O. (2003). Effect of soaking, dehulling, cooking and fermentation with Rhizopus oligosporus on the oligosaccharides, trypsin inhibitor, phytic acid and tannins of soybean (*Glycine max* Merr.), cowpea (*Vigna unguiculata* L. Walp) and groundbean (*Macrotyloma geocarpa* Harms). *J Food Eng.*, vol.56, no. 2-3, pp. 249-54. doi: 10.1016/S0260-8774(02)00262-5.

43. Mujica M. V., Granito M., Soto N. (2009). Importance of the extraction method in the quantification of total phenolic compounds in *Phaseolus vulgaris* L. *Interciencia*, vol. 34, no. 9, pp. 650-654.

44. Friedman, M., Jürgens, H. S. (2000). Effect of pH on the stability of plant phenolic compounds. *J Agric Food Chem.*, vol. 48, no. 6, pp. 2101-2110. doi: 10.1021/jf990489j.

45. Towo E.E., Svanberg U., Ndossi G.D. (2003). Effect of grain pre-treatment on different extractable phenolic groups in cereals and legumes commonly consumed in Tanzania. *J Sci Food Agric.*, vol. 83, no. 9, pp. 980-986. doi: 10.1002/jsfa.1435.

46. Cuevas M. S., Rodrigues C. E., Meirelles A. J. (2009). Effect of solvent hydration and temperature in the deacidification process of sunflower oil using ethanol. *J Food Eng.*, vol. 95, no. 2, pp. 291-297. doi: 10.1016/j.jfoodeng.2009.05.009.

47. Valdés S.T., Coelho C.M.M., Michelluti D.J., Tramonte V.L.C.G. (2011). Association of genotype and preparation methods on the antioxidant activity, and antinutrients in common beans (Phaseolus vulgaris L.). *LWT-Food Sci Technol.*, vol. 44, no. 10, pp. 2104-2111. doi: 10.1016/j.lwt.2011.06.014.

48. Douglas, I., Alam, K., Maghenda, M., Mcdonnell, Y., McLean, L., Campbell, J. (2008). Unjust waters: climate change, flooding and the urban poor in Africa. *Environ Urban.*, vol. 20, no.1, pp. 187-205. doi: 10.1177/0956247808089156

49. Sridhar K. R., Seena S. (2006). Nutritional and antinutritional significance of four unconventional legumes of the genus *Canavalia* – a comparative study. *Food Chem.*, vol. 99, no.2, pp.267-288. doi: 10.1016/j.foodchem.2005.07.049.

50. Ekanayake S., Skog K., Asp N.-G. (2007). Canavanine content in sword beans (*Canavalia gladiata*): analysis and effect of processing. *Food Chem Toxicol*., vol. 45, no. 5, pp. 797-803. doi: 10.1016/j.fct.2006.10.030.

51. Guillon F., Champ M. J. (2002). Carbohydrate fractions of legumes: uses in human nutrition and potential for health. *Br J Nutr.*, vol. 88, no. 3, pp. 293-306. doi: 10.1079/BJN2002720.

IRSTI 34.15.23; 34.15.25; 34.31.27; 34.31.31

*[1]A.K. Rakhmetullina, [2]M. Régnier, [1]A.T. Ivashchenko

[1]al-Farabi Kazakh National University, Almaty, Kazakhstan
[2] Ecole Polytechnique, Paris, France
*e-mail: zhanullina1994@gmail.com

The characteristics of miRNA binding sites with mRNA of MYB plant transcription factors

Abstract: miRNA regulates the expression of a large number of genes, including plant transcription factors. It is important to reveal miRNA associations with the corresponding targets in order to increase plant productivity and resistance to biotic and abiotic stresses. One of such targets is the group of MYB transcription factor genes, involved in the regulation of some of the most important physiological processes. The search for miRNA target genes was performed using the MirTarget program, which calculates the free energy (ΔG) of miRNA binding with mRNA; position and schemes of the potential binding sites. The relative amount of free energy (ΔG/ΔGm) was used as a comparative criterion for evaluating the degree of interaction of miRNA and mRNA. The binding sites for tae-miR1127b-3p, tae-miR159a,b-3p, tae-miR164-5p, tae-miR171a-3p, tae-miR319-3p, tae-miR397-3p, tae-miR444a,b-3p, tae-miR5084-3p, tae-miR531-5p, tae-miR5384-3p, tae-miR9652-5p, tae-miR9663-5p, tae-miR9666a-3p, tae-miR9676-5p, tae-miR9778-5p, tae-miR9779-3p, tae-miR9780-3p were found in mRNAs of 258 MYB family genes in *Triticum (T.) aestivum*. miRNAs orthologs of *T. aestivum*, *Arabidopsis thaliana*, *Zea mays* and *Oryza sativa* had binding sites in mRNAs of MYB family genes of these and other plant species. tae-miR159a,b-3p binding sites are located in the CDS and encode the WSSIRSK oligopeptide, conserved in the proteins of the MYB transcription factors of 22 plant species. Amino acid sequences of the MYB family proteins containing ELPSNQ oligopeptide are encoded by tae-miR159a,b-3p binding sites located in the third open reading frame in the mRNAs of the other 20 plant species. For each miRNA, groups of target genes of transcription factors are established. The schemes of interaction of the nucleotide sequences of the studied miRNAs with the nucleotide sequences of the mRNA genes of the transcription factors of the MYB family were constructed. Considered associations of miRNAs and genes can be used as markers of control of plant physiological processes in plant growth selection and regulation.
Key words: miRNA, mRNA, gene, binding site, oligopeptide, plant, transcription factor, MYB.

Introduction

Regulation of gene expression on transcriptional level facilitates large number of important biological processes, including responses to different kinds of biotic and abiotic stresses, growth and development, differentiation, metabolism and other [1-5]. Transcription factors (TFs) play significant role in regulation of cellular processes. MYB proteins are among the most well-known, characterized by their highly conserved domains. A number of studies has shown that miRNAs can influence physiological processes in plants by miRNAs [6-10]. The established regulatory roles of miRNAs in gene expression unveil new opportunities to control plant productivity and resistance [11-14]. Nevertheless, in these works, no direct association of miRNAs with mRNAs of MYB transcription factors was not established. Therefore, the principal goal of our research was to establish miRNA associations and their MYB target genes using bioinformatic approaches, which in turn leads to significant reductions in material costs of search for such associations.

The MirTarget program that we created allows us to work with a large number of genes and miRNAs, predicting with high precision the associations of miRNAs and their target genes [15; 16].

In the present work, we focused on identification of miRNAs that have potential to bind to the mRNA genes of the MYB family in *Triticum (T.) aestivum*, *Oryza (O.) sativa, Arabidopsis (A.) thaliana and Zea (Z.) mays.*

Materials and methods

Nucleotide sequences of MYB genes of *T. aestivum, O. sativa, A. thaliana and Z. mays* were obtained from Plant Transcription Factor Database v.4.0 (http://planttfdb.cbi.pku.edu.cn/index.php; http://www.ncbi.nlm.nih.gov). Nucleotide sequences of miRNAs in genomes of studied plants were obtained from the database miRBase v.22 (http://www.mirbase.org/). The search for miRNA target genes was determined using the MirTarget program [15; 16]. It calculates the free energy (Δ*G*, kJ/mole) of miRNA binding, the relative value of free energy (ΔG/ΔGm, %), the position and schemes of potential binding sites (BSs). The ΔGm for miRNA binding was defined as the free energy of miRNA binding to the fully complementary nucleotide sequence. Relative amount of free energy (ΔG/ΔGm) was used as a comparative criterion to evaluate the degree of interaction of miRNA and mRNA. Unique properties of MirTarget program include consideration of nucleotide interaction in miRNA with mRNA of target genes not only between adenine (A) and uracil (U), guanine (G) and cytosine (C), but also between A and C, G and U via single hydrogen bond [17; 18]. The distance between A-C and G-U is equal to distance value between G-C and A-U.

List of abbreviated names of plant species of the following transcription factors were used in this work: *Aegilops tauschii – Ata, Aethionema arabicum – Aar, Arabidopsis halleri – Aha, Arabidopsis lyrata – Aly, Arabidopsis thaliana – Ath, Arabis alpina – Aal, Boechera stricta – Bst, Brachypodium distachyon – Bdi, Brachypodium stacei – Bsa, Brassica napus – Bna, Camelina sativa – Csa, Dichanthelium oligosanthes – Dol, Eragrostis tef – Ete, Leersia perrieri – Lpe, Musa acuminata – Mac, Oryza barthii – Oba, Oryza brachyantha – Obr, Oryza glaberrima – Ogl, Oryza glumaepatula – Ogu, Oryza longistaminata – Olo, Oryza meridionalis – Ome, Oryza nivara - Oni, Oryza punctata – Opu, Oryza rufipogon – Oru, Oryza sativa subsp. japonica – Osa j, Panicum hallii – Pha, Raphanus raphanistrum – Rra, Raphanus sativus – Rsa, Setaria italica – Sit, Setaria viridis – Svi, Sorghum bicolor – Sbi, Tarenaya hassleriana – Tha, Triticum aestivum – Tae, Zea mays – Zma.*

Results and discussion

Study of 125 miRNAs binding to mRNAs of 258 MYB family genes of *T. aestivum* revealed that only 34 genes were targets for 19 miRNA (Table 1).

Table 1 – Characteristics of miRNA BSs in CDS mRNA of MYB transcription factors genes of *T. aestivum*

Gene	miRNA	Start of site, nt	ΔG, kJ/mole	ΔG/ΔGm, %	Length, nt
Traes_2BL_79F1B50DF.1	tae-miR1127b-3p	706	-96	87	21
Traes_2AL_41B71F83C.1	tae-miR1127b-3p	691	-96	87	21
Traes_6DS_A0EC5D808.1	tae-miR159a,b-3p	688	-100	90	21
TRAES3BF027700010CFD_t1	tae-miR159a,b-3p	956	-98	88	21
Traes_2DL_912473A86.1	tae-miR159a,b-3p	54	-98	88	21
Traes_2BL_855A1170C.2	tae-miR159a,b-3p	141	-98	88	21
Traes_2AL_0A21FB42C.1	tae-miR159a,b-3p	141	-98	88	21
Traes_6AS_5562B97F7.1	tae-miR159a,b-3p	760	-96	87	21
Traes_1BL_CF98E922B.1	tae-miR159a,b-3p	839	-96	87	21
TRAES3BF034000040CFD_t1	tae-miR164-5p	629	-102	87	21
Traes_2BL_7CEC6A8D7.1	tae-miR164-5p	545	-102	87	21
Traes_2BL_03F3475CD.1	tae-miR164-5p	545	-102	87	21
Traes_2AL_AF9357B4C.1	tae-miR164-5p	548	-102	87	21
Traes_2AL_962A9D448.1	tae-miR164-5p	545	-102	87	21
Traes_1DS_5EEED86AD.2	tae-miR171a-3p	232	-96	87	21
Traes_1BS_403DBC53C.1	tae-miR171a-3p	577	-96	87	21
Traes_1AS_61D017632.2	tae-miR171a-3p	577	-96	87	21
TRAES3BF027700010CFD_t1	tae-miR319-3p	955	-102	89	21
Traes_1BL_CF98E922B.1	tae-miR319-3p	838	-102	89	21

Continuation of table 1

Gene	miRNA	Start of site, nt	ΔG, kJ/mole	ΔG/ΔGm, %	Length, nt
Traes_4DS_7BFAC49C2.1	tae-miR397-3p	206	-104	89	21
TRAES3BF024100110CFD_t1	tae-miR444a,b-3p	707	-100	87	21
TRAES3BF012200030CFD_t1	tae-miR444a,b-3p	1151	-100	87	21
Traes_3B_934488D20.1	tae-miR444a,b-3p	1106	-100	87	21
Traes_3AL_152A7186A.1	tae-miR444a,b-3p	1052	-100	87	21
Traes_7DS_E27ECBC6E.1	tae-miR5084-3p	464	-106	86	24
Traes_7BS_D28CCE3B8.1	tae-miR5084-3p	413	-106	86	24
Traes_7AS_A337F362A.1	tae-miR5084-3p	413	-106	86	24
TRAES3BF026500080CFD_t1	tae-miR531-5p	157	-110	90	21
Traes_2DS_61B920833.1	tae-miR5384-3p	502	-108	89	21
TRAES3BF063000030CFD_t1	tae-miR9652-5p	214	-93	86	22
TRAES3BF026500080CFD_t1	tae-miR9663-5p	652	-96	87	21
Traes_2BL_361925B62.1	tae-miR9666a-3p	407	-106	88	21
Traes_7DL_5BD0D4BD1.1	tae-miR9676-5p	439	-104	87	22
Traes_7AL_04D939077.1	tae-miR9676-5p	439	-104	87	22
Traes_5BL_C1D4586B1.2	tae-miR9778-5p	431	-98	87	21
TRAES3BF012200020CFD_t1	tae-miR9779-3p	284	-96	92	20
Traes_2DS_3F5D36630.1	tae-miR9780-3p	958	-115	90	21

tae-miR1127b-3p, tae-miR159a,b-3p, tae-miR164-5p, tae-miR171a-3p, tae-miR319-3p, tae-miR397-3p, tae-miR444a,b-3p, tae-miR5084-3p, tae-miR531-5p, tae-miR5384-3p, tae-miR9652-5p, tae-miR9663-5p, tae-miR9666a-3p, tae-miR9676-5p, tae-miR9778-5p, tae-miR9779-3p, tae-miR9780-3p bind with mRNAs of these genes. For tae-miR159a, b-3p, there are 10 target genes with ΔG/ΔGm value ranging from 86 to 92%. tae-miR164-5p and tae-miR444a,b-3p had five and four target genes with ΔG/ ΔGm value of 87%. tae-miR171a-3p and tae-miR5084-3p bind to mRNAs of three MYB genes. ΔG/ΔGm value of interaction of tae-miR171a-3p and tae-miR5084-3p with mRNA of these genes was 87% and 86%, respectively. tae-miR1127b-3p, tae-miR319-3p tae-miR9676-5p had BSs in the mRNA of two target genes. The remaining miRNAs had only one target genes with a ΔG/ΔGm value ranging from 87 to 92%. The miRNA BSs in the mRNA genes of the MYB family of *T. aestivum* are located only in the coding sequence (CDS).

Not only MYB family genes of *T. aestivum*, but also genes of other plant species were targets for miRNAs. For instance, tae-miR159a,b-3p has binding sites in the mRNAs of *T. aestivum* Traes_2DL_912473A86.1, Traes_2BL_855A1170C.2, Traes_2AL_0A21FB42 C.1 genes as well as in *O. sativa* LOC_Os04g46384.1 gene, *A. thaliana* AT3G60460.1 gene, and *Z. mays* GRMZM2G311059_P01, GRMZM2G046443_P01 genes, which are the members of the MYB family of these plant species (Table 2).

Since the characteristics of miRNA159-3p interaction with mRNA genes of different plant species were close, here we provide data only for the miR159-3p family. The interaction patterns of the nucleotide sequences of miRNA with the mRNAs of these genes are presented in Figure 1.

It is important to note that the nucleotide sequence of tae-miR159a,b-3p is similar in the *T. aestivum*, *O. sativa, A. thaliana* and *Z. mays* genomes in which it was found (miRBase).

Six miRNAs of the zma-miR159a,c,d,f,j,k-3p family were bound to mRNAs of GRMZM2G311059_P01 and GRMZM2G046443_P01 genes with a ΔG/ΔGm value of 87 – 89%. Three members of ath-miR159a,b,c-3p family were bound to mRNA of AT3G60460.1 gene with a ΔG/ΔGm value of 86% and above. Two miRNAs of the osa-miR159a.1,f-3p and tae-miR159a,b-3p had two and three target genes, respectively (Table 2). The tae-miR159a,b-3p binding sites are located in the CDS and encode the WSSIRSK oligopeptide, which is conserved in the 27 proteins of the MYB transcription factors for 22 plant species (Table 3).

Table 2 – Characteristics of miR159-3p BSs in CDS mRNA of MYB transcription factors genes of *T. aestivum*, *O. sativa, A.thaliana*, *Z. mays*

Gene	miRNA	Start site, nt	ΔG, kJ/mole	ΔG/ΔGm, %
Traes_2DL_912473A86.1	tae-miR159a,b-3p	54	-98	88
Traes_2BL_855A1170C.2	tae-miR159a,b-3p	141	-98	88
Traes_2AL_0A21FB42C.1	tae-miR159a,b-3p	141	-98	88
LOC_Os04g46384.1	osa-miR159f-3p	199	-100	90
LOC_Os04g46384.1	osa-miR159a.1-3p	198	-98	88
AT3G60460.1	ath-miR159a-3p	182	-98	90
AT3G60460.1	ath-miR159c-3p	182	-98	88
AT3G60460.1	ath-miR159b-3p	182	-93	86
GRMZM2G311059_P01	zma-miR159a,f,j,k-3p	1393	-98	88
GRMZM2G311059_P01	zma-miR159c,d-3p	1394	-100	89
GRMZM2G046443_P01	zma-miR159c,d-3p	292	-100	89
GRMZM2G046443_P01	zma-miR159a,f,j,k-3p	292	-96	87

Gene,miRNA, site,region of mRNA, characteristics of binding	Gene,miRNA, site,region of mRNA, characteristics of binding
Traes_2DL_912473A86.1, tae-miR159b-3p, 55, -96, 87 5'-U**G**GAGCUCCAUUC**G**AUCCAAA-3' 3'-G**U**CUCGAGGGAAG**U**UAGGUUU-5'	AT3G60460.1, ath-miR159c-3p, 182, -98, 88 5'-UGGAGCUCCAUUC**G**AUCCAAA-3' 3'-UCCUCGAGGGAAG**U**UAGGUUU-5'
Traes_2BL_855A1170C.2, tae-miR159b-3p, 142, -66, 87 5'-U**G**GAGCUCCAUUCGAUCCAAA-3' 3'-G**U**CUCGAGGGAAGUUAGGUUU-5'	GRMZM2G311059_P01, zma-miR159a-3p, 1394, -96, 87 5'-**UG**GAGCUCCAUUC**G**AUCCAAA-3' 3'-**GU**CUCGAGGGAAG**U**UAGGUUU-5'
LOC_Os04g46384.1, osa-miR159a.1-3p, 198, -98, 88 5'-CUGGAGCUCCAUUC**G**AUCCAAA-3' 3'-GUC-UCGAGGGAAG**U**UAGGUUU-5'	GRMZM2G311059_P01, zma-miR159f-3p, 1394, -96, 87 5'-**UG**GAGCUCCAUUC**G**AUCCAAA-3' 3'-**GU**CUCGAGGGAAG**U**UAGGUUU-5'
LOC_Os04g46384.1, osa-miR159f-3p, 199, -100, 90 5'-U**G**GAGCUCCAUUC**G**AUCCAAAG-3' 3'-A**U**CUCGAGGGAAG**U**UAGGU-UC-5'	GRMZM2G311059_P01, zma-miR159j-3p, 1394, -96, 87 5'-**UG**GAGCUCCAUUC**G**AUCCAAA-3' 3'-**GU**CUCGAGGGAAG**U**UAGGUUU-5'
AT3G60460.1, ath-miR159a-3p, 182, -98, 90 5'-U**G**GAGCUCCAUUC**G**AUCCAAA-3' 3'-A**U**CUCGAGGGAAG**U**UAGGUUU-5'	GRMZM2G046443_P01, zma-miR159a-3p, 292, -96, 87 5'-**UG**GAGCUCCAUUC**G**AUCCAAA-3' 3'-**GU**CUCGAGGGAAG**U**UAGGUUU-5'
AT3G60460.1, ath-miR159b-3p, 182, -93, 86 5'-U**G**GAGCUCCAUUC**G**AUCCAAA-3' 3'-U**U**CUCGAGGGAAG**U**UAGGUUU-5'	GRMZM2G046443_P01, zma-miR159j-3p, 292, -96, 87 5'-**UG**GAGCUCCAUUC**G**AUCCAAA-3' 3'-**GU**CUCGAGGGAAG**U**UAGGUUU-5'
The bold type indicates the nucleotide of non-canonical pairs U-G, A-C.	

Figure 1 – Schemes of miR159-3p interaction with mRNAs of MYB transcription factor genes in *T. aestivum*, *O. sativa, A.thaliana*, *Z. mays*

Table 3 – The variability of amino acid sequences of the MYB family proteins containing oligopeptide WSSIRSK encoded by the binding sites of miR159-3p in the mRNA of genes

Gene	Abbreviated names	Region of transcription factor containing oligopeptide WSSIRSK
GRMZM2G311059_P01	*Zma*	LLRHVLVHGPRD**WSSIRSK**GFLPRTGKSCRL
GRMZM2G046443_P01	*Zma*	LRRHVMENGPRE**WSSIRSK**GLLPRTGKSCRL
LOC_Os04g46384.1	*Osaj*	LLEHVRTHGPMD**WSSIRSK**GLLPRTGKSCRL
Traes_2DL_912473A86.1	*Tae*	LLEHVRTHGPRD**WSSIRSK**GALQRTGKSCRL
Traes_2BL_855A1170C.2	*Tae*	LLEHVRTHGPRD**WSSIRSK**GALQRTGKSCRL
Traes_2DL_912473A86.1	*Tae*	LLEHVRTHGPRD**WSSIRSK**GALQRTGKSCRL
Traes_2BL_855A1170C.2	*Tae*	LLEHVRTHGPRD**WSSIRSK**GALQRTGKSCRL
Traes_2AL_0A21FB42C.1	*Tae*	LLEHVRTHGPRD**WSSIRSK**GALQRTGKSCRL
AT3G60460.1	*Ath*	LINHVKRYGPRD**WSSIRSK**GLLQRTGKSCRL
Bradi5g17600.2.p	*Bdi*	LLEHVRTHGPCD**WSSIRSK**GILPRTGKSCRL
Brast09G163900.1.p	*Bsa*	LLEHVRAHGPCD**WSSIRSK**GILPRTGKSCRL
Do012459.1	*Dol*	LLEHVRAHGPCD**WSSIRSK**GLLPRTGKSCRL
462873087	*Ete*	LREHVRTHGPRD**WSSIRSK**GLLPRTGKSCRL
LPERR04G16870.1	*Lpe*	LREHVRTHGPRE**WSSIRSK**VGLPRTGKSCRL
GSMUA_Achr1P01660_001	*Mac*	LMEYVRKHGPRD**WSSIRSK**GLLARTGKSCRL
OBART04G20790.1	*Oba*	LLEHVRTHGPMD**WSSIRSK**GLLPRTGKSCRL
OB04G27810.1	*Obr*	LLQHVRAHGPMD**WSSIRSK**GLLPRTGKSCRL
ORGLA04G0178400.1	*Ogl*	LLEHVRTHGPMD**WSSIRSK**GLLPRTGKSCRL
OGLUM04G20730.1	*Ogu*	LLEHVRTHGPMD**WSSIRSK**GLLPRTGKSCRL
KN540032.1_FGP006	*Olo*	LLEHVRTHGPMD**WSSIRSK**GLLPRTGKSCRL
OMERI04G17240.1	*Ome*	LLEHVRTHGPMD**WSSIRSK**GLLPRTGKSCRL
OPUNC04G18480.1	*Opu*	LLEHVRTHGPMD**WSSIRSK**GLLPRTGKSCRL
ORUFI04G22380.1	*Oru*	LLEHVRTHGPMD**WSSIRSK**GLLPRTGKSCRL
Pahal.F00780.1	*Pha*	LLRHVREHGPRE**WSSIRSK**GLLPRTGKSCRL
Sobic.006G169700.1.p	*Sbi*	LLEHVRVHGPRD**WSSIRSK**GFLPRTGKSCRL
Seita.6G211500.1.p	*Sit*	LLRHVREHGPRE**WSSIRSK**GLLPRTGKSCRL
Sevir.6G218900.1.p	*Svi*	LLRHVREHGPRE**WSSIRSK**GLLPRTGKSCRL

The zma-miR159c,d,e,f,j,k-3p family consists of zma-miR159c,d-3p, zma-miR159e-3p and zma-miR159f,j,k-3p different in 5’ and 3’ ends of nucleotide sequences. Therefore, their binding sites are identical. Table 4 shows the binding characteristics of mir159-3p with the mRNA of MYB family genes. All sites are located in the CDS of the mRNA target. The binding characteristics of miR159-3p in the mRNAs CDS of Traes_6DS_A0EC5D808.1, AT2G32460.1, AC217264.3_FGP005, GRMZM2G070523_P01 genes are shown on Figure 2.

The nucleotide sequences of miR159-3p interacted along the entire length with the corresponding mRNA. Data from the analysis of miR159-3p binding to the mRNA of 23 genes in 20 plant species are listed in Table 5.

Table 4 – Characteristics of miR159-3p BSs in CDS mRNA of MYB transcription factors genes of *T. aestivum*, *O. sativa, A.thaliana*, *Z. mays*

Gene	miRNA	Start site, nt	ΔG, kJ/mole	ΔG/ΔGm, %
AT2G32460.1	ath-miR159a-3p	1016	-100	92
AT2G32460.1	ath-miR159b-3p	1016	-96	88
LOC_Os06g46560.1	osa-miR159d-3p	1064	-100	89
Traes_6DS_A0EC5D808.1	tae-miR159a,b-3p	688	-100	90
Traes_6AS_5562B97F7.1	tae-miR159a,b-3p	760	-96	87
AC217264.3_FGP005	zma-miR159a-3p	1377	-96	87
GRMZM2G070523_P01	zma-miR159a-3p	1044	-96	87
AC217264.3_FGP005	zma-miR159c,d-3p	1377	-98	87
GRMZM2G070523_P01	zma-miR159c,d-3p	1044	-98	87
AC217264.3_FGP005	zma-miR159e-3p	1377	-110	100
GRMZM2G070523_P01	zma-miR159e-3p	1044	-110	100
AC217264.3_FGP005	zma-miR159f,j,k-3p	1377	-96	87
GRMZM2G070523_P01	zma-miR159f,j,k-3p	1044	-96	87

Gene, miRNA, site, region of mRNA, characteristics of binding	Gene, miRNA, site, region of mRNA, characteristics of binding
Traes_6DS_A0EC5D808.1, tae-miR159a-3p, 688, -100, 90 5'–CAGGAGCUCCCUUC**G**AACCAAU–3' 3'–GUC–UCGAGGGAAG**U**UAGGUUU–5'	AC217264.3_FGP005, zma-miR159c-3p, 1377, -110, 100 5'–UGGAGCUCCCUUCAAACCAAU–3' 3'–ACCUCGAGGGAAGUUUGGUUA–5'
AT2G32460.1, ath-miR159a-3p, 1016, 100, 92 5'–UAGAGCU**U**CCUUCAAACCAAA–3' 3'–AUCUCGA**G**GGAAGUUAGGUUU–5'	GRMZM2G070523_P01, zma-miR159c-3p, 1044, -110, 100 5'–UGGAGCUCCCUUCAAACCAAU–3' 3'–ACCUCGAGGGAAGUUUGGUUA–5'
The bold type indicates the nucleotide of non-canonical pairs U-G, A-C.	

Figure 2 – Schemes of miR159-3p BSs interaction in CDS of *T. aestivum*, *A.thaliana, Z. mays* MYB transcription factor genes mRNAs

Table 5 – The variability of amino acid sequences of the MYB family proteins containing oligopeptide ELPSNQ encoded by the binding sites of miR159-3p in the mRNA of different plant genes

Gene	Abreviated names	Region of transcription factor containing oligopeptide ELPSNQ
AC217264.3_FGP005	*Zma*	LPPLSPSPGPRV**ELPSNQ**YGQPAPPTSAAA
GRMZM2G070523_P01	*Zma*	PPLSPSPCPRVV**ELPSNQ**YAQPTPPASAAA
AT2G32460.1	*Ath*	SSFPLGLDNSVL**ELPSNQ**RPTHSFSSSPII
Traes_6DS_A0EC5D808.1	*Tae*	PGMPPLVPPAVQ**ELPSNQ**SPADAGGPLEML
Traes_6AS_5562B97F7.1	*Tae*	LGMPPLVPPSAQ**ELPSNQ**SPADAGGPLEML
LOC_Os06g46560.1	*Osaj*	SSGLPPLPNRPR**ELPSNQ**FETATSGGGGGC
KFK31122.1	*Aal*	GMIKPTSFPLGL**ELPSNQ**TPTHSFTSNTIL
AA32G00526	*Aar*	NITPNSFLLQNL**ELPSNQ**TTSNTNKNGVFL
Araha.1971s0002.1.p	*Aha*	SSFPLGLENSVL**ELPSNQ**TPTHSFSSNPIL
482173	*Aly*	SSFPLGLENSVL**ELPSNQ**TPTHSFSSNPIL

Continuation of table 5

GSBRNA2T00006425001	*Bna*	SYFSLGLDTTVL**ELPSNQ**TPCTSNIMHDNN
XP_013634909.1	*Tha*	SYFSLGLDTTVL**ELPSNQ**TPTQSCTSNIML
Csa05g024410.1	*Csa*	SSFPLGLENTVL**ELPSNQ**TTIDSFTSNPIL
Bostr.23794s0867.1.p	*Bst*	SSFPLGLGNTVL**ELPSNQ**TPTHSFTSNPIL
RrC14648_p1	*Rra*	SYFSLGLDNTVL**ELPSNQ**TPTQLCTSNIML
Rsa1.0_01027.1_g00010.1	*Rsa*	SYFSLGLDNTVL**ELPSNQ**TPTQLCTSNIML
ORUFI06G26670.1	*Oru*	HAXLPPLPNRPR**ELPSNQ**FETATSGGGGGC
ONIVA06G28020.1	*Oni*	SSGLPPLPNRPR**ELPSNQ**FETATSGGGGGG
OMERI06G24960.1	*Ome*	SPSASQANSPPR**ELPSNQ**FETATSGGGGGD
OGLUM06G26120.1	*Ogu*	SSGLPPLPNRPR**ELPSNQ**FETATSGGGGGG
Do015678.1	*Dol*	YSGLPPLPTRPQ**ELPSNQ**FDTSSSGGGGAG
EMT12896	*Ata*	LPGLPPLPTRPR**ELPSNQ**IETASCSGGADG
EMT06644	*Ata*	PGMPPLVPPAVQ**ELPSNQ**SPADAGGPLEML

This data indicates that the relationship between miR159-3p and mRNA of target genes arose millions of years ago, which suggests its important functional significance.

The nucleotides of miR159-3p binding sites are homologous, but encode different oligopeptides (Figure 3 A, B).

Figure 3 – Variability of amino acid region of MYB family proteins on the example of tae-miR159a,b-3p binding sites. Note: **(A)** – oligopeptide WSSIRSK encoded by tae-miR159a,b-3p binding sites in mRNAs of different plant species; **(B)** – oligopeptide ELPSNQ encoded by tae-miR159a,b-3p binding sites located in the third open reading frame in the mRNAs of other plant species

The data in Figure 3 is explained by the fact that mRNA nucleotide sequences can encode different oligopeptides in different reading frames. Therefore, miRNA binding sites in mRNA can also encode different oligopeptides. The binding sites of some miRNAs have homologous nucleotide sequences that can be read in different open reading frames. For example, the nucleotide sequence of miR159j-3p binding sites UGGAGCUCCAUUCGAUCCAAA in the first reading frame will encode the WSSIRSK oligopeptide, and in the third reading frame, miR159e-3p will encode the ELPSNQ oligopeptide (Figure 4).

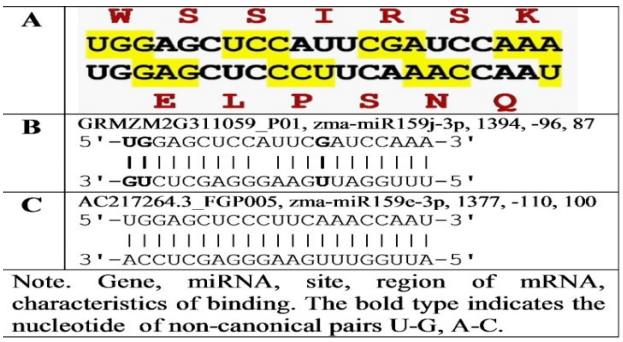

Note. Gene, miRNA, site, region of mRNA, characteristics of binding. The bold type indicates the nucleotide of non-canonical pairs U-G, A-C.

Figure 4 – Scheme of zma-miR159j-3p and zma-miR159e-3p interaction with mRNAs of GRMZM2G311059_P01 and AC217264.3_FGP005 genes. Note: **A** – WSSIRSK and ELPSNQ oligopeptide coding scheme by zma-miR159j-3p and zma-miR159e-3p binding sites, respectively (yellow color indicates codons in different open reading frames); **B** – scheme of zma-miR159j-3p interaction with mRNA of GRMZM2G311059_P01gene; **C** – scheme of zma-miR159e-3p interaction with mRNA of AC217264.3_FGP005 gene.

Thus, on the example of interaction of zma-miR159j-3p and zma-miR159e-3p, having homologous nucleotide sequences, with mRNAs of the transcription factor genes of numerous plants, miRNAs binding is observed independently of the reading frame in which mRNA nucleotide sequence is translated. Similar data was obtained when analyzing the binding sites of miRNAs in animal mRNAs [19; 20].

Conclusion

Current work has shown that miRNA families can interact with mRNAs of MYB transcription fac-

tor genes and regulate their expression. In mRNAs of MYB genes of *Triticum aestivum*, *Oryza sativa, Arabidopsis thaliana*, *Zea mays* all binding sites to mir159-3p were located in protein coding part. These binding sites were homologous and encoded oligopeptides WSSIRSK and ELPSNQ. It is important to note that miRNA binding to CDS of the mRNAs encoded by the transcription factor genes is not accidental. Such localization of miRNA binding sites in mRNAs indicates conserved relationship for a many millions of years of divergence in the studied plant species. Analysis of interactions of miR159-3p with the different plants of MYB indicates the conserved structure of miRNA binding sites. A high ΔG/ΔGm ratio of miRNAs binding to miRNAs shows that the expression of genes of MYB family can be suppressed strongly by miR159-3p. The established associations of miRNAs and target genes can be used to create plant varieties that are highly productive and resistant to abiotic and biotic stresses.

References

1. Ambawat S., Poonam S., Neelam R.Y., Ram C.Y. (2013) MYB transcription factor genes as regulators for plant responses: an overview. *Physiol Mol Biol. Plants.,* vol. 19, no. 3, pp. 307-321.

2. Roy S. (2016) Function of MYB domain transcription factors in abiotic stress and epigenetic control of stress response in plant genome. *Plant Signal Behav.,* vol. 11, no. 1, pp. 1-7.

3. Liu L., Tang X., Huang Y., Du H., Sun Z., Tang Y. (2008) The roles of MYB transcription factors on plant defense responses and its molecular mechanism. *Hereditas (Beijing),* vol. 30, no. 10, pp. 1265-1271.

4. Martin C., Paz-Ares J. (1997) MYB transcription factors in plants. *Trends in Genetics,* vol. 13, no. 2, pp. 67-73.

5. Dubos C., Stracke R., Grotewold E., Weisshaar B., Martin C., Lepiniec L. (2010) MYB transcription factors in Arabidopsis. *Trends in Plant Science,* vol. 15, no. 10, pp. 573-581.

6. Rogers K., Chen X. (2013) Biogenesis, turnover, and mode of action of plant microRNAs. *Plant Cell*, vol. 25, no. 7, pp. 2383-2399.

7. Navarro L., Dunoyer P., Jay F., Arnold B., Dharmasiri N. (2006) A plant miRNA contributes to antibacterial resistance by repressing auxin signaling. *Science*, vol. 312, no. 5772, pp. 436-439.

8. Phillips J.R., Dalmay T., Bartels D. (2007) The role of small RNAs in abiotic stress. *FEBS Lett*., vol. 581, no. 9, pp. 3592-3597.

9. Bari A., Sagaidak I., Pinskii I., Orazova S., Ivashchenko A. (2014) Binding of miR396 to mRNA of Genes Encoding Growth-Regulating Transcription Factors of Plants. *Russ J Plant Physiol*., vol. 61, no. 6, pp. 807-810.

10. Bari A., Orazova A., Ivashchenko A. (2013) miR156- and miR171-binding sites in the protein-coding sequences of several plant genes. *BioMed Research Int.*, vol. 2013, pp. 1-7.

11. Zhou M., Luo H. (2013) MicroRNA-mediated gene regulation: potential applications for plant genetic engineering. *Plant Mol Biol.*, vol. 83, no. 2, pp. 59-75.

12. Zhang L., Zheng Y., Jagadeeswaran G., Li Y., Gowdu K., Sunkar R. (2011) Identification and temporal expression analysis of conserved and novel microRNAs in Sorghum, *Genomics*, vol. 98, no. 6, pp. 460-468.

13. Zhang B., Pan X., George P.C., Todd A.A. (2006) Plant microRNA: A small regulatory molecule with big impact. *Dev Biol*., vol. 289, no. 1, pp. 3-16.

14. Zhao Y., Wen H., Teotia S., Du Y., Zhang J., Li J., Sun H., Tang G., Peng T., Zhao Q. (2017) Suppression of microRNA159 impacts multiple agronomic traits in rice (Oryza sativa L.). *BMC Plant Biolog.,* vol. 17, no. 215, pp. 1-13.

15. Ivashchenko A.T., Pyrkova A.Y., Niyazova R.Y., Alybayeva A., Baskakov K. (2016) Prediction of miRNA binding sites in mRNA. *Bioinformation*, vol. 12, no. 4, pp. 237-240.

16. Ivashchenko A., Berillo O., Pyrkova A., Niyazova R., Atambayeva S. (2014). MiR-3960 binding sites with mRNA of human genes. *Bioinformation*, vol. 10, no. 7, pp. 423-427.

17. Kool E.T. (2001) Hydrogen bonding, base stacking, and steric effects in DNA replication. *Annu Rev Biophys Biomol Struct.,* vol. 30, pp. 1-22.

18. Leontis N.B., Stombaugh J., Westhof E. (2002) The non-Watson-Crick base pairs and their associated isostericity matrices. *Nucleic Acids Res*., vol. 30, no. 16, pp. 3497-3531.

19. Atambayeva S., Niyazova R., Ivashchenko A. (2017) The binding sites of miR-619-5p in the mRNAs of human and orthologous genes. *BMC Genomics*, vol. 18, no. 1, pp. 428-438.

20. Niyazova R., Berillo O., Atambayeva Sh. (2015) miR-1322 binding sites in paralogous and orthologous genes. *BioMed Research Int*., vol. 1, pp. 1-7.

IRSTI 34.03.21

[1*]A.Y. Sikhymbayev, [2]N.K. Aralbay, [3]S.M. Sikhimbayeva,
[1]R.U. Mamykova, [1]T.A. Zhgitekov, [1]B.E. Narbota

[1]Silkway International University, Shymkent, Kazakhstan
[2]Kazakh Research Institute of Horticulture, Almaty, Kazakhstan
[3]M. Auezov South Kazakhstan State University, Shymkent, Kazakhstan
*e-mail: amirbek.sikimbay@gmail.com

Current state of natural ecosystems of Western Tanirtau (Tien Shan) and taxonomical structures of the region's dendroflora

Abstract: Special reports on the Western Tanirtau dendroflora are currently absent. The essence of the floristic analysis given in this paper is identification of taxonomical structure of the Western Tanirtau dendroflora at the level of superfamily groups, families and genera. The objectives of the study are identification of the current state of natural ecosystems in the region. The study of the Western Tanirtau dendroflora was conducted from 2008 to 2017. The study was conducted in the region of the Kazakh part of the Western Tanirtau in the south of Kazakhstan. Collection and processing of materials was carried out by the method of A.K. Skvortsov. All species of hardy-shrub plants observed on all mountain altitudinal belts, including ranges, gorges and anthropogenically-urbanized ecosystems were recorded. During the analysis of the materials collected in the Western Tanirtau territory and review of previously collected materials identified 396 taxa of dendroflora belonging to 130 genera and 50 families. The proposed material is actual reflection of the current state of the Western Tanirtau dendroflora within Kazakhstan and for the first time a floristic spectrum of hardy-shrub plants was developed at the modern level of taxonomy and nomenclature. For the first time, the most complete list of the Western Tanirtau dendroflora, numbering 396 species of the hardy-shrub plants, is given. The data of the conducted researches testify that the Western Tanirtau dendroflora is a large center for enrichment of the genofond of plants in Kazakhstan. The complete list of the species is recommended for use in the compilation of the Plant Identifier in the vicinity of Shymkent city, as well as in the theoretical analysis of the Western Tanirtau flora. In addition, the results of the study are proposed for use in the development of resource and environmental activities in the region.
Key words: floristic spectrum, dendroflora, Western Tien Shan, flora, Kazakhstan.

Introduction

Development of scientific foundations for the optimal and sustainable use of natural resources and effective conservation of nature is impossible without multi-vector study of the plant world, as the plant world is the basic and functional basis for the existence of the biosphere, both on planetary and regional scales [1-5]. In this regard, the study of phytobiota, including in-depth floristic studies of individual natural regions and individual groups of plants, is very important. Concerning the issues of bioresources, it is necessary to emphasize the imperishable importance of dendroflora in the composition of the general flora of a particular region.

The mountain vegetation of Central Asia and Kazakhstan has attracted the attention of many scientists, therefore it is no accident that many works are devoted to the history of mountain forests and their genesis [6-9]. Almost all researchers recognize that the modern forests of Central Asia and southern Kazakhstan are the result of the successive development of tertiary vegetation and represent "depleted forest refugium" [6; 10]. M.G.Popov [6] expressed a complete and demonstrative idea of the decisive role of the process of xerophilization of tertiary vegetation and transformation of subtropical forests of the Ginkgo flora into xerophilic forests of the Ancient Middle-earth, which resulted in the formation of wild fruit plants, including apple tree. According to his concept, subtropical forests in the Neogene have experienced three stages of transformation into xerophilic forests: walnut, oak, juniper-pistachio [11].

According to its plant diversity among the mountain systems of Central Asia the Tien Shan takes a special place. In the works of such scientists as Kamelin R.V. [5], Berg L.S. [12] the Tien Shan is divided into three parts: western, central (internal) and northern.

The natural conditions of the Western Tanirtau are described in great detail in the works of V.N. Pavlov [13]. In the geographical nomenclature, onomastics and toponomy of modern sovereign Kazakhstan, the original name Tanirtau is used instead of the term Tien Shan [3]. In the first works of P.P. Semenov, later P.P. Semenov-Tianshansky, called these mountains "the heavenly range" [14].

The Western Tanirtau is one of the most interesting, original and distinctive regions of Kazakhstan. The peculiarity and originality of the region is predetermined by the following factors:

– the Western Tanirtau is the richest floristic mountain ecosystem of Kazakhstan [15], here bioclimatic zones from deserts to glaciers are represented in all diversity;

– the generic flora coefficient of the Western Tanirtau is the highest in Kazakhstan and reaches 4.12 [5; 13]. At the same time this indicates a high degree of autonomy and originality of the Western Tanirtau flora.

– the Western Tanirtau is located in the middle of the Central Asian center of origin of cultivated plants [16], therefore it is ancient center of civilization.

One of the main characteristics of flora are spectra of floras, which express the main features of systematic composition, as well as botanical-geographical patterns [3; 4].

The floristic spectrum of the Western Tanirtau dendroflora is compiled according to the system of A.L. Takhtadzhyan [1; 2], which formed the basis of the concept of the second edition of "Flora of Kazakhstan" [3]. This work does not give the characteristics of the entire Western Tanirtau dendroflora within Kazakhstan.

There are no special reports on the Western Tanirtau dendroflora. Scientific data and characteristics of the regional hardy-shrub plant species are given in Flora and reports of Kazakhstan and Central Asia as a whole [7; 8; 16-23].

Floristically, the most studied area is Aksu-Zhabagly Reserve with 1312 species [24]. Taking into account flora of western spurs of Talas Alatau, 1491 species are known (which constitute 28% of the flora of the vascular plants of Kazakhstan) [25]. Recently, for the South-Western Tien Shan (part of Uzbekistan) Tadjibayev K.Sh. described 2056 species [26].

Kamelin R.V. [5] determined about 1500 plant species for the Mashat Mountains.

According to the data of V.N. Pavlov, the entire flora of the Western Tanirtau has 2844 species [13]. If proceed from this figure, then the dendroflora of the Kazakh part of the Western Tanirtau is 13.92% of the entire Western Tanirtau flora, i.e. in the flora of the region, each "seventh" species is represented by the life form of trees, shrubs and semishrubs, and according to C. Raunkier's system – phanerophytes and chamephytes [27]. According to Ye.P. Korovin [7; 8], the dendroflora of the whole Central Asia has 500 species. Thus, the Western Tanirtau dendroflora represents 79.20% of the total species composition of the hardy-shrub plants in Central Asia, which characterizes the region as one of the most significant and important centers of the rich diversity of the phytogenofond of Central Asia, as well as Kazakhstan.

The flora of Kazakhstan for the Western Tanirtau comprises more than 2 700 species, from 587 genera, from 118 families [17]. The first report for the dendroflora of Kazakhstan gives for the region under the study 729 species, from 145 genera, from 46 families [28; 29]. In 1993-1999, the flora of the Kazygurt Mountain was studied [30; 31], the results of which provided significant data on the Western Tanirtau dendroflora. In addition, N. Aralbay [3] supplemented these data in the compilation of the State Cadaster of Plants of the South Kazakhstan Region.

The analysis of the flora is based on a program of floristic studies of varying degrees of activity [4].

Due to the study and analysis of the urban flora of Shymkent city, information on the Western Tanirtau dendroflora was supplemented with completely new data [32].

But nevertheless, in these studies, the Western Tanirtau dendroflora within Kazakhstan was not thoroughly studied. This served as the basis for determining the current state of the natural ecosystem and taxonomical structure of the dendroflora.

The essence of our floristic analysis is identification of taxonomical structure of the flora at the level of superfamily groups, families and genera (floristic, family and generic spectra). Identification of these parameters is necessary for assessing the flora's identity and developing a scheme for floristic zoning [33].

The object of the study is the species composition of the hardy-shrub plants collected and noted in all natural, anthropogenically-urbanized ecosystems of the Western Tanirtau.

The objectives of the study are identification of the current state of natural ecosystems in the region; inventory of the species composition of the Western

Tanirtau dendroflora; compilation of floristic spectrum of the dendroflora; determination of its position in the Western Tien Shan system of the Afghan-Turkestan province.

The area of the study is characterized by the following parameters:

Relief. The Western Tanirtau includes a number of mountain ranges, which are part of the Tanitrau Mountains system. The axial range of this part is the Talas Alatau up to 74º30\ of the east longitude [13;14]; it also has the highest altitude (the Manas Mountains, 4882 m). The most western low part of the range is called the Mashat Mountains. The spurs of the southern slope of the range bear parallel to each other, forming as a whole the angle, open to the west – the "western corner" of M.G. Popov [6]. The most western position is occupied by the Karzhantau Range, further to the east are Ugam, Pskem (with the eastern Koksu spur), Chatkal with Kuramin and Mogoltau, Atoinak and Uzunakhmat ranges.

The Western Tanirtau territory has complex relief, in which powerful mountain ranges alternate with deep intermountain valleys. Geomorphologically, the entire complex system of the Western Tanirtau ranges is grandiose branching structure on the western end of the Talas Alatau, forming a single geoblock – arched block massive [13; 14; 34; 35].

The Karzhantau range stretches from the north-east to the south-west (Figure 1). With its northern part, it joins with Ugam, forming at the junction Sairam plexus of mountains (Sairam peak – 4227 m). The northern part of the range is the highest, the range falls to the south-west and has height of about 2000 m in the middle, flattened leveled ridge and low gradient soft slopes. On the southern segment, the ranges rise again (near Mynbulak peak to 2840 m), the ridge in this part of the range is rocky, the slopes are steep and stony. The total length of the range is about 80 km [13; 14].

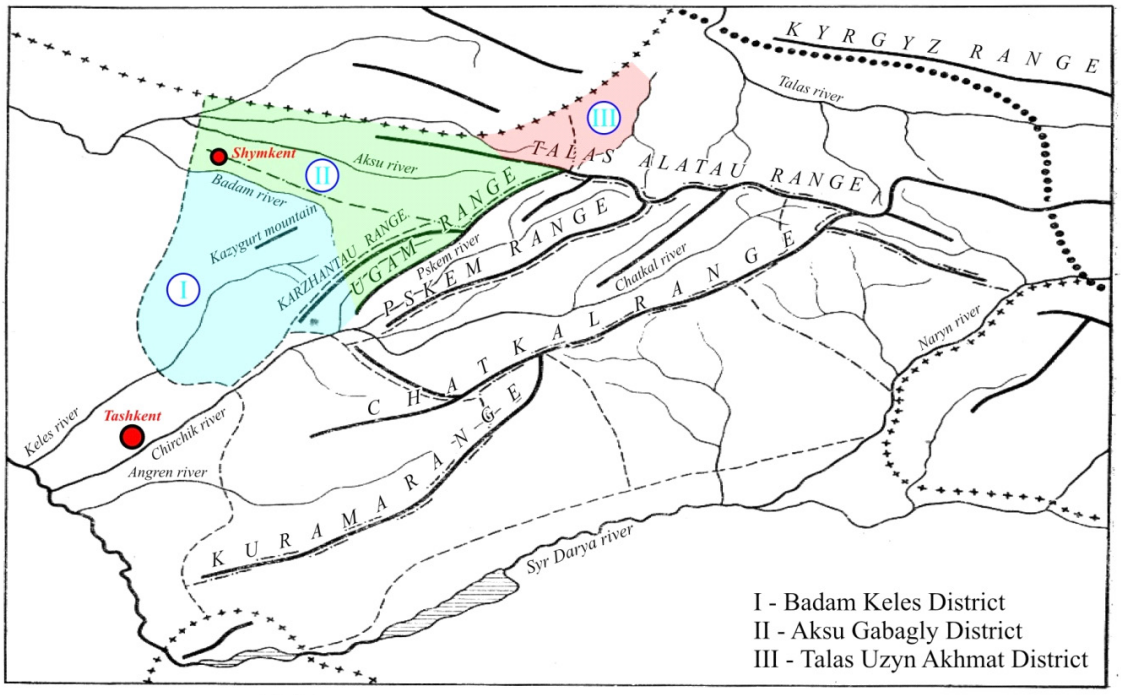

Figure 1 – Schematic map of the Western Tanirtau

The higher Ugam Range stretches to the east of Karzhantau. The southern edge of the range for about 10 km is relatively low (900-1100 m) and flat, the soft slopes are now mostly plowed. Further to the north-east, the ridge of the range increases rather sharply and at a great extent in the middle part its height is not lower than 2800-3000 m, and separate peaks are even higher – 3504 (the Tepar Mountain), 3627, 3729 and 3812 m (the Ayutyur Mountain). In its middle part, the Ugam Range is asymmetric – the north-west slope is flat, the south-east – steep and more stony [13; 14].

The height of the snow line in the Western Tanirtau varied between 3450-4000 m. There is a regular

increase in the snow line from the west to the east from the periphery into the depths of the mountain ridges. Despite the great absolute heights of the snow line, the snow banks persist on the northern slopes (2000-3000 m) until the end of June and the middle of July, and longer in the long snow years [13; 14; 35].

Climate. The climatic features of the Western Tanirtau are due to its location on the border between the moderate and subtropical climatic zones [13; 14; 36]. The dendroflora's richness is explained by the subtropical belt and location of axes of the ridges. For the subtropical belt, the air masses of temperate latitudes predominate in winter over its territory (with the exception of cases of separate northern occurrences), in summer – tropical masses. However, in mountainous conditions these common climatic features are transformed under the influence of relief and other local causes. The most important direction of the axes of the mountain ridges in relation to the winds of the western quarter of the horizon, which is due to penetration of moist air masses deep into the system and precipitations on the slopes. In general, the climate is sharply continental [13; 14]. It is expressed in relatively large fluctuating amplitudes of air temperature, both winter and summer, and day and night. The absolute maximum reaches +35÷38ºC, and the minimum (-25)÷(-29)ºC. The average annual air temperature varies between 9÷11ºC. As noted by some authors [13; 14; 37; 38], the atmospheric circulation, expressed in the cyclonic activity of the West Asian (Iranian) branch of the polar front, plays important role in the seasonal heat distribution in the Western Tanirtau [13]. The above cyclonic activity also determines the amount of precipitation and its seasonal distribution. On average, in the study area, the average annual rainfall rises with the spring minimum of cyclonic activity in Central Asia [13; 14; 38].

There are differences in climatic parameters (air temperature, amount of precipitation, soil moisture, etc.) on the slopes of the northern and southern exposures. Thus, the slopes of the north-western exposition are most moistened in comparison with the south-eastern ones. In general, the Western Tanirtau is characterized by climatic heterogeneity. Increased solar radiation, contrast of temperatures, irregular precipitation and local phenomena of atmospheric circulation create conditions for variegated mosaic of vegetation cover [13; 14].

The annual heat balance in the Western Tanirtau territory is approaching 45-50 kcal/cm^2 [39]. The highest values were recorded at altitudes of up to 1200 m, higher they naturally decrease.

Typical for all mountainous Central Asia, the climatic continentality in the Western Tanirtau is expressed in high summer temperature peaks, observed to high altitudes. The absolute maximum of the lowest part (-41.2°C) differs from the known maxima of high points (+32.4°C) by less than 10°C [13; 14].

The atmospheric circulation plays important role in seasonal heat distribution. The Western Tanirtau is located in the cyclonic zone of the West Asian (Iranian) branch of the air front [38]. Due to the presence of ridges of latitudinal strike, which protect it from the invasion of the European cold masses, the Western Tanirtau is characterized by mild winters. The average temperature in January in Pskem, Chimgan is not lower than -5°C, which is only 2-4°C less than in the same months in Tashkent and Shymkent, although the difference in the heights of these places reaches 1300 m [13; 14].

The cyclonic activity determines the amount and seasonal distribution of precipitation. The annual precipitation amounts in various parts of it fluctuate within considerable limits: from 134 to 996 mm. The amount of precipitation naturally increases with the ascent, while the rate of increase by 100 m varies with altitude on the slopes of different ridges and in different areas [13; 14].

For the Western Tanitau, a long period of summer drought is associated with the annual minimum of precipitation. As the ascent increases, the duration of the dry period decreases. The annual amounts of precipitation change regularly from the west to the east [13; 14; 40].

In the Western Tanirtau, differences in climatic indices in the northern and southern exposures are clearly evident. Especially significant is difference in soil moisture regime at different exposures and slopes. On the southern slopes, a considerable part of the moisture is lost due to rapid melting of the snow (partially evaporating), since in the spring melt waters form solifluction streams and rapid ground water runoff [13; 14; 41; 42]. In general, it is possible to speak about significant climatic heterogeneity of the Western Tanirtau. This explains diversity of vegetation cover, including dendroflora. If culture of some subtropical plants is possible in the southern and western parts when watering [43], even tomatoes do not ripen in the upper part of the mountain valleys [13; 14].

Soil cover. As noted by V.N. Pavlov [13; 14], in the mountains the most important factors of soil formation are, on the one hand, altitude zonality and, on the other hand, exposure of slopes, emphasizing

that these phenomena are of different order and they cannot be countered.

According to V.N. Pavlov [13; 14], the main vertical belt spectrum of soils of the Western Tanirtau is as follows:

I. Low mountains – ordinary (typical) and dark gray soils (in the upper part mountain gray-brown, ordinary soils and dark gray dry steppe – on the slopes of the northern exposures);

II. Middle mountains – light and dark-brown (black-brown) soils, brown and dark brown (black-brown), in some places (under spruce-fir forests) – mountain dark-colored forest;

III. Uplands – mountain light-brown, meadow-steppe, brown, chernozem soils under subalpine meadows and meadow-steppes, mountain meadow sod semi-peaty leached, mountain sod-brown dry steppe [6; 13].

It should be noted that many studies by other researchers have been devoted to the belt distribution of the Western Tanirtau [5; 7-9; 44]. In the most modern work [31; 45], the authors, using the classification of K.Z. Zakirov [46], offer the following classification of soil and vegetation belts of the Western Tanirtau:

Shol (Chul). Foothills and low mountains (500-800 m, sometimes up to 1300 m). Ephemeral desert steppes, grass-sagebrush deserts, gypsophilous shrubs and semi-shrubs are characteristic for this type of vegetation. The climate is very hot, extra-arid. The soils are gray soils, in some places low-carbonate gray soils.

Adyr. The type of vegetation in the interval 800 (1300)-1700 m of absolute altitude. The main dominants of this belt are grasses and a variety of dry grass (semi-savannas), as they move upwards they are replaced by xerophilous shrubs and trees (shiblyak, badal). The climate is arid and subarid. The soils are light brown, rank and stony.

Tau. The type of vegetation, characteristic of absolute altitude of 1700-2800 m. From the phytocenotic point of view, this belt is very rich and diverse. This belt is characterized by all the unique features of the Western Tanirtau. Steppe groups, subarid, humid, petrophilic groups, mesophilic walnut forests, mixed forests, juniper stands and spruce, conifer forests, mesophilous shrubs, meadows and meadow grounds, petrophilous cenoses, etc. are found nearby. The upper boundary of this belt is characterized by subalpine and alpine meadows. The climate is subhumid (in the lower part) and humid. The soils are brown and rank or rank dark brown.

Zhailau (yailau). The vegetative type of the zone is 2800-3400 (above 3500) m of absolute height. The main type of vegetation is alpine meadows. The climate is cryophilic-humid. The soils are cryohydromorphic, in the nival belt – low-power and incompletely-formed.

In this paper, we recognize the chorologic rank of the Western Tanirtau as a phytogeographical province. And the internal division into districts take according to V.N. Pavlov [13; 14].

According to V.N. Pavlov [13; 14], in the natural boundaries of the Western Tanirtau, nine districts are naturally and clearly distinguished according to the complex natural and climatic characteristics: I – Aksu-Zhabagly; II – Talas-Uzunakhmat; III – Badam-Keles; IV – Upper Chirchik; V – Parkent; VI – Santalash-Chatkal; VII – Aflatun-Karasu; VIII – Kuraminsk; IX – South Chatkal.

The Kazakh part of the Western Tanirtau is represented within the Aksu-Zhabagly, Talas-Uzunakhmat (partially) and Badam-Keles districts. Therefore, during the floristic analysis of the Western Tanirtau dendroflora, we studied only in these three districts (Figure 1).

Materials and methods

The study of the Western Tanirtau dendroflora was carried out by us in different seasons with numerous field visits conducted during the period from 2008 to 2017. The basis of the study was the outline of the Western Tanirtau dendroflora [47]. Collection and processing of material for the present work was carried out according to the generally accepted method of A.K. Skvortsov [48].

All species of hardy-shrub plants observed on all mountain altitudinal belts, including ranges, gorges and agrocenoses, anthropophytons were recorded. The studies were carried out by the route-reconnaissance method.

The study was conducted in the region of the Kazakh part of the Western Tanirtau in the south of Kazakhstan (68° of the north latitude, 42° of the east longitude), where the flora stretches over a vast area, about 13200-13800 km^2 (selected areas I, II and III in Figure 1).

The floristic analysis of the dendroflora was carried out on the basis of the ecology-system approach, theoretical aspects of which in Kazakhstan for the last 20-30 years are widely reflected in the works [49-53]. 396 taxa of the dendroflora have been identified during the identification of materials collected during the expedition in the Western Tanirtau territory, as well as viewing of previously collected material stored in the Herbarium of the Institute of Botany and

Phyto-Introduction of the Ministry of Education and Science of the Republic of Kazakhstan, the Institute of the Genetic Fund of Flora and Fauna of the Academy of Sciences of the Republic of Uzbekistan.

Results and discussion

396 species of hardy-shrub plants from 130 genera and 50 families, presented in Table 1, were recorded within the Kazakh part of the Western Tanirtau, based on the study of herbarium funds in Almaty, Shymkent (Kazakhstan), Tashkent (Uzbekistan), literature data and own research.

It should be noted that 205 species from of 396, or 51.76% of them are characteristic of oases, agrophytocenoses, urbanized ecosystems, altered under the influence of anthropogenic impact, i.e. for anthropophyton. The floristic spectrum was compiled according to the system of A.L. Takhtadzhyan [1; 2], taking into account the latest nomenclatural changes [23].

Table 1 – Floristic spectrum of the Western Tanirtau dendroflora

Taxa	Genera	Species
Section *MAGNOLIOPHYTA*		
Group *MAGNOLIOPSIDA*		
Subclass A. *Magnoliidae:*		
Magnoliaceae	2	2
	2	2
Subclass B. *Ranunculiidae*		
Berberidaceae	1	7
Ranunculaceae	2	6
	3	13
Subclass C. *Caryophyllidae:*		
Chenopodiaceae	2	2
Polygonaceae	2	9
Limoniaceae	1	2
	5	13
Subclass D. *Hamamelididae:*		
Platanaceae	1	1
Fagaceae	2	7
Betulaceae	3	8
Juglandaceae	3	6
	9	22
Subclass E. *Dilleniidae*		
Tamaricaceae	2	7
Salicaceae	2	23
Capparaceae	1	1
Ebenaceae	1	1
Brassicaceae	1	1
Tiliaceae	1	4
Malvaceae	1	1
Ulmaceae	2	8
Celtidaceae	1	5
Moraceae	4	1
	16	52
Subclass F. *Rosidae*		
Saxifragaceae	1	2
Grossulariaceae	2	7
Rosaceae	21	106
Fabaceae	17	31
Sapindaceae	1	1
Aceraceae	1	12
Hippocastanaceae	1	2
Rutaceae	1	1
Simarubaceae	1	1
Anacardiaceae	3	5
Celastraceae	1	5
Rhamnaceae	3	4
Eleagnaceae	2	4
Vitaceae	2	5
Punicaceae	1	1
Cornaceae	2	5
Araliaceae	1	1
Caprifoliaceae	2	18
Viburnaceae	1	2
Sambucaceae	1	2
	65	215
Subclass G. *Lamiidae*		
Rubiaceae	2	3
Oleaceae	5	15
Solanaceae	2	3
Bignoniaceae	1	3
Lamiaceae	7	22
	17	46
Subclass H. *Asteridae*		
Asteraceae	5	11
	5	11
Total:	122	374
Section Pynophyta		
Group Gnetopsida		
Ephedraceae	1	3
	1	3
Group Ginkgoopsida		
Ginkgoaceae	1	1
	1	1
Group Pinopsida		
Pinaceae	3	8
Cupressaceae	3	10
	6	18
Total:	8	22
Total: 50 families	130	396

This floristic spectrum shows the main features of the systematic structure of the Western Tanirtau dendroflora, which is expressed in the following: the dendroflora is represented by representatives of only two divisions of the plant world, while the entire regional flora consists of representatives of five plant sections.

According to our results, almost 95% (94.44%) of the dendroflora species composition are represented by taxa of *Magnoliophyta* section, i.e. flowering plants, the distinctive feature of the floristic spectrum is the fact that all *Magnoliophyta* are in their entirety and completely representatives of the group *Magnoliopsida* – dicotyledons. There is no one representative of *Liliopsida*, monocotyledons, even in cultural cenoses – anthropophyton they are not recorded. In classical florogenetic analyzes the ratio of dicotyledons and monocotyledon is important botanical-geographical indicator. Thus, in the regional flora of the Western Tanirtau [13; 14], the ratio of dicotyledons and monocotyledons is 4.4:1. For comparison – a similar ratio in Zaisan hollow is 4.5:1 [49].

In general, such ratio of dicotyledons and monocotyledons is characteristic of the territory of the eastern part of the Ancient Middle-earth [9]. Complete absence of monocotyledons in the formation of the Western Tanirtau dendroflora indicates that, mainly, the dendroflora consists of boreal, moderately warm species. In more detail, this can be traced by considering the ratio of the large systematic groups of the flora under the study (Table 2).

Table 2 – Ratio of the main systematic groups of the Western Tanirtau dendroflora

Systematic groups	Amount of			% from the total number of species
	families	genera	species	
I. Pynophyta	4	8	22	5.55
Gnetopsida	1	1	3	0.75
Ginkgoopsida	1	1	1	0.25
Pinopsida	2	6	18	4.54
II. Magnoliophyta	46	122	374	94.44
Magnoliopsida	46	122	374	94,44
Magnoliidae	1	2	2	0.50
Ranunculiidae	2	3	13	3.28
Caryophyllidae	3	5	13	3.28
Hamamelididae	4	9	22	5.55
Dilleniidae	10	16	52	13.13
Rosidae	20	65	215	54.29
Lamiideae	5	17	46	11.61
Asteriidae	1	5	11	2.77
Total:	50	130	396	100

As can be seen, from the Table 2, gymnosperms in the Western Tanirtau dendroflora are represented by only 22 species and compose weakly noticeable share of only 5.55%. From *Magnoliophyta*, a large number of species are concentrated in the subclasses of, *Dilleniales*, *Lamiales* and *Hamamelinaceous*, in each of which there are 1-2, rarely more families, abundant genera and species. It should be emphasized that among the major subclasses is *Rosidae*, which exceeds according to the number of species other subclasses by 5-9 times. More than half of the species of the Western Tanirtau dendroflora are concentrated in this subclass. This gives grounds for confident assumption that many large families and genera of the Western Tanirtau dendroflora will be in this subclass. This also indicates that the dendroflora formation history can be largely related to the phylogeny of families and genera of *Rosales* of *Rosidae* subclass.

The species diversity of *Salicaceae, Lamiaceae, Caprifoliaceae, Oleaceae* exceeds the average from 2 to 3 times (Figure 2).

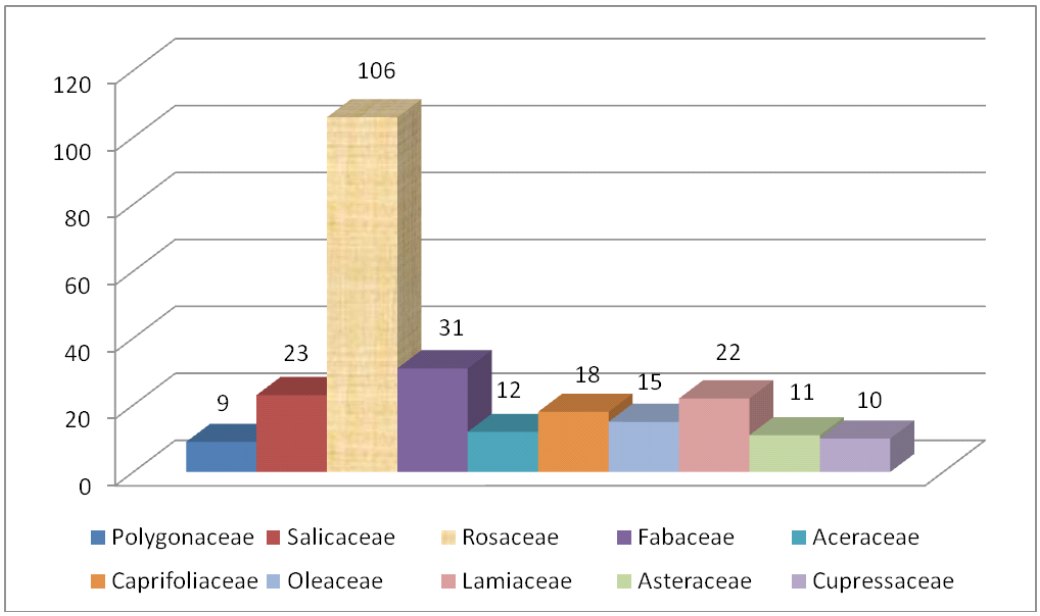

Figure 2 – Spectrum of the leading families of the Western Tanirtau dendroflora

The average level of species diversity of the Western Tanirtau dendroflora families is 7.92, or on average for each family there are almost 8 species. The average level of species diversity is 2.60, i.e. on average for each family there are about 3 genera.

From 10 leading families, 4 – *Rosaceae, Fabaceae, Caprifoliaceae, and Aceraceae*, represent the subclass *Rosidae.* They contain 167 species or 42.5% of the species composition of the regional dendroflora. Hyperpolymorphous family of the Western Tanirtau dendroflora is *Rosaceae*, the species diversity of which exceeds the average level by more than 13 times. A very polymorphous family is *Fabaceae*, species diversity of which exceeds the average level by a little more than 3 times.

A special feature of the species diversity of *Rosaceae* family plants is that from 106 species 51 (48.1%) are represented by anthropophyton – agrocenoses, cultural landscapes, urbanized ecosystems and oases. The species composition of such genera as *Malus, Crataegus, Cerasus,* and *Sorbus* in the Western Tanirtau dendroflora exceeds the species composition of these genera in the natural flora of Kazakhstan by 1.1-3.7 times, eg. *Malus* by 3.7 times, *Crataegus* by 1.2 times, *Cerasus* by 1.1 times, *Sorbus* by 1.75 times. The aforementioned species composition is primarily represented by fruit-bearing and beautifully flowering trees and shrubs, the majority of species belongs to *Anthropophyton*.

The species composition of such genera as *Acer, Berberis, Quercus, Ulmus* and *Fraxinus* in the Western Tanirtau dendroflora exceeds the species composition of these genera in the natural flora of Kazakhstan by 1.1-6.5 times, eg. *Acer* by 6.5 times, *Berberis* by 1.1 times, *Quercus* by 6 times, *Ulmus* by 3 times, *Fraxinus* by 3 times.

This allows to make affirmative conclusion about the enrichment of phytogenous fund of the Western Tanirtau and Kazakhstan as a whole. The data of the conducted research testifies that the Western Tanirtau dendroflora is a large center for enrichment of the gene fund of Kazakhstani plants.

Conclusion

The proposed material is actual reflection of the current state of the Western Tanirtau dendroflora within Kazakhstan. For the first time the floristic spectrum of hardy-shrub plants was developed by us at the modern level of taxonomy and nomenclature. For the first time, the most complete list of the Western Tanirtau dendroflora, numbering 396 species of the hardy-shrub plants, belonging to 130 genera and 50 families, is given. The data presented in the paper is recommended for use in the preparation of the Kazakhstan National Strategy for Conservation and Balanced Use of Biological Diversity, and under discussion for inclusion in the "Plant Identifier of the Republic of Kazakhstan". The complete list of the species is recommended for use in the compilation of the Plant Identifier in the vicinity of Shymkent city, as well as in the theoretical analysis of the Western

Tanirtau flora. In addition, the results of the study are proposed for use in the development of resource and environmental activities in the region.

Acknowledgment

The authors are grateful to the staff of the Institute of Botany and Phyto-Introduction of the Ministry of Education and Science of the Republic of Kazakhstan, the Institute of the Genetic Fund of Flora and Fauna of the Academy of Sciences of the Republic of Uzbekistan, represented by Professors U.P. Pratov and K.Sh. Tozhibayev, whose materials were used in the preparation of the paper.

References

1. Tahtadzhjan A.L. (1970) Proishozhdenie i rasselenie cvetkovyh rastenij. Leningrad: Nauka, p. 145.
2. Tahtadzhjan A.L. (1987) Sistema magnoliofitov. Leningrad: Nauka, p. 439.
3. Aralbaj N.K. (2016) Koncepcija jenciklopedicheskogo spravochnika «Қazaқstannyң flora-sy». Ust'-Kamenogorsk: Izd-vo «Media-Al'jans», p. 104.
4. Jurceva B.A. (1987) Teoreticheskie i metodicheskie problemy sravnitel'noj floristiki. Leningrad: Nauka, p. 296.
5. Kamelin R.V. (1973) Florogeneticheskij analiz estestvennoj flory gornoj Srednej Azii. Lenin-grad: Nauka, p. 356.
6. Popov M.G. (1940) Rastitel'nyj pokrov Kazahstana. Trudi Kazakhskoi Akademiĭ nauk Fil-iala Akademii nauk SSSR, vol.18, p. 216.
7. Korovin E.P. (1961) Rastitel'nost' Srednej Azii i Juzhnogo Kazahstana. Tashkent: Izda-tel'stvo Akademii nauk Uzbekskoj SSR, vol. 1, p. 452.
8. Korovin E.P. (1962) Rastitel'nost' Srednej Azii i Juzhnogo Kazahstana. Tashkent: Izda-tel'stvo Akademii nauk Uzbekskoj SSR, vol. 2, p. 549.
9. Kamelin R.V. (1967) O nekotoryh zamechatel'nyh anomalijah vo flore gornoj Srednej Aziatskoj provincij. *Botanicheskij zhurnal*, vol. 52, no. 4, pp. 447-460.
10. Dzhangaliev A.D. (1977) Dikaja jablonja Kazahstana. Almaty: Nauka, p. 284.
11. Popov M.G. (1928/1929) Dikie plodovye derev'ja i kustarniki Srednej Azii. Trudy po pri-kladnoj botanike, genetike i selekcii, vol. 22, no. 3, pp. 241-483.
12. Berg L.S. (1937) Priroda SSSR. Moscow: Geografgiz, p. 287.
13. Pavlov V.N. (1980) Rastitel'nyj pokrov Zapadnogo Tjan'-Shanja. Moscow: MGU, p. 248.
14. Semenov P.P. (1858) Pervaja poezdka na Tjan'-Shan' ili nebesnyj hrebet do verhov'ja r. Jak-Sarta ili Syr-Dar'i dejstvitel'nogo chlena P.P. Semenova v 1857 g. s kartoju. St.-Petersburg: Vesti Imperatorckogo Russkogo Obshestva, chast' 22.
15. Bajtulin I.O. (1999) Nacional'naja strategija po sohraneniju i sbal. ispol'zovaniju BR v Ka-zahstane. Kokshetau: IntelService, p. 356.
16. Zhukovskij P.M. (1974) Kul'turnye rastenija. Zhizn' rastenij. vol. 1, pp. 162-173.
17. Pavlova N.V. (1956-1966) Flora Kazahstana. Almaty: Fylym, vol. I-IX.
18. Korovin Ye.P. (1961-1991) Opredelitel' rastenij Srednej Azii. Tashkent: FAN, , vol. I-II.
19. Illjustrirovannyj opredelitel' rastenij Kazahstana (1969-1972). Alma-Ata: Nauka, vol. 1, p. 640.
20. Illjustrirovannyj opredelitel' rastenij Kazahstana (1969-1972). Alma-Ata: Nauka, vol. 2, p. 572.
21. Aralbaev N.K., Kudabaeva G.M., Veselova P.V., Danilov M.P., Zakirova R.O., Nelina N.V., Zhamangara A.K., Nigmatova S.A., Samojlova V.A., Shadrina N.V., Muhtubaeva S.K., Kurmantaeva A. A., Isaev E.B., Sihymbaev A.E. (2002) Gosudarstvennyj kadastr rastenij Juzhno-Kazahstanskoj oblasti. Konspekt vidov vysshih sosudistyh rastenij. Almaty: NIC «Ғylym», p. 314.
22. Cherepanov S.K. (1995) Sosudistye rastenija Rossii i sopredel'nyh gosudarstv (v predelah byvshego SSSR). St.-Petersburg: Mir i Sem'ja, p. 990.
23. Stanjukovich K.V. (1973) Rastitel'nost' gor SSSR. Dushanbe: Donish, p. 416.
24. Karmysheva N.H. (1973) Flora i rastitel'nost' zapovednika Aksu-Dzhabagly. Alma-Ata: Nauka, p. 180.
25. Karmysheva N.H. (1982) Flora i rastitel'nost' zapadnyh otrogov Talasskogo Alatau. Alma-Ata: Nauka, p. 162.
26. Tozhibaev K.Sh. (2010) Flora Jugo-Zapadnogo Tjan'-Shanja (v predelah Respubliki Uzbekistan) Tashkent: FAN, p. 100.
27. Raunkiaer C. (1934) The life form plants and statistical plant geography. Oxford: Clarendon press, vol. 2, pp. 37-50.
28. Mushegjan A.M. (1962) Derev'ja i kustarniki Kazahstana. Alma-Ata: Kajnar, vol. 1, p. 364.
29. Mushegjan A.M. (1966) Derev'ja i kustarniki Kazahstana. Alma-Ata: Kajnar, vol. 2, p. 344.
30. Sikhymbayev, A.Ye. (1999) Flora of the Kazygurt Mountain. Abstract of thesis of candidate of biological sciences, Tashkent: Tashkent State University, p. 24.

31. Sihymbaev A.E. (2012) Kazygurt tauynyn florasy (monografija). Shymkent: Nurly bejne, p. 176.

32. Sihimbaeva S.M. (2014) Shymkent kalasynyn urbanoflorasy. Shymkent: Alem, p. 184.

33. Malyshev L.I. (1987) Sovremennye podhody k kolichestvennomu analizu i sravneniju flor. Teoreticheskie i metodicheskie problemy sravnitel'noj floristiki: Materialy 2 rabochego soveshhanija po sravnitel'noj floristike. Leningrad: Nauka. pp. 142-149.

34. Svarichevskaja Z.A. (1965) Geomorfologija Kazahstana i Srednej Azii. Leningrad: Izda-tel'stvo Leningradskogo gosudarstvennogo universiteta, p. 296.

35. Meshherjakov Ju.A. (1972) Rel'ef SSSR (morfostruktura i morfoskul'ptura). Moscow: Mysl', p. 520.

36. Rybin N.G. (1952) Ustrojstvo poverhnosti Kazahstana. Ozera Kazahstana. Ledniki Kazah-stana. V knige: Ocherki po fizicheskoj geografii Kazahstana. Alma-Ata: Nauka, p. 512.

37. Alisov B.P. (1956) Klimat SSSR. Mocsow: Izdatel'stvo Moskovskogo gosudarstvennogo universiteta, p. 127.

38. Borisov A.A. (1970) Klimatografija Sovestkogo Sojuza. Leningrad: Izdatel'stvo Leningrad-skogo gosudarstvennogo universiteta, p. 331.

39. Ivanov N.N. (1959) Pojasa kontinental'nosti Zemnogo shara. Izvestija vsesojuznogo geo-graficheskogo obshhestva, vol. 91, no. 5, pp. 29-34.

40. Kuvshinova K.V. (1968) Klimat. V knige: Srednjaja Azija. Moscow: Nauka, p. 192.

41. Shhul'c V.L. (1949) Reki Srednej Azii. Zapadnoe Vsesoiuznoe Geograficheskoe Obshestvo. Novaja serija, vol. 8, pp. 27-35.

42. Stepanov I.N. (1975) Jekologo-geograficheskij analiz pochvennogo pokrova Srednej Azii. Moscow: Nauka, p. 168.

43. Paravjan A.V. (1960) Opyt akklimatizacii kustarnikov v gornyh uslovijah Srednej Azii. Al-ma-Ata: Institut botaniki Akademii nauk Kazahskoj SSR, p. 266.

44. Kul'tiasov M.V. (1955) Osobennosti jekologii vysokogornyh rastenij Zapadnogo Tjan'-Shanja. Moscow: Izdatel'stvo Akademii nauk SSSR, p. 127.

45. Aralbaj N.K., Tagajbekova D.S., Isaev E.B. (2016) Batys Tjan'-Shan' osimdikter duniesinin beldeulik taralu erekshelikterine taldau. V sbornike: Atyrau Altaj arasy – Kazaktyn baj flo-rasy, Almaty: Ulagat, pp. 68-72.

46. Zakirov K.Z., Zakirov P.K. (1971) Zakonomernosti raspredelenija rastitel'nogo pokrova i principy vysotnoj zonal'nosti. V knige: Rastitel'nyj pokrov Uzbekistana. Tashkent: FAN, vol. 1, p. 155.

47. Sihymbaev A.E. (2017) Materialy k dendroflore Zapadnogo Tanirtau (monografija). Shymkent: Izdatel'stvo Juzhno-Kazahstanskogo pedagogicheskogo universiteta, p. 122.

48. Skvorcov A.K. (1977) Gerbarij. Posobie po metodike i tehnike. Moscow: Nauka, p. 198.

49. Aralbaj N.K. (2015) Flora Zajsanskoj kotloviny (monografija). Almaty: Ulagat, p. 364.

50. Bajtulin I.O. (1987) Sostojanie i perspektivy ohrany rastenij Kazahstana. Ohrana redkih vi-dov rastenij i rastitel'nosti Kazahstana. Almaty: Nauka, pp. 3-19.

51. Bajtulin I.O. (1993) Garmonizacija problem jekonomiki i jekologii v razvitii obshhestva. Izvestija Nacional'noj akademii nauk Respubliki Kazahstan. Serija Biologija, vol.1, pp. 3-8.

52. Bajtulin I.O. (1996) Sistemnyj podhod k sohraneniju i sblansirovannomu ispol'zovaniju biologicheskogoraznobrazija. Podgotovitel'nyj jetap razrabotki Nacional'noj strategii i plana dejstvij sohranenija i sbalansirovannogo ispol'zovanija biologicheskogo raznoobrazija: respublikanskij seminar. Almaty, pp. 12-23.

53. Bajtulin I.O., Kurochkina L.Ja., Aralbaev A.K. (1996) Nacional'naja programma dejstvij po bor'be s opustynivaniem v RK (rasshirennyj referat). Almaty, p. 31.

IRSTI 34.29.25

[1]B.A. Turalin, [1]N.V. Kurbatova, [1]M.S. Kurmanbayeva,
[1*]K.T. Abidkulova, [2]A.A. Bazargaliyeva, [3]A.N. Kupriyanov

[1]al-Farabi Kazakh National University, Almaty, Kazakhstan
[2]Aktobe Regional State University named after K. Zhubanov, Aktobe, Kazakhstan
[3]Institute of Human ecology, Siberian branch of the Russian Academy of Science, Kemerovo, Russia
*e-mail: Karime.Abidkulova@kaznu.kz

Anatomy of the vegetative organs of rare and endangered species *Crambe tatarica* Sebeok. (Brassicaceae) growing in the conditions of the Aktobe region

Abstract: The article presents the results of a study of the anatomy of the vegetative organs (roots, leaves and petioles) of rare and endangered plant species *Crambe tatarica* Sebeok, growing in the Aktobe region of Kazakhstan. The studied plants were collected from two populations: the first population was found in the chalk mountains of Akshatau, in the vicinity of the village of Koktogay, the Wilsky district, and the second population was found in the chalk mountains of Ishkargantau, the village of Karabulak, the Khobdinsky district. This species belongs to mesoxerophytes and calcephytes. According to the available literature, in Kazakhstan *C. tatarica* has the status of 3b (R) – rare, relict species. Some representatives of the genus *Crambe* L. are important economic species because they are oilseed, melliferous, fodder and medicinal plants. Study of the roots of *C. tatarica* revealed the presence of the phloem parenchyma, radial rays, xylem parenchyma and cells of a mechanical tissue, brachisclereids. In the internal structure of leaf numerous starch grains were noted in the parenchyma; brachisclereides were often found on periphery of the leaf, and sclerenchyma cells were apparent in the center of vascular bundles. Large number of vascular bundles was noted in the petioles; the outer wall of the epidermis cells was thickened. In the studied organs, no large cells with a liquid content were found. The obtained information on features of the anatomical structure of roots, leaves and petioles of *C. tatarica* will be used in the future for diagnostics of the raw plant material, and in the studies of its phytochemical composition.
Key words: anatomical, morphological features, vegetative organs, rare, endangered species.

Introduction

Study of the biology of rare and endangered plant species as the most vulnerable elements of changing ecosystems is closely related to the conservation of biological diversity. Such species are carriers of a valuable biological information; they are good indicators of a scientific value of a certain territory for its further assignment to the status of specially protected. One of such species is *Crambe* (*C.*) *tartarica* Sebeok.

Genus *Crambe* L. has a broad area of distribution, from the Macaronesian archipelago to the west of China and North India and from the Arctic Polar Circle on the Scandinavian Peninsula to 5º Latitude South in the north of Tanzania. This genus is represented in Macaronesia, Euro-Siberian, Mediterranean, Sindico-Sahara, Iranian-Turkish, and Sudan-Zambezian (Ethiopia and Tanzania) regions [1].

A critical review of the species composition of the genus *Crambe* is presented in the works of I.I. Khalilov [2]. According to the author, genus includes 33 species belonging to 7 sections and 6 subsections. Prina [3] provided a taxonomic review of 16 species and 5 intraspecific taxa of the genus *Crambe* encountered from Eastern and Northern Europe to Central Asia. In Kazakhstan, there are four species of *Crambe*: *C. tatarica*, *C. kotschyana* Boiss., *C. edentula* Fisch. et C.A. Mey. ex Karelin, and *C. orientalis* L. [4], but only one species, *C. tatarica*, is included in the latest edition of the Red Book of Kazakhstan as a rare species of the IInd category [5].

C. tatarica is a southern European and Mediterranean species. This is a perennial polycarpic, up to 90 cm tall. Root 60-120 cm long, fusiform, juicy.

Plants single- or multi-stemmed, stems erect, with sparse short stiff hairs, later naked. Leaves fleshy, grey-green in colour; basal leaves large, on petioles, up to 30 cm in length and 20 cm in width, twice pinnate, with oblong-linear, toothed or incised lobes, with stiff hairs, especially on the abaxial side, later exposed; the uppermost leaves are linear, entire. Flowers in dense paniculate inflorescence, with honey smell; white, 4.5-5 mm in length. Pods spherical, the upper segment of the pod is 4-5 mm in diameter, tetragonous, mesh-rugose, with four sharply prominent ribs, on the stalks up to 10 mm in length. Dispersal is by seeds. Flowers are produced in April – May, fruits in June – August. The species occurs in steppes, on stony-gravelly slopes, and chalky outcrops. In Kazakhstan, it is found in the Northern Pre-Caspian, Aktobe, Atyrau and Kostanay regions, where the eastern border of its range is located. Outside of Kazakhstan, the species is found in the south of the European part of the former USSR, in the Crimea, Caucasus, Western Siberia (exclusively as an alien species) and in southern Europe [5-8].

The rarity of the species, its vulnerability to anthropogenic impact resulted in the inclusion of *C. tatarica* in the Red Books of the Ukraine, Moldova and southern regions of Russia (Kursk, Belgorod, and Volgograd regions) [9; 10].

Some members of the genus *Crambe* L. are of great importance as oilseeds, melliferous, fodder and medicinal plants, eg., *C. abyssinica* Hochst. The protein content of the seeds of this species is 45-50%, and the oil content is up to 35%; the latter contains 55-60% of erucic acid [11]. Such characteristics make it a valuable plant material in the production of animal feed, biodiesel, and for some industrial and pharmaceutical applications. As a consequence, this species has been well studied [11-16].

Among Central Asian species, *C. orientalis* L. and *C. kotschyana* Boiss. have been studied in Uzbekistan [17; 18].

C. tatarica has been studied in the Crimea and the Lugansk natural reserve [6; 7]. The composition of the oil obtained from the seeds of *C. orientalis* and *C. tataria var. tataria* from Turkey and the chemical composition and properties of the fibers [19; 20] have also been studied. In their studies, scientists from the Czech Republic compared the biochemical composition of *C. tatarica* plants obtained from the Ukraine and grown *in vitro* and *in vivo* [21].

Due to the above, this species is of scientific and practical interest, which justifies its further study. It should be noted that anatomical studies of the Kazakhstani species *C. tatarica* have been carried out for the first time.

Materials and methods

As a result of the field surveys in Aktobe region, two *C. tatarica* populations were found: population 1, in the chalk mountains of Akshatau, in the vicinity of Koktogai settlement, Uilsky district; and population 2, in the chalk mountains of Ishkargantau, Karabulak settlement, Hobdinsky district. The studied species belongs to the Pliocene desert-steppe relics and is represented in the calcephylic floristic complex of the Aktobe region [22-24]. *C. tatarica* belongs to mesoxerophytes and calcephytes. According to the information on rare and endangered plants of the Aktobe region, the species has the status of 3b (R) – rare, relict species [25].

Anatomical preparations were produced following the methods accepted in plant anatomy [26]. For microscopic examination, the vegetative organs of *C. tatarica* were taken. The microscopic studies were conducted using plant material, which has been fixed in a mixture of 96% ethanol, glycerine and water in a ratio of 1: 1: 1.

In accordance with the guidelines, the cross sections of the vegetative organs were produced in the flowering phase, since it is in this phase that the structural anatomical elements of the plant organs have the greatest integrity.

The root sections were produced in the basal part of the roots, every 2-3 cm along their entire length. For the study, plants of a certain age were taken, but the main attention was paid to the middle-aged generative plants, which provide the bulk of the raw material for the study of the species.

Anatomical preparations were produced using a microtome with an OL-ZSO freezing device (Inmedprom, Russia), and also by hand using ordinary razors with a biconcave blade. The thickness of the anatomical sections was 10-15 microns. For quantitative analysis, morphometric parameters were measured using an MOV-1-15 eyepiece micrometer (LOMO, Russia); with a lens x 10; magnification x 10, 20). Microphotographs of anatomical sections were taken on an MC 300 microscope (Micros, Austria) with a CAM V400 / 1.3M video camera (jProbe, Japan).

Descriptions of morphological and anatomical characteristics were made in accordance with the requirements of the State Pharmacopoeia XI [27; 28].

Results and discussion

As a result of the field trips in the Aktobe region during the spring-summer of the growing season of 2018, two populations of *C. tatarica* were found and surveyed.

Anatomical studies of the vegetative organs of *C. tatarica* showed the following results. In the anatomical structure of a root (cross section) with 10x10 and 10x20 magnification, the primary cortex and central cylinder were clearly visible. The outer layer was represented by a loose layer of periderm cells. Cells with lateral appendages, that is, root hairs, were noticed. The primary cortex consisted of thin-walled cells of the parenchyma, oval in shape and closely spaced. The primary sclerenchyma was located along the edges of the primary cortex and represented by groups of brachisclereid (isodiametric sclereides) with lignified walls. The conductive elements of the secondary phloem were thin-walled, polygonal, and brownish in colour; they were arranged in small groups. The gaps between the conductive elements were filled with parenchymal cells. Next to the phloem was the cambial ring. The xylem was represented by vessels forming radial rays. The primary xylem was of a diarch type. The xylem vessels were arranged in cords along the radii of the root in the form of rays. The larger vessels were located in the center of the root, and next to them, towards the surface of the root, were the vessels with a smaller diameter. The biometric indicators were as follows: the thickness of the primary cortex was 134.17 ± 2.80 *μm, the diameter of the central cylinder,* 85.61 ± 7.86 μm, the area of the xylem vessels, 133.25 ± 10.10 μm^2. In the center of the root there was a core parenchyma consisting of small loosely arranged cells; round-shaped starch-containing inclusions were also present (Figure 1).

In a cross section of a leaf of *C. tatarica,* large cells of the upper epidermis with poorly sinuous walls, slightly thickened cuticle layer and a small number of stomata were visible on the surface (20x); the thickness of the upper epidermis was on average 22.17 ± 0.20 μm, and the thickness of the lower epidermis, 28.21 ± 0.24 μm. The stomata on both sides of the leaf were surrounded by 2-4 periustic cells (anomocytic type). In the upper epidermis, small, rare, sessile, colorless or light brown glands consisting of 2-4 cells were found. The leaf of *C. tatarica* was a typical dorsoventral, hypostomatic leaf with the adaxial side formed by tangently elongated cells. The cells of the abaxial (spinal) epidermis had the same structure, however their dimensions were sometimes smaller. On the adaxial (abdominal) and abaxial sides of the leaf, simple trichomes were located, mainly concentrated along the veins. Large trichomes were formed in the area of the main vein on the basal multicellular protrusions. The mesophyll was poorly differentiated. The palisade tissue was represented by three layers of cells slightly elongated perpendicular to the surface, with numerous chlorophyll-bearing inclusions. The spongy tissue was also formed by three layers of isodiametric, closely arranged cells with small intercellular spaces. The vein was a closed collateral bundle. In the leaves of population 1 (Figure 2, a), there were two, occasionally three conductive beams in the central vein, whereas in the leaves of population 2 the number of beams reached 4-5. A parenchymal lining was formed around the group of conductive beams. In the central part, collenchyme cells were located, which can be both above and below the vein (Figure 2, c).

The diagnostic features of this species include the presence of numerous starch grains in the leaf (Figure 3), in the peripheral part of the leaf there were often brachisclereides or stony cells that form mechanical elements of an approximately equal diameter in all directions, otherwise they were parenchymal cells with very thick walls, and in the center of the group of conducting beams there were sufficiently developed collenchyme cells (Figure 4).

The anatomical structure of a petiole of *C. tatarica* is characterized by the following features. The petioles of plants collected in populations 1 and 2 had an identical structure; they were of a radial type with well-developed numerous (15-27) bundles. In cross section, a petiole had a grooved, rounded shape. The abaxial (dorsal side) was rounded, and on the side of the adaxial (abdominal) part there were scleretised parts of the petiole. The uppermost layer was represented by large epidermal cells of the oval and round shape, 15-20 μm in length and 30-45 μm in height. The outer wall of the epidermal cells was slightly thicker, up to 1-3 μm. The outer wall of the epidermal cells had appendages. The cuticle was 1-1.8 μm thick, evenly thickened, smooth; it evenly covered the petiole. Under the epidermal layer of cells there were from one to three layers of large collenchyme cells, 15-30 μm in diameter. From the periphery to the center, there was an assimilation tissue consisting of 5-7 layers of chlorenchyma cells. The chlorenchyma thin-walled cells, round or irregular in shape, varied in size from 10 to 60 μm. Collateral conductive bundles of different size were arranged in an orderly manner in the central part of the petiole.

The bundles were round and V-shaped. There were 8-10 large bundles, 3-4 of medium size and 4-5 small bundles. The parenchyma found between bundles was not lignified. The xylem of the bundles faced the center, and the phloem, the surface of the petiole. The mechanical tissue was well defined and formed by sclerenchyma cells, adjacent to the phloem (Figures 5 and 6).

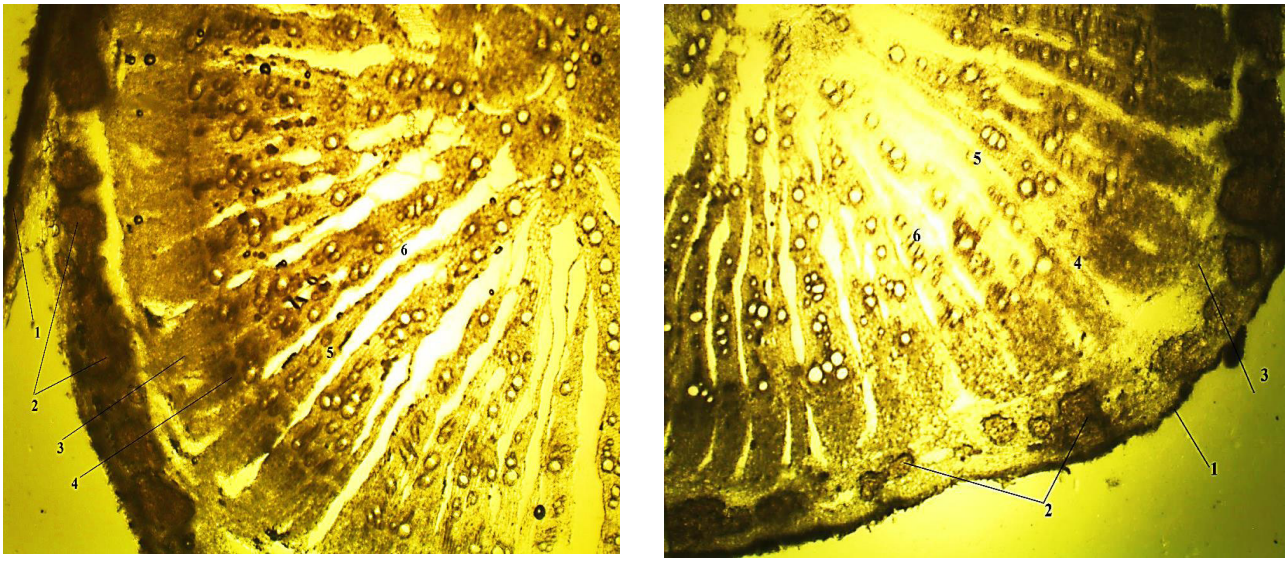

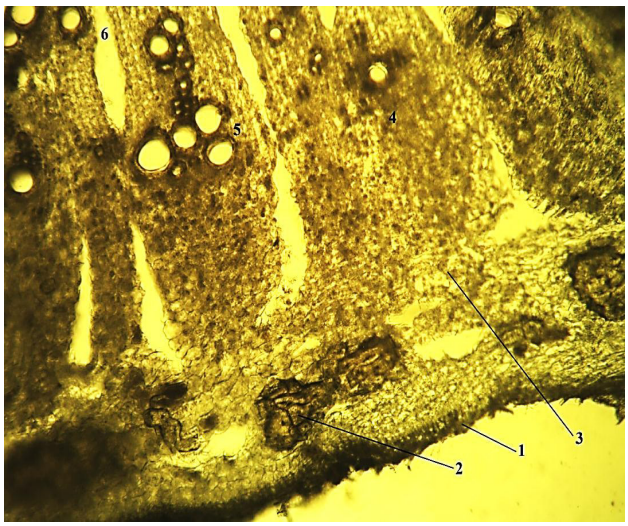

Figure 1 – Anatomical section of the root (magnification 10x10 – a, b; 10x20 – c) of *C. tatarica*. Note: 1 – periderm, 2 – brachisclereides; 3 – primary cortex; 4 – phloem; 5 – xylem; 6 – radial parenchymal rays; a – the first population, b – the second population, c – the general diagnostic signs of the two populations

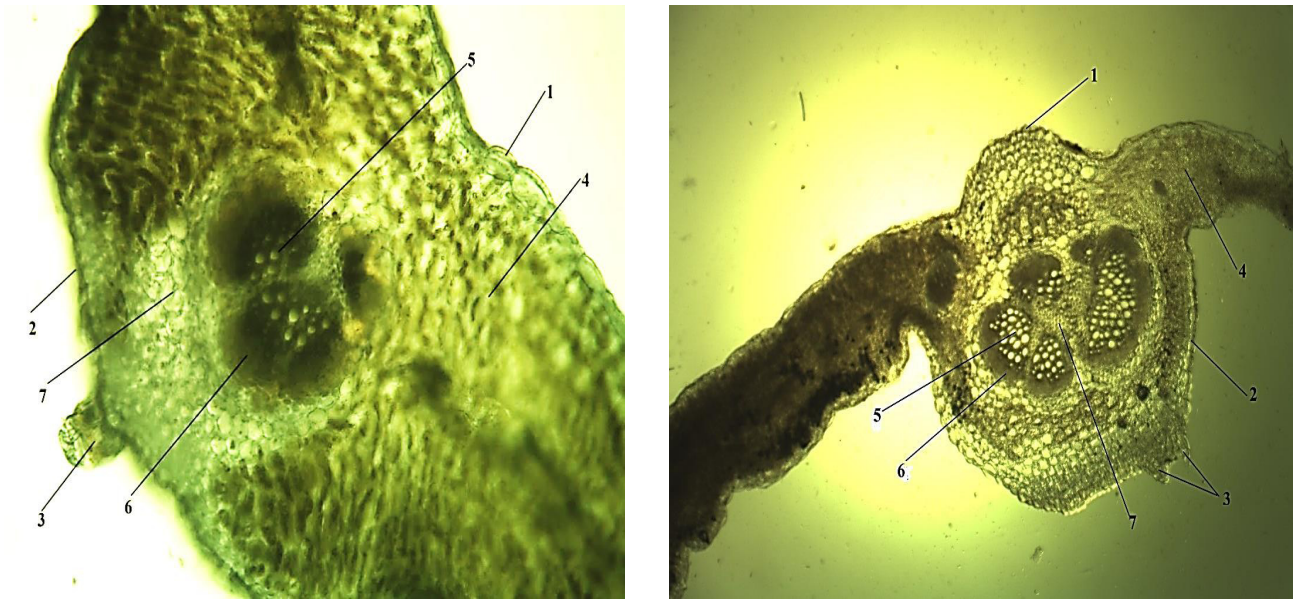

a b

Figure 2 – Anatomical section of the leaf of *C. tatarica*. Note: 1 – upper epidermis, 2 – lower epidermis, 3 – trichomes with multicellular base, 4 – mesophyll, 5 – xylem, 6 – phloem, 7 – collenchyma; a – the first population (magnification10x10), b – the second populations (magnification 4x10)

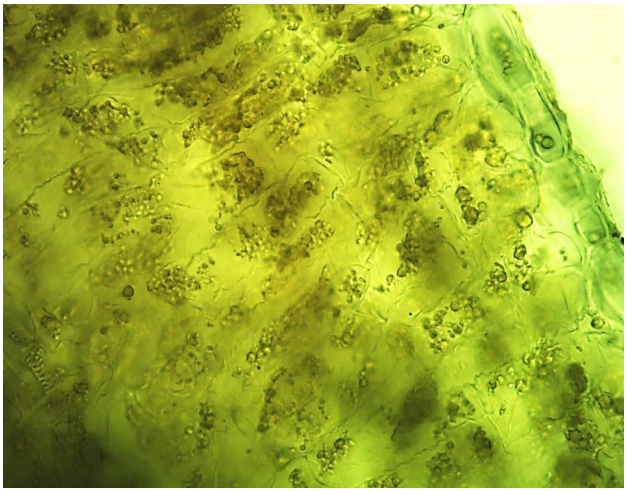

Figure 3 – Mesophyll cells of the leaf of *C. tatarica* with starchy grains (magnification10 x 40)

Figure 4 – Collenchyma cells in the center of the group of conducting bundles of *C. tatarica* (magnification10 x 40). Note: 1 – lower epidermis, 2 – mesophyll, 3 – sclerenchyma, 4 – phloem, 5 – xylem vessels, 6 – collenchyma

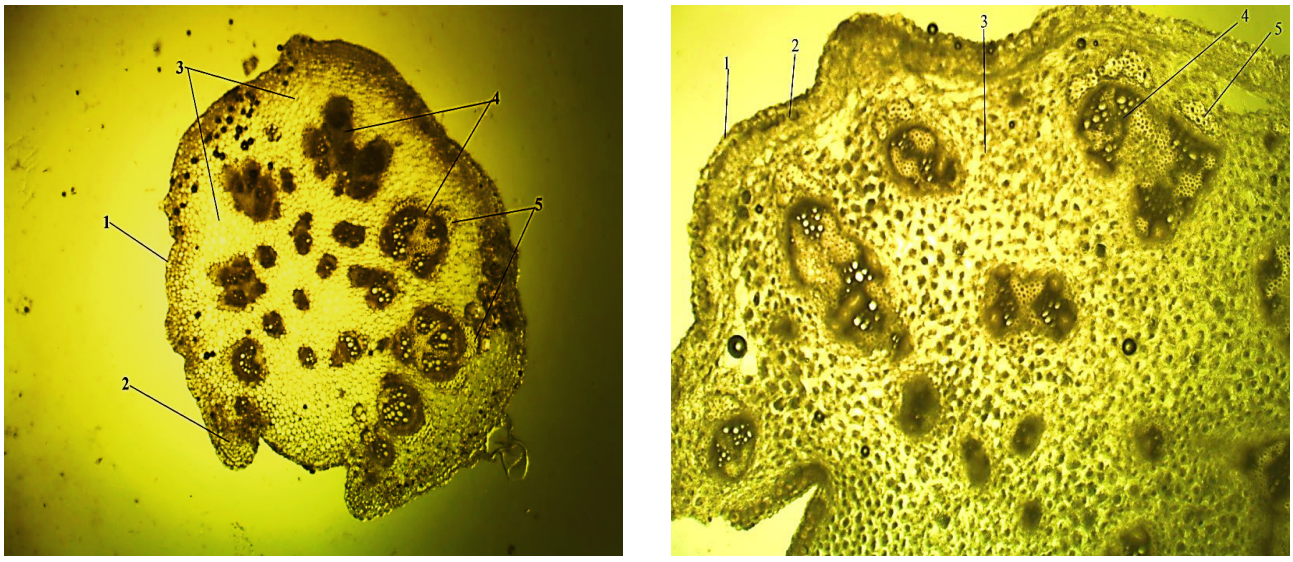

a b

Figure 5 – Anatomical section of the petiole of *C. tatarica*. Note: 1 – epidermis, 2 – angle-shaped collenchyme, 3 – chlorenchyma, 4 – collateral beams, 5 – sclerenchyma; a – first population (magnification 4x10), b – second population (magnification 10x10)

Figure 6 – Anatomical section of the petiole of *C. tatarica*, first population (magnification 10x10). Note: 1 – epidermis, 2 – angle-shaped collenchyma, 3 – chlorenchyma, 4 – xylem, 5 – phloem, 6 – sclerenchyma, 7 – collenchyme

When comparing the obtained results with the data available from the literature [6], similar features of the anatomical structure of the vegetative organs of *C. tatarica* were noted. Thus, the layering of the xylem and phloem parenchyma, and the well-developed primary cortex enable roots to perform the storage function, which is indicated by a large amount of starch-bearing grains in the root parenchyma. The abundance of the parenchyma in combination with weak differentiation of mechanical tissues or lack thereof is characteristic of highly specialized contractile roots, which makes it possible to retract the reproductive buds below the soil surface and thus protect them from adverse conditions. The structure of a leaf of *C. tatarica* revealed xeromorphic features: the presence of a thickened cuticle, weak pubescence, thickening of the outer walls of the epidermis, a small volume of intercellular spaces, and the presence of a mechanical lining of the bundle. Leaves developing in bright light had a higher degree of xeromorphism. In addition, a feature of an anatomical structure characteristic of mesophytes was revealed: the predominance of the spongy tissue over the palisade tissue.

Conclusion

Thus, as a result of the study of the anatomical structure of the vegetative parts (roots, leaves, and petioles) of the plants of *C. tatarica*, it was found that the phloem parenchyma, radial rays and xylem parenchyma were well developed in roots, which did not interfere with root contractility; brachisclereides (cells of mechanical tissue) were also present. In addition, roots were characterized by an abundance of non-lignified parenchymal tissues. In the case of leaves, diagnostic characters included the presence of numerous starch grains in the parenchyma; in the

peripheral part, brachisclereides were often found; and in the center of the conducting bundles, well-developed sclerenchyma cells. The structure of a leaf was also characterized by the presence of numerous round-shaped inclusions with liquid contents. The stomatal apparatus was of an anomocytic type. The petiole had a radial structure with well-developed numerous bundles, the outer walls of epidermis cells were thickened, the cuticle covering the petiole was uniformly thickened. Repositories were absent in all organs. The characteristic features of the anatomical structure of roots, leaves, and petioles point to the characteristics of mesoxerophytic and calcephytic plants, which also include the species under study. The data obtained can be used in the future for diagnostics of *C. tatarica* raw material of, and in the study of the phytochemical composition of this species.

References

1. Leppik E., White G. (1975) Preliminary Assessment of Crambe germplasm resources. *Euphytica*, vol. 24, pp. 681-689.

2. Khalilov I.I. (1992) Monografija roda Srambe L. [Monograph of the genus Crambe L.]. Abstract for the degree of candidate of biological sciences. – St. Petersburg, p.19.

3. Prina A. (2009) Taxonomic review of the genus Crambe sect. Crambe (Brassicaceae, Brassiceae). Anales del Jardín Botánico de Madrid, vol. 66, no. 1, pp.7-24.

4. Abdulina S.A. (1999) Spisok sosudistyh rastenij Kazahstana [Checklist of vascular plants of Kazakhstan / ed. R.V. Kamelin] / pod red. R.V. Kamelina. Almaty, p. 187.

5. Krasnaya kniga Kazaxstana. Tom 2. Chast` 1. Rasteniya (2014) [The Red Data Book of Kazakhstan vol. 2. Part I. Plants]. Almaty, p. 452.

6. Mihajlova O.A., Biryuleva E.G. (2013) Osobennosti anatomicheskogo stroeniya vegetativnyh organov nekotoryh ohranyaemyh vidov roda Crambe L. [Features of Anatomical Structure of the Vegetative Organs of Some Protected Species from Genus Crambe L.]. Byuleten' DNBS, 2013, no. 106, pp. 83-88.

7. Gouz G.V. (2016) The spatial distribution of Crambe tataria (Brassicaceae) across Striltsivsky steppe. Proceedings of the 4th international conference "Rare plants and fungi of Ukraine and adjacent areas: implementing conservation strategies". Kyiv, PALYVODA A.V., pp. 67-69.

8. Flora Kazakhstana / pod red. N.V. Pavlova [Flora of Kazakhstan / ed. N.V. Pavlov] (1961), Alma-Ata: AN KazSSR, no. 4, pp. 304-305.

9. Chervona kniga Ukraïni. Roslinnij svit / pid. red. Ya. P. Diduxa [The Red Book of Ukraine. Vegetable world / ed. J.P. Didukh] (2009), K.: Globalkonsalting, p. 912.

10. Pânzaru P., Negru A., Izverschi T. (2002) Taxoni rari din flora Republicii Moldova. Chişinău, 148 p.

11. Palmer C.D., Keller W.A. (2011) Somatic embryogenesis in Crambe abyssinica Hochst. ex R.E. Fries using seedling explants. *Plant Cell Tissue and Organ Culture*, vol. 104, no 1, pp. 91-100.

12. Vargas-Lopez J. M., Wiesenborn D., Tostenson K., Cihacek L. (1999) Processing of Crambe oil and isolation of erucic acid. *Journal of the American Oil Chemists' Society*, vol. 76, no. 1, pp. 801-809.

13. Capelle A., Tittonel E.D. (1999) Crambe, a potential non-food oil crop. Production. *Agro Food Industry Hi-Tech*, vol. 10, no. 1, pp. 22-27.

14. Szmatoła M., Chrobak J., Grabowski R., Iłowska J., Woch J., Szwach I., Semeniuk I., Drabik J., Wrona M., Kozdrach R., Orlińska B., Grymel M. (2018) Spectroscopic methods in the evaluation of modified vegetable base oils from *Crambe abyssinica*. *Molecules*, vol. 23, no. 12, pp. 1-18.

15. Tito G.A., Chaves L.H.G., Fernandes J.D., Monteiro D.R., Vasconcelos A.C.F.D. (2014) Effect of copper, zinc, cadmium and chromium in the growth of Crambe. *Agricultural Sciences*, vol. 5, pp. 975-983.

16. Werner E.T., Milanez C.R.D., Gontijo A.B.P.L., Soares T.C.B., Amaral J.A.T. (2018) Leaf anatomy changes related to cultivate in vivo and in vitro and during pre-acclimatization of Crambe abyssinica Hochst. *Plant Cell Cult Micropropag*., vol. 14, no. 1, pp. 10-17.

17. Nigmatullaev B.A., Rahmatov H.A., Ohunov I.I., Karimov U.T., Aripova S.F. (2017) Rasproctranenie i syr'evye zapasy *Crambe kotschyana* i *C. orientalis* (sem. *Brassicaceae*) v Uzbekistane [Distribution and raw materials reserves of *Crambe kotschyana* and *C. orientalis* (fam. *Brassicaceae*) in Uzbekistan]. Uzbekskij biologicheskij zhurnal, no. 1,. pp.61-70.

18. Duschanova G.M., Ohunov I.I., Karimov U.T., Aripova S.F. (2017) Anatomy of vegetative organs of *Crambe kotschyana* Boiss. (*Brassicaceae*). *Uzbekskij biologicheskij zhurnal*, no. 4, pp. 47-55.

19. Komplekcioglu N., Karaman S., Ilcim A. (2008) Oil composition and some morphological

characters of Crambe orientalis var. orientalis and Crambe tataria var. tataria from Turkey. *Nat Prod Res*., vol. 22, no. 6, pp. 525-532.

20. Tutus Ah., Komplekcioglu N., Karaman S., Mehmet A. (2010) Chemical Composition and Fiber Properties of *Crambe orientalis* and *C. tataria. Int J Agric Biol.*, vol. 12, pp. 286–290.

21. Pushkarova N., Kalista M., Kharkhota M., Rakhmetov Dzh., Kuchuk M. (2016) Crambe tataria Sebeók seeds and plants grown in vitro and in vivo fatty acid composition comparison. Potravinarstvo. vol. 10, no. 1. pp. 494-498.

22. Ajpeisova S.A. (2012) Konspekt flory` Aktyubinskogo floristicheskogo okruga [Floristic complexes of Aktobe floristic district]. Aktobe, p. 175.

23. Ajpeisova S.A. (2016) Floristicheskie kompleksy` Aktyubinskogo floristicheskogo okruga [Floristic complexes of Aktobe floristic district]. Aktobe, p. 160.

24. Izbastina K.S., Kurmanbaeva M.S., Bazargalieva A.A., Erezhepova N.Sh., Aldibekova A.R. (2018) Floristicheskij sostav rastitel'nyh soobshhestv s uchastiem populjacii redkogo vida Anthemis trotzkiana Claus v Aktjubinskoj oblasti [Floristic composition of plant communities with the participation of a population of a rare species Anthemis trotzkiana Claus in the Aktobe region]. *Exp Biol*., vol. 74, no. 1, pp. 4-19.

25. Ajpeisova S.A. (2011) Redkie i ischezajushhie rastenija Aktjubinskoj oblasti [Rare and endangered plants of Aktobe region]. Aktobe, p. 165.

26. Barykina R.P. (2004) Spravochnik po botanicheskoj mikrotehnike. Osnovy i metody [Handbook of botanical microtechnique. Basics and methods]. M.: Izd-vo Moskovskogo universiteta, p. 312.

27. Gosudarstvennaja farmakopeja Respubliki Kazahstan, vol. 1. (2008) [State Pharmacopoeia of the Republic of Kazakhstan, T. 1]. Almaty, p. 592.

28. Gosudarstvennaja farmakopeja Respubliki Kazahstan, vol. 2. (2009) [State Pharmacopoeia of the Republic of Kazakhstan, T. 2]. Almaty, p. 804.

IRSTI 34.29.35.

[1*]K.B. Yernazarova, [1]Zh.T. Abdrassulova, [1]S.T. Tuleuhanov, [1]G.A. Tussupbekova,
[2] N.N. Salybekova, [2]G. Isayev, [3]H. Basim

[1]Laboratory of Chronobiology and Ecological Physiology, Almaty, Kazakhstan
[2] Laboratory of Biotechnology, Turkestan, Kazakhstan
[3]Laboratory of Molecular Biology, Akdeniz University, Antalya, Turkey
*e-mail: kamilya_002@mail.ru

Biological features of the medicinal plant *Plantago major* L.

Abstract: Paper provides an overview of the therapeutic, morphological, anatomical and phytochemical features of *Plantago major* L. For studies, plant samples were collected four times from April to September 2018 in the Almaty region, with freshly harvested plants used for morphological and anatomical studies, and specially dried leaves used for phytochemical studies. Anatomical sections were produced using the classic blade method. Chemical composition, including vitamins B1 (thiamine chloride), B2 (riboflavin), B3 (pantothenic acid), B6 (pyridoxine), C (ascorbic acid), E (tocopherol), tannins was studied at the research laboratory for assessing the quality and safety of food products of the Almaty Technological University. Vitamins were determined according to the State Standard 31483-2012, with the help of the device "Kapel105-M" by the method of capillary electrophoresis (M-04-41-2005). Tannins were estimated by titration of margon-acid potassium using the classical method according to the State Standard 24027.2-80. As a result of a phytochemical study, large amount of vitamin C (ascorbic acid) was determined among vitamins, on average of 0.432 mg/100g. This means that preparations obtained from *Plantago major L.* can be used in the treatment of bleeding gums, against viral and other diseases. However, vitamin E was not detected in the plant. Amount of tannins was around 77.94 mg/100g; which indicates its high antimicrobial, hemostatic properties and prevents the replenishment of the gastrointestinal tract. The results of this study can be used as an additional material in the educational process in such courses as "Botany", "Medicinal plants", "Anatomy and morphology of plants".
Key words: *Plantago major* L.*,* xylem, phloem, ascorbic acid, tannins.

Introduction

Plantago (*P.*) *major L.* (large plantain) is a pharmacological plant, which belongs to the family *Plantoginacae*. The area of its distribution is very wide. Plants belonging to the Plantoginacae family grow around the globe, with about 260 species known. Large plantain can be found on the territory of all CIS countries. Despite the fact that it grows on the soil with different mechanical composition and moisture content, it is quite demanding for moisture and light, so it falls in the widespread and exposed areas of the shadowy regions. It is common in residential areas, open terraces, along the roads and pastures and never grows into large groups [1; 2]. There are 16 species in all regions of Kazakhstan. Among them there are large plantains (*P. major*), average plantain (*P. media*) and flat plantains (*P. lanceolata*). They grow on the banks of the river-lake, in the mountains, deserts, in slopes where weeds are grown, along the road, in the vicinity. The height of the stem is about 20–70 cm. The leaves are oval, flat, with the whole edge, they grow around the roots. Occasionally, they are on the opposite of the stem, but sometimes tend to alternate. The tiny flowers are light brown, rarely light blue, in the form of grains. In the period from May to September it will bloom and give fruits and it is dioecious. The fruit bursts open when it is ripen. Seeds and leaves contain glycosides, carotene, phytoncid, and are therefore used in medicine [3].

Plantain is one of the most ancient medicinal plants. Even in China for medical purposes it was collected for more than 3,000 years ago. The ancient Greeks and Romans used plantain seeds for dysentery, inflammatory conditions of the stomach, intestines and other diseases. Hippocrates and Galen used it. Avicenna believed it was extremely good for ul-

cers. Leaves prevent bleeding, and when dried, promote healing of old and fresh ulcers. Avicenna used plantain leaves as a wound healing and hemostatic agent [4; 5].

The pharmacological value of the plantain carries a great deal of interest to many researchers and the work of both Kazakhstani and foreign scientists can be considered as a proof. In 2013 at the stomatology school in the University of Indiana, United States, Rayna E. studied *P. major* and determined its tumor and anti-inflammatory properties [6]. Levent A. at the University of Batman in Turkey has developed a new, simpler method for high-quality liquid chromatography for simultaneously identifying the retinol, retinol palmitate, beta-carotene, α-tocopherol and vitamin C from rat's serum treated with *P. major* and 7,12-dimethylbenzanthracene [7]. In 2015, Kazakh scientist Alimova U.S. identified the pharmacological and pharmaceutical aspects of construction of the suppositories with the added extracts of sweet flag and large plantain (*Acorus calamus* L. and *P. major*) [8]. This year, Dilbarhanov R.D. *et al.* studied antimicrobial activity of CO_2-extracts of sweet flag and large plantain [9].

In 2016, at the Rungta Dental Society of India, Sharma H. had studied the microbial effects of *P. major* [10]. This year at the Swedish University of Agricultural Sciences, Zubair M. has carried out a research to prove the application of a large plantain in traditional medicine [11]. In 2017, in Surabaya University of Indonesia there were investigated the effects of the precipitations and chemical compounds of *Plantago* on the proliferation of cytokines and cancer cells the inflammatory and antitumoral properties [12]. In June 2017 at the Plovdiv Medical University in Bulgaria, Lukova P. studied the medicinal properties of the *P. major* plant, including the fermented hydrolysis of polysaccharides extracted from the leaves [13]. In 2017 at the Malaysian International Islamic University, Adom M.B., has conducted an investigation to determine the chemical components and medical advantages of *P. major* [14]. In March 2018, in the Neurogenic Inflammation Research Center at the Mashhad Medical University in Iran Naji Ebrahim checked dexorubicin-induced nephropathic protection in mice [15]. Same year, in Columbia at the University of Cartagena Karo D.S. studied the healing properties of anxiety and insomnia of a large plantain [16], in Mashhad Medical University in Iran Enezar H.N. studied the protective effect of *P. major* on liver inflammation caused by daxorubin [17].

The aim of the current research is to study morpho-anatomical and phytochemical characteristics of *P. major*, growing in Almaty region, and assess its pharmacological value.

Materials and methods

Samples of the medicinal plants were collected four times from April to September 2018 in the Almaty region. Morpho-anatomical studies were carried out at the laboratory of collective use "Physical and chemical methods of research in biology" No. 216 of al-Farabi Kazakh National University. To carry out this experimental work, freshly harvested plants, their leaves and roots were used. Anatomical sections were prepared by the classical method, cutting off a thin plate with a razor blade. Photos of the plant were taken with a camera Canon EOS1200D 5472x3648 (20,0 million pixels) (Canon, Japan). Morphometric parameters of the plant were measured and anatomic images were examined with MT6300 microscope (Meiji Techno, Japan), eyepieces SWH10x F.N. 22 (O.D. 30 мм), software Vision Capture 2.1. Statistical processing of morphometric indicators was conducted in Microsoft Excel 2010.

Phytochemical parameters of *P. major* were studied on dried leaves. Collected leaves were dried by the shade method, under a well ventilated canopy, without sunlight [18]. The research was conducted at the Almaty Technological University on June 11-22, 2018 in the Research Laboratory for the Assessment of Quality and Safety of Food Products. Test conditions: temperature – 21±1°C, relative humidity – 81%. In the composition of *P. major* the water-soluble vitamins (B_1, B_2, B_3, B_6, C, E) were determined according to GOST 31483-2012, with the device Kapel 105-M (Lumex, Russia), using the method of capillary zone electrophoresis (M-04-41-2005) in accordance with the general provisions, stated in the TU 4215-023-20506233-98 regulatory document. According to the aforementioned regulatory document, the sample to be analyzed is introduced into a capillary pre-filled with electrolyte. After high voltage is applied to the ends of the capillary, the components of the mixture begin to move through the capillary at different speeds, depending on their structure, molecular weight and charge, and reach the detector located at the end of the capillary. The electrophoregram obtained is a sequence of peaks, each of which corresponds to a strictly defined substance. The Kapel 105-M system consists of the following main elements: quartz capillary; devices for filling the capillary with liquid, introducing the liquid sample into the capillary and supplying voltage from the high voltage source to the ends of the capillary (herein-

after referred to as the sample introduction device); high-voltage unit of positive, negative or switchable polarity, consisting of a high voltage source and a switching device; a detector to determine when the components of the sample reach the detection zone.

The Kapel 105-M system is available with a high-voltage switchable polarity unit, a photometric switch with a switchable wavelength, an automatic sample changing system and a water capillary cooling system. The vitamins were determined on capillary zone electrophoresis, using the wavelength exchange program by their absorption at 200 nm and 240 nm wavelengths [19]. The amount of tannins in medicinal plants has been estimated according to the state standard 24027.2-80 by the classical method, involving titration with manganese acid potassium [20]. All photos presented in the paper were taken by the authors.

Results and discussion

All of the plantain types are annual and perennial, some of them are weed. Leaves are often rarely seen and covered with roots. The flowers are small, two-sided, and actinomorphic, have upper-ended heads or germ-like flowerpots, often four-membered. Its tray has four blades or four blades. The crown of the flower is deciduous, has four blades, colored or dyed. The coenycarpal gynoecium consists of two fertilized leaves that form two upper nodules [21; 22].

Plantains usually reproduce by the wind, but sometimes they come in contact with insects. The fruits are cenocarpus: a hawk with a cap. Seeds are small, with boar, small vertical seeds and nutritious endosperma; it falls off the covered foliage and spreads through the wind [23].

Large plantain (*P. major*) is a perennial herbaceous plant with the height of 10-50 (70) cm, one or more flower foliage and stem layers, 12 cm long plate, wide egg or ellipsoid, the side has a rarely uneven tooth (slightly thin), three to seven arched pipe tubes (Figure 1). The crusher is equal to the length of the leaf plate or slightly longer, rarely short. The pulp is lessened and the thin roots are pulled out from it [24].

The study of morphometric parameters of large plantains revealed changes in quantitative parameters (Table 1).

Figure 1 – Large plantain (*Plantago major* L.), growing on the territory of al-Farabi KazNU

Table 1 – Morphometric parameters of *Plantago major* L.

Parameters	April-June	July-September
Total length of the large plantain	17±3.02	40±3.10
Number of leaves	7±3.00	12±3.00
Length of the leaves, cm	1.4-4.80	4.1-21.30
Width of the leaves, cm	1-2.90	3.6-8.20
Number of leaf bands	5±1.00	8±1.00
Length of the root, cm	9±2.50	10±2.06
Number of roots	40±4.00	45±5.00
Number of fruits in a bush	-	234±20.00

Total length of the plant increased from April to June in the range of 17-20 cm, and from July to September – 40-44 cm. The number of leaves per plant within the first months ranged from 7 to 10, and from July to September it reached 12-15. During the general development of the leaf, the length of the leaves increased from 1.4 to 21.3 cm and width up to 1-8.2 cm. The number of leaf bands in the first sample increased from 5-6 to 8-9 at the end of the summer. The number of rhizomes reached 40-44, the length increased to 9-11.5 cm from April to June, and from July to September the number of rhizomes reached 45-50, the length reached 10-12 cm. Since the flowering period of *P. major* starts in June, the number of fruits has been tested since July and on one of these flowers there were 234-254 of them.

Plantago major L. has its own semiconductor, mechanical, separating and storing elements. These tissues combine all members of the plant into one system.

There are two types of conductive tissue – xylem (gr. Chylon – wood) and phloem (gr. Phloios – shell, sponges). They have structural and functional differences. The conductive elements of xylem consist of dead cells. They transfer water and dissolved substances from the roots to the leaves. Fluid in conductive elements preserves living protoplasts [25]. In the absorption zone, rhizodermatellular cells form the vascular bundles (Figure 2).

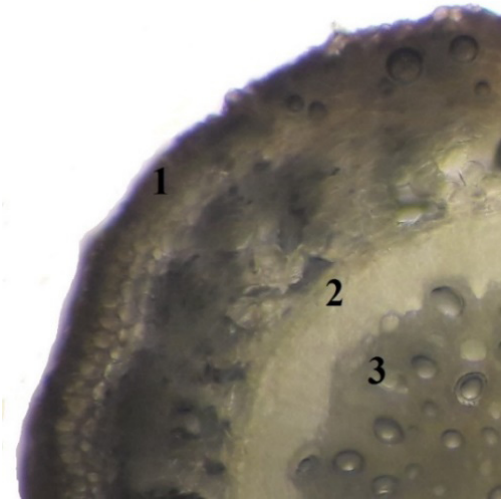

Figure 2 – Anatomical structure of *Plantago major* root, magnification x100.
Note: 1 – rhizoderm, 2 – phloem, 3 – xylem

The flowering shrub is directed upwards, decorated with thin, long cylindrical spikelets and dense small-sized fflowers. There are four, 1.5-2.5 mm long, petals, in the flower receptacle; flowers in the crown are actinomorphic; cylinder tubes are formed on the underside. Four male parts are attached to the flower crown tube with twice as long purple pollen. Female parts have two nodes.

Anatomical structure of the large plantain leaf is specific to the herbaceous plants. Insular conductive bundles are located in the mesophyll. Xylem is located at the top of the leaf, and phloem is at the bottom. Xylem consists of round twisted tubules, and phloem of filter-shaped tubes with very large supportive cells. Leaf plate endurance is ensured at the expense of the subepidermal crown of collenchyma or sclerenchyma (Figure 3).

Figure 3 – Anatomical structure of *Plantago major* leaf, magnification x100.
Note: 1 – xylem, 2 – phloem, 3 – sclerenchyma, 4 – collenchyma

Drugs (fresh and canned juice, emulsion and ointment) with different pharmacological effects (antiinflammatory, wound healing and antimicrobial) produced from plantain leaves, may be used in treatment of broad range of diseases, including stomach ulcers, laryngitis, hypotension, bronchial asthma and tuberculosis [26-28]; aqueous extracts show properties of lowering cholesterol and sclerosis [29; 30]. Galen's drugs (extract, juice) are used in the treatment of inflammatory diseases of mouth and throat, skin injuries, chronic gastric ulcers, burns, flegmonia, cholera, and purulent wounds [31]. Herbal preparations and fresh leaves have bacteriostatic effect on the pathogenic microbes of traumatic infections; the surface of the wound cleanses quickly from the purgation, inflammation stops, and the wound healing rapidly speeds up [32].

Quantitative indicators of vitamins and tannins are shown in table 2.

According to our results, the amount of vitamin C in the medicinal plant is the highest, with an average of 0.432 mg per 100 g of the raw material (Table 3).

Vitamin C (ascorbic acid) inhibits the formation of harmful substances during the biological oxidation, subsequently increasing the resistance of an organism (bones, tooth, liver, cardiovascular system) to infectious diseases. Insignificant amount of vitamin C leads to growing fatigue of the human body, blockage of saline shells and bleeding of gum. In case of long deprivation, due to increased gum disease, person is exposed to scurvy with further deteriorioration of the nervous system [33].

Table 2 – Vitamins and tannins content of *Plantago major* leaves

Indicators, unit of measurement	Precise results	Regulatory documents of research methods
Vitamins, mg/100 g:		
-B_1	0.0137±0.0027	M-04-41-2005
-B_2	0.0350±0.0147	
-B_3	0.180±0.036	
-B_6	0.0317±0.0063	
-C	0.432±0.148	
-E	Undefined	
-Tannin	77.94	State Standard 24027.2-80

Table 3 – Quantitative indicators of vitamins content in *Plantago plant* leaves

No.	Time, min	Component	Height	Start	End	Area	Concentration, mg/L	Concentration, mg/100g
1	4.587	B_1 (thiaminechloride)	0.085	4.540	4.725	6.376	0.0025	0.0137±0.0027
2	6.032	B_2 (riboflavin)	0.403	5.938	6.123	20.45	0.0064	0.0350±0.0147
3	7.265	B_6 (pyridoxine)	0.857	7.207	7.403	25.84	0.0058	0,0317±0.0063
4	8.677	C (ascorbic acid)	0.574	8.513	8.847	43.28	0.079	0.432±0.148
5	10.142	B_3 (pantothenic acid)	0.626	9.938	10.185	43.59	0.033	0.180±0.036

B_3 (pantothenic acid) is involved in biochemical reactions, such as high fat and amino acids biosynthesis and oxidation. According to our results, its content comprises 0.180 mg in average per 100 g of the raw material. The lack of pantothenic acid can lead to a large spectrum of abnormalities, including dermatitis, neuritis, pneumonia, etc. It is applied at such conditions as postoperative intestinal atony, as well as renal insufficiency, osteoarthritis in lesions of the skin and mucous membranes, photosystatosis in different types of arthritis, dry skin, hair loss, etc. [34].

B_2 (riboflavin) participates in significant oxidation processes. According to our results, its content comprises 0,0350 mg in average per 100 g of the raw material. It stimulates quick healing of traumas and maintains the eyesight. In case of insufficiency, lips become dried, and the body injuries are healed slowly. In addition, vitamin B_2 is used in treatment of burns, phototherapy, chronic hepoxy, insufficient carbohydrate feeding, or in the treatment of acute infectious diseases.

Vitamin B_6 (pyridoxine) is involved in amino acids exchange. According to our results, its content comprises 0,0317 mg in average per 100 g of the raw material. Vitamin deficiency slows down the growth in children, causes blood loss and leads to dark facial spots in pregnant women [35]. During pyridoxine avitaminosis, the amino acids and proteins exchange is disrupted, blood formation gets worse, total amount decreases and anemia develops. Vitamin B_6 is involved in maintaining sodium and potassium in the body fluid. This, in turn, is of great importance to the nervous system.

B_1 (thiamine chloride) is necessary for the proper metabolism. According to our results, its content comprises 0.037 mg in average per 100 g of the raw material. The lack of this vitamin causes fatigue and problems with digestion process. Vitamin B_1 interacts with unsaturated fatty acids responsible for the development of urolithiasis and gallbladder pathologies. It helps to relieve skin inflammation, has good effect on the condition of mucous membranes. It is used against typhoid, neurodermatitis, pulse, burn injuries, scabies, and has a positive effect on the intellectual functions [36]. When vitamin B_1 is insufficient, amino acid metabolism results in significant issues.

Estimation of specific vitamins was performed using capillary zone electrophoresis, with the wavelength exchange program at 200 nm and 240 nm

wavelength. The wave diagram is characterized by the appearance of vitamins in a time frame indicated on Figure 4.

In addition to detecting some vitamins, we also aimed to detect the tannins, which are considered to be the only indication of the healing properties of the plant. Scientific data indicates that plant tannins not only serve as antioxidants, but also display antiinflammatory, antibacterial, antitumoral and antifungal activities. Tannins have a positive effect on gastrointestinal tract activity, fighting harmful microorganisms and stopping the bleeding. They can also be used for external hemorrhage and internal bleeding. Thus, tannins are used to treat various diseases in medicine [37]. According to our results, the amount of tannins in *P. major* medicinal plant constitutes in average as much as 77.94 mg of tannins per 100 g of raw material.

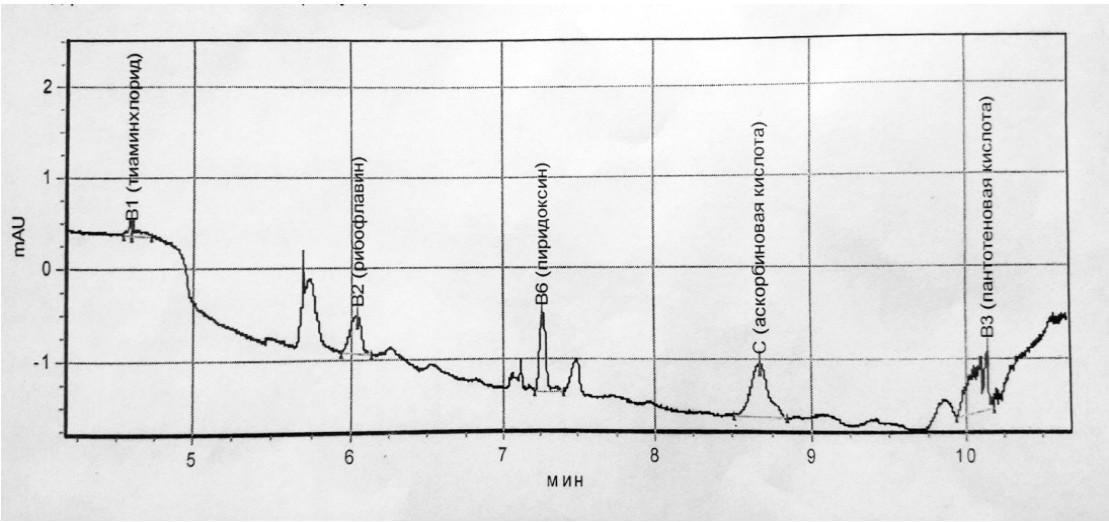

Figure 4 – The electrophoregram of the vitamin amount in leaves of the plant *Plantago major L.*
Note: min-off time (output of the vitamin indicator in the chromatography);
mAU – peak height (height indication of vitamin A peak)

Conclusion

Plantago major L. is a valuable object of research interest. Besides anatomical, morphological and phonological studies, research on its pharmacological effect was conducted. Latter was performed at the laboratory of collective use "Physical and chemical methods of research in biology" No.216 of al-Farabi Kazakh National University and commercially in the Research Laboratory for the Assessment of Quality and Safety of Food Products of Almaty Technological University in the period of April-September, 2018. The amount of vitamin B_1 (thiaminine chloride), B_2 (riboflavin), B_3 (pantothenic acid), B_6 (pyridoxine), C (ascorbic acid) in *Plantago major* L. medicinal plant leaves was determined by the capillary zone electrophoresis, while such of tannins has been estimated according to the state standard 24027.2-80 by the classical method, involving titration with manganese acid potassium. The results show that vitamin C (ascorbic acid) can be used to treat various infectious diseases, such as the inflammatory diseases of the colon and others. Vitamin E (tocopherol) was not found in the plant composition. The amount of tannins was 77.94 mg/100g of plant raw material, and this is a good indication that extracts from *Plantago major* L. plants may have high action to bacterial, bleeding and inflammatory processes in the gastrointestinal tract. Taking into consideration the importance of the identified vitamins and the therapeutic properties of the tannins, we conclude that *Plantago major* L. has also got a high phytochemical value.

References

1. Sosnina S.A. (2007) Kolichestvennoye opredeleniye polisakharidov v list'yakh podorozhnika bol'shogo, podorozhnika srednego i podorozhnika lantsetnogo [Quantitative determination of polysaccharides in the leaves of the large plantain, the middle plantain and the plantain lanceolate]. Vestnik

Perm'skoy gos. farmatsevticheskoy akademii, vol. 2, pp. 285-288.

2. Knyazeva I.V. Mudrik V.A., Pigulevskaya T.K. (2001) Ekofiziologicheskie harakteristiki nekotoryh vidov Plantago [Ecophysiological characteristics of some species of Plantago]. Vestn. Bashkir, vol. 2, no. 1, pp. 43-45.

3. Nysanbaev A. (2002) Kazakhstan ulttyk enciklopediya [Kazakhstan national encyclopedia]. Almaty: Kazakh enciklopediyasy, vol. 2, pp. 316-317.

4. Budancev A.L., Lesiovskaya E.E. (2001) Dikorastushie rasteniya [Wild plants]. SPb: SPHFA, vol. 1, pp. 643.

5. Korsun V.F., Trumpe E.E., Korsun E.V., Ershov N.V., Ogrenich N.A. (2016) Fitoterapiya protiv diadeta. Travy zhizni [Herbal medicine against diabetes. Grass life] ZAO "Izdatel'stvo Centrpoligraf", no. 1, pp. 115-116.

6. Reina E., Al-Shibani N., Allam E., Gregson K.S., Kowolik M., Windsor L.J. (2013) The Effects of Plantago major on the Activation of the Neutrophil Respiratory Burst. *J Tradit Complement Med.*, vol. 3, no. 4, pp. 268-272.

7. Levent A., Oto G., Ekin S., Berber I. (2013) Method validation and simultaneous determination of retinol, retinyl palmitate, β-carotene, α-tocopherol and vitamin C in rat serum treated with 7,12 dimethylbenz [a] anthracene and Plantago major L. by high-performance liquid chromatography using diode-array detection. Comb Chem High Throughput Screen, vol. 16, no. 2, pp. 142-149.

8. Alimova U.S. (2015) Razrabotka suppozitoriev na osnove uglekislotnogo ekstrakta podorozhnika bol'shogo I aira bolotnogo [Development of suppositories based on carbon dioxide extract of large plantain and calamus swamp]. Sank-Piterburgskaya gosudarstvennaya himiko – farmacevticheskaya akademiya: Informagenstvom "Severnaya Zvezda", no. 3, pp. 161-164.

9. Dil'barhanov R.D., Ustenova G.O., Orynbasarova K.K., Strel'nikov L.S., Strilec O.P., Yudin Yu.V., Gladuh E.V. (2015) Izuchenie antimikrobnoi aktivnosti CO2-ekstraktov podorozhnika bol'shogo i aira bolotnogo [The study of the antimicrobial activity of CO2-extracts of the plantain large and calamus swamp]. OK-MFA Habarshysy, vol. 2, no. 71, pp. 56-59.

10. Sharma H., Yunus G.Y., Mohapatra A.K., Kulshrestha R., Agrawal R., Kalra M. (2016) Antimicrobial efficacy of three medicinal plants *Glycyrrhiza glabra, Ficus religiosa*, and *Plantago major* on inhibiting primary plaque colonizers and periodontal pathogens: an *in vitro* study. *Indian J Dent Res.*, vol. 27, no. 2, pp. 200-204.

11. Zubair M., Nybom H., Lindholm C., Brandner J.M., Rumpunen K. (2016) Promotion of wound healing by Plantago major L. leaf extracts-ex-vivo experiments confirm experiences from traditional medicine. *Nat Prod Res*., vol. 30, no. 5, pp. 622-624.

12. Kartini-Piyaviriyakul S., Thongpraditchote S., Siripong P., Vallisuta O. (2017) Effects of Plantago major Extracts and Its Chemical Compounds on Proliferation of Cancer Cells and Cytokines Production of Lipopolysaccharide-activated THP-1 Macrophages. *Pharmacogn Mag.*, vol. 13, no. 51, pp. 393-399.

13. Lukova P.K., Karcheva-Bahchevanska D.P., Bivolarski V.P., Mladenov R.D., Iliev I.N., Nikolova M.M. (2017) Enzymatic hydrolysis of water extractable polysaccharides from leaves of *Plantago major* L. Folia Med (Plovdiv), vol. 59, no. 2, pp. 210-216.

14. Adom M.B., Taher M., Mutalabisin M.F., Amri M.S., Abdul Kudos M.B., Wan Sulaiman M.W.A., Sengupta P., Susanti D. (2017) Chemical constituents and medical benefits of *Plantago major*. Biomed Pharmacother, vol. 96, pp. 348-360.

15. Naji Ebrahimi Yazd Z., Hosseinian S., Shafei M.N., Ebrahimzadeh Bideskan A., Entezari Heravi N., Parhizgar S., Shahraki S., Samadi Noshahr Z., Mahzari S., Khajavi Rad A. (2018) Protection against Doxorubicin-induced nephropathy by *Plantago major* in rat. *Iran J Kidney Dis.*, vol. 12, no. 2, pp. 99-106.

16. Caro D.C., Rivera D.E., Ocampo Y., Franco L.A., Salas R.D. (2018) Pharmacological Evaluation of Mentha spicata L. and Plantago major L., Medicinal Plants Used to Treat Anxiety and Insomnia in Colombian Caribbean Coast. *Evid Based Complement Alternat Med.*, vol. 27, pp. 7.

17. Entezari H.N., Hosseinian S., Naji Ebrahimi Y.Z., Shafei M.N., Ebrahimzadeh B.A., Shahraki S., Samadi N.Z., Motejadded F., Beheshti F., Mohebbati R., Parhizgar S., Khajavi R.A. (2018) Doxorubicin-induced renal inflammation in rats: Protective role of Plantago major. *Avicenna J Phytomed.*, vol. 8, no. 2, pp. 179-187.

18. Grechanyi I.A. (2013) Polnyi spravochnik lekarstvennyh trav i celitel'nyh sborov [Complete handbook of herbal and healing fees]. Knizhnyi klub "Klub semeinogo dosuga", no. 1, pp. 357-359.

19. GOST 31483-2012 Premiksy, Opredelenie soderzhaniya vitaminov: B(1) (tiaminhlorida), B(2) (riboflavina), B(3) (pantotenovoi kisloty), B(5) (nikotinovoi kisloty i nikotinamida), B(6) (piridoksina), B(c) (folievoi kisloty), C (askorbinovi kisloty) metodom kapillyarnogo elektroforeza) [Premixes Determination of the content of vitamins: B (1) (thia-

mine chloride), B (2) (riboflavin), B (3) (pantothenic acid), B (5) (nicotinic acid and nicotinamide), B (6) (pyridoxine), B (c) (folic acid), C (ascorbic acid) by capillary electrophoresis].

20. GOST 24027.2-80 Syr'e lekarstvennoe rastitel'noe. Metody opredeleniya vlazhnosti, soderzhaniya zoly, ekstraktivnyh I dubil'nyh veshestv, efirnogo masla [Raw medicinal plant. Methods for determining the moisture content of ash, extractive and tannins, essential oil].

21. Maevskii, P. F. (1964) Flora srednei polosy Evropeiskoi chasti SSSR [Flora of the middle belt of the European part of the USSR]. Kolos, vol. 8, pp. 134-139.

22. Kanaev, A. T., Kanaeva, Z.K. (2016) Paidaly osimdikter zhane olardy daiyndau biptehnologiyasy [Useful plants and biotechnology for their preparation]. Almaty: Kazakh Universiteti, no. 1, pp.187-189.

23. Yakovlev, G.P. (2018) Botanika [Botany]. SpecLit, no. 1, pp. 303-305.

24. Muhitdinov, N.M., Mamurova, A.T. (2013) Darilik osimdikter [Medicinal plants]. Almaty, no. 3, pp. 236.

25. Viktorov, V.P., Gulenkova, M.A., Elenevskii A.G., Shorina N.I. (2001) Praktikumpo anatomii I morfologii rastenii [Workshop on the anatomy and morphology of plants]. Izdatel'skii centr: Akademiya, no. 2, pp. 59.

26. Zakharova O.A., Musaeva R.F., Musaev F.A. (2014) Lekarstvennye rasteniya [Medicinal plants]. Knizhnyi dom, no. 2, pp. 656.

27. Turishchev S.N. (2003) Fitoterapiya revmaticheskih boleznei [Herbal medicine for rheumatic diseases]. *Farmaciya*, vol. 6, pp. 46-48.

28. Aziz S.A., See T.L., Khuay L.Y., Osman K., Abu Bakar M.A. (2005) In vitro effects of Plantogo major extract on urolithiasis. *Malaysian Jornal of Medical Sciences*, vol. 12, no. 2, pp. 22-26.

29. Maksiutina N.P., Nikitina N.I., Lipkan G.N., Gorin A.G., Voitenko I.N. (1978) Chemical composition and hypocholesteremic effect of several preparations from the leaves of the great plaintain. I. Polyphenol compounds. *Farm Zh.*, vol. 4, pp. 56-61.

30. Kurennov I.P. (2018) Entsiklopediya lekarstvennykh rasteniy [Encyclopedia of medicinal plants]. Martin, vol. 1, pp. 357.

31. Tsitsilin A. (2015) Lekarstvennyye rasteniya: Atlas-spravochnik [Medicinal Plants: Atlas-Reference]. Medical Academy for the whole family, vol. 1, pp. 238.

32. Pailer V.M., Haschke-Hofmeister E. (1969) Inhaltstoffe aus *Plantago major. Planta Med.*, vol. 17, pp. 139-145.

33. Scott-Moncrieff C. (2006) The Vitamin Alphabet: Your Guide to Vitamins, Minerals and Food Supplements. Collins & Brown, vol. 10, pp. 11-13.

34. Gerald F. Combs Jr. (2012) The Vitamins. Academic Press, vol. 4, pp. 158-162.

35. Rebeille F., Douce R. (2011) Advances in Botanical Research. Academic Press, vol. 58, pp. 165-178.

36. Zempleni J., Suttie J.W., Jesse F.G., Stover P.J. (2013) Handbook of Vitamins. CRC Press, vol. 5, pp. 435-436.

37. Ormanov N.Zh., Ormanova L.Zh. (2013) Farmakologiya [Pharmacology]. Almaty: Evero, vol. 1, pp. 405-406.

IRSTI 57.017.35:633.31/.37

[1]B.A. Zhumabayeva, [1*] Z.G. Aytasheva, [1]E.D. Dzhangalina,
[2*]A. Esen, [1]L.P. Lebedeva

[1]Laboratory of cell and applied biotechnology, Almaty, Kazakhstan
[2]Virginia Polytechnic Institute and State University, Blacksburg, Virginia, United States of America
[*]e-mail: zaure.aitasheva@kaznu.kz; aevatan@vt.edu

Screening of domestic common bean cultivar for salt tolerance during *in vitro* cell cultivation

Abstract: One of the principal limitations in application of cell and tissue culture techniques for improving crop plants resistance to adverse environmental stresses, such as high salinity, is insufficient knowledge of cellular and molecular-genetic basics of this type of tolerance. This approach will provide opportunity to identify new salt-tolerant cultivars, which arisen from somatic mutations increasing the pool of salt-tolerant breeding lines. It is well known that salinity causes sharp reduction in bean productivity and thus significant losses in quality and quantity of products derived from it. Choosing salt-tolerant plant genotypes for cultivation may solve this problem. The aim of this study is to trace tolerance and accompanying changes in lectin accumulation in calli of common bean (*Phaseolus vulgaris L.*) grown under the conditions of tissue culture. In our experiment, induction of certain common bean cultivars by *in vitro* cell cultures have been optimized. The most appropriate composition of the nutrient media for the induction of callusogenesis have been established together with the cultivars possessing high callus-forming ability. We have not observed strict correlation between callus-forming propensity and morphogenic calli generation. However, we noticed that under-passaging in selective conditions calli leads to gradual growth decline and browning, as well as slow growth and in some cases death of cell cultures. Nevertheless, we have identified common bean cultivars with average salt tolerance and high propensity to callusogenesis for use as a starting material for breeding. Differences in lectin content between morphogenic and non-morphogenic calli let us suggest that lectin content depends on hormonal composition of the nutrition medium since morphogenic type of callus was formed when the media contained NAA and low concentrations of 2,4-D. The cultivars used in this study have demonstrated moderate salt tolerance and high callusogenesis efficiency thus regarded as suitable material to breeding for salt tolerance.

Key words: common bean, cultivar samples, *in vitro* culture, calli, salt tolerance, lectins.

Introduction

Salinity is one of the most critical environmental factors leading to decrease in crops productivity under growing salt concentrations in the soil, and this issue keeps on growing [1]. Principal reason for increasing soil salinity is the use of irrigation. This matter may be solved using efficient agricultural practices, improved irrigation methods, and completely or partly desalted water for sprinkle irrigation.

Common bean is a pulse vegetable crop with high activity of lections [2]. Study of the protein composition of the common bean seed is particularly relevant nowadays because there is a need to develop new cultivars, which may serve as the source of protein. This can be achieved by deploying biotechnological approaches towards their identification, selection and their uses in different sectors of agriculture.

Within the last decades, there is a growing need in new sources for extraction of nutritional and anti-nutritional protein components to study their action on different cell models, advanced methods for their isolation, and further use to obtain new plant protection reagents as well as drugs and diagnostics [3; 4].

In the cultivation and use of common bean, lectins (including intracellular) are of particular concern, since they are involved in a number of undesirable reactions, like wounding, cold, drought, osmotic shock and salinity of the growth medium, increasing their hemagglutinating activities [5]. It has been reported that lectin gene expression is induced by low humidity and high salinity stress [6]. Consequently,

development of salt-tolerant cultivars received much attention in common bean breeding lately.

Salt tolerance is thought to be genetically controlled trait in beans [7]. Although it is shown to be monogenic in soybean, the consensus is that it is a polygenic trait. Variability for salt tolerance within the plant species is shown by various surveys [4]. In contrast, there are species with no such type of variability [5].

One of the principal limitations in application of cell and tissue culture techniques for improving crop plants resistance to adverse environmental stresses, high salinity, in particular, is insufficient knowledge of cellular and molecular-genetic basics of such tolerance.

Selection at the cellular level is used in the majority of cases to obtain plant forms that are tolerant or resistant to stress factors, such as salt (including ion stress), diseases, chemical stress caused by herbicides, etc. The aim of this study was to investigate salt tolerance and accompanying changes in lectin accumulation in calli of common bean cultivars (cvs.) grown under tissue culture conditions

Materials and methods

Seeds of 10 domestic and international cvs. of common bean were used for this study. They were: Aktatti, Nazym, Talgat (Kazakhstan), Katka, Luna, Zuzka (Czech Republic), Bijchanka, Ufimskaya (Russian Federation), Camelia, and Red Goya (USA).

Cell and tissue culture work was carried out under strictly aseptic conditions, and thus, sterility was maintained throughout the whole study, i.e., from preparation of glassware and instruments to preparation of seed stocks and nutritional media. In order to obtain aseptic seedlings of common bean, seeds were sterilized sequentially in 60% sulphuric acid for 3 min, 5% chloramine for 5 min, 0.1% mercuric chloride for 10-15 min and 70% ethanol for 1-2 min.

Seeds were then washed thrice in sterile distilled water and planted on the agaric Murashige-Skoog (MS) medium containing half the concentration of macro- and microelements and no growth regulators [8]. After germination, seedlings were grown at 20-25 °C and 16-hour photoperiod.

Then, epicotyls and hypocotyls of 10-15 day-old sterile seedlings were used as explants. Epicotyls were rooted using MS medium without growth regulators to obtain sufficient amount of explants preserving their initial genotype. All nutrition media were autoclaved at 120 °C for 25 min. Analysis of calli formation and morphogenic capacity were performed on Uchimiya-Murashige nutritional medium [9]. 2,4-Dichlorophenoxyacetic acid (2,4-D), kinetin, 1-naphthylacetic acid (NAA), 6-benzylaminopurine (BAP) and yeast extract were used as phytohormone and organic additives.

Sodium chloride (NaCl) concentrations of 0.17 M, and 0.26 M were used as selective agent for salinity tolerance, and the normal medium (no added NaCl) served as control.

Identification and selection of salt-tolerant cell lines were carried out by direct stair-step selection in callus cultures on MS medium containing the above-mentioned NaCl concentrations. Tissues were cultivated at each concentration of NaCl for 8 weeks, and then on the media inducing callusogenesis (4 weeks) and media inducing somatic embryogenesis (4 weeks), respectively. Growth characteristics of calli and biomass accumulation were estimated on all of selective media. Biomass of calli was measured under sterile conditions of laminar box using the torsion scales, whereas the growth activity of calli was assessed microscopically using an MBS-10 device (Levenhuk, Russia).

Biomass of morphogenic calli was proliferated every fortnight by 3-4 times by transferring on fresh modified Uchimiya-Murashige medium, containing 2 mg/L 2,4-D and 0.25 mg/L kinetin. Increased biomass of calli was measured every 28 days.

Basic method of lectin isolation from cell biomass of common bean was developed for seeds and described by Alexidze et al. [10]. We applied it to calli cultures using more gentle homogenization of plant tissue and reduced extraction time.

Statistical analysis of the data was performed using standard methods of statistical research, methods of correlation and variation analyses [11].

Results and discussion

The main objective of this study was to identify and select salt-resistant common bean cultivars by screening domestic cultivar samples within *in vitro* culture. To meet this objective, it was necessary to develop approaches that will allow obtaining highly morphogenic common bean cell cultures.

Callus-forming and somatic embryogenic capacity of common bean. At the earlier stage of this investigation, effective methods of seed and explant sterilization were tested. It was found that duration of seed sterilization differed prior to the time of exposure to chloramine and ethanol solutions, when chloramine concentration was kept at 5% and ethanol concentration achieved 70%. These tests showed that optimal

time for sterilization in chloramine and ethanol would be 5 and 1-2 min, respectively. In subsequent experiments, we carried out extensive screening of Kazakh common bean cultivars to determine their ability to generate calli and promote somatic embryogenesis in tissue culture so that genotypes with high morphogenetic potential can be identified. In this study, 10 cultivars of domestic and foreign origin were examined. Screening was carried out under the following conditions: callusogenesis induction on Uchimiya and Murashige medium (UM) (2,4-D – 2 mg/L, kinetin – 0.25 mg/L) and somatic embryogenesis induction on the same UM medium with other additives (NAA – 0.05 mg/l, BAP – 0.5 mg/L). Epicotyls and hypocotyls of 7-10 day-old sterile seedlings were used as explants. Results showed that both types of explants demonstrated callus formation in 7 to 10 days after the onset of cultivation. However, there were differences respectively to the callus proliferation and the amount of callusogenesis, depending on genotypes and explant sources.

Callus formation started on all nutrition media on 7 to 10 days after cultivation. Comparative analysis of the frequency of callusogenesis dependent on the explant type indicated that the epicotyl and the hypocotyl were capable of forming calli, but the epicotyl was more suitable than the hypocotyl for the induction of callus formation. There was substantially greater mass of the cotyledonary leaves on the epicotyl, increasing the final yield of the callus much higher than that on hypocotyls. Moreover, the proportion of explants forming callus varied from 75 to 95% in most cultivar samples, as shown in the Table 1.

Table 1 – Frequency and amount of callus formation and production of somatic embryoids from the epicotyls of domestic and foreign common bean cultivars

Genotype	Frequency of callusogenesis, %	Intensity of callusogenesis, points	Frequency of morphogenic calli,%	Average number of embryoids per callus
Aktatti	81±0.54	1.9 ±0.14	20±0.31	0±0.21
Bijchanka	84±0.41	1.6±0.21.	14±0.22	7±0.20
Camelia*	93±0.42	3.6±0.32	35±0.11	11±0.17
Katka	89±0.67	3.3±0.17	0	0
Luna	75±0.31	2.0±0.11	18±0.14	9±0.14
Nazym	79±0.42	2.2±0.21	19±0.17	7±0.15
Red Goya*	95±0.71	2.9±0.31	33±0.21	10±0.9
Talgat	82±0.56	2.1±0.26	15±0.17	7±0.11
Ufimskaya	87±0.31	2.7±0.11	13±0.19	8±0.16
Zuzka	80±0.42	2.1±0.12	11±0.23	5±0.12

As can be seen from the Table 1, cvs. Ufimskaya, Camelia, Katka and Red Goya showed the highest callus yields, achieving 87%, 93%, 89% and 95%, respectively. Intensity of the callus formation was assessed by the five-point scale. The highest percentage of the callus formation (more than 2 points) was also observed in the same cultivar samples. Callus tissues differed within and between genotypes with respect to morphology, color and density, and they were subdivided into the following types: 1) friable, granular, weakly watery, heterogenous, white yellow; 2) dense, moisture-deficient, homogeneous, light green; and 3) extensively hydrated, homogeneous, white. Of these calli, their morphology, color, density the first type turned out to be embryogenic.

Within a given common bean genotype, morphology of calli showed less variability than that between the genotypes. It should be noted that we could not experimentally confirm the presence, if any, of a strong correlation between the frequency of callusogenesis and the propensity to produce morphogenic calli.

According to the results, which were obtained using Student-test method, the difference between cvs. Red Goya and Camelia is equal to 2.44 ($p<0.01$), between Katka and Ufimskaya is 2.70 ($p<0.01$), between Talgat and Biichanka is 2.88, and between Luna and Nazym is 7.66. Thanks to this data, which might be considered as statistically significant, we can prove, that all of the cultivars, listed in Table 1, belong to the different lines.

Different investigators emphasize the importance of the relationships between calli morphology and the ability to regenerate plants. Specific features of morphogenic calli may vary among plant species [12]. In this study, we observed that dense, compact callus had reduced morphogenic ability. In our study, formation of morphogenic structures was observed only in cvs. Red Goya and Camelia (Figure 1), whereas cvs. Katka and Ufimskaya produced friable, globular calli. Cv. Katka appeared to have high frequency of callusogenesis (3 points and higher) by its growth. However, it showed only further proliferation of callus, but no somatic embryoid formation or morphogenic calli.

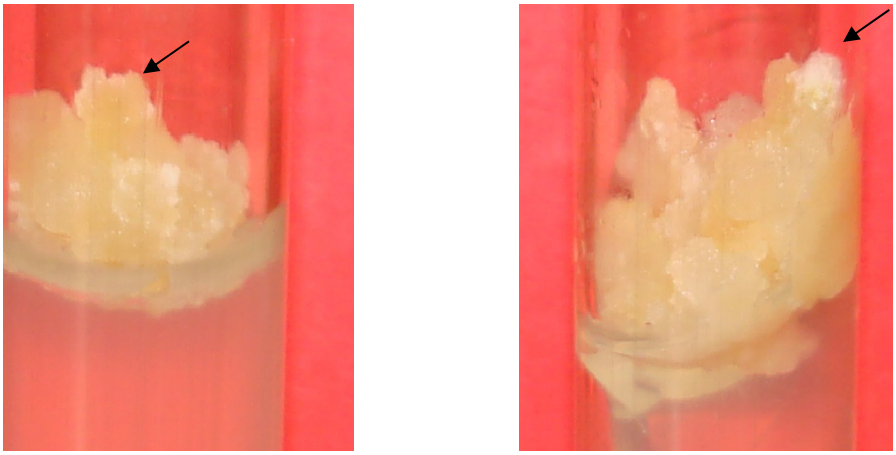

a b

Figure 1 – Induction of morphogenic calli in tissue culture of common bean cvs. Red Goya (a) and Camelia (b). Note: Morphogenicity is determined by the form, color and density of the callus and the presence of morphogenic tubercules are shown by arrows

Thus, sterilization conditions for the different types of explants were determined along with the optimal cultivation media composition, as well as the relationship between the callusogenesis and morphogenesis *in vitro*. Epicotyls from cvs. Katka, Camelia and Red Goya exhibited maximal callus-generating ability when cultivated in modified Uchimiya-Murashige medium.

As for the relationship between the intensity of callusogenesis and morphological structures of the calli, tight, compact calli had lower morphogenic potency. Morphogenic structures were observed only in cvs. Camelia and Red Goya, which formed loose, globular calli. In callus-producing cultures, the induction of calli was observed upon two-three weeks of cultivation in Murashige-Skoog medium containing NAA (0.05 mg/L) and BAP (0.5 mg/L) (Figure 2).

Before the emergence of green meristematic foci on the light surface of the calli, bud formation was detected. Frequency of morphogenesis in epicotyls was substantially higher than that in hypocotyls, the value varying from 11.1% to 19.3% (Figure 3), whereas the morphogenic capacity in hypocotyls was in the range of 6.5-14.2%.

Next stage of the present study was focused on cellular level selection for salt tolerance in callus cultures of common bean. Subsequent to cultivation under light conditions for a month, part of the calli obtained was transferred on to a selective medium containing varying (0.17 M to 0.26 M) concentrations of NaCl to investigate the accumulation of the callus biomass. The results showed that calli proliferated at 0.17 M/L NaCl concentration but their biomass was decreased by 14 to 48%, depending on the genotype when compared to salt-free control. At 0.26 M NaCl concentration, calli of all cultivars completely stopped accumulating the biomass (Table 2).

Under the increasing salt (NaCl) concentration in the growth medium up to 0.26 M, the calli developed necrotic areas, especially in those genotypes that are more susceptible to salinity. These genotypes turned necrotic already after the first passage of cultivation on medium containing 0.17 NaCl (Figure 4).

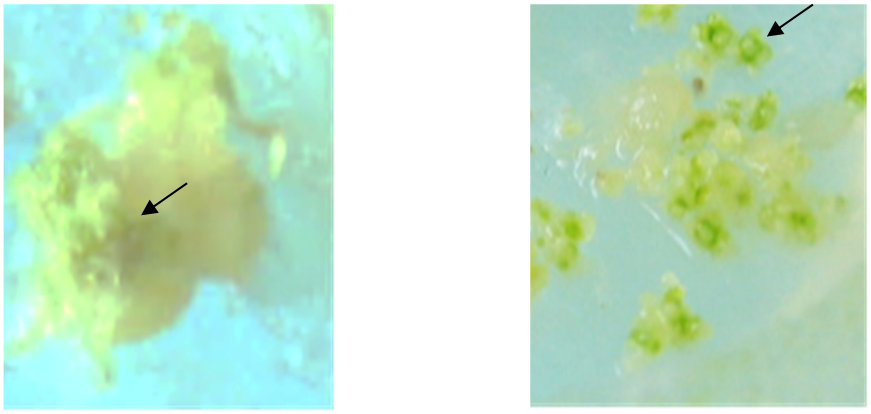

a b

Figure 2 – Induction of meristematic foci on the surface of the calli in common bean cvs. Red Goya (A), Camelia (B). Note: Shoots are shown by arrows

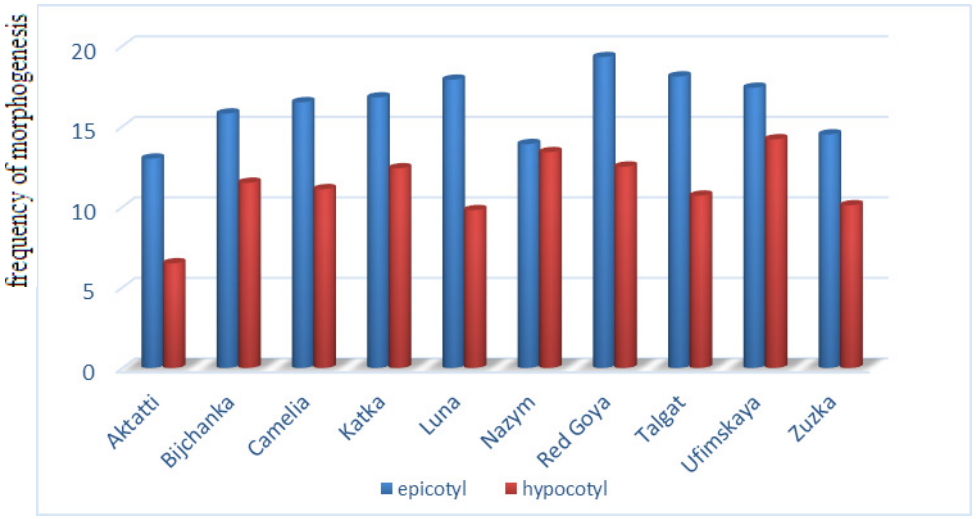

Figure 3 – Dependence of the frequency of morphogenesis on the type of explant in different cultivars of common bean

Table 2 – Accumulation of the biomass by common bean calli on selective medium simulating soil salinity

Genotype	Initial average mass, mg	Mass of callus in the absence of salt, mg (blank)	Mass of callus on stressor-containing medium, mg
Aktatti	101.67 ± 1.41	118.71 ± 1.23	102.92 ± 1.37
Bijchanks	86.42 ± 1.82	106.71 ± 1.98	86.45 ± 3.24
Camelia	120.66 ± 2.34	152.72 ± 1.45	136.58 ± 1.79
Katka	132.75 ± 1.71	166.81 ± 2.46	130.18 ± 1.63
Luna	85.32 ± 1.83	163.71 ± 1.56	85.74 ± 1.36
Nazym	84.59 ± 1.10	110.83 ± 1.53	84.69 ± 2.74
Red Goya	112.66 ± 2.93	158.62 ± 2.45	135.93± 1.84
Talgat	92.79 ± 1.89	126.61 ± 1.34	93.92 ± 1.49
Ufimskaya	119.55 ± 1.85	145.73 ± 1.47	125.73 ± 1.55
Zuzka	94.79 ± 1.95	125.83 ± 0.67	94.5 ± 1.38

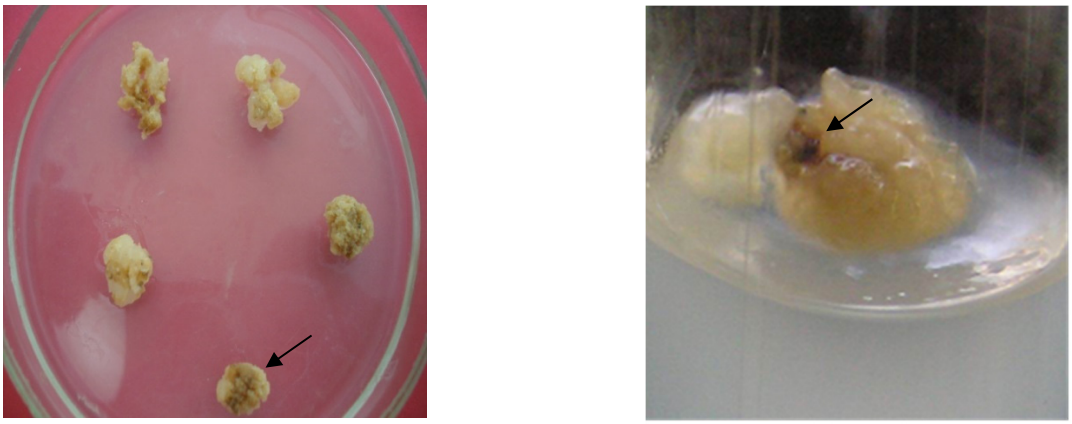

a b

Figure 4 – Change in the callus tissue morphology (shown by the arrows) from genotypes Nazym and Talgat after 30-day cultivation in the medium containing 0.17 M/L NaCl.
Note: a – growth and development inhibition in the callus tissue of cultivar Nazym;
b – necrosis of the callus tissue from cultivar Talgat

Our results indicate that the reduction of growth under salinity conditions in comparison to control was especially remarkable in the calli of such highly salt-susceptible genotypes as Aktatti, Bijchanka, Zuzka, Luna, Katka, Nazym, and Talgat. Although all genotypes have displayed susceptibility to salinity. American cvs. Red Goya and Camelia were less sensitive to salinity than other cultivars tested. In addition, we observed substantial differences among cultivars with respect to calli morhology in that the calli of less susceptible genotypes under the salinity stress (during the first passage) were more dense, and they retained their original color and consistency. In contrast, the calli of strongly salt-susceptible genotypes began to darken and become necrotic even under minimal salt concentration.

Selection of resistant cell clones under salt stress was done on the basis of two criteria: growth and maintenance of morphogenetic capability. However, morphogenetic potency weighted more heavily than growth characteristics during the selection. Cv. Red Goya was a standout candidate for selection because it was able to grow and form tolerant morphogenic calli for a long period.

Performing cell selection in two stages allowed us to estimate the degree of resistance of common bean genotypes to salinity, including those that maintain callus morphogenicity.

As a rule, *in vitro* growth and accumulation of biomass tend to decline as concentration of the stressor (i.e., NaCl) in nutrient medium increases. This is evident from the data (presented in Table 2) that growth decreases under the saline stress compared to control in all of the calli of the following genotypes: Aktatti, Bijchanka, Zuzka, Luna, Katka, Nazym and Talgat. Thus, we conclude that only American cvs. Red Goya and Camelia are relatively salt-resistant. Therefore, out of the 10 cultivars used in this study, only these two cultivars may be used as source material to breed salt resistant cultivars in further studies. All in all 1016 explants and 926 calli of common bean were planted on the NaCl-containing selective media, and of this total, 201 callus lines were passed for regeneration yielding 21 regenerated plants (the yield of 7.6%).

The other focus of our study was on lection accumulation in callus tissues of common bean and its relationship to salinity. The first evidence of protective properties of lectins under salinity was reported in conjunction with the description of a protein encoded by Sal T gene in rice, *Oryza sativa* L. [13]. This protein was a cytosolic mannose-specific lectin [14; 15], and it was not detectable under normal conditions but was induced and detectable in roots subjected to salt stress or drought [16; 17]. Nonetheless, even after induction by abiotic stress factors, it was not highly expressed.

The generic functions attributed to lectin are binding to carbohydrates with high degree of specificity, and their postulated role in cell division [18; 19]. Hence, lectins may play essential roles in morphological and physiological processes and intracellular interactions, which are crucial for cellular and tissue differentiations. Lectins may also be involved in induction of somatic embryogenesis in tissue cultures [20; 21]. With these

consideration in mind, we performed , comparative analysis of lectin content in callus tissues of common bean cultivars. Calli of these cultivars differing by morphogenetic potency were obtained under optimized conditions. The analysis indicated significant differences in lectin content among callus tissues of common bean cultivars, namely, high lectin concentration being a characteristic of the morphogenic type callus. This consistent pattern was not genotype-dependent. Although the analysis of extracts from callus cultures showed variability with respect to lectin content, maximal lectin levels were always observed in calli extracts from morphogenic callus tissue (Figure 5).

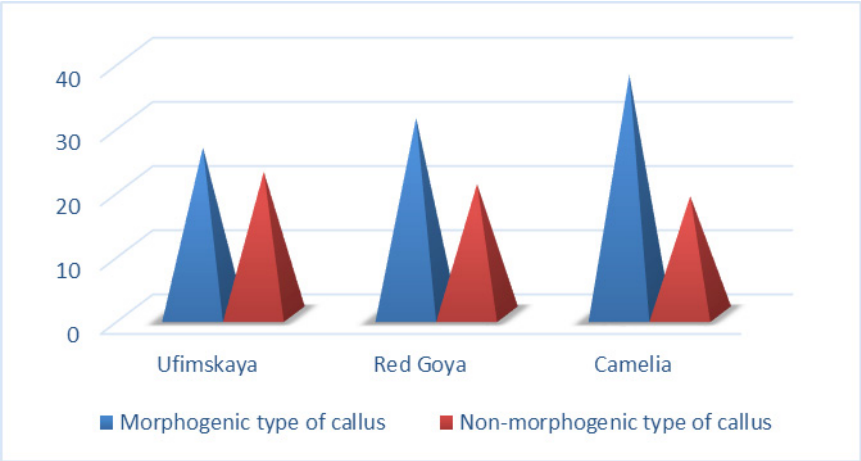

Figure 5 – Lectin content in common bean calli (mg/ 100g of fresh weight)

According to the results presented in Figure 5, lectin concentration in the morphogenic calli ranges between 26.0 mg/100 g of fresh weight in cv. Ufimskaya and 37.3 mg/100 g of fresh weight in cv. Camelia. Callus tissues from non-morphogenic cultivars contained low lectin concentrations, which ranged from 18.4 to 25.2 mg/100 g of fresh weight.

Conclusion

Salt tolerance is not necessarily manifested at the level of the whole plant as the mechanisms of cellular and organismic adaptations may differ. That is why screening and selection for salt tolerance *in vitro* should not be used without prior establishment of substantial correlation between the whole plant and cell culture responses to stress by performing appropriate experiments [22].

Tissue culture technology may facilitate investigations on salt tolerance at cellular level in order to identify germplasm to be used as source material in breeding for salinity tolerance [23]. In addition, this approach will provide opportunity to identify new salt-tolerant variants arising from somatic mutations increasing the pool of salt-tolerant breeding lines.

The correlation linkage between biomass accumulation in calli under osmotic stress and plant drought resistance traits *in vivo* is shown [24; 25]. Consequently, the ability to grow and accumulate biomass under stress conditions may be critical indicators of genotype resistance to stress.

Our data shows that by using NaCl-containing media, it is possible to conduct a primary evaluation of salt tolerance among genotypes based on morphological characteristics of callus tissues and growth inhibition as measured by the degree of reduction in biomass accumulation. Such preliminary evaluation will pave the way to further studies using *in vitro* cultures for selecting salt-tolerant and salt-sensitive common bean cultivars.

Differences in lectin content between morphogenic and non-morphogenic calli suggest that lectin content is dependent on hormonal composition of the nutrition medium since morphogenic type of callus was formed when the media contained NAA and low concentrations of 2,4-D. It is known from the literature [26; 27] that the synthesis of lectins is triggered by abscisic acid (ABA), and high concentrations of 2,4-D reduce the ABA content.

It was discovered that the common bean cultivars used in this study possess average salt tolerance and high callusogenesis potency; and they are suitable to be used as a source material for breeding salt tolerant lines.

References

1. Shrivastava P., Kumar R. (2015) Soil salinity: A serious environmental issue and plant growth promoting bacteria as one of the tools for its alleviation. *Saudi J Biol Sci*., vol. 22, no. 2, pp. 123-131. https://doi.org/10.1016/j.sjbs.2014.12.001

2. Roy F., Boye J.I., Simpson B.K. (2010) Bioactive proteins and peptides in pulse crops: pea, chickpea and lentil. *Food Res Int*., vol. 43, no. 2, pp. 432-442. https://doi.org/10.1016/j.foodres.2009.09.002

3. Saetae D., Worapot Suntornsuk W. *(2011)* Toxic Compound, Anti-Nutritional Factors and Functional Properties of Protein Isolated from Detoxified *Jatropha curcas* Seed Cake. *Int J Mol Sci.*, vol. *12, no. 1*, pp. 66-77. https://doi.org/10.3390/ijms12010066

4. Li J.W.-H., Vederas J.C. (2009) Drug discovery and natural products: end of an era or an endless frontier? *Science, v*ol. 325, no. 5937, pp. 161-165. https://doi.org/10.1126/science.1168243

5. Shakirova F.M., Bezrukova M.V., Hajrullin R.M. (1993) Stimulyaciya uvelicheniya urovnya lektina v prorostkah pshenicy pod vliyaniem solevogo stressa. [Stimulation of increasing of lectin level in wheat seedlings under saline stress], *Izv RAN Ser biol.,* vol. 1. pp. 143-145.

6. Zhang W., Peumans W., Barre A. et al. (2000) Isolation and characterization of a jacalinrelated mannose-binding lectin from salt-stressed rice (Oryza sativa) plants, *Planta*, vol. 210. pp. 970-978. https://doi.org/10.1007/s004250050705

7. *Singh A.K., Bhatt B.P., Upadhyaya A., Kumar S., Sundaram P.K.,Singh B.K., Chandra N., Bharati R.C.* Improvement of faba bean (*Vicia faba L.*) yield and quality through biotechnological approach: a review (2012). *African J Biotech.*, vol. 11, no. 87, pp. 15264-15271.

8. Murashige, T., & Skoog F. (1962) A revised medium for rapid growth bioassays with tobacco tissue cultures. *Physiol Plant.*, vol. 15, no. 3, pp. 473-493. https://doi.org/10.1111/j.1399-3054.1962.tb08052.x

9. Uchimiya H., Murashige T. (1997) Quantative analysis of the fate of exogenous DNA in *Nicotiana* protoplasts, *Plant Physiol*., vol. 59, pp. 301-308. https://doi.org/10.2307/4264723

10. Aleksidze G.YA. (2002) Model' organizacii na membrane tilaktoidov cikla Kalvina s uchastiem lektina fotosistemy [Model of Kalvin cycle organization on the membrane of thylakoids with participation of lectin photosystem], *Fiziologiya rastenij*, vol. 49, no. 1. pp. 148-154.

11. Rokickij P.F. (1973) Biologicheskaya statistika. [Biological statistics] Minsk. Vysshaya shkola. 319 p.

12. Mitrofanova I. V. (2009) Somaticheskij ehmbriogenez kak sistema in vitro kul'turnyh rastenij. [Somatic embryogenesis as a system of agricultural plants in vitro], *Fiziologiya i biohimiya kul'turnyh rastenij*, vol. 41, no. 6, pp. 496-508.

13. George E.F., Hall M.A., De Klerk G.J. (eds.) (2007). *Plant propagation by tissue culture: the* background. Springer Science & Business Media, vol. 1, 374 p.

14. Hirano K., Teraoka T., Yamanaka H. et al. (2000) Novel mannose-binding rice lectin composed of some isolectins and its relation to a stress-inducible Sal T gene, *Plant Cell Physiol.,* vol. 41, pp. 258-267. https://doi.org/10.1093/pcp/41.3.258

15. Zhang W., Peumans W., Barre A. et al. (2000) Isolation and characterization of a jacalin-related mannose-binding lectin from salt-stressed rice (*Oryza sativa*) plants, *Planta*, vol. 210. pp. 970-978. https://doi.org/10.1007/s004250050705

16. De Souza Filho G., Ferreira B.S., Dias J.M.R. et al. (2003) Accumulation of Sal T protein in rice plants as a response to environmental stresses, *Plant Sci.,* vol. 164, pp. 623-628. https://doi.org/10.1016/S0168-9452(03)00014-1

17. Engler J.A., Claes B. et al. (1998) The expression of the salt-responsive gene Sal T from rice is regulated by hormonal and developmental cues, *Planta*, vol. 207, pp. 172-180.

18. Wati K.R., Theppakorn T., Benjakul S., Rawdkuen S. (2009) Three-phase partitioning of trypsin inhibitor from legume seeds, *Process Biochem.*, vol. 44, pp. 1307-1314. https://doi.org/10.1016/j.procbio.2009.07.002

19. Benedito V.A., Torres-Jerez I., Murray J.D. et al. (2008) A gene expression atlas of the model legume Medicago truncatula, *Plant J*., vol. 55, pp. 504-513. https://doi.org/10.1111/j.1365-313X.2008.03519.x

20. Lubyanova A. R., Fathutdinova R. A., Bezrukova M. V., SHakirova F. M. (2009) Roststimuliruyushchij i zashchitnyj ehffekty fitogemagglyutinina na rasteniya fasoli [The effect of phytohemagglutinin on plant grow promotion and protection of lectins]. *Vestnik Harkivs'kogo nacional'nogo agrarnogo universitetu, seriya biologiya,* vol. 16, no. 1, pp. 39-44.

21. Babosha A.V. (2008) Inducibel'nye lektiny i ustojchivost' rastenij k patogennym organizmam i abioticheskim stressam [Inducible lectins and plant resistance to pathogenic organisms and abiotic stressors], *Biohimiya*. vol. 73, no. 7, pp. 1007-1022.

22. Smethurst C.F., Gill W.M., Shabala S. (2009) Using excised leaves to screen lucerne for salt tolerance. *Plant Signal Behav*., vol. 4, pp. 39-41. https://doi.org/10.4161/psb.4.1.7269

23. Baranova E.N., Gulevich A.A., Polyakov V.Yu. (2007) Effekty NaCl, Na2SO4 i mannita na utilizaciyu zapasnogo krahmala i formirovanie plastid v semyadolyah i kornyah prorostkov lyucerny [Effects on NaCl, Na2SO4 and mannit on utilization of spare starch and plastid formation in cotyledon of roots of alfalfa seedlings], *Fiziologiya rastenij*. vol. 54, pp. 59-67.

24. Tardieu F. (2005) Plant tolerance to water deficit: physical limits and possibilities for progress. *Com Rend Geosci*., vol. 337, pp. 57-67. https://doi.org/10.1016/j.crte.2004.09.015

25. Lia L.-H., Lva M.-M., Lia X., Yea T.-Z., Hea X., Ronga S.-H., Donga Y.-L., Guana Y., Gaoa X.-L., Zhua J.-Q., Xu Z.-J. (2018) Semejstvo OSDUF810 risa: OSDUF810.7 mozhet byt' vovlechen v mekhanizmy sole- i zasuhoustojchivosti1 [OSDUF810.7 might be involved in mechanisms of saline and drought tolerance], *Molekulyarnaya biologiya*, vol. 52, no. 4, pp. 567-575.

26. Raikhel N.V., Lee H.-I., Broekaert W.F. (1993) Structure and function of chitin-binding proteins. *Annu Rev Plant Physiol Plant Mol Biol*., vol. 44, pp. 591-615.

27. Bouiamrine El H., Diouri M., Halimi R. El, Chillasse L. (2013). Callus growth and plant regeneration in durum wheat (*Triticum durum* Desf.) immature embryos under abscisic acid (ABA) treatment. *IJB*, vol. 3, no. 2, pp. 87-98.

IRSTI 31.23.17

[1*]M.Zh. Zhumagul, [1]M.S. Kurmanbayeva, [2]N.O. Kudrina,
[1]K.D. Tolenova, [3]A.S. Seilkhan, [4]Mária Höhn

[1]Laboratory of plant anatomy and morphology, Almaty, Kazakhstan
[2]Central Laboratory for Biocontrol, Almaty, Kazakhstan
[3]Kazakh National Agrarian University, Almaty, Kazakhstan
[4]Szent István University, Budapest, Hungary
[*]e-mail: moldirzhumagul@gmail.com

GC-MS analysis of the lipophilic compounds of medicinal plant *Rhodiola rosea* L.

Abstract: *Rhodiola (R.) rosea* L. is one of the most popular adaptogenic agents. *Rhodiola rosea* L. (fam. *Crassulaceae*) commonly known as golden root or roseroot, is an insect-pollinated dioecious perennial that has been traditionally used as an immunomodulatory agent in many countries, including Kazakhstan. Plant extracts can be used both against somatic and infectious diseases, psychiatric and neurological diseases as well as in healthy people to relieve fatigue and increase concentration, memory, and productivity. There is growing evidence that the long-term effects of stressful life events and depression are associated with significant behavioral, endocrinological and neurobiological changes in human. *R. rosea* is a relatively rare and valuable medicinal plant and grows at high altitudes (up to 2280 m above the sea level) in the arctic and mountainous regions of Central Asia, Europe and North America. Study of the phytochemical composition of *R. rosea* is required in order to introduce it into official practice. Several mechanisms of action that are potentially responsible for the observed stress resistance, anti-aging and anti-cancer effects of *R. rosea* extracts and its active compounds have been identified in *in vitro* cell culture systems and on *in vivo* animal models. *R. rosea* extracts and its main biologically active compound salidroside appear to have multi-targeted effects. The results of our research showed that *R. rosea* in addition to adaptogenic, has several other pharmacological properties: antioxidant, antidepressant, immunomodulatory. Phytochemical study of *R. rosea* in Kazakhstan has been conducted for the first time. As a result of the conducted work, 28 compounds were identified in its composition.
Key words: *Rhodiola rosea* L., phytochemical composition, medicinal plants, extracts, biological activity, essential oil, pharmacotherapeutic group.

Introduction

The flora of Kazakhstan includes 68 species of trees, 266 species of shrubs, 433 species of semi-shrubs and semi-herbs, 2,598 species of perennial grasses, 849 species of annual herbs. There are more than six thousand plant species in Kazakhstan, of which 515 are endemics, 303 plant species are listed as rare and endangered, including various groups of useful plants. *Crassulaceae* family concludes 30 genera and about 1,500 varieties of succulent plants, out of which some are included into the Red Book of Kazakhstan, including *Rhodiola (R.) rosea* L. [1-3].

Healing potential of its extracts is known for many centuries. As previously, medicinal plants sustain as sources of necessary compounds for the maintenance of vital activity. The range of biologically active compounds based on medicinal and food plants used in medical practice, food industry and agriculture has however enlarged. It is important to emphasize that naturally produced biologically active compounds have pronounced physiological effect on the body and its main regulatory and metabolic processes, with lack of additive effects [4].

The importance of biologically active compounds as protective agents that prevent diseases, including such caused by adverse environmental factors and stresses is obvious. Some medicinal plants stand out for their stimulating effects on the immune system of the body and prevention of various pathological processes. One of such plants is *R. rosea* or golden root [5; 6].

R. rosea is a widespread and very polymorphic species, i.e. morphological features of this plant in different habitats vary greatly. This applies primarily to the number and density of branches, location of leaves and inflorescences, their shape and size [7-9].

Its root is a strong stimulant and increases the resistance of the human body to adverse factors. Rhizome resembles a human hand with five half-bent fingers, it is almost on the surface of the soil, and the coniferous roots go deep inside. Brownish rhizome is covered with scaly leaves of golden color with a peculiar pearlescence [10].

Leaves are pulpy, oblong-ovoid and pointed at the end. Flowers are yellow and collected in dense corymbose inflorescence. Male and female flowers are located on different bushes, male flowers are brighter and more visible, female flowers often remain green even during the flowering. Fruits – oblong leaflets of red or green color, 6-8 mm in length. Seeds are very small and light, up to 2 mm in length [11-13].

According to the literature sources 23 compounds of different nature: flavonoids, phenylpropanoids, flavolignans, monoterpenes and sterols were isolated from *R. rosea* rhizome, including such compounds as phenylpropanoids – rosin, rosavin, rosarin, cinnamon alcohol, caffeic acid, phenolic compounds – tyrosol, salidroside, gallic acid, gallicin (methyl gallate), flavonoids – rhodiolin (flavolignan gerbecetin), rhodionine, rhoiosin, 3-methyl, 3-methyl-gallate, 3-methylate, rhodoline, rhodoline, 3-methyl-gallate, rhodoline, 3-methyl-gallate, rhodoline, 5-methyl-galvanic acid, rhodoline, 5-sylphane, rhodoline, 3-methyl-gallate; tricine, tricine-5-O-glucoside, terpenoids – rosidol, roziridin, β-sitosterol, daucosteric [14-20].

Essential oils of *R. rosea*, making 0.03 to 0.2% of total compounds, vary and are of particular interest to the modern cosmetics industry. For instance, *R. rosea*, which grows in Norway, contains such components as monoterpenic acids, monoterpenic alcohols, and aliphatic alcohols in the composition of essential oils. Geraniol, in ratio of up to 65%, is a key component affecting its smell. Geranyl acetate, benzyl alcohol, phenylethyl alcohol, geranyl formate are also contained in the essential oil. The enhancers of the flower odor of the rhizomes of the *R. rosea* are linalool and its oxides, nonanal, decanal, nerol and cinnamon alcohol [20-22].

R. rosea may affect cognitive function and general nervous system. It was revealed that after a course of treatment with *R. rosea* extract significant improvement in the central nervous system occurs as the root extract increases such indicators as mobility and strength. In patients with neuroses, there is an improvement in sleep, memory, attention, and appetite; the increased irritability and unpleasant vibrations in the heart region disappear. In pharmacology, the liquid extract of *R. rosea* has a positive effect on the correction of the side effects of psychotropic therapy for schizophrenia, Parkinsonism, asthenia, etc. [23; 24]. In addition, *R. rosea* helps to prevent the negative effects of free radicals [25].

R. rosea as an adaptive organism resists the effects of chemical, biological, physical stress. In turn, the adaptogen is a catalyst for resistance to significant number of human diseases and enhances the metabolism that stimulates the hypothalamic-pituitary-adrenal system, which contributes to the processes of synthesis, improves oxygen transport to muscles and nervous system, and affects the development of red blood cells and resistance to hypoxic stress [26; 27].

Results of many studies have shown that *R. rosea* root extract stimulates and increases physical performance [9-14]. Under the experimental conditions, the possibility of correcting the free radical oxidation of membrane lipids in the blood plasma and liver tissue of animals by introducing adaptogens of extracts of *Eleutherococcus* (*E.*) *senticosus, R. rosea* and *Glycyrrhiza glabra* was investigated. Their effectiveness has been shown to increase the body's resistance under stress conditions – the effects of prooxidant factors, such as cold load and ultraviolet radiation. The administration of extracts of *E. senticosus* and *R. rosea* has a more pronounced antioxidant effect and stress-protective activity under conditions of induction of lipid peroxidation by exposure to cold, as evidenced by a decrease in the content of peroxidation products in the blood and liver of animals [28].

Currently, the possibility of using *R. rosea* preparations as hepatoprotectors is widely considered. That is, the pharmacotherapeutic group of dissimilar drugs, which prevent the destruction of cell membranes and stimulate the regeneration of hepatocytes, thereby exerting a positive effect on liver function [29].

Considering the unique medicinal properties of *R. rosea*, it is necessary to study its phytochemical composition.

Materials and methods

The object of the study is the aerial part of *R. rosea*, harvested in the flowering phase in the highlands of the Kazakhstani part of the Altai mountain system (Figure 1). Raw materials collected and dried in accordance with the requirements of the State Pharmacopoeia of the Republic of Kazakhstan, Ist edition [30; 31].

The crushed air-dry raw material was subjected to extraction by the method of infusion (maceration) with 96% ethanol, at the room temperature for 3 days. Extraction was repeated twice. The combined extract was concentrated and dried under vacuum.

Research was carried out in the Laboratory Ecology of the Biosphere, RSE Al-Farabi KazNU, SSE Center for Physical and Chemical Methods of Research and Analysis, and Laboratory of plant anatomy and morphology, Al-Farabi KazNU (Figure 2).

Figure 1 – Altai's *R. rosea*. Flowering stage. Kazakhstan, East Kazakhstan region, the northern slope of the Ivanovsky Belok ridge, 1800 m. above s.l., August 2017. Photo by Olga Kuznetsova

Figure 2 – Work with *Rhodiola rosea* L. at the laboratory of plant anatomy and morphology, KazNU, by Moldir Zhumagul

For the identification and quantitative estimation of compounds in the plant sample method using gas chromatography-mass spectrometry (GC-MS, Agilent 6890N/5973N, USA) was applied. Analysis conditions: sample volume 0.5 µl, sample entry temperature 250 °C, without dividing the flow. The separation was carried out using a DB-WAXetr (Agilent, USA) chromatographic capillary column with a length of 30 m, an internal diameter of 0.25 mm and a film thickness of 0.25 µm at a constant carrier gas (helium) rate of 1 mL/min. The chromatographic temperature was programmed from 40 °C (holding 0 min) to 200 °C with a heating rate of 10 °C/min (holding 15 min). Detection was carried out on the SCAN mode m/z 34-750. Agilent MSD ChemStation software was used to control the gas chromatography system, record and process the results and data obtained (version 1701EA). Data processing included evaluation of retention times, peak areas, as well as processing of spectral information obtained using a mass spectrometric detector. The Wiley 7th edition and NIST'02 libraries were used to decipher the mass spectra obtained (total number of spectra in libraries – more than 550,000 units).

Results and discussion

Gas-liquid chromatography is used for the analysis, separation and purification of synthetic polymers, drugs, detergents, proteins, hormones and other biologically important compounds. The use of highly sensitive detectors allows working with tiny amounts of compounds (10^{-11}-10^{-9} *g*), which is extremely important in the biological research.

In this regard, the composition of the obtained extract was analyzed.

GC-MS chromatogram of *R. rosea* ethanol extract is presented on Figure 3.

As a result of the study of the chemical composition of ethanol extract of *R. rosea*, obtained by treating the raw material with 96% ethanol, 28 components of different chemical nature were identified using GC-MS technique (Figure 3). The results of the analysis allow us to describe compounds whose content exceeded 0.5 mg %.

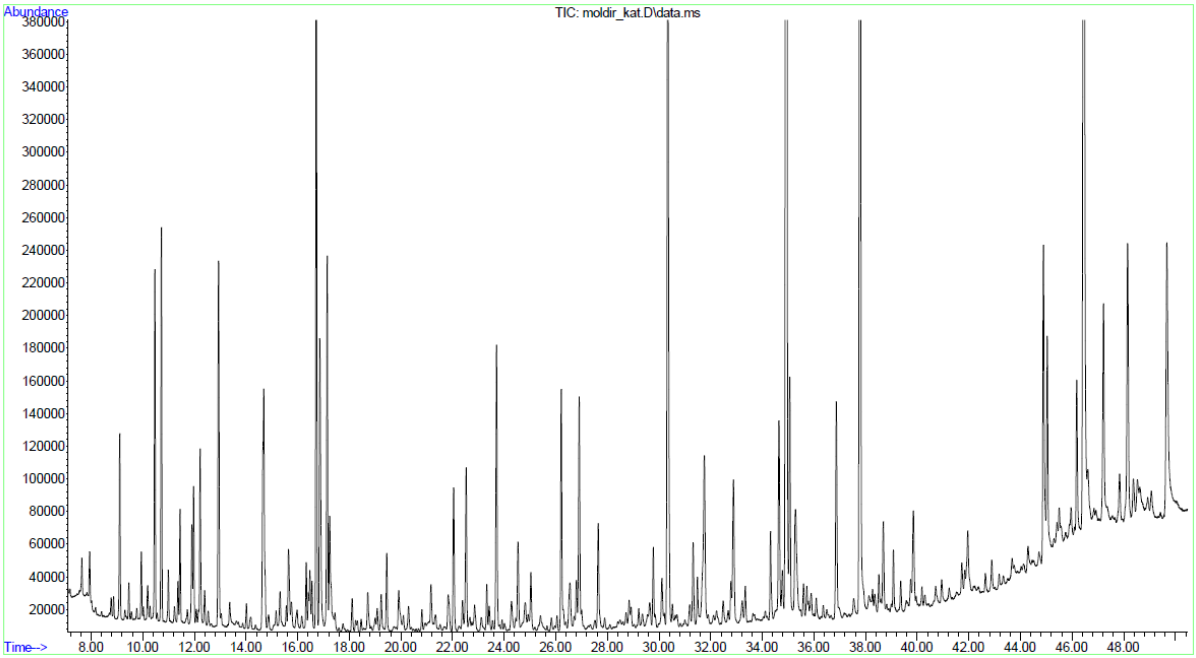

Figure 3 – Chromatogram of GC-MS analysis of *R. rosea* ethanol extract

Table 1 – The results of chromatographic analysis of the extract

No.	RT	Compound	Formula	Percentage, %	Activity	Literature
1	9.11	β-pinene beta-pinene; 6,6-dimethyl-2-methylenebicyclo [3.1.1]-heptane	$C_{10}H_{16}$	0.98	anti-inflammatory, antiviral antimicrobial activities	[32]
2	10.72	1,3-cyclopentadiene, 5,5-dimethyl-2-ethyl	C_9H_{14}	1.99	flavoring spirits, used to extract oils and fats	[33]
3	11.97	benzene-1-methyl-3-(1-methyl-1)	$C_{10}H_{14}$	0.70	antiinflammatory, used in perfumery for its citrus effect	[34]
4	12.22	ethanone, 2-hydroxy-1-phenyl	$C_8H_8O_2$	1.01	antiseptic, used as a disinfecting and drying agent and antiseptic	[35]
5	12.93	2-propanone, 1-hydroxy	$C_9H_{12}O$	2.20	antiseptic	[36]
6	14.68	citral (lemarome, 3,7-dimethyl-2,6-octadienal)	$(CH_3)_2C = CHCH_2CH_2C(CH3) = CHCHO$	2.38	antiseptic and antiinflammatory, used in perfumery for its citrus effect, used as a flavor and for fortifying lemon oil, has strong antimicrobial qualities, and pheromonal effects in insects, used in the synthesis of vitamin A, ionone and methylionone	[37]
7	16.72	2.6-dimethyl-1,3,5,7-octatetraene	$C_{10}H_{16}O$	4.03	antiseptic, used as bactericidal agent	[38]
8	16.86	acetic acid	CH_3COOH	2.25	antiseptic, used as a fungicide and bactericidal agent	[39]
9	17.14	propanoic acid, 2-oxo-, methyl ester	$C_4H_6O_3$	2.01	antioxidant, has propionic acid, inhibits the growth of mold and some bacteria	[40]
10	22.04	2-furanmethanol	$C_5H_6O_2$	0.96	used to dissolve nitrocellulose, GOST 28960-91 Furfuryl Alcohol	[40]

Continuation of table 1

No.	RT	Compound	Formula	Percentage, %	Activity	Literature
11	23.70	2.6-octadienal, 3,7-dimethyl-	$C_{10}H_{16}O$	1.81	antiseptic and antiinflammatory, used in perfumery for its citrus effect	[41]
12	26.21	geraniol	$C_{10}H_{18}O$	1.53	used for making perfume compositions, flavoring soap and detergent, used in synthesis of other fragrant substances	[42]
13	26.90	benzyl-alcohol	C_7H_8O	1,45	flavoring, psychostimulant, appetite regulator, used for disinfection of oil solutions of drugs for intramuscular injection in pharmacology	[43]
14	30.33	cinnamaldehyde	C_9H_8O	6,26	hypoglycemic agent, EC 4.3.1.24 inhibitor (phenylalanine ammoniales), vasodilator agent, antifungal agent	[44]
15	31.75	1,3-diaxol -2-one, 4.5-dimethyl-		1,81	antiviral activity	[45]
16	32.88	2-hydroxy-gamma-butyrolactone	$C_4H_6O_3$	1.15	EC 4.3.1.24 inhibitor, flavoring agent, plant metabolite and sensitizer	[46]
17	34.64	4h-pyran-4-one, 2,3-dihydro-3.5-dihydroxy-6methyl-		1.54	compound with flavonoid fraction, important bioactive chemical, exhibits antifungal activity to inhibit growth or spore germination	[47]
18	34.92	2-propen-1-ol,3-phenyl-(hydroxytyrosol)	C_9H_{10}	24.07	antioxidant, antiinflammatory	[48]
19	35,06	tricosane	$C_{23}H_{48}$	1,50	antimicrobial activity, radical scavenging effect	[49]
20	36.86	benzofuran	C_8H_6O	1.48	antioxidants, used in preparation of rubber, as medicines	[49]
21	37.78	2-butonic acid, 2-methyl-, 3-methylbutil ester	$C_{10}H_{18}O_2$	14.71	flavoring agents	[50]
22	44.89	n-hexadecanoic acid	$C_{16}H_{32}O_2$	2.37	anti-inflammatory, antioxidant, hypocholesterolemic, antibacterial, activities	[50]
23	45.04	1-docosanol, acetate	$C_{22}H_{46}O$	1.52	saturated fatty alcohol antiviral agent, used traditionally as an emollient, emulsifier, and thickener in cosmetics, and nutritional supplement (as an individual entity and also as a constituent of policosanol)	[51]
24	46,08	behenic alcohol	$C_{22}H_{46}O$	1,04	antiviral agent, in humans causes an increase in blood cholesterol	[52]
25	46.45	4-hydroxy-benzeneethanol	$C_8H_{10}O_2$	12.45	phenolic antioxidant, used as a pharmaceutical intermediate to produce metoprolol, betaxolol and salidroside, etc.	[52]
26	47.21	squalene	$C_{30}H_{50}$	1.55	antihypoxant, intermediate in the biological synthesis of steroids, including cholesterol (through lanosterol), participates in metabolism	[53]
27	48.15	tetracosyl acetate	$C_{26}H_{52}O_2$	2.30	used as a component of fruit essences	[54]
28	46.97	n-tetracosanal-1	$C_{24}H_{48}O$	2.97	not fully explored	[54]

According to the results presented in the Table 1, 28 compounds were identified using GC-MS analysis: of which β-pinene was found in the greatest amount (0.98%), 1,3-cyclopentadiene, 5,5-dimethyl-2-ethyl benzene1-methyl-3-(1-methyl1), ethanone, 2-hydroxy-1-phenyl-, 2-propanone, 1-hydroxy-, citral, 2.6-dimethyl-1,3,5,7-octatetraene,e,e-, acetic acid, propanoic acid, 2-oxo-, methyl ester, 2-furanmethanol, 2.6-octadienal, 3,7-dimethyl-, geraniol, benzyl-alcohol, cinnamaldehyde, 1,3-diaxol-2-one, 4.5-dimethyl-, 2-hydroxy-gamma-butyrolactone, 4h-pyran-4-one, 2,3 dihydro-3.5-dihidroxy-6-methyl-, 2-propen-1-ol, 3-phenyl-, tricosane, benzofuran, 2-butonic acid, 2-methyl-3-methylbutil1 ester, n-hexadecanoic acid, 1-docosanol, acetate, behenic alcohol, benzeneethano l,4-hydroxy-, squalene, tetracosyl acetate, n-tetracosanal-1.

It should be noted that 2-(4-hydroxyphenyl) ethanol serves as a pharmaceutical intermediate for metoprolol, betaxolol and salidroside. Metoprolol is a beta-adrenergic blocking agent and is used to treat high blood pressure. Betaxolol is a cardioselective 1-adrenergic blocker, whereas salidrozide can enhance immunity, slow down aging, resist radiation and tumors and protect the cardiovascular system, etc. [34].

Lipophilic compounds exhibit a wide range of biological activities, e.g., cinnamaldehyde, contained in the quantity of 6.26%, may serve as a hypoglycemic agent, EC 4.3.1.24 (phenylalanine ammonia-lyase) inhibitor, vasodilator, antifungal agent, flavoring agent, plant metabolite and sensitizer [44].

Hydroxytyrosol – one of the main phenolic components of the roots (24.07%), is also beneficial for health, its protective action has been shown in preclinical studies against several diseases.

Numerous studies have demonstrated the importance of natural dietary polyphenols in supporting cardiovascular health. Reactive oxygen species (ROS) are critically involved in the endothelial dysfunction that contributes to atherosclerosis development. Oxidative stress-induced endothelial dysfunction probably represents one of the first stages in the development of atherosclerotic lesions. Accordingly, walls of atherosclerotic vessels contain increased levels of ROS, which affect several redox-sensitive pathways in vascular cells, resulting in a markedly altered cellular composition of the tissue. Migration and proliferation of vascular smooth muscle cells in the area is induced, as well as expression of adhesion molecules and chemotactic factors by the endothelium. Direct reduction of ROS levels and/or stimulation of antioxidant defense at these levels could possibly help to avoid the development of atherosclerosis. Mechanisms of action include potent antioxidant and antiinflammatory effects, among others [48].

P-tyrosol, contained in the quantity of 12.45%, is recognized as a good antioxidant, which counteract the damaging effects of oxidation in animal tissues. Anti-arrhythmia agents are often divided into four main groups according to their mechanisms of action: sodium channel blockade, beta-adrenergic blockade, repolarization prolongation, or calcium channel blockade [49]. Agents used for the treatment or prevention of cardiac arrhythmias may affect the polarization-repolarization phase of the action potential, its excitability or refractoriness, impulse conduction or membrane responsiveness within cardiac fibers. Another important compound is squalene [53].

By chemical composition, the essential oil, obtained from the rhizomes of *R. rosea* differs in composition. The composition of the oil is affected by the place of plant growth. As known from the literature data, main components of the essential oil of *R. rosea* grown in Bulgaria are geraniol and myrtenol [55], in China – geraniol and octanol [56], and in India – phenylethyl alcohol [57], in Kazakhstan – for the first-time cinnamon alcohol was found, and earlier cinnamon alcohol was found only in samples from Bulgaria [55]. Based on the our results, it can be concluded that, as representatives of a succulent species, *R. rosea* contains in plant roots not only a set of vitamin groups, but also biologically active compounds that, according to conducted research and literature review, can favorably affect the human body.

Conclusion

Rhodiola rosea L. is a plant with a whole spectrum of biological activities (increases mental activity in healthy people; reduces anxiety and fear with fatigue syndrome; significantly increases the amount of dynamic and static work; normalizes metabolic processes). According to the literature data, plant roots contain essential oil, tannins, more than 20 valuable trace elements, like iron, phosphorus, magnesium, manganese, etc., ascorbic and nicotinic acids.

As mentioned, before GC-MS (Agilent 6890N/5973N, USA) analysis was used for identification and quantitative estimation of compounds in the plant. Data obtained in this work includes the general chemical profile of the essential oil, percentage content and retention could be useful in estimating its chemical characteristics. Such components as β-pinene (0.98%), benzene 1-methyl-3-(1-methyl 1) (0.70%), 2-furanmethanol (0.96%) were identified

in small amounts, largest amount was revealed for 2-propen-1-ol,3-phenyl (24.07%), 2-butonic acid, 2-methyl-3-methylbutil1 ester, (14.71%) and benzeneethano l,4-hydroxy (12.45%). By the profile of their biological activity, proven compounds show high antioxidant potential.

References

1. Zinchenko E.S. (2014) Rhodiola rosea. In: The Red Book of Kazakhstan, vol. 2. Part 1. Plants, Almaty, p. 133.
2. Vasiliev A.N. (1972) Rhodiola – Rhodiola L. In: Flora of Kazakhstan, Alma-Ata: Publishing House of the Academy of Sciences of the Kazakh SSR, vol. 2, pp. 345-352.
3. Brown R.P., Gerbarg P.L., Ramazanov Z. (2002) Rhodiola rosea: a phytomedicinal overview. *Journal of the American Botanical Council*, vol. 56, pp. 40-52.
4. Kittredge J.S. (1974) Behavioral bioassays and biologically active compounds. In: Food-drugs from the sea, Proceedings, pp. 467-475.
5. McGuffin M., Kartesz J.T., Leung A.Y., Tucker A.O. (2000) Herbs of Commerce. 2nd ed. Silver Spring, MD: American Herbal Products Association, 421 p.
6. Ballmann C.G., Maze S.B., Wells A.C., Marshall M.M., Rogers R.R. (2019) Effects of short-term Rhodiola Rosea (Golden Root Extract) supplementation on anaerobic exercise performance. *J Sports Sci.*, vol. 37, no. 9, pp. 998-1003.
7. Moran R.V. (2009) Rhodiola. In: Flora of North America North of Mexico, ed. by Flora of North America Association, vol. 8, pp. 164-167.
8. European Medicines Agency Committee on Herbal Medicinal Products (2011) Assessment report on Rhodiola rosea L. rhizoma et radix. London, United Kingdom, pp. 1-32.
9. Amsterdam J.D., Panossian A.G. (2016) Rhodiola rosea L. as a putative botanical antidepressant. *Phytomedicine*, vol. 23, no. 7, pp. 770-783.
10. Kurkin V.A., Zapesochnaya G.G., Shchavlinskii A.N., Nukhimovskii E.L., Vandyshev V.V. (1985) Method of analysis of identity and quality of Rhodiola rosea rhizome. *Khim Farm Zh.*, vol. 19, no. 3, pp. 185-190.
11. WHO (2013) Rhodiola quadrifida Fisch & Mey and Rhodiola rosea L. Medicinal Plants in Mongolia. Geneva, Switzerland, pp. 163-172.
12. Powdered Rhodiola rosea extract. USP 40-NF 35 (2017) Rockville, MD: United States Pharmacopeial Convention, pp. 6809-6810.
13. Yousef G.G., Grace M.H., Cheng D.M., Belolipov I.V., Raskin I., Lila M.A. (2006). Comparative phytochemical characterization of three Rhodiola species. *Phytochem*., vol. 67, no. 21, pp. 2380-2391.
14. Kurkin V.A. (2015) Rhodiola rosea (Golden root): drugs production and standardization: Monography. Samara: Ofort ltd, Samara State Medical University MHRF, p. 240.
15. Galambosi B. (2005) Rhodiola rosea L. from wild collection to field production. *Med Plant Cons*., vol. 11, no. 1, pp. 31-35.
16. Galambosi B., Galambosi Zs., Slacanin I. (2007) Comparison of natural and cultivated roseroot (Rhodiola rosea L.) roots in Finland. *Z. Arznei-Gewurzpfla*, vol. 12, no. 3, pp. 141-147.
17. Rohloff J. (2002) Volatiles from rhizomes of Rhodiola rosea L. *Phytochem*., vol. 59, no. 6, pp. 655-661.
18. Chevallier A. (2016). Encyclopedia of Herbal Medicine. DK/Penguin Random House. p. 127.
19. Furmanowa M., Skopinska-Rozewska E., Rogala E., Malgorzata H. (1998) Rhodiola rosea in vitro culture: phytochemical analysis and antioxidant action. *Acta Societis Botanicorum Poloniae*. vol. 76, no. 1, pp. 69-73.
20. Bykov B.A., Zapesochnaya G.G., Kurkin B.A. (1999) Rhodiola rosovaya (Rhodiola rosea L.): Tradisionniye y biotechnologichnye aspecti poluchenie lekarstvennih sredstv (obzor) [Rhodiola rose traditional and biotechnological aspects the preparation of medicaments]. *Chem Pharm J.*, vol. 33, no. 1, pp. 28-37.
21. Rhodiola crenulata. In: Pharmacopoeia of the Peoples Republic of China (2010). *China Medical Science*, vol. 1, pp. 376-377.
22. Rhodiola. In: Wu Y.-Z., Raven P.H., eds. Flora of China. Vol 8. Beijing, China and St. Louis, MO: Missouri Botanical Garden Press, 2001. pp. 251-268. pp. 13.
23. Bohm B.A. (2009) The geography of phytochemical races. Springer, Netherlands, 358 p.
24. Krasnov E.A., Vejc L.A. (1968) Issledovanie jefirnogo masla rodioly rozovoj [Research essential oil Rhodiola L.] (*Rhodiola rosea* L.). In: Central nervous system stimulation. Tomsk. vol. 2, pp. 18-21.
25. Cuerrier A., Ampong-Nyarko K. (2014). Traditional herbal medicines for modern times. Rhodiola rosea. CRC Press, Taylor & Francis group, 304 p.
26. Petkov V.D., Yonkov D., Mosharoff A. et al. (1986) Effects of alcohol aqueous extract from *Rhodiola rosea* L. roots on learning and memory. *Acta Physiol Pharmacol Bulg*., vol. 12, no. 1, pp. 3-16.

27. Mattson M.P., Pedersen W.A., Duan W., Culmsee C., Camandola S. (1999) Cellular and molecular mechanisms underlying perturbed energy metabolism and neuronal degeneration in Alzheimer's. *Ann NY Acad Sci*., vol. 893, pp. 154-175.

28. Simonova N.V., Dorovskih V.A., Shtarberg M.A. (2011) Adaptogeny v korrekcii processov perekisnogo okislenija lipidov biomembran, inducirovannyh vozdejstviem holoda i ul'trafioletovyh luchej [Adaptogens in the correction of lipid peroxidation of biomembranes induced by exposure to cold and ultraviolet rays]. *Bulletin of physiology and pathology of respiration*, no. 40, pp. 66-71.

29. Kulagin O.L., Kurkin V.A., Careva A.A., Dodonova N.A. (2010) Primenenie fitopreparatov rodioly rozovoj v kachestve vozmozhnyh gepatoprotektorov [The use of herbal remedies Rhodiola Rosea as possible hepatoprotectors]. *Proceedings of the Samara Scientific Center of the Russian Academy of Sciences*, vol. 12, no. 1-8, pp. 2065-2068.

30. Sal'nik A.S., Cherdyncev S.G., Eulusheva V.A., Kapustina V.A. (1968) K mehanizmu stimulirujushhego dejstvija jekstrakta jeleuterokokka, rodozina i piridrola pri myshechnyh nagruzkah [The mechanism of the stimulating effect of the extract of Eleutherococcus, rhodosin and pyridrol under muscle loads]. In: Stimulants of the central nervous system. Tomsk, vol. 2, pp. 89-91.

31. Simonova N.V. (2009) Phytodrugs in correction of lipids peroxidation processes of biomembranes, induced by UV radiation. Reporter of Krasnoyarsk State Agrarian University, no. 2, pp. 119-125.

32. Gosudarstvennaja Farmakopeja RK. [State Pharmacopoeia RK], 2008, vol. 1, 591 p.

33. Gosudarstvennaja Farmakopeja RK. [State Pharmacopoeia RK], 2009, vol. 2, 802 p.

34. Rivas da Silva A.C., Monteiro Lopes P., Barros de Azevedo M.M. et al. (2012) Biological Activities of aMyrzagaliyeva A.B., Ibatayev Zh.A., Iskakova Zh.B., Samarkhanov T.N., Medeubayeva B.Z. Himija rastitel'nogo syr'ja [Chemistry of plant material], 1/05, no. 3, 72 p.

35. Rodin I.A., Smirnov R.S., Smolenkov A.D., Krechetov P.P., Shpigun O.A. (2012) Transformation of unsymmetrical dimethylhydrazine in soil. Eur Soil Sci., Maik Nauka/Interperiodica Publishing. vol. 45, p. 46.

36. Mohandes F., Salavati-Niasari M. (2014) Particle size and shape modification of hydroxyapatite nanostructures synthesized via a complexing agent-assisted route. Materials Science & Engineering. *Materials for Biological Applications*, vol. 40, pp. 288-298.

37. Freitag J., Díez M.T.S., Tuma D.1, Ulanova T.V., Maurer G. (2004) High-pressure multiphase behavior of the ternary systems (ethene + water + 1-propanol) and (ethene + water + 2-propanol): part I: experimental investigation. *J Supercrit Fluids*, vol. 32, no. 1-3, pp. 1-13.

38. Duarte M.C., Figueira G.M., Sartoratto A., Rehder V.L., Delarmelina C. (2005) Anti-candida activity of Brazilian medicinal plants. *J Ethnopharmacol*., vol. 97, no. 2, pp. 305-311.

39. El-Sayed A.M., Byers J.A., Manning L.M. et al. (2008) Floral scent of Canada thistle and its potential as a generic insect attractant. *J Econ Entomol*., vol. 101, no. 3, pp. 720-727.

40. Cortesia C., Vilchèze C., Bernut A. et al. (2014) Acetic acid, the active component of vinegar, is an effective tuberculocidal disinfectant. *Chemother*., vol. 53, 3197-3204

41. Thompson A.M., Rewcastle G.W., Tercel M. et al. Tyrosine kinase inhibitors. 1. Structure-activity relationships for inhibition of epidermal growth factor receptor tyrosine kinase activity by 2,3-dihydro-2-thioxo-1H-indole-3-alkanoic acids and 2,2'-dithiobis(1H-indole-3-alkanoic acids). *Med Chem*., vol. 17, pp. 2459-2469.

42. Arnoldi M., Negroni A.D'Agostina (1998) Effect of antioxidants on the formation of volatiles from the Maillard reaction. *Dev Food Sci.*, vol. 40, pp. 529-534.

43. Sun Y., Hayakawa S., Chuamanochan M., Fujimoto M., Innun A., Izumori K. (2006) Antioxidant effects of Maillard reaction products obtained from ovalbumin and different D-aldohexoses. *Biosci Biotechnol Biochem.*, vol. 70, no. 3, pp. 598-605.

44. Bergeron S., Chaplin D.A., Edwards J.H. et al. (2006) Nitrilasecatalyzed desymmetrization of 3-hydroxyglutaronitrile: preparation of a statin side-chain intermediate. *Org Process Res Dev.*, vol. 10, pp. 661-665.

45. Rahuman A.A., Gopalakrishnan G., Ghouse B.S., Arumugam S., Himalayan B. (2000) Effect of Feronia limonia on mosquito larvae. *Fitoterapia*, vol. 71, pp. 553-555.

46. Goldberg K., Schroer K., Lütz S., Liese A. (2007) Biocatalytic ketone reduction-a powerful tool for the production of chiral alcohols-part II: whole-cell reductions. *Appl Microbiol Biotechnol*., vol. 76, pp. 249-255.

47. Aparna V., Dileep K.V., Mandal P.K., Karthe P., Sadasivan C., Haridas M. (2012) Anti-inflammatory property of n-hexadecanoic acid: structural evidence and kinetic assessment. *Chem Biol Drug Res*.,

vol. 80, pp. 434-439.

48. Hollingsworth R.I. (1999) Taming carbohydrate complexity: a facile, high-yield route to chiral 2,3-dihydroxybutanoic acids and 4-hydroxytetrahydrofuran-2-ones with very high optical purity from pentose sugars. *J Org Chem.*, vol. 64, pp. 7633-7634.

49. Kumar P.P., Kumaravel S., Lalitha C. (2010) Screening of antioxidant activity, total phenolics and GC-MS study of Vitex negundo. *Afr J Biochem Res.*, vol. 4, pp. 191-195.

50. Fickert B., Schieberle P. (1998) Nahrung. Food, vol. 42, pp. 371-375.

51. Buttery R.G., Takeoka G.R., Naim M., Rabinowitch H., Nam Y. (2001) Analysis of furaneol in tomato using dynamic headspace sampling with sodium sulfate. *J Agric Food Chem.*, vol. 49, pp. 4349-4351.

52. De Clercq E., Li G. (2016) Approved antiviral drugs over the past 50 years. *Clin Microbiol Rev*., vol. 29, no. 3, pp. 695-747.

53. Wegener R., Schulz S., Meiners T., Hadwich K., Hilker M. (2001) Analysis of volatiles induced by oviposition of elm leaf beetle Xanthogaleruca luteola on Ulmus minor. *J Chem Ecol.*, vol. 27, no. 3, pp 499-515

54. Zídek Z., Kmonícková E., Holy A. (2005) Biomed. Pap. Med. Fac. Univ. Palacky Olomouc Czech. Repub., vol. 315, p. 149.

55. Kosakowska O., Baczek K., Przybyl J.L. et al. (2018). Antioxidant and antibacterial activity of roseroot (Rhodiola rosea L.) dry extracts. *Molecules,* vol. 23, no. 7, p. 1767.

56. Mao Y., Li Y., Yao N. (2007). Simultaneous determination of salidroside and tyrosol in extracts of Rhodiola L. by microwave assisted extraction and high-performance liquid chromatography. *J Pharm Biomed Anal*., vol. 45, no. 3, pp. 510-515.

57. Bhardwaj A.K., Singh B., Kaur K., Roshan P. et al. (2018). In vitro propagation, clonal fidelity and phytochemical analysis of Rhodiola imbricata Edgew: a rare trans-Himalayan medicinal plant. *Plant Cell Tissue Organ Cult*., vol. 135, no. 3,

IRSTI 34.45.21

[1]P. Ramezannezhad, [1*]S. Heidari-Soureshjani, [2]T. Suhan

[1]Shahrekord University of Medical Sciences, Shahrekord, Iran
[2]University of Michigan, Department of Pediatrics-Hematology/Oncology, Ann Arbor, MI, USA
*e-mail: heidari_62@yahoo.com

Protective effects of some medicinal plants against myocardial hypoxia

Abstract: Myocardial hypoxia is one of the main complications of myocardial ischemic injury which have high morbidity and mortality. The aim of this review is to investigate the protective effects of medicinal plants in myocardial hypoxia. The words cardiomyocytes alongside with hypox* or myocardial hypoxia, in combination with some herbal terms such as medicinal plant, phyto* and herb*, were used to search for relevant publications indexed in the Institute for Scientific Information (ISI) and PubMed. Finally after all revisions, 74 articles were included in this study. Available evidence shows that certain medicinal plants and herbal derivatives can exert their myocardial protective effects against hypoxia using several pathways. These mechanisms include antioxidant properties such as savaging reactive oxygen species (ROS) and activation antioxidant pathways, suppressing pro-apoptotic genes and regulate apoptosis pathways, regulating autophagy and related pathways, reducing inflammation and suppress proinflammatory cytokines and pathways, inhibiting intracellular Ca^{2+} influx, antiplatelet aggregation, stimulating the adenosine triphosphate (ATP) generation in mitochondria and mitochondrial respiration, promoting autophagy, regulating hypoxia-inducible factor 1-alpha (HIF-1α) expression, decreasing the expression of angiotensin, reducing cardiac troponin I (cTnI) and creatine kinase-MB (CK-MB) and up-regulation of epoxyeicosatrienoic acids (EETs). Thus, clinicians can use the medicinal herbs as an effective treatment against myocardial hypoxia. Post-ischemia and chronic treatment of cardioprotection maybe consider as a therapeutic strategies than short term and pre-treatment methods in clinical setting. Nevertheless, more clinical trial studies are required in order to obtain more reliable results.
Key words: antihypoxic, medicinal plants, reactive oxygen species, myocardial ischemic injury.

Introduction

Myocardial ischemic injury occurs due to severe dysfunction of coronary blood supply and is a leading cause of morbidity and mortality worldwide [1]. This disorder is closely associated with cardiac dysfunction, in particular some aspects of it, such as myocardial stunning, left ventricular remolding, inflammation, fibrosis, neurohormonal activation, cardiomyocyte necrosis, reperfusion injury, haemorhage and microvascular obstraction are causes heart failure [2]. Myocardial ischemic injury is a pathological process that includes augmented cell death, namely, oncosis, apoptosis and infarction [3]. Cardiomyocytes consume large quantities of energy and are very sensitive to lack of energy. During heart attack and eventually hypoxia, cardiac myocytes switch their metabolism to anaerobic respiration, which causes ATP depletion, lactate accumulation, Na^+ and Ca^{2+} overload and due to myocardial contractile dysfunction. Reperfusion results in generation of reactive oxygen species (ROS), what contributes to apoptosis and inflammation and finally myocardial infarction and ischemic reperfusion injury [4].

Currently there are several therapeutic strategies used for treatment, not as effective as could be [4]. As a result, new investigations are considered necessary in this area. Medicinal plants are the cheapest and conventional approach to confronting numerous diseases especially for treatment of heart failure [5-13]. Given that the magnitude of heart disease in human mortality and necessity for new therapeutic strategies to treatment of chronic heart failure are high, this review was prepared to find out the protective effects of medicinal plants in myocardial hypoxic condition and its related complications.

Search for strategies and study design

Key words of interest, such as cardiomyocytes alongside with hypox* or myocardial hypoxia, in combination with some herbal terms, namely medicinal plant, phyto*, and herb* were used to search for relevant publications indexed in the Institute for Scientific Information (ISI) and PubMed. Finally, 74 articles were found with Endnote software (Table 1).

Table 1 – Number of studies present in subsequent databases

Hypox* + Cardiomyocyte + Medicinal plant	PubMed	3
	ISI	1
Hypox* + Cardiomyocyte + Phyto*	PubMed	3
	ISI	1
Hypox* + Cardiomyocyte + Herb*	PubMed	22
	ISI	19
Myocardial hypoxia + Medicinal plant	PubMed	15
	ISI	6
Myocardial hypoxia + Phyto*	PubMed	9
	ISI	9
Myocardial hypoxia+ Herb*	PubMed	68
	ISI	46
Total	PubMed	120
	ISI	82

A standard form, which included items as purpose or the title of the study, intervention, outcome, variables, journal name, intervention period, and article number, was designed. Selection process is presented on Figure 1.

First, full text articles relevant to the purpose of the study were recorded in the form and entered into the study with agreement of researchers. Then, the plants and their products that were reported to be effective to treat myocardial hypoxia and related complications were selected for the study. Articles, where full texts were not accessible, non-English language articles, studies with non-positive effects, review articles, and studies that were not relevant to the principle aim of the current study were excluded after all authors' agreement was achieved. Finally, 74 articles were included into the study.

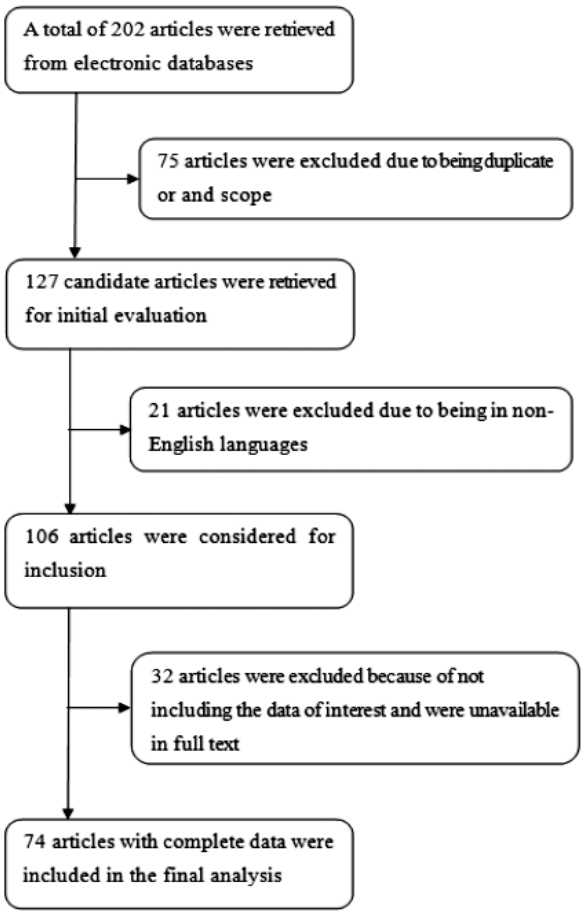

Figure 1 – The process of selection of articles for final analysis.

Results and discussion

Medicinal plants and their compounds can be effective against myocardial hypoxia via various mechanisms of action. Summary of analysis for some of them is provided in Table 2.

Table 2 – Medicinal plants, formula and compounds with cardioprotective effects and mechanisms of action against myocardial hypoxia

Medicinal plants				
References	**Main effects or mechanisms**	**Type of administration**	**Study design**	**Scientific name of the plant**
[14]	Diminishing levels of oxidants generated during hypoxia and within exposure to the mitochondrial site III inhibitor antimycin A and decreasing cell death	Aqueous extract	Experimental (*in vitro*)	*Scutellaria baicalensis* Georgi
[15]	Reducing degenerative intra mitochondrial areas. In addition insert protective effect to reducing number of ATPase particles at the inner mitochondrial membranes and increasing of myocardial capacity for ATP production	Extract	Experimental (*in vitro and in vivo*)	*Ginkgo biloba*
[16]	Increasing the expressions of hypoxia-inducible factor 1alpha (HIF-1alpha), hypoxia-inducible factor 1beta (HIF-1beta) and vascular endothelial growth factor (VEGF) mRNAs and the expressions of HIF-1alpha and VEGF proteins	Solution	Experimental (*in vitro and in vivo*)	Radix et rhizoma *Rhodiolae kirilowii*
[17]	Decreasing $[Ca(^{2+})]i$ contents in cardiac muscel cells and inhibiting the changes induced by Potassium chloride (KCl) in single cardiac myocytes	Powder extract	Experimental (*in vitro*)	*Rhododendron dauricum L.*
[18]	Decreasing the level of MDA, intracellular ROS, release of LDH and apoptosis. Besides enhancement the activity of SOD	Aqueous and ethanolic extract	Experimental (*in vitro*)	*Pseudostellaria heterophylla*
[19]	Increasing mitochondrial ATP-generation capacity (ATP-GC) and ADP-stimulating state 3 respirations and increasing antioxidant capacity. In addition enhancement of cellular glutathione redox cycling and reducing apoptosis	Dried extract	*Ex-vivo*	*Cistanche deserticola*
[20]	Protected myocyte cells against hypoxia via ROS scavenger	Aqueous extract	Experimental (*in vitro*)	*Pogostemon cablin* Blanco
[21]	Reducing apoptosis and oxidative stress via activation of PI3 K/Akt signaling pathway	Aqueous extract	Experimental (*in vitro*)	*Dictamnus dasycarpus* Turcz
[22]	Reducing calcium accumulation, inhibiting caspase-3 activation, and down-regulating protein expression of p-JNK and p-p38MAPK	Extract	Experimental (*in vitro and in vivo*)	*Trichosanthes cucumerina*
Medicinal plants formula				
References	**Main effects or mechanisms**	**Type of administration**	**Study design**	**Herbal compounds/ derivatives**
[23]	Inhibited reduced GSH and also a reduced sensitivity to Ca^{2+}-induced mitochondrial permeability transition. In addition activated both ERK/Nrf2 and PKC epsilon/m ATP-sensitive potassium channel (K-ATP) pathways	Decoction	Experimental (*in vitro*)	Danshen and Gegen composed of *Salviae miltiorrhizae* and *Puerariae lobatae*
[24]	Decreasing calcium accumulation and reducing cell apoptosis by protecting cell membrane skeleton integrity and the mitochondrial function.	Decoction	Experimental (*in vitro*)	Danshen and Gegen

Continuation of table 2

[25]	Up-regulation of epoxyeicosatrienoic acids (EETs)-generating cytochrome P450 enzymes	Extracted Pill	Experimental (*in vitro and in vivo*)	Danshen composed of *Salviae Miltiorrhizae, Notoginseng Radix* and *Borneolum Syntheticum*
[26]	enhancing antioxidant capacity and calcium handling and lead to reducing apoptosis rates	Solution	Experimental (*in vitro*)	Danshen composed of *Salviae Miltiorrhizae, Notoginseng Radix* and *Borneolum Syntheticum*
[27]	Promoting autophagy via activation of the mitogen activated protein kinase/ERK pathway	Solution	Experimental (*in vitro*)	Tongxinluo composed of *Radix ginseng, Hirudo, Eupolyphaga seusteleophaga, Buthus martensi, Scolopendra subspinipes, Periostracum cicadae, Semen ziziphi spinosae, Radix paeoniae rubra, Lignum santali albi, Lignum dalbergiae odoriferae,* and *Borneolum syntheticum*
[28]	Up-regulating proteins which involving in regulation of metabolic process, cell proliferation and stress response.	Solution	Experimental (*in vitro*)	Tongxinluo
[29]	Activating Angptl4-mediated regulation of endothelial barrier integrity through the PPAR-α pathway	Solution	Experimental (*in vitro and in vivo*)	Tongxinluo
[30]	Increasing cell viability and SOD levels and decreased MDA levels. Besides suppressing MDA, cTnT and inflammatory cytokines.	Extract capsule	Experimental (*in vitro and in vivo*)	Yindanxinnaotong composed of *Ginkgo biloba*, *Salvia miltiorrhizae*, *Gynostemma, ynostemmatis*, *Erigerontis herba*, *Allii sativi bulbus*, Radix/rhizoma *notoginseng*, *Crataegi fructus* and *Borneolum*
[31]	Inhibition of mitochondrial permeability transition pore (mPTP) opening via attenuating Ca^{2+} overload and ROS generation	Extract	Experimental (*in vitro*)	Danhong composed of *Salvia miltiorrhiza* Bge and *Carthamus tinctorius* L.
[32]	Reducing in MDA, LDH, cardiac troponin I (cTnI) and creatine kinase-MB (CK-MB) and reducing expression of cleaved caspase-3, 8-hydroxydeoxyguanosine (8-OHdG), and increasing SOD activity, Bcl-2/Bax ratio and regulating Akt/Nrf2/HO-1 signaling	Solution	Experimental (*in vitro and in vivo*)	Danhong injection composed of *Salvia miltiorrhiza and Carthamus tinctorius L*+ hydroxysafflor yellow A that are the main active ingredients of Radix *Salvia miltiorrhiza*
[33]	Inhibiting myocardial apoptosis, probably by regulating hypoxia-inducible factor 1-alpha (HIF-1α) expression in cardiomyocytes	Extract Pill	Experimental (*in vitro and in vivo*)	Qishen Yiqi Droping Pill composed of *Salvia miltiorrhiza* Bge, *Pannax notoginseng,* and *Dalbergia odorifera* T. Chen.
[34]	Reducing inflammation of the endothelial cells, inhibiting the activity of LDH, CK and decreasing the level of MDA and increasing SOD activity	Extract	Experimental (*in vivo*)	Yi-Qi-Fu-Mai composed of *Panax ginseng, Ophiopogon japonicas* and *Schisandra* chinensis
[13]	Inhibiting mitochondrial mediated apoptosis and modulating AMP-activated protein kinase (AMPK) activation mediating mitochondrial fission	Powder	Experimental (*in vitro and in vivo*)	Yi-Qi-Fu-Mai
[35]	Reducing $[Ca^{(2+)}]i$ accumulation induced by hypoxia-reoxygenation in ventricular myocytes via supressing I_{NaL} and I_{CaL}	Extract	Experimental (*in vitro*)	Wenxin Keli composed of *Nardostachys chinensis Batal, Codonopsis, Notoginseng, amber,* and *Polygonati*

Continuation of table 2

[36]	Inhibiting autophagy through regulating AMPK-mTOR signaling pathways and increasing cell viability and consequently reduced apoptosis.	Decoction	Experimental (*in vitro*)	XuefuZhuyu decoction composed of *Angelica sinensis (Oliv.) Diels Rehmannia glutinosa Libosch Prunu persica (L.), Batsch, Carthamus tinctorius L., Paeonia Lactiflora Pall. Bupleurum chinense DC, Citrus aurantium L., Glycyrrhiza uralensis Fisch., Platycodon grandiflorum (Jacq.) A.DC. Ligusticum chuanxiong Hort.* and *Achyranthes bidentata Blume*
[37]	Increasing cardiomyocytes survival by regulating stress-responsive mitogen-activated protein kinases (MAPK) pathways and phosphatidylinositol 3-kinase (PI3K)-Akt pathway for cell survival was restored by the herbal compounds	Solution	Experimental (*in vitro*)	Tanshinone IIA from S*alvia miltiorrhiza Bunge* and astragaloside IV from *Astragalus membranaceus*
[38]	Decreasing myocardium infarct size, reducing apoptosis and myocardial myeloperoxidase (MPO). In addition decreasing MDA, calcium accumulation, LDH, creatine kinase MB isoenzyme (CK-MB), and cardiac troponin I (cTn-I) activity	Solution	Experimental (*in vitro and in vivo*)	Sheng-Mai-San composed of ginsenoside Rb1 (ginsenosides of *Panax ginseng*), ruscogenin, (saponins of radix *ophiopogonis*) and schisandrin (lignans of *Fructus schisandrae*)
[39]	Activating of Peroxisome proliferator activated receptor gamma co-activator (PGC-1α) and maintenance of mitochondrial functions via involving the activation of AMPK phosphorylation	Decoction	Experimental (*in vitro and in vivo*)	Yiqihuoxue *Astragalus membranaceus, Angelica sinensis, Panax ginseng, Ligusticum wallichii,* and *Panax notoginseng*
[40]	Regulating of Ca^{2+} influx, reducing oxidative stress and apoptotic proteins (Mainly by *Salvia miltiorrhiza Bunge*)	Aqueous extract	Experimental (*in vitro*)	Xin-Ke-Shu that composed of *Salvia miltiorrhiza Bge, Pueraria lobata, Ohwi, Panax notoginseng F.H. Chen., Crataegus pinnatifida Bunge* and *Aucklandia lappa Decne*
[41]	Promoting mitochondrial function through increasing respiration, ATP-coupled respiration, and spare capacity of mitochondria in response to hypoxia	Solution	Experimental (*in vitro and in vivo*)	Shenmai formula composed of *Panax ginseng* and *Ophiopogonis*
[42]	Activating RISK pathway and reducing apoptosis. In addition insert cardioprotective effects by antioxidant activity	Decoction	Experimental (*in vitro*)	Gualou Xiebai composed of *Trichosanthis Fructus* and *Allii Macrostemonis Bulbus*
Medicinal plants compounds				
References	**Main effects or mechanisms**	**Type of administration**	**Study Design**	**Herbal compounds/ derivatives**
[43]	Improving hypoxic contractile recovery. Main mechanism associated with restoration of tissue ionic concentrations and reducing the release of ATP metabolites and creatine kinase from the hypoxic hearts	Solution	Experimental (*in vivo*)	Tanshinone VI derived from S*alvia miltiorrhiza Bunge*
[44]	Reducing infarct size and preventing the increase in superoxide dismutase-mRNA and inhibition of $45Ca^{2+}$ influx	Solution	Experimental (*in vivo*)	Trilinolein derived from *Panax pseudoginseng*
[45]	Increasing in Cu.Zn-superoxide dismutase (SOD) activity and indicating antioxidant effect that insert its myocardial protective effect	Solution	Experimental (*in vivo*)	Trilinolein derived from *Panax pseudoginseng*

Continuation of table 2

[46]	Augmenting the force recovery from reperfusion and arrhythmia via decreasing [Cl-] i in non-hypoxic myocytes and modulation of intracellular Cl- homeostasis	Extract	Experimental (*in vitro and in vivo*)	Sasanquasaponin derived from *Camellia oleifera*
[47]	Decreasing lactate dehydrogenase (LDH) release, malondialdehyde, oxidized glutathione (GSSG) contents and reactive oxygen species (ROS) levels. In addition increasing activities of Glutathione (GSH) contents and superoxide dismutase, catalase and glutathione peroxidase. Besides reducing calcium accumulation in cardiomyocytes.	Extract	Experimental (*in vitro*)	Sasanquasaponin derived from *Camellia oleifera*
[48]	Reducing in oxidized glutathione and lipid peroxidation	Extract	Experimental (*in vivo*)	Oleuropein derived from *Olea europaea* oil
[49]	Protecting rat aorta endothelial cells against hypoxia and stimulating nitric oxide (NO) release from endothelial cells, cytoprotection, KATP channel opening and venous thrombosis inhibiting	Solution	Experimental (*in vitro*)	Cyclovirobuxine D derived from *Buxus microphylla*
[50]	Up-regulating of GSH and inhabitation of deplete cellular GSH level. The 12-O-tetradecanoylphorbo-13-acetate response element or the antioxidant response element may be involved in the transactivating actions of andrographolide on the catalytic subunit (GCLC) and modifier subunit (GCLM) promoters	Solution	Experimental (*in vitro*)	Andrographolide derived from *Andrographis Paniculata*
[51]	Down-regulating gene expression levels of pro-apoptotic genes such as Bax and Fas proteins. But it up-regulating Bcl-2 and Bcl-xl proteins. In addition inducing the anti-oxidant enzymes SOD and CAT	Extract	Experimental (*in vitro*)	Leonurine derived from *Herba leonuri*
[52]	Insert anti-apoptotic effects by activating the PI3K/AKT/GSK3β pathway and reduced apoptosis	Solution	Experimental (*in vitro and in vivo*)	Leonurine
[53]	Increasing the Akt phosphorylation, reducing gene expression of Bcl-2, but it reducing the gene expression of Bax in vivo. In addition increasing the expression of HIF-1α but also the expression of survivin and VEGF	Extract	Experimental (*in vitro and in vivo*)	Leonurine
[54]	Down-regulating gene expression levels of proapoptotic genes (Bax, Fas and caspase-3) and up-regulating Bcl-2. Besides it can increasing in SOD content	Methanolic extract	Experimental (*in vitro*)	Hirsutine derived from *Uncaria rhynchophylla*
[55]	Modulating the PI3K/Akt pathway and reducing hypoxia-induced apoptosis	Solution	Experimental (*in vitro*)	3,5-dimethoxy-4-(3-(2-carbonyl-ethyldisulfanyl)-propionyl) derived from *Herba Leonuri*
[56]	Reducing cardiac Troponin I (cTnI) secretion in serum and attenuated the Ca2+ overload in cardiomyocytes and modulated the ATP-sensitive potassium channel (KATP) signaling pathway	Solution	Experimental (*in vitro and in vivo*)	Saponins derived from *Panax ginseng*
[57]	Attenuating A/R-induced inflammatory response and apoptosis that related to the TLR4/NF-κB signaling pathway	Solution	Experimental (*in vitro*)	Resveratrol derived from wide variety of plant species

Continuation of table 2

[58]	Up-regulating miR-133 expression via activating MAPK ERK1/2 pathway and enhanced cell resistant to hypoxic condition	Extract	Experimental (*in vitro*)	Tanshinone IIA derived from *Salvia miltiorrhiza*
[59]	Reducing myocardial infarct size, serum levels of TNF-alpha, and platelet aggregation. Besides reducing apoptosis via down-regulated the expression of cleaved caspase-3, and up-regulating the expression of phosphorylated Akt	Solution	Experimental (*in vitro and in vivo*)	Citric acid and L-malic acid derived from *Fructus choerospondiatis*
[60]	Attenuating inflammation of cardiomyocytes via inhibiting ERK1/2 and JNK signaling pathways	Solution	Experimental (*in vitro*)	Sparstolonin B derived from *Sparganium stoloniferum*
[61]	Inhibiting the adhesion between human cardiac microvascular endothelial cells (HCMECs) and polymorphonuclear leukocyte(PMN), through down regulation of the expression and phosphorylationofp38 MAPK	Extract	Experimental (*in vitro*)	Astragalus polysaccharide derived from *Astragulus*
[62]	Attenuating myocardial iscemic via activating hypoxia inducible factor-1a (HIF-1 α)/inducible nitric oxide synthase (iNOS) pathway. Besides up-regulating of the Bcl2 protein and down-regulating of the caspase3 protein	Solution	Experimental (*in vitro*)	Astragaloside IV derived from *Astragalus membranaceus*
[63]	Stimulated the mitochondrial ATP generation and mitochondrial respiration. Up-regulating of cellular glutathione redox cycling and reducing apoptosis	Solution	*Ex-vivo*	β-sitosterol derived from *Cistanche deserticola*
[64]	Protecting hypoxia induced inflammation by attenuating cyclooxygenase-2 (COX-2) mediated cell apoptosis, and the death of endothelial cells through oxidative stress reduction	Decoction	Experimental (*in vitro and in vivo*)	Baicalein sulfates/ glucuronides and wogonin ssulfates/glucuronides derived from *Scutellaria baicalensis* Georgi
[65]	Decreasing LDH release and increasing in Bcl-2 and a decrease in active caspase-3 expression and suppress apoptosis by activating the PI3K/ Akt/eNOS signaling pathway	Solution	Experimental (*in vitro and in vivo*)	Breviscapine derived from *Erigeron breviscapus*
[66]	Decreasing serum levels of CK-MB, TNF-α, IL-6, LDH, SOD, and MDA. Besides, can cause increasing SOD activity and decreased MDA content in myocardial tissue. In addition preventing myocardial injury via regulation of Nox/NF-κB/AP1 pathway	Solution	Experimental (*in vitro and in vivo*)	Salidroside derived from *Rhodiola rosea*
[67]	Reversing Bax/Bcl-2 ratio and inhibiting the activities of caspase-3 and caspase-9, increasing mitochondrial function, by reducing ROS accumulation, improving mitochondrial membrane potential and decreasing intracellular calcium concentration and supressing apoptotic myocyte death by reducing Akt/GSK-3β pathway activating	Solution	Experimental (*in vitro*)	Asiatic acid derived from *Centella asiatica*
[68]	Inhibiting apoptosis by reversing mitochondrial dysfunction, due to activation of GLP-1R and PI3K/AKT signaling pathway and reducing oxidative stress.	Solution	Experimental (*in vitro*)	Geniposide derived from *Gardenia jasminoides* J. Ellis

Continuation of table 2

[69]	Activating AMPK-mTORC1 signaling pathway to initiate autophagy and improving the Beclin 1/Bcl-2 interaction by regulating their phosphorylation to prevent further autophagy	Solution	Experimental (*in vitro*)	Orientin derived from *Polygonum orientale L.*
[70]	Decreasing fibrosis, oxidative stress, inflammatory response, and hypoxia induce cardiomyocyte apoptosis and activating the eNOS/NO signaling cascades	Solution	Experimental (*in vitro and in vivo*)	Orientin
[71]	Alkaloeid compound increasing cell viability	Extract	Experimental (*in vitro*)	hexahydrobenzo[c] phenanthridine alkaloids derived from *Corydais ambigua* var. *amurensis*
[72]	Protective effects toward H9c2 cells injury by increasing cell viability	Extract	Experimental (*in vitro*)	C21 steroidal glycosides derived from *Cynanchum stauntonii*
[73]	Decreasing apoptosis and inhibited the activities of renin and angiotensin-converting enzyme and reducing the expression of angiotensin	Extract	Experimental (*in vitro and in vivo*)	Trans-polydatin derived from *polygonum cuspidatum*
[74]	Diminishing the protein level of cleaved caspase-3, LC3-II, Beclin1 and Sirt1 and suppressing autophagy and apopotosis	Extract	Experimental (*in vitro*)	Coptisine derived from *Rhizoma coptidis*
[75]	Up-regulation of autophagy and enhancement of mitochondrial biogenesis via Sirt3 activity	Solution	Experimental (*in vitro and in vivo*)	Polyphenolic derived from *Polygonum cuspidatum*
[76]	Increasing pyruvate dehydrogenase-mediated aerobic metabolism and restoration of aerobic glucose oxidation	Solution	Experimental (*in vitro*)	*Panax notoginseng* saponin derived from *Panax notoginseng*
[77]	Enhancement of autophagic flux and removal of dysfunction of mitochondria	Solution	Experimental (*in vitro and in vivo*)	Gastrodin derived from *Gastrodia elata*
[78]	Reducing oxidative stress and apoptosis via affecting ERα and GPR30 to activation PI3K pathway and its downstream apoptosis proteins	Solution	Experimental (*in vitro*)	Notoginsenoside R1 derived from *Panax notoginsenosides*
[79]	Regulation of mitochondrial pathway (mediated by 14-3-3η signaling pathway)	Solution	Experimental (*in vitro*)	Luteoloside derived from several Chinese medicines
[80]	Down-regulating miR-22 expression and activating the PI3K/AKT and JAK1/STAT3 pathways and reduced apoptosis	Solution	Experimental (*in vitro*)	*Angelica sinensis* polysaccharide
[81]	Recovering the Activated Peroxisome Proliferator- Receptor-γ (PPAR- γ) and eNOS pathway activity and reduced apoptosis and inflammatory response	Solution	Experimental (*in vitro*)	Emodin derived from *Rheum palmatum L.*
[82]	Attenuating oxidative abnormalities and modulating the antiapoptotic proteins.	Methanolic extract	Experimental (*in vitro*)	Rutin derived from *Spermococe hispida*
[83]	Restoration autophagic flux via activation of PI3K/Akt/mTOR signaling pathway	Ethanolic extract	Experimental (*in vitro and in vivo*)	Lactone derived from *Ligusticum chuanxiong*
[84]	Rising cellular antioxidant defense capacity via inducing the phosphorylation of AKT and subsequently activating the Nrf2/HO-1 signaling pathway	Solution	Experimental (*in vitro and in vivo*)	Total flavonoids derived from *Clinopodium chinense*

Continuation of table 2

[85]	Inhibiting self-cleavage of OMA1, causing to attenuate OPA1 cleavage and reducing apoptosis	Solution	Experimental (*in vitro*)	Epigallocatechin gallate derived from *Camellia sinensis*
[86]	Inhibiting PI3K/AKT-mediated ER stress, apoptosis and oxidative stress	Solution	Experimental (*in vitro and ex vivo*)	Tournefolic acid B derived from *Clinopodium chinense*

Medicinal plants and their derivatives analyzed in Table 2 provide their cardioprotective effects through several mechanisms, such as follows.

Antioxidant activity. Oxidative stress and ROS have been proven to be a potent inducer of oxidative injury, programmed cell death i.e. apoptosis [87]. ROS, which have highly toxic and reactive properties, generated due to ischaemia and augment the degree of myocardial damage sustained by the ischaemic myocardium. To cope with these toxic agents humans developed a natural defense system. The defense mechanisms include enzymes, such as SOD, GPX, CAT, guaiacol peroxidase (POX), peroxiredoxins (Prxs), ascorbate-glutathione (AsA-GSH), ascorbate peroxidase (APX), monodehydroascorbate reductase (MDAR), dehydroascorbate reductase (DHAR) and glutathione reductase (GR) [88]. Another cardioprotective mechanism is preventing myocardial injury via regulation or or activation of pathways that contribute to antioxidant activity. For instance, herbal compounds regulatied Nox/NF-κB/AP1 pathway, which causes nonmitochondrial cellular ROS and inflammatory cytokines generation through the multiple signal pathways [66]. Another antioxidant pathway is activation of eNOS. Phytochemicals can increase NO production in heart and inhibit superoxide by quenching it [70]. Also activation of PI3 K/Akt signaling pathway can suppress mitochondrial-dependent apoptosis and oxidative stress, by activating HO-1 and NQO1, which are Nrf2 mediated-antioxidants [21; 84]. Under pathological conditions, for instance, myocardium infraction and stroke, this defense system is disrupted. Consequently, generation of free radicals increases and the scavenging effects of antioxidants, leading to oxidative damage to cardiomyocytes. Medicinal herbs contain polyphenols that attenuate the level of oxidizing agents and can directly scavenge hydrogen peroxide, superoxide and hydroxyl radicals, increasing the cardiomyocytes viability and reducing the infarct size [14].

Anti-apoptotic properties. ROS induces cell dysfunction and cardiomyocytes necrosis via other mechanisms. They stimulate and activate calpains and metalloproteinases, mitochondrial permeability transition pore (MPTP) opening which cause to swelling and lysis of cardiomyocytes. This process may cause release of pro-apoptotic factors in the cytosol, so this mechanism is contributing to cell death [89]. Hence, another cardioprotective mechanism of medicinal plants and their derivatives is regulating pro-apoptotic genes in cardiomyocytes hypoxic condition. They can down-regulating gene expression levels of pro-apoptotic genes such as Bax, Fas, caspase-3 and caspase-9 proteins. In addition they can up-regulating Bcl-2 and Bcl-xl proteins [51; 54; 57]. Another protective mechanism is prevented a reduction in cell viability, decreased the amount of lactate dehydrogenase (LDH) activity release, which is used as indicators of cardiomyocyte injury and improved cell viability [57]. Also they can protect cardiomyocytes against hypoxia via suppress multiple signaling pathways such as PKC epsilon/mK ATP and redox-sensitive ERK/Nrf2 and TLR4/NF-κB pathways, which attributed ROS arising from CYP-catalyzed processes and apoptosis trigger [23; 57]. They also can suppress apoptosis through activating the AMPK, PI3K/Akt/eNOS, GLP-1R, PI3K/AKT, JAK1/STAT3 and Akt/GSK-3β signaling pathways that plays important roles in cell survival and apoptosis [13; 33; 67; 68; 80] and regulating Akt/Nrf2/HO-1 signaling. Up-regulation of eNOS can protect against myocardial infarction injury via suppressing vascular cell adhesion molecule expression and preventing excessive leukocyte tissue infiltration. In addition phytochemicals increasing hemeoxygenase-1 (HO-1), which is an inducible enzyme with potent antioxidant activity [32]. Thus, phytochemicals up-regulating MAPK ERK1/2 pathway and modulating the PI3K/Akt pathway and reduced apoptosis in cardiomyocytes [55; 58]. Besides, phytochemical prevented cytochrome c release to protect cardiomyocytes from apoptosis via activation some pathways [85].

Reducing the calcium influx. During the acute myocardial ischemia, results in reduction of ATP production and cell metabolism switch to anaerobic

glycolysis due to lack of oxygen. It can cause a drop in intracellular pH and the production of lactate. This induces ion pump function unbalance and the Na^+-H^+ exchanger to extrude H+ and causes in intracellular Na+ accumulation, which activates the $2Na^+$-Ca^{2+} exchanger to function in inverse to throw out Na+ and results intracellular Ca^{2+} overload [4]. Polyphenols, such as flavonoids components, inhibited [$Ca^{(2+)}$] i contents in cardiac muscle cells and prevented the changes induced by KCl in cardiac myocytes and K-ATP channel-opening in the cardiac myocytes has been may attributed to reduced Ca^{2+} influx. They can consequently prolong hypoxia endurance time in cardiac myocytes [17; 56]. Besides in molecule assay, they reduced sensitivity to Ca^{2+}-induced mitochondrial permeability transition (MPT) pore opening and reduced necrotic and apoptotic cell death in hypoxic/reoxygenated cardiac myocytes [23]. Also medicinal plants suppress increased in the late sodium current (INaL) that induce intracellular Na(+) overload and finally intracellular $Ca^{(2+)}$ overload through activated reverse $Na^{(+)}$ – $Ca^{(2+)}$ exchange [35].

Antiinflammatory properties. After cardiac reperfusion, inflammatory cascade is triggered and a lot of amounts of pro-inflammatory cytokines like TNF-alpha, IL-1beta, IL-6, and IL-8 are produced and released. These cytokines as main factors in cardiac dysfunction activate neutrophils and endothelial cells and exacerbate myocardial ischemic injury [90]. Therefore inflammation is a detrimental factor in myocyte hypoxia. It has been proven that TLR2 and TLR4 are expressed in cardiomyocytes during myocardial infarction injury and their stimulation by local endogenous ligands results to the up-regulation of their own expression. These two toll-like receptors are mediate to inflammatory receptors. Some medicinal derivatives can attenuate hypoxia–reoxygenation-induced inflammation, via extracellular signal-regulated kinase 1 or 2 (ERK1/2) and c-Jun NH2-terminal kinase (JNK) signaling pathways [60]. ROS generation during hypoxia causes inflammatory responses that activate including the expression of COX-2 and intercellular adhesion molecule1 (ICAM-1), which plays a pivotal role in the linkage between inflammation and apoptosis [91]. Inhibitory effect of medicinal plants on expression of inflammatory neutrophils or gene response and consequently this property can increase cell viability and reduce necrosis volume [57; 64]. One of these related mechanisms is decreasing peroxidase enzyme like MPO, which has both oxidative and inflammatory effects in cardiomyocytes [38]. MPO is an inflammatory marker, elevated in ischemic cases [92]; so inhibiting that is one of the anti inflammatory effects of medicinal herbs. HIF-1 α is known as principal regulator of the molecular hypoxic response and has regulator effect on the cellular and systemic homeostatic responses to hypoxic circumstances by activating the transcription of several genes, consisting those involved in energy metabolism, apoptosis, angiogenesis, other genes, the protein products of which augment oxygen delivery or assist metabolic adaptation to hypoxia [93]. HIF-1 α has a vital role in triggering cellular protection and metabolic alterations in response to oxygen deprivation during myocardial ischemia and adaptive response to cell ischemia and hypoxia [94].

Some herbal compounds can attenuate myocardial ischemia reperfusion injury by up-regulating HIF-1 α expression which transmits a survival signal to the myocardium [62]. For example, promoting HIF-1α expression causes the inhibition of ROS generation, maintenance of mitochondrial membrane potential (MMP) and reduction of calcium influx, so inhibiting the mitochondrial-mediated apoptosis in hypoxic cardiomyocytes [67]. Even so, some studies reported that HIF-1 is negatively attributed to bcl-2 expression and enhancement apoptosis [33; 95]. Several plants can implement their cardioprotective effects by decreasing HIF-1α expression after several weeks [33].

The role of autophagy in myocardial hypoxic injury is still controversial. It is believed that cardiomyocyte necrosis may occur via autophagy up-regulation and through excessive degradation of the necessary cellular components and self-digestion after hypoxia/reoxygenation or ischemic injury [96]. Medicinal plants active compounds can act as the inhibitor of autolysosome, suggesting that they may inhibit autophagosome generation that consequently enhanced cell viability and decreased apoptosis [36; 74]. However some studies indicate that medicinal plants and their derivatives insert their protective effects through up-regulating autophagy along with enhanced autophagic flux via the activation of various pathways [27; 77; 83]. Clearly, autophagy is dysregulated in the process of myocardial hypoxia injury and herbal compounds can restore unbalance in autophagy process and regulating phosphorylation to prevent excessive autophagy.

Conclusion

It should be noted that plant and their derivatives are not always beneficial and their misuse can lead to irreparable complications. For instance, application of methylcysteine, derived from *Allium sativum*

in mice caused toxic effects to the heart. High dose consumption of this compound causes up-regulation of apoptotic genes (Bax and caspase3), hypoxia inducible factor 1 alpha (HIF1a) and down-regulation of the anti-apoptotic marker, Bcl2. It causes hypoxia induced cardiomyocyte apoptosis attributed by engulfment of mitochondria by nucleus [97]. Most of the reviewed studies were carried out on animal hypoxic or ischemic models and on H9c2 cells; so they cannot be generalized in human and it was one of the main limitations of the studies. Medicinal herbs can be used as an effective treatment against myocardial hypoxia mainly through antioxidant, anti apoptosis, anti-inflammatory properties, inhibiting calcium accumulation, HIF-1 α signaling regulation and autophagy regulation. Post-ischemia and chronic treatment of cardioprotection maybe consider as a therapeutic strategies than short term and pre-treatment methods in clinical setting. More clinical trial studies are required in order to obtain more reliable results.

References

1. Mozaffarian D., Benjamin E.J., Go A.S., Arnett D.K., Blaha M.J., Cushman M., et al. (2015). Heart disease and stroke statistics-2015 update: a report from the American Heart Association. *Circulation*, vol. 131, no. 4, pp. e29-322.

2. Cahill T.J., Kharbanda R.K. (2017). Heart failure after myocardial infarction in the era of primary percutaneous coronary intervention: mechanisms, incidence and identification of patients at risk. *World J Cardiol.*, vol. 9, no. 5, pp. 407-415.

3. Neri M., Riezzo I., Pascale N., Pomara C., Turillazzi E. (2017). Ischemia/Reperfusion injury following acute myocardial infarction: a critical issue for clinicians and forensic pathologists. *Media Inflam*., vol. 2017, no., pp. 7018393-7018393.

4. Hausenloy D.J., Yellon D.M. (2013). Myocardial ischemia-reperfusion injury: a neglected therapeutic target. *J Clin Invest.*, vol. 123, no. 1, pp. 92-100.

5. Heidari-Soreshjani S., Asadi-Samani M., Yang Q., Saeedi-Boroujeni A. (2017). Phytotherapy of nephrotoxicity-induced by cancer drugs: an updated review. *J Nephropathol.*, vol. 6, no. 3, pp. 254-263.

6. Memarzadeh E., Luther T., Heidari-Soureshjani S. (2018). Effect and mechanisms of medicinal plants on dry eye disease: a systematic review. *J Clin Diagn Res.*, vol. 12, no. 9, pp. NE1-NE4.

7. Shabanian G., Heidari-Soureshjani S., Rafieian-Kopaei M., Saadat M., Shabanian M. (2017). Therapeutic effects of *Quercus persica* fruit skin on healing of second-degree burn wounds in animal model. *J Zanjan Univ Med SciHealth Servs.*, vol. 25, no. 113, pp. 81-92.

8. Shabanian S., Khalili S., Lorigooini Z., Malekpour A., Heidari-Soureshjani S. (2017). The effect of vaginal cream containing ginger in users of clotrimazole vaginal cream on vaginal candidiasis. *J Adv Pharm Technol Res*., vol. 8, no. 2, pp. 80-84.

9. Shirani M., Raeisi R., Heidari-Soureshjani S., Asadi-Samani M., Luther T. (2017). A review for discovering hepatoprotective herbal drugs with least side effects on kidney. *J Nephropharmacol*., vol. 6, no. 2, pp. 38-48.

10. Yavangi M., Rabiee S., Nazari S., Farimani-Sanoee M., Amiri I., Bahmanzadeh M., et al. (2018). Comparison of the Effect of Oestrogen Plus Foeniculum vulgare Seed and Oestrogen alone on Increase in Endometrial Thickness in Infertile Women. J. Clin. Diagn. Res., vol. 12, no. 1, pp. QC01–QC04.

11. Heidari-Soreshjani S., Asadi-Samani M., Yang Q., Saeedi-Boroujeni A. (2017). Phytotherapy of nephrotoxicity-induced by cancer drugs: an updated review. *J Nephropathol.*, vol. 6, no. 3, pp. 254-263.

12. Shirani-Boroujeni M., Heidari-Soureshjani S., Keivani Hafshejani Z. (2017). Impact of oral capsule of Peganum harmala on alleviating urinary symptoms in men with benign prostatic hyperplasia; a randomized clinical trial. *J Renal Inj Prev*, vol. 6, no. 2, pp. 127-131.

13. Li F., Fan X., Zhang Y., Pang L., Ma X., Song M., et al. (2016). Cardioprotection by combination of three compounds from ShengMai preparations in mice with myocardial ischemia/reperfusion injury through AMPK activation-mediated mitochondrial fission. *Sci Rep.*, vol. 6, 37114.

14. Shao Z.H., Li C.Q., Vanden Hoek T.L., Becker L.B., Schumacker P.T., Wu J.A., et al. (1999). Extract from Scutellaria baicalensis Georgi attenuates oxidant stress in cardiomyocytes. *J Mol Cell Cardiol.*, vol. 31, no. 10, pp. 1885-1895.

15. Fitzl G., Welt K., Wassilew G., Clemens N., Penka K., Mukke N. (2001). The influence of hypoxia on the myocardium of experimentally diabetic rats with and without protection by *Ginkgo biloba* extract. III: Ultrastructural investigations on mitochondria. *Exp Toxicol Pathol.*, vol. 52, no. 6, pp. 557-568.

16. Gao X.F., Shi H.M., Sun T., Ao H. (2009). Effects of Radix et rhizoma *Rhodiolae kirilowii* on expressions of von Willebrand factor, hypoxia-inducible factor 1 and vascular endothelial growth factor in myocardium of rats with acute myocardial infarction. *Zhong Xi Yi Jie He Xue Bao*, vol. 7, no. 5, pp. 434-440.

17. Zhang B.N., Hou Y.L., Liu B.J., Liu Q.M., Qiao G.F. (2010). The *Rhododendron dauricum* L. flavonoids exert vasodilation and myocardial preservation. *Iran J Pharm Res.*, vol. 9, no. 3, pp. 303-311.

18. Wang Z., Liao S.G., He Y., Li J., Zhong R.F., He X., et al. (2013). Protective effects of fractions from *Pseudostellaria heterophylla* against cobalt chloride-induced hypoxic injury in H9c2 cell. *J Ethnopharmacol*, vol. 147, no. 2, pp. 540-545.

19. Wong H.S., Ko K.M. (2013). Herba Cistanches stimulates cellular glutathione redox cycling by reactive oxygen species generated from mitochondrial respiration in H9c2 cardiomyocytes. *Pharm Biol.*, vol. 51, no. 1, pp. 64-73.

20. Lim C.Y., Kim B.Y., Lim S.H., Cho S.I. (2015). Effects of *Pogostemon cablin* Blanco extract on hypoxia induced rabbit cardiomyocyte injury. *Pharmacogn Mag.*, vol. 11, no. 42, pp. 311-319.

21. Li L., Zhou Y., Li Y., Wang L., Sun L., Zhou L., et al. (2017). Aqueous extract of Cortex Dictamni protects H9c2 cardiomyocytes from hypoxia/reoxygenation-induced oxidative stress and apoptosis by PI3K/Akt signaling pathway. *Biomed Pharmacother.*, vol. 89, no., pp. 233-244.

22. Yang G., Min D., Yan J., Yang M., Lin G. (2018). Protective role and mechanism of snakegourd peel against myocardial infarction in rats. *Phytomed.*, vol. 42, no., pp. 18-24.

23. Chiu P.Y., Leung H.Y., Leong P.K., Chen N., Zhou L.M., Zuo Z., et al. (2012). Danshen-Gegen decoction protects against hypoxia/reoxygenation-induced apoptosis by inhibiting mitochondrial permeability transition via the redox-sensitive ERK/Nrf2 and PKC epsilon/mK ATP pathways in H9c2 cardiomyocytes. *Phytomed.*, vol. 19, no. 2, pp. 99-110.

24. Hu F., Koon C.M., Chan J.Y., Lau K.M., Fung K.P. (2012). The cardioprotective effect of danshen and gegen decoction on rat hearts and cardiomyocytes with post-ischemia reperfusion injury. *BMC Complement Altern Med.*, vol. 12, p. 249.

25. Xu M., Hao H., Jiang L., Wei Y., Zhou F., Sun J., et al. (2016). Cardiotonic pill reduces myocardial ischemia-reperfusion injury via increasing EET concentrations in rats. *Drug Metab Dispos.*, vol. 44, no. 7, pp. 878-887.

26. Wei W., Liu Y., Zhang Q., Wang Y., Zhang X., Zhang H. (2017). Danshen-Enhanced cardioprotective effect of cardioplegia on ischemia reperfusion injury in a human-induced pluripotent stem cell-derived cardiomyocytes model. *Artif Organs.*, vol. 41, no. 5, pp. 452-460.

27. Cui H., Li X., Li N., Qi K., Li Q., Jin C., et al. (2014). Induction of autophagy by Tongxinluo through the MEK/ERK pathway protects human cardiac microvascular endothelial cells from hypoxia/reoxygenation injury. *J Cardiovasc Pharmacol.*, vol. 64, no. 2, pp. 180-190.

28. Li Q., Cui H.H., Yang Y.J., Li X.D., Chen G.H., Tian X.Q., et al. (2017). Quantitative Proteomics Analysis of Ischemia/Reperfusion Injury-Modulated Proteins in Cardiac Microvascular Endothelial Cells and the Protective Role of Tongxinluo. *Cell Physiol Biochem.*, vol. 41, no. 4, pp. 1503-1518.

29. Qi K., Li X., Geng Y., Cui H., Jin C., Wang P., et al. (2018). Tongxinluo attenuates reperfusion injury in diabetic hearts by angiopoietin-like 4-mediated protection of endothelial barrier integrity via PPAR-alpha pathway. *PLoS One*, vol. 13, no. 6, pp. e0198403.

30. Wang W., Wang L., Yang H., Wang J., Yin X., Xu H., et al. (2014). Protective effects of yindanxinnaotong capsule in a rat model of myocardial ischemia/reperfusion injury. *J Tradit Chin Med.*, vol. 34, no. 6, pp. 699-709.

31. Duan Z.Z., Li Y.H., Li Y.Y., Fan G.W., Chang Y.X., Yu B., et al. (2015). Danhong injection protects cardiomyocytes against hypoxia/reoxygenation- and H2O2-induced injury by inhibiting mitochondrial permeability transition pore opening. *J Ethnopharmacol.*, vol. 175, no., pp. 617-625.

32. Hu T., Wei G., Xi M., Yan J., Wu X., Wang Y., et al. (2016). Synergistic cardioprotective effects of Danshensu and hydroxysafflor yellow A against myocardial ischemia-reperfusion injury are mediated through the Akt/Nrf2/HO-1 pathway. *Int J Mol Med.*, vol. 38, no. 1, pp. 83-94.

33. Yu F.C., Xu Y.J., Tong J.Y., Lu Z.Z., Zhang X.H. (2015). Therapeutic effects of Qishen Yiqi Dropping Pill on myocardial injury induced by chronic hypoxia in rats. *Chin J Nat Med.*, vol. 13, no. 10, pp. 776-780.

34. Feng Y.Q., Ju A.C., Liu C.H., Wang T., Yu B.Y., Qi J. (2016). Protective effect of the extract of Yi-Qi-Fu-Mai preparation on hypoxia-induced

heart injury in mice. *Chin J Nat Med.*, vol. 14, no. 6, pp. 401-406.

35. Luo A., Liu Z., Cao Z., Hao J., Wu L., Fu C., et al. (2017). Wenxin Keli diminishes $Ca^{(2+)}$ overload induced by hypoxia/reoxygenation in cardiomyocytes through inhibiting INaL and ICaL. *Pacing Clin Electrophysiol.*, vol. 40, no. 12, pp. 1412-1425.

36. Shi X., Zhu H., Zhang Y., Zhou M., Tang D., Zhang H. (2017). XuefuZhuyu decoction protected cardiomyocytes against hypoxia/reoxygenation injury by inhibiting autophagy. *BMC Complement Altern Med.*, vol. 17, no. 1, p. 325.

37. Wang D., Liu Y., Zhong G., Wang Y., Zhang T., Zhao Z., et al. (2017). Compatibility of Tanshinone IIA and astragaloside IV in attenuating hypoxia-induced cardiomyocytes injury. *J Ethnopharmacol.*, vol. 204, pp. 67-76.

38. Li F., Fan X.X., Chu C., Zhang Y., Kou J.P., Yu B.Y. (2018) A strategy for optimizing the combination of active components based on Chinese medicinal formula Sheng-Mai-San for myocardial ischemia. *Cell Physiol Biochem.*, vol. 45, no. 4, pp. 1455-1471.

39. Li F., Guo S., Wang C., Huang X., Wang H., Tan X., et al. (2018). Yiqihuoxue decoction protects against post-myocardial infarction injury via activation of cardiomyocytes PGC-1alpha expression. *BMC Complement Altern Med.*, vol. 18, no. 1, pp. 253.

40. Sun L., Jia H., Ma L., Yu M., Yang Y., Liu Y., et al. (2018). Metabolic profiling of hypoxia/reoxygenation injury in H9c2 cells reveals the accumulation of phytosphingosine and the vital role of Dan-Shen in Xin-Ke-Shu. *Phytomed.*, vol. 49, no., pp. 83-94.

41. Wang Y., Zhao Y., Jiang W., Zhao X., Fan G., Zhang H., et al. (2018). iTRAQ-based proteomic analysis reveals recovery of impaired mitochondrial function in ischemic myocardium by Shenmai formula. *J Proteome Res.*, vol. 17, no. 2, pp. 794-803.

42. Zhang W.Y., Yu Y., Yan L.L., Li C., Han J.Y., Qin Z.F., et al. (2018). Discovery of cardioprotective constituents of Gualou Xiebai Decoction, a classical traditional Chinese medicinal formula. *Phytomed*., vol. 15, no. 54, pp. 318-327.

43. Yagi A., Okamura N., Tanonaka K., Takeo S. (1994). Effects of tanshinone VI derivatives on post-hypoxic contractile dysfunction of perfused rat hearts. *Planta Med.*, vol. 60, no. 5, pp. 405-409.

44. Chan P., Hong C.Y., Tomlinson B., Chang N.C., Chen J.P., Lee S.T., et al. (1997). Myocardial protective effect of trilinolein: an antioxidant isolated from the medicinal plant *Panax pseudoginseng*. *Life Sci*., vol. 61, no. 20, pp. 1999-2006.

45. Chan P., Niu C.S., Tomlinson B., Hong C.T., Chen J.P., Hong C.Y., et al. (1997). Effect of trilinolein on superoxide dismutase activity and left ventricular pressure in isolated rat hearts subjected to hypoxia and normoxic perfusion. *Pharmacol.*, vol. 55, no. 5, pp. 252-258.

46. Lai Z.F., Shao Z., Chen Y.Z., He M., Huang Q., Nishi K. (2004). Effects of sasanquasaponin on ischemia and reperfusion injury in mouse hearts. *J Pharmacol Sci.*, vol. 94, no. 3, pp. 313-324.

47. Chen H.P., He M., Huang Q.R., Liu D., Huang M. (2007). Sasanquasaponin protects rat cardiomyocytes against oxidative stress induced by anoxia-reoxygenation injury. *Eur J Pharmacol.*, vol. 575, no. 1-3, pp. 21-27.

48. Manna C., Migliardi V., Golino P., Scognamiglio A., Galletti P., Chiariello M., et al. (2004). Oleuropein prevents oxidative myocardial injury induced by ischemia and reperfusion. *J Nutr Biochem.*, vol. 15, no. 8, pp. 461-466.

49. Hu D., Liu X., Wang Y., Chen S. (2007). Cyclovirobuxine D ameliorates acute myocardial ischemia by K(ATP) channel opening, nitric oxide release and anti-thrombosis. *Eur J Pharmacol.*, vol. 569, no. 1-2, pp. 103-109.

50. Woo A.Y., Waye M.M., Tsui S.K., Yeung S.T., Cheng C.H. (2008). Andrographolide up-regulates cellular-reduced glutathione level and protects cardiomyocytes against hypoxia/reoxygenation injury. *J Pharmacol Exp Ther.*, vol. 325, no. 1, pp. 226-235.

51. Liu X.H., Xin H., Hou A.J., Zhu Y.Z. (2009). Protective effects of leonurine in neonatal rat hypoxic cardiomyocytes and rat infarcted heart. *Clin Exp Pharmacol Physiol.*, vol. 36, no. 7, pp. 696-703.

52. Xu L., Jiang X.J., Wei F., Zhu H.L. (2018). Leonurine protects cardiac function following acute myocardial infarction through anti-apoptosis by the PI3K/AKT/GSK3 beta signaling pathway. *Mol Med Rep.*, vol. 18, no. 2, pp. 1582-1590.

53. Liu X., Pan L., Gong Q., Zhu Y. (2010). Leonurine (SCM-198) improves cardiac recovery in rat during chronic infarction. *Eur J Pharmacol.*, vol. 649, no. 1-3, pp. 236-241.

54. Wu L.X., Gu X.F., Zhu Y.C., Zhu Y.Z. (2011). Protective effects of novel single compound, Hirsutine on hypoxic neonatal rat cardiomyocytes. *Eur J Pharmol.*, vol. 650, no. 1, pp. 290-297.

55. Liu C., Guo W., Maerz S., Gu X., Zhu Y. (2013). 3,5-dimethoxy-4-(3-(2-carbonyl-ethyldisulfanyl) - propionyl)-benzoic acid 4-guanidino-butyl ester: a novel twin drug that prevents primary cardiac myocytes from hypoxia-induced apoptosis. *Eur J Pharmacol.*, vol. 700, no. 1-3, pp. 118-126.

56. Li H.X., Han S.Y., Ma X., Zhang K., Wang L., Ma Z.Z., et al. (2012). The saponin of red ginseng protects the cardiac myocytes against ischemic injury in vitro and in vivo. *Phytomed.*, vol. 19, no. 6, pp. 477-483.

57. Zhang C., Lin G., Wan W., Li X., Zeng B., Yang B., et al. (2012). Resveratrol, a polyphenol phytoalexin, protects cardiomyocytes against anoxia/reoxygenation injury via the TLR4/NF-kappaB signaling pathway. *Int J Mol Med.*, vol. 29, no. 4, pp. 557-563.

58. Zhang L., Wu Y.L., Li Y.M., Xu C.Q., Li X.L., Zhu D.L., et al. (2012). Tanshinone IIA improves miR-133 expression through MAPK ERK1/2 pathway in hypoxic cardiac myocytes. *Cell Physiol Biochem*., vol. 30, no. 4, pp. 843-852.

59. Tang X., Liu J., Dong W., Li P., Li L., Lin C., et al. (2013). The cardioprotective effects of citric acid and L-malic acid on myocardial ischemia/reperfusion injury. *Evid Based Complement Alternat Med.*, vol. 2013, no., pp. 820695.

60. Liu Q., Wang J., Liang Q., Wang D., Luo Y., Li J., et al. (2014). Sparstolonin B attenuates hypoxia-reoxygenation-induced cardiomyocyte inflammation. *Exp Biol Med.*, vol. 239, no. 3, pp. 376-384.

61. Zhu H.Y., Gao Y.H., Wang Z.Y., Xu B., Wu A.M., Xing Y.W., et al. (2013). Astragalus polysaccharide suppresses the expression of adhesion molecules through the regulation of the p38 MAPK signaling pathway in human cardiac microvascular endothelial cells after ischemia-reperfusion injury. *Evid Based Complement Alternat Med.*, vol. 2013, 280493.

62. Si J., Wang N., Wang H., Xie J., Yang J., Yi H., et al. (2014). HIF-1alpha signaling activation by post-ischemia treatment with astragaloside IV attenuates myocardial ischemia-reperfusion injury. PLoS One, vol. 9, no. 9, pp. e107832.

63. Wong H.S., Chen N., Leong P.K., Ko K.M. (2014). beta-sitosterol enhances cellular glutathione redox cycling by reactive oxygen species generated from mitochondrial respiration: protection against oxidant injury in H9c2 cells and rat hearts. *Phytother Res.*, vol. 28, no. 7, pp. 999-1006.

64. Chao C.L., Lin S.P., Hou Y.C., Chao P.D.L., Chang N.C., Huang Y.C., et al. (2015). Metabolites of *Scutellariae radix* inhibit injury of endothelial cells in hypoxia device. *J Med Biol Eng*., vol. 35, no. 4, pp. 492-499.

65. Wang J., Ji S.Y., Liu S.Z., Jing R., Lou W.J. (2015). Cardioprotective effect of breviscapine: inhibition of apoptosis in H9c2 cardiomyocytes via the PI3K/Akt/eNOS pathway following simulated ischemia/reperfusion injury. *Pharmazie*, vol. 70, no. 9, pp. 593-597.

66. Zhu L., Wei T., Chang X., He H., Gao J., Wen Z., et al. (2015). Effects of salidroside on myocardial injury *in vivo in vitro* via regulation of Nox/NF-kappaB/AP1 pathway. *Inflammation*, vol. 38, no. 4, pp. 1589-1598.

67. Huang X., Zuo L., Lv Y., Chen C., Yang Y., Xin H., et al. (2016). Asiatic acid attenuates myocardial ischemia/reperfusion injury via Akt/GSK-3beta/HIF-1alpha signaling in rat H9c2 cardiomyocytes. *Molecules*, vol. 21, no. 9, pp.1248.

68. Jiang Y.Q., Chang G.L., Wang Y., Zhang D.Y., Cao L., Liu J. (2016). Geniposide prevents hypoxia/reoxygenation-induced apoptosis in H9c2 cells: improvement of mitochondrial dysfunction and activation of GLP-1R and the PI3K/AKT signaling pathway. *Cell Physiol Biochem.*, vol. 39, no. 1, pp. 407-421.

69. Liu L., Wu Y., Huang X. (2016). Orientin protects myocardial cells against hypoxia-reoxygenation injury through induction of autophagy. *Eur J Pharmacol.*, vol. 776, no., pp. 90-98.

70. Li F., Zong J., Zhang H., Zhang P., Xu L., Liang K., et al. (2017). Orientin reduces myocardial infarction size via eNOS/NO signaling and thus mitigates adverse cardiac remodeling. *Front Pharmacol.*, vol. 8, no., pp. 926.

71. Liu Z.H., Li Q., Chang S., Yang Z.Y., Han N., Yin J. (2016). Protective effect of hexahydrobenzo[c] phenanthridine alkaloids isolated from *Corydalis ambigua var. amurensis* on myocardial ischemia-hypoxia cells. *Phytochemistry Letters*, vol. 17, pp. 258-262.

72. Lei Q.S., Zuo Y.H., Lai C.Z., Luo J.F., Pang S.W., Zhou H., et al. (2017). New C-21 steroidal glycosides from the roots of *Cynanchum stauntonii* and their protective effects on hypoxia/reoxygenation induced cardiomyocyte injury. *Chinese Chemical Letters*, vol. 28, no. 8, pp. 1716-1722.

73. Ming D., Songyan L., Yawen C., Na Z., Jing M., Zhaowen X., et al. (2017). trans-polydatin protects the mouse heart against ischemia/reperfusion

injury via inhibition of the renin-angiotensin system (RAS) and Rho kinase (ROCK) activity. *Food Funct.*, vol. 8, no. 6, pp. 2309-2321.

74. Wang Y., Wang Q., Zhang L., Ke Z., Zhao Y., Wang D., et al. (2017). Coptisine protects cardiomyocyte against hypoxia/reoxygenation-induced damage via inhibition of autophagy. *Biochem Biophys Res Commun*., vol. 490, no. 2, pp. 231-238.

75. Zhang M., Zhao Z., Shen M., Zhang Y., Duan J., Guo Y., et al. (2017). Polydatin protects cardiomyocytes against myocardial infarction injury by activating Sirt3. *Biochim Biophys Acta Mol Basis Dis.*, vol. 1863, no. 8, pp. 1962-1972.

76. Zhao X., Zhang F., Wang Y. (2017). Proteomic analysis reveals Xuesaitong injection attenuates myocardial ischemia/reperfusion injury by elevating pyruvate dehydrogenase-mediated aerobic metabolism. *Mol Biosyst*., vol. 13, no. 8, pp. 1504-1511.

77. Fu S., Chen L., Wu Y., Tang Y., Tang L., Zhong Y., et al. (2018). Gastrodin pretreatment alleviates myocardial ischemia/reperfusion injury through promoting autophagic flux. *Biochem Biophys Res Commun.*, vol. 503, no. 4, pp. 2421-2428.

78. Li G., Xing X.Y., Luo Y., Deng X.H., Lu S., Tang S.M., et al. (2018). Notoginsenoside R-1 prevents H9c2 cardiomyocytes apoptosis against hypoxia/reoxygenation via the ERs/PI3K/Akt pathway. *Rsc Advances*, vol. 8, no. 25, pp. 13871-13878.

79. Liu Z., Yang L., Huang J., Xu P., Zhang Z., Yin D., et al. (2018). Luteoloside attenuates anoxia/reoxygenation-induced cardiomyocytes injury via mitochondrial pathway mediated by 14-3-3eta protein. *Phytother Res*., vol. 32, no. 6, pp. 1126-1134.

80. Pan H., Zhu L. (2018). Angelica sinensis polysaccharide protects rat cardiomyocytes H9c2 from hypoxia-induced injury by down-regulation of microRNA-22. *Biomed Pharmacother*., vol. 106, pp. 225-231.

81. Shou X.L., Zhou R.F., Zhu L.Y., Ren A.H., Wang L., Wang Y., et al. (2018). Emodin, A Chinese Herbal Medicine, Inhibits Reoxygenation-Induced Injury in Cultured Human Aortic Endothelial Cells by Regulating the Peroxisome Proliferator-Activated Receptor-gamma (PPAR-gamma) and Endothelial Nitric Oxide Synthase (eNOS) Signaling Pathway. *Medical Science Monitor*, vol. 24, pp. 643-651.

82. Sundaram R.L., Sali V.K., Vasanthi H.R. (2018). Protective effect of rutin isolated from Spermococe hispida against cobalt chloride-induced hypoxic injury in H9c2 cells by inhibiting oxidative stress and inducing apoptosis. *Phytomed*., vol. 51, pp. 196-204.

83. Wang G., Dai G.L., Song J., Zhu M.M., Liu Y., Hou X.F., et al. (2018). Lactone component from *Ligusticum chuanxiong* alleviates myocardial ischemia injury through inhibiting autophagy. *Frontiers in Pharmacology*, vol. 9, 301.

84. Zhang H.J., Chen R.C., Sun G.B., Yang L.P., Zhu Y.D., Xu X.D., et al. (2018). Protective effects of total flavonoids from Clinopodium chinense (Benth.) O. Ktze on myocardial injury in vivo and in vitro via regulation of Akt/Nrf2/HO-1 pathway. *Phytomed*., vol. 40, pp. 88-97.

85. Nan J., Nan C., Ye J., Qian L., Geng Y., Xing D., et al. (2019). EGCG protects cardiomyocytes against hypoxia-reperfusion injury through inhibition of OMA1 activation. *J Cell Sci.*, vol. 132, no. 2, pii. jcs220871.

86. Yu Y., Xing N., Xu X., Zhu Y., Wang S., Sun G., et al. (2019). Tournefolic acid B, derived from *Clinopodium chinense* (Benth.) Kuntze, protects against myocardial ischemia/reperfusion injury by inhibiting endoplasmic reticulum stress-regulated apoptosis via PI3K/AKT pathways. *Phytomed*., vol. 52, no., pp. 178-186.

87. Uttara B., Singh A.V., Zamboni P., Mahajan R.T. (2009). Oxidative stress and neurodegenerative diseases: a review of upstream and downstream antioxidant therapeutic options. *Curr Neuropharmacol.*, vol. 7, no. 1, pp. 65-74.

88. Caverzan A., Casassola A., Brammer S.P. (2016). Reactive oxygen species and antioxidant enzymes involved in plant tolerance to stress, Abiotic and biotic stress in plants-recent advances and future perspectives. InTech.

89. Neri M., Riezzo I., Pascale N., Pomara C., Turillazzi E. (2017). Ischemia/reperfusion injury following acute myocardial infarction: a critical issue for clinicians and forensic pathologists. *Mediators Inflamm.*, vol. 2017, 7018393.

90. Kleinbongard P., Heusch G., Schulz R. (2010). TNFα in atherosclerosis, myocardial ischemia/reperfusion and heart failure. *Pharmacology & therapeutics*, vol. 127, no. 3, pp. 295-314.

91. Millar T.M., Phan V., Tibbles L.A. (2007). ROS generation in endothelial hypoxia and reoxygenation stimulates MAP kinase signaling and kinase-dependent neutrophil recruitment. *Free Radic Biol Med.*, vol. 42, no. 8, pp. 1165-1177.

92. Omran M.M., Zahran F.M., Kadry M., Belal A.A.M., Emran T.M. (2018). Role of myeloperoxidase in early diagnosis of acute myocardial infarction in patients admitted with chest pain. *J Immunoassay Immunochem.*, vol. 39, no. 3, pp. 337-347.

93. Semenza G.L. (2012). Hypoxia-inducible factors in physiology and medicine. *Cell*, vol. 148, no. 3, pp. 399-408.

94. Lee S.H., Wolf P.L., Escudero R., Deutsch R., Jamieson S.W., Thistlethwaite P.A. (2000). Early expression of angiogenesis factors in acute myocardial ischemia and infarction. *N Engl J Med.*, vol. 342, no. 9, pp. 626-633.

95. Carmeliet P., Dor Y., Herbert J.-M., Fukumura D., Brusselmans K., Dewerchin M., et al. (1998). Role of HIF-1α in hypoxia-mediated apoptosis, cell proliferation and tumour angiogenesis. *Nature*, vol. 394, no. 6692, pp. 485.

96. Wang Z.G., Wang Y., Huang Y., Lu Q., Zheng L., Hu D., et al. (2015). bFGF regulates autophagy and ubiquitinated protein accumulation induced by myocardial ischemia/reperfusion via the activation of the PI3K/Akt/mTOR pathway. *Sci. Rep.*, vol. 5, pp. 9287.

97. El-Magd M.A., Abdo W.S., El-Maddaway M., Nasr N.M., Gaber R.A., El-Shetry E.S., et al. (2017). High doses of S-methylcysteine cause hypoxia-induced cardiomyocyte apoptosis accompanied by engulfment of mitochondaria by nucleus. *Biomed. Pharmacother.*, vol. 94, pp. 589-597.

IRSTI 31.23.39

[1]A.A. Kudaibergen, [1]M.A. Dyusebaeva,
[2]A. Ydyrys, [3]Y. Feng, [1*]J. Jenis

[1]Research Center for Medicinal Plants of al-Farabi Kazakh National University, al-Farabi ave. 71, Almaty, Kazakhstan
[2]al-Farabi Kazakh National University, Faculty of Biology and Biotechnology, department of biophysics and biomedicine, al-Farabi ave. 71, Almaty, Kazakhstan
[3]Griffith Institute for Drug Discovery, Griffith university, QLD 4111, Brisbane, Australia
e-mail: janarjenis@mail.ru

Investigation of chemical constituents of medicinal Plant *Spiraea Hypericifolia* L.

Abstract: In this work, the quantitative analysis of phytochemical constituents of medicinal plant *Spiraea hypericifolia* L. from Kazakhstan has been made for the first time. Total bioactive components aerial and underground parts of plants material *S. hypericifolia* L. such as organic acids (0.28 %), (0.35 %), flavonoids (0.77 %), (5.36 %), coumarins (0.04 %), (0.21 %), saponins (2.09 %), (0.98 %), tannins (1.31 %), (1.62 %), and together with moisture content (4.72 %), (3.84 %), total ash (5.11 %), (5.41 %), were determined. Eleven macro-micro elements from the ash of plant were identified, main contents of them were Ca (362.20 μg/ml), (344.750 μg/ml), K (69.670 μg/ml), (57.8075 μg/ml), and Mg (24.270 μg/ml), (34.480 μg/ml), by using the method of multi-element atomic emission spectral analysis. In addition, twenty amino and eight fatty acids were analyzed from the plant. The results showed that major contents of amino acids were glutamate (1741 mg/100g), (1710 mg/100g), aspartate (845 mg/100g), (820 mg/100g), and alanine (560 mg/100g), (523 mg/100g), as well as in fatty acid was linoleic (81.1 %), (79.7 %) acid, respectively.
Key words: *Spiraea hypericifolia* L., bioactive constituents, macro-micro elements, amino-, fatty acids.

Introduction

Studies on phytochemicals have attracted the attention of plant scientists due to the development of new and sophisticated techniques. These techniques played a significant role in giving the solution to systematic problems on the one hand and in the search for additional resources of raw materials for pharmaceutical industry on the other hand [1]. The genus *Spiraea* L., spirea, represents deciduous shrubs of the family *Rosaceae Juss*., subfamily *Spiraeoideae* Focke, respectively the family *Spiraeaceae* Humb., Bonpl. & Kunth in the narrower concept. The genus is widespread in the temperate and the subtropical zone of the northern hemisphere having more than 100 species [2-3]. *S. hypericifolia* L. has the most extensive Eurasian range and is considered one of the most evolutionarily advanced representatives of the genus [4]. In Europe, beside two native species, *S. hypericifolia* L. and *S. salicifolia* L., cultivated evidently already in the 16th or 17th century, the first species being imported from overseas were East American *S. tomentosa* L. and *S. alba* Du Roi. A species with an extensive natural geographic range in Eurasia. The typical subspecies is distributed from East Europe to Central Asia, West Mongolia, North China and SouthEast Siberia (Transbaikalia), while the subsp. *obovata* occurs in SouthWest Europe [5]. Deciduous shrub 0, 5-1, 6 m height. Crohn thick, sprawling. Branches are numerous, spreading or arcuate, brown. Very thin, curved, angular, red-brown, first pubescent, then naked[6]. In the leaves of *S. hypericifolia* L. detected, p-hydroxybenzoic, coffee, ferulic, chlorogenic acid, flavones apigenin, luteolin and 5-glucosides of flavonols isoquercitrin and avicularin [7]. In the hydrolysates of *S. hypericifolia* L. discovered quercetin, chlorogenic, p- coumaric and caffeic acids in extracts – hyperoside, isoquercitrin, avicularin[8].

This study has made the investigation of the chemical constituents from Kazakh medicinal plants of *S. hypericifolia* L. grown in Almaty region of Kazakhstan for the first time.

Materials and methods

Plant material. The aerial and underground parts of plants material *S. hypericifolia* L. was collected in Almaty region Kazakhstan in October, 2018. The air dried aerial and underground parts of *S. hypericifolia* L. was cutted into small pieces and stored at room temperature.

Experimental part. The quantitative determination of detected groups of natural compounds is carried out according to the method of the State Pharmacopoeia and the methodology developed by the author of phytochemical analysis [9-12]

In the "Center of Physical and Chemical methods of research and analysis", Republican State Enterprise Kazakh National Al-Farabi University, Ministry of Education and Science of RoK using the method of multi-element atomic emission spectral analysis in the ash of *S. hypericifolia* L. were analyzed elemental constituents. To determine the mineral composition of ashes was used Shimadzu 6200 series spectrometer.

Method for the determination of amino acids. 1 g of the analyte, hydrolyzed in 5 ml of 6N hydrochloric acid at 105 ºC for 24 hours, in ampoules sealed under a stream of argon. The resulting hydrolyzate is evaporated three times to dryness on a rotary evaporator at a temperature of 40-50 ºC and a pressure of 1 atm. The resulting precipitate is dissolved in 5 ml of sulfosalicylic acid. After centrifugation for 5 minutes, the packed liquid is passed through a column of ion exchange resin at a rate of 1 drop per second. After this, the resin is washed with 1-2 ml of deionized water and 2 ml of 0.5N acetic acid; then the resin is washed to neutral pH with deionized water. To elute the amino acids from the column, 3 ml of a 6N NH_4OH solution is passed through it at a rate of 2 drops per second. The eluate is collected in a round bottom flask together with distilled water, which is used to wash the column to a neutral pH medium. The contents of the flask are then evaporated to dryness on a rotary evaporator at a pressure of 1 atm and a temperature of 40-50 ºC. After adding a drop of freshly prepared 1.5% $SnCl_2$ solution, 1 drop of 2,2-dimethoxypropane and 1-2 ml of propanol saturated with hydrochloric acid, it is heated to 110 ºC, keeping this temperature for 20 minutes, and then the contents are again evaporated from the flask on a rotary evaporator. In the next step, 1 ml of freshly prepared acetyl reagent (1 volume of acetic anhydride, 2 volumes of triethylamine, 5 volumes of acetone) is introduced into the flask and heated at a temperature of 60 ºC for 1.5-2 minutes. The sample is again evaporated on a rotary evaporator to dryness and 2 ml of ethyl acetate and 1 ml of a saturated NaCl solution are added to the flask. The contents of the flask are thoroughly mixed and as the two layers of liquids are clearly formed, an upper layer (ethyl acetate) is taken for gas chromatographic analysis.

To determine the amino acids composition was made erenow [13] of the raw material used GC/MS device. GC/MS analysis: the aerial and underground parts of *S. hypericifolia* L. were analyzed by Gas Chromatograph coupled to Mass Spectrometer using polar mixture of 0.31% carbowax 20 m, 0.28% silar 5 CP and 0.06% lexan in chromosorb WA-W-120-140 mesh., column (400 x 3 mm). The column temperature was programmed from 110ºC (held for 20 min), at 6ºC/min from 110ºC to 180ºC, at 32ºC/min from 185ºC to 290ºC. When it reaches to 250ºC, it should stay constant till finishing analysis of all existed amino acids. The chromatogram is counted according to an external standard.

Determination of the fatty acids composition of dried plants aerial and underground parts of *S. hypericifolia* L. extracted with a chloroform- methanol mixture (2:1) for 5 minutes, the extract is filtered through a paper filter and concentrated to dryness. Then, to taked extract add 10 ml of methanol and 2-3 drops of acetyl chloride and further methylation at 60-70°C in a special system for 30 minutes. The methanol is removed by rotary evaporation and the samples are extracted with 5 ml of hexane and analyzed using a gas chromatograph together with MS by applying the same method in investigation of amino acids.

As a result, chromatograms of methyl esters of fatty acids were obtained. By comparison with reliable samples by the time of exit from the column, eight fatty acids were identified. To determine the components was used the internal normalization method.

Results and discussion

The quantitative analysis of biologically active constituents together with moisture content, total ash were determined from aerial and underground parts of *S. hypericifolia* L. The results are shown in Table 1.

Moisture and ash contents depend on many factors, such as the method of collection and the method of drying. These indicators have a certain limit. For example, for my plant limit is 12%. Based on the results we can say that the goodness of the plant *S. hypericifolia* L has been proven. This plant might be used in the pharmaceutical industry.

As values were determine with a purpose to find out the total amount of inorganic solutes present in the medicinal plant material. Quite a few herbal therapies make use of ash. It is very obvious that ash of any plant does not contain any organic material and therefore inorganic salts are used medicinally. It is also interesting to know about the different solubility of the components of ash. Therefore, the solubility of ash in water and hydrochloric acid was tested in the present study. Organic acids play an important role in maintaining the acid-base balance of the human body. Organic acids are responsible for the taste, the flavour, the microbial stability, and the product consistence of plant derived beverages and are used in food preservation because of their effects on bacteria. Flavonoids are a class of compounds presented broadly in nature. Concerns about their extensive profitable bioactive benefits, including anti-viral/bacterial, anti-inflammatory, cardio protective, anti-diabetic, anti-cancer, anti-aging, have long been received great attention and well supported by numerous studies. Mostly, phytochemicals from the group of flavonoids have been reported as the major contributor to the biological activities. It is believed that the significant biological activities exhibited by the herbal materials are due to the presence of flavonoids acting as antioxidants.

Table 1 – Quantitative analysis of bioactive constituents of *S. hypericifolia* L.

Content, %							
Plants	Moisture content	Ash	Organic acids	Flavanoids	Coumarins	Saponins	Tannins
Aerial part of S. hypericifolia L.	4.72	5.11	0.28	0.77	0.04	2.09	1.31
Underground part of S. hypericifolia L.	3.84	5.41	0.35	5.36	0.21	0.98	1.62

Macro-micro elemental composition

In "Center of Physical and Chemical methods of research and analysis", Republican State Enterprise Kazakh National Al-Farabi University, Ministry of Education and Science of RoK using the method of multi-element atomic emission spectral analysis in the ash of *S. hypericifolia* L. there were determined eleven macro- and microelements, shown in Table 2 and Figure 1,2 and major of them was Ca (362.20 μg/ml), (344.750 μg/ml), K (69.670 μg/ml), (57.8075 μg/ml) and Mg (24.270 μg/ml), (34.480 μg/ml). The information helps to select plants with high quantity of each nutrient. This will intern confirm the efficacy of the medicinal activity of the plant. An analysis of macro and microelements showed a large variability. The present study showed a large variation in the contents of nutrients and protein %, thereby offering opportunity by scientists working on medicinal. 2 medicinal plants were grouped based on the maximum content of macro and micro elements. Potassium is an electrolyte, a substance that conducts electricity in the body. K is crucial to heart function and plays a key role in skeletal and smooth muscle contraction, making it important for normal digestive and muscular function[14]. The role of K in the human body is complex intervening in the forming proteins, maintaining cellular balance, acid-base balance, transport of oxygen and carbon dioxide in the blood, nerve impulse management, muscle contraction in cardiac muscle specuila, glycogenesis[15]. Magnesium is involved in hundreds of enzyme reactions in the body as it performs an array of biological functions as activation of muscles and nerves, digestion of proteins, carbohydrates, fats, building block for RNA and DNA synthesis. In the human body calcium, helps alongside phosphorus, the formation and strengthening of bones and teeth. Performs a number of functions among which the muscular contraction, nerve impulse transmission, immunity, promotes the absorption of iron and vitamin B12 is a blood clotting activator of various enzymes[16].

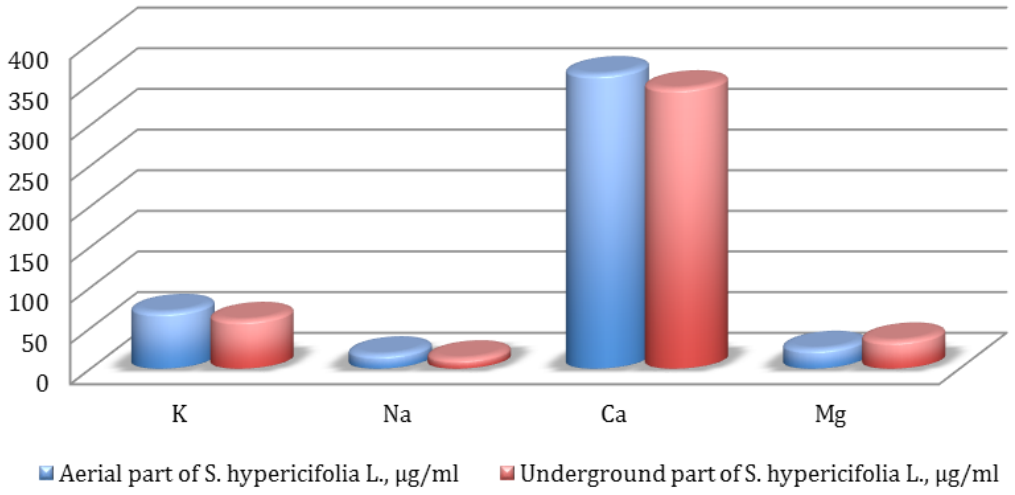

Figure 1 – Contents of macro elements of plants *S. hypericifolia* L.

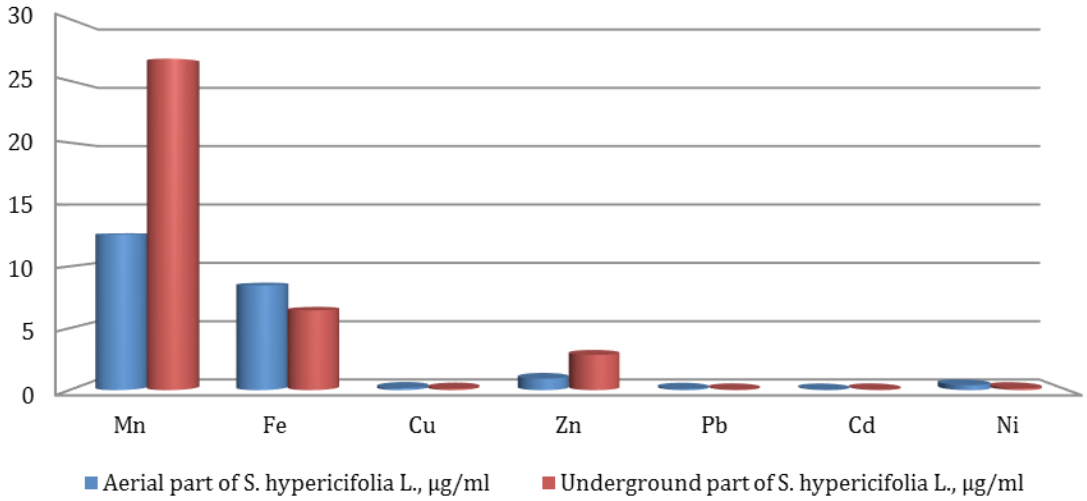

Figure 2 – Contents of micro elements of plants *S. hypericifolia* L.

Table 2 – Composition of macro-micro elements in the ash of plants *S. hypericifolia* L.

Element, µg/ml	K	Na	Ca	Mg	Mn	Fe	Cu	Zn	Pb	Cd	Ni
Aerial part	69.670	17.487	362.200	24.270	12.595	8.468	0.169	0.927	0.105	0.045	0.402
Under-ground part	59.807	12.542	344.750	34.480	26.785	6.448	0.122	2.846	0.055	0.055	0.156

Amino acid composition

Thus, in the quantitative determination of the amino acid composition of the aerial and underground parts of S. hypericifolia by the method of gas-liquid chromatography, 20 amino acids were detected. Their main content is represented by glutamate (1741 mg/100g), (1710 mg/100g), aspartate (845 mg/100g), (820 mg/100g) and alanine (560 mg/100g), (523 mg/100g). A smaller amount contains ornithine and oxyproline. The results shown in Table 3.

Table 3 – Amino acids contents of *S. hypericifolia* L.

№	Amino acids	Molecular formula	Amount in aerial part, mg/100g	Amount in underground part, mg/100g
1	Alanine	$C_3H_7NO_2$	560	523
2	Glycine	$C_2H_5NO_2$	180	161
3	Leucine	$C_6H_{13}NO_2$	320	295
4	Isoleucine	$C_6H_{13}NO_2$	294	270
5	Valine	$C_5H_{11}NO_2$	230	211
6	Glutamate	$C_5H_9NO_4$	1741	1710
7	Threonine	$C_4H_9NO_3$	218	202
8	Proline	$C_5H_9NO_2$	302	180
9	Methionine	$C_5H_{11}NO_2S$	50	41
10	Serine	$C_3H_7NO_3$	188	134
11	Aspartate	$C_4H_7NO_4$	845	820
12	Cysteine	$C_3H_7NO_2S$	29	22
13	Oxyproline	$C_5H_9NO_3$	1	2
14	Phenylalanine	$C_9H_{11}NO_2$	278	256
15	Tyrosine	$C_9H_{11}NO_3$	300	82
16	Histidine	$C_6H_9N_3O_2$	236	218
17	Ornithine	$C_5H_{12}N_2O_2$	1	2
18	Arginine	$C_6H_{14}N_4O_2$	328	305
19	Lysine	$C_6H_{14}N_2O_2$	212	190
20	Tryptophan	$C_{11}H_{12}N_2O_2$	66	53

Therefore, according to the results, *S. hypericifolia* L. could be one of the most valuable sources of these amino acids and might be widely used in medicine due to the fact that glutamate is one of the most abundant of the amino acids. In addition to its role in protein structure, it plays critical roles in nutrition, metabolism and signaling. Post-translational carboxylation of glutamyl residues increases their affinity for calcium and plays a major role in hemostasis [17]. Aspartic acid increases immunity, metabolism, deactivates ammonia, participates in the formation of ribonucleic acids, promotes the removal of chemicals, including drugs, restores working capacity. Studies conducted by scientists have proved the effectiveness of taking asparaginic acid preparations for increasing testosterone levels. Aspartic acid is taken as an additive by bodybuilding athletes to improve strength, increase libido and testosterone in the blood [18]. Alanine also increases immunity and provides energy for brain and central nervous system, the muscle tissue. This amino acid protects against the development of cancer of the pancreas and prostate gland [19].

Fatty acids composition

The result of gas-liquid chromatography determined the amount of 8 fatty acids. Quantitative composition of fatty acids in the aerial and underground parts of *S. hypericifolia* L. mostly contained in linoleic acid (81.1 %), (79.7 %), showed in Table 4.

Table 4 – Fatty acids contents of *S. hypericifolia* L.

№	Fatty acids	Molecular formula	Amount in aerial part, %	Amount in underground part, %
1	Myristic acid $C_{14:0}$	$C_{14}H_{28}O_2$	2.3	2.2
2	Pentadecanoic acid $C_{15:0}$	$C_{15}H_{30}O_2$	2.4	2.0
3	Palmitic acid $C_{16:0}$	$C_{16}H_{32}O_2$	5.2	4.9
4	Palmitoleic acid $C_{16:1}$	$C_{16}H_{30}O_2$	0.9	0.8
5	Stearin acid $C_{18:0}$	$C_{18}H_{36}O_2$	3.0	2.8
6	Oleic acid $C_{18:1}$	$C_{18}H_{34}O_2$	6.3	6.1
7	Linoleic acid $C_{18:2}$	$C_{18}H_{32}O_2$	81.1	79.7
8	Linolenic acid $C_{18:3}$	$C_{18}H_{30}O_2$	1.8	1.5

As can be seen from the table, the figure for linoleic acid is much higher than that of other fatty acids. That's why *S. hypericifolia* L. could be utilized to obtain linoleic acid. As regards the qualities of linoleic acid, it is an essential fatty acid in nutrition and is used in the biosynthesis of prostaglandins and cell membranes [20].

Conclusion

In conclusion, quantitative analysis of total bioactive constituents and the moisture, total ash, organic acids, flavonoids, coumarins, saponins and tannins of *S. hypericifolia* L. were determined. Besides, macro-micro elements in the ash of the medicinal plant were investigated, and total eleven macro-micro elements were identified by the method of multi-element atomic emission spectral analysis. Meanwhile, twenty amino and eight fatty acids were determined from *S. hypericifolia* L. Of the identified amino acids of the aerial part, glutamate, aspartate and alanine predominate, while in the underground their content is slightly less. Fatty acid is mainly linoleic acid. The plants *S. hypericifolia* L. has high research potential and demands multidimensional study.

References

1. Mojab F., Kamalinejad M., Naysanch Ghaderi, Hamid Reza Vahidipour. (2003) Phytochemical Screening of Some Species of Iranian Plants, *Iranian Journal of Pharmaceutical Research,* 2(2), pp. 77-82.

2. Yü, T. T. & LU, L. T. (1974) Spiraea L. – In: Yü, T.T. (ed.), Flora Reipublicae Popularis Sinicae, *Science Press*. – Beijing, 36, pp. 3–67.

3. Yü, T. T., LU, L. T. & KU, T. C. (1975), *Acta Phytotax. Sinica*, 13 (1), pp. 99–101.

4. Slavkina T. I. (1972) Species of the genus Spiraea introduced in the Botanical Garden of UzSSR // Dendrology of Uzbekistan [Dendrologiya Usbekistana]. Vol. 4. Rosaceae. – Tashkent, pp. 196–304.

5. Rehder A. (1940) Manual of Cultivated Trees and Shrubs Hardy in North America, 2nd ed. corrected reprint – Macmillan Co., New York. 1958, p. 996 .

6. Businský R., Businská L. (2002) *Acta Pruhoniciana*, 72, pp. 1-165

7. Chumbalov T. K., Pashinina L. T., Storozhenko N. D. (1975) Flavons and its 5-glycosides from Spiraea hypericifolia, *Chemistry of natural compounds,* No. 3. pp. 425–426.

8. Karpova E. A., Khramova E. P. (2014) Phenolic composition and content of representatives of genus *Spiraea* L. under industrial pollution in Novosibirsk, *Contemporary Problems of Ecology,* Vol. 7, iss. 2. pp. 228–236.

9. Kazakhstan State Pharmacopeia (2008), Almaty: Zhibek zholy, 1, pp. 592–609.

10. Muzychkina R.A., Korulkin D.Yu. (2006) Bio-Active Plant Substances. Extraction, Separation and Analysis, Almaty: Atamura, p. 438.

11. Mamonov L.K., Muzychkina R.A. (2008) Introduction to Phytochemical Researches and Detection of Biological Activity of Plant Substances, Almaty: XXI Century School, p. 216.

12. Muzychkina R.A., Korulkin D.Yu. (2012) Methodology of Research of Natural Metabolites, Almaty: MV-Print, p. 324.

13. Tulembetova A.K., Jenis J. (2013) Amino acid composition of badan (*Bergenia crassifolia*), *News of Scientific-Technical Society «KACAK»,* 2, pp. 47-49.

14. Gorbachev V.V., Gorbacheva V.N. (2002) Vitamins, micro- and macro elements **[**Vitaminy, mikro- i makroelementy]. Interpresservis, Belorussia. ISBN 985-428-547-2.

15. K. Lux-Sparschuh. (1989), *IPI Berna*, no.3, pp. 8-10.

16. K.O. Soetan, C.O. Olaiya, O.E. Ozewole. (2010), *African Journal of Food Science*, 4(5): pp. 200-220.

17. Stacey S. W., Shahriar K. G. (2013), *International Journal of Biological Sciences*, pp. 948-959

18. Katane M, Kanazawa R, Kobayashi R, Oishi M, Nakayama K, Saitoh Y, Miyamoto T, Sekine M, Homma H. (2017), *Proteins and Proteomics*, vol. 1865, pp. 1129-1140.

19. Liu L, Chen Y, Yang L. (2014), *Analytical Biochemistry*, 467, pp. 28-30.

20. Yang B, Chen H, Stanton C, Ross RP, Zhang H, Chen YQ, Chen W. (2015), *Journal of Functional Foods*, 15, pp. 314-325.

IRSTI 31.21.25; 76.31.35

[1]L. Figueroa-Valverde, [2]M. Rosas-Nexticapa,
[3]F. Díaz-Cedillo, [1]T. Lopez-Gutierez, [1]M. López-Ramos,
[1]L.Hau-Heredia, [2]E. Pool-Gómez, [2]P. Hernandez-Vasquez

[1]Laboratory of Pharmaco-Chemistry, Faculty of Chemical Biological Sciences, University Autonomous of Campeche, Av. Agustín Melgar s/n, Col Buenavista C.P. 24039 Campeche, Camp., México.
[2]Facultad de Nutrición, Universidad Veracruzana, Médicos y Odontologos s/n C.P. 91010, Unidad del Bosque Xalapa Veracruz, México.
[3]Escuela Nacional de Ciencias Biológicas del Instituto Politécnico Nacional. Prol. Carpio y Plan de Ayala s/n Col. Santo Tomas, México, D.F. C.P. 11340.
*e-mail: lfiguero@uacam.mx; lauro_1999@yahoo.com

Synthesis and theoretical activity evaluation of a new steroid-oxazolone derivative against COX1-1 and COX-2

Abstract: There are some reports for the preparation of several drugs as COX-inhibitors; however, some reagents used in the preparation are expensive and difficult to handle. The aim of this study was to synthesize a steroid-oxazolone derivative using some reactions such as *i*) hydroxylation-amiination; *ii*) amidation; *iii*) alkynyl-addition; *iv*) aldolization and *iv*) imination. In addition, a theoretical assessment was carried out to evaluate the interaction of both COX-1 and COX-2 with the steroid-oxazolone derivative using indomethacin and rofecoxib as controls in a docking model. The structure of the compounds obtained was confirmed through elemental analysis, spectroscopy and spectrometry data. The results showed that the steroid-oxazolone derivative has a higher affinity for COX 1 compared to indomethacin; however, it exhibits a lower affinity for COX-2 in comparison with rofecoxib. These data suggest that the steroid-oxazolone derivative could be a good candidate as COX-1 inhibitor translated as a possible drug for treatment of pain.
Key words: inhibitor, hydroxylation-amiination, amidation, alkynyl-addition.

Introduction

For years, several inhibitors of the enzyme cyclooxygenase have been used for the treatment of both inflammation and pain such as ketorolac, naproxen, acetylsalicylic acid, paracetamol ibuprofen, indomethacin [1, 2] and others. However, some of these drugs can produce side effects such as bronchospam, vasomotor thinitis, and angioedema [3], renal dysfunction, meningeal syndrome, and bone marrow depression, headache, vertigo, [4-6]. In the search of other alternative therapeutics for treatment of these clinical pathologies, several drugs have been prepared such as 1-morpholinocyclohexanecarbonitrile from both morpholine and cyclohexanone [7]. Other data showed the reaction of Ethyl 5-(4-nitrophenyl) furan-2-carboxylate with hydrazine to form 5-(4-nitrophenyl) furan-2-carbohydrazide [8]. In addition, a series of 3-(4-biphenyl)-5-substituted phenyl-2-pyrazolines were synthesized from both chalcones and hydrazine with biological activity to pain [9]. Also, a study showed the synthesis of 4-aminopiperidine derivative with analgesic activity through of reaction of (1-Benzylpiperidin-4-yl)-[2-(3,4-dimethoxyphenyl)ethyl]-amine with 5-bromo-2-(3,4-dimethoxyphenyl)-2-(methylethyl) pentanenitrile [10]. All these data indicate that some methods are available for synthesis of drugs with analgesic activity; nevertheless, expensive reagents and special conditions are required. Therefore, the aim of this study was to synthesize a steroid-oxazolone derivative for evaluating their theoretical activity evaluation against both COX1-1 (2OYU) and COX-2 (3LN1) [11] using a docking model.

Material and Methods

General methods

2-nitroestrone was prepared using a previously method reported [12]; in addition, the others reagents

used in this investigation were acquired from Sigma-Aldrich Co., Ltd. The melting point for compounds was determined on an Electrothermal (900 model). Infrared spectra (IR) were recorded using KBr pellets on a Perkin Elmer Lambda 40 spectrometer.^{1}H and ^{13}C NMR spectra were recorded on a Varian VXR300/5 FT NMR spectrometer at 300 MHz in $CDCl_3$ using TMS as internal standard. EIMS spectra were obtained with a Finnigan Trace Gas Chromatography Polaris Q-Spectrometer. Elementary analysis data were acquired from a Perkin Elmer Ser. II CHNS/02400 elemental analyzer.

Chemical Synthesis

(13S)-3-((1-hydroxyethyl)amino)-13-methyl-2-nitro-6,7,8,9,11,12,13,14,15,16-decahy- dro-17H-cyclopenta[a]phenanthren-17-one (2)

In a round bottom flask (10 ml), 2-nitroestrone (200 mg, 0.63 mmol) and acetonitrile (5ml) were stirred to reflux for 12 h. The solution obtained was reduced pressure and purified through a crystallization using the methanol:water (4:1) system; yielding 44% of product; m.p. 166-168 °C; IR (V_{max}, cm^{-1}) 3430, 3400, 1712 and 1544: ^{1}H NMR (500 MHz, Chloroform-*d*) δ_H: 0.90 (s, 3H), 1.20-1.34 (m, 4H), 1.44 (s, 3H), 1.54-2.46 (m, 8H), 3.02-3.10 (m, 3H), 5.60 (m, 1H), 6.56 (m, 1H), 7.72 (broad, 2H), 8.42 (m, 1H) ppm. ^{13}C NMR (500 MHz, Chloroform-*d*) δ_C: 13.82, 21.70, 24.90, 25.50, 27.55, 28.94, 31.06, 35.00, 37.25, 46.43, 48.34, 50.12, 76.62, 115.44, 124.70, 128.92, 137.2, 141.00, 147.80, 219.74 ppm. EI-MS m/z: 358.18. Anal. Calcd. for $C_{20}H_{26}N_2O_4$: C, 67.02; H, 7.31; N, 7.82; O, 17.85. Found: C, 67.00; H, 7.24.

(12aS)-8,12a-dimethyl-2,3,3a,3b,4,5,7,8,10b,11,12,12a-dodecahydro-1H-cyclopenta [7,8]phenanthro[2,3-d]oxazol-1-one (3)

In a round bottom flask (10 ml), compound **2** (200 mg, 0.58 mmol), potassium carbonate (45 mg, 0.33 mmol), and 5 ml of dimethyl sulfoxide were stirred to reflux for 12 h. The solution obtained was reduced pressure and purified through a crystallization using the methanol:water:hexane (4:1:1) system; yielding 67% of product; m.p. 122-124 °C; IR (V_{max}, cm^{-1}) 3432, 1710 and 1210: ^{1}H NMR (300 MHz, Chloroform-*d*) δ_H: 0.90 (s, 3H), 1.18 (s, 3H), 1.22-1.90 (m, 7H), 2.10-3.10(m, 8H), 6.24 (m, 1H), 6.43-6.54 (m, 2H), 7.22 (broad, 1H) ppm. ^{13}C NMR (300 MHz, Chloroform-*d*) δ_C:13.80, 19.91, 21.82, 25.84, 27.55, 28.92, 31.50, 35.40, 37.56, 46.90, 48.12, 50.40, 83.50, 107.22, 110.92, 131.32, 133.26, 136.02, 144.00, 220.70 ppm. EI-MS m/z: 311.18. Anal. Calcd. for $C_{20}H_{25}NO_2$: C, 77.14; H, 8.09; N, 4.50; O, 10.28. Found: C, 77.10; H, 10.19.

(12aS)-7-(2-chloroacetyl)-8,12a-dimethyl-2,3,3a,3b,4,5,7,8,10b,11,12,12a-dodecahydro-1H-cyclopenta[7,8]phenanthro[2,3-d]oxazol-1-one (4)

In a round bottom flask (10 ml), compound **3** (200 mg, 0.64 mmol), chloroacetyl chloride (50 µl, 0.63mmol) and triethylamine (100 µl, 0.71 mmol) in 5 mL of methanol was stirring for 72 h to room temperature. The solution obtained was reduced pressure and purified through a crystallization using the methanol:water (4:2) system; yielding 54% of product; m.p. 136-138 °C; IR (V_{max}, cm^{-1}) 1712, 1632 and 1210: ^{1}H NMR (300 MHz, Chloroform-*d*) δ_H: 0.90 (s, 3H), 1.22-1.36 (m, 4H), 1.40 (s, 3H), 1.55-2.20 (m, 7H), 2.46-2.62 (m, 4H), 3.92-4.00 (m, 2H), 6.40 (m, 1H), 6.73-7.30 (m, 2H) ppm. ^{13}C NMR (300 MHz, Chloroform-*d*) δ_C:13.80, 19.90, 21.74, 25.70, 27.63, 28.92, 31.32, 35.30, 37.45, 42.42, 46.87, 48.10, 50.22, 82.84, 109.40, 116.23, 133.00, 134.00, 135.40, 152.97, 160.82, 220.30 ppm. EI-MS m/z: 387.16. Anal. Calcd. for $C_{22}H_{26}ClNO_3$: C, 68.12; H, 6.76; Cl, 9.14, N, 3.61; O, 12.37. Found: C, 68.06; H, 6.70.

(12aS)-7-(7-hydroxyhept-2-ynoyl)-8,12a-dimethyl-2,3,3a,3b,4,5,7,8,10b,11,12,12a-dodecahydro-1H-cyclopenta[7,8]phenanthro[2,3-d]oxazol-1-one (5)

In a round bottom flask (10 ml), compound **4** (310 mg, 0.80 mmol), 5-hexyn-1-ol (90 µl, 0.82 mmol) and Copper(II) chloride (110 µl, 0.82 mmol) in 5 mL of methanol was stirring for 72 h to room temperature. The solution obtained was reduced pressure and purified through a crystallization using the methanol:water (4:1) system; yielding 65% of product; m.p. 106-108 °C; IR (V_{max}, cm^{-1}) 3400, 2196, 1712, 16390 and 1212: ^{1}H NMR (300 MHz, Chloroform-*d*) δ_H: 0.90 (s, 3H), 1.22-1.36 (m, 4H), 1.40 (s, 3H), 1.55 (m, 1H), 1.58-1.72 (m, 4H), 1.80-1.90 (m, 2H), 1.94 (broad, 1H), 2.10-2.20 (m, 4H), 2.25-2.26 (m, 2H), 2.46-2.62 (m, 4H), 3.62-(m, 2H), 6.40 (m, 1H), 6.60-7.40 (m, 2H) ppm. ^{13}C NMR (300 MHz, Chloroform-*d*) δ_C:13.80, 17.62, 19.00, 21.74, 25.71, 25.75, 27.60, 28.92, 30.04, 31.35, 35.32, 37.42, 46.87, 48.10, 50.24, 62.05, 73.96, 82.95, 90.12, 109.52 116.02, 133.10, 133.92, 135.40, 149.62, 152.82, 220.30 ppm. EI-MS m/z: 435.24. Anal. Calcd. for $C_{27}H_{33}NO_4$: C, 74.45; H, 7.64; N, 3.22; O, 14.69. Found: C, 74.40; H, 7.60

8-((12aS)-8,12a-dimethyl-1-oxo-2,3,3a,3b,4,5,10b,11,12,12a-decahydro-1H-cyclopenta [7,8]phenanthro[2,3-d]oxazol-7(8H)-yl)-8-oxooct-6-ynal (6)

In a round bottom flask (10 ml), compound **5** (200 mg, 0.46 mmol) 5 mL of dimethyl sulfoxide was stirring for 72 h to reflux. The solution obtained was reduced pressure and purified through a crystallization using the methanol:water:hexane (4:1:1) system; yielding 48% of product; m.p. 116-118 °C; IR (V_{max}, cm^{-1}) 2194, 1726, 1710 and 1210: ^{1}H NMR (300 MHz, Chloroform-*d*) δ_H: 0.90 (s, 3H), 1.22-1.36 (m, 4H), 1.40 (s, 3H), 1.55 (m, 1H), 1.70-1.76 (m, 4H), 1.80-2.10 (m, 4H), 2.12 (m, 1H), 2.13-2.14 (m, 2H), 2.20-2.54 (m, 3H), 2.56 (m, 2H), 2.62-2.63 (m, 2H), 6.40 (m, 1H), 6.60-7.40 (m, 2H), 9.70 (d, 1H, J = 1.00 Hz) ppm. ^{13}C NMR (300 MHz, Chloroform-*d*) δ_C:13.80, 18.15, 19.00, 21.70, 22.10, 25.71, 25.76, 27.62, 28.93, 31.34, 35.32, 37.42, 44.57, 46.86, 48.10, 50.22, 73.97, 82.97, 91.32, 109.52, 116.02, 133.10, 133.92, 135.40, 149.61, 152.82, 202.44, 220.30 ppm. EI-MS m/z: 447.24. Anal. Calcd. for $C_{27}H_{33}NO_4$: C, 75.14; H, 7.43; N, 3.13; O, 14.30. Found: C, 75.10; H, 7.38.

(12aS)-7-((1Z,4E)-1,4-diazacyclododeca-4,12-dien-6-yn-5-yl)-8,12a-dimethyl-2,3,3a,3b,4,5,7,8,10b,11,12,12a-dodecahydro-1H-cyclopenta[7,8]phenanthro[2,3-d]oxazol-1-one (7)

In a round bottom flask (10 ml), compound **6** (200 mg, 0.45 mmol), ethylenediamine (50 µl, 0.74 mmol) and boric acid (50 mg, 0.80 mmol) in 5 mL of methanol was stirring for 72 h to room temperature. The solution obtained was reduced pressure and purified through a crystallization using the methanol:water (4:1) system; yielding 65% of product; m.p. 146-148 °C; IR (V_{max}, cm^{-1}) 3322, 2196, 1712 and 1212: ^{1}H NMR (300 MHz, Chloroform-*d*) δ_H: 0.85 (m, 1H), 0.90 (s, 3H), 1.22-1.36 (m, 4H), 1.46 (m, 2H), 1.55 (m, 1H), 1.57 (s, 3H), 1.58 (m, 2H), 1.80-2.20 -2.54 (m, 6H), 2.30 (m, 2H), 2.46-3.10 (m, 4H), 4.30-4.50 (m, 1H), 6.60 (m, 1H), 6.70 (m, 1H), 6.80 (m, 1H), 6.88 (m, 1) ppm. ^{13}C NMR (300 MHz, Chloroform-*d*) δ_C: 13.80, 19.42, 19.91, 21.70, 23.03, 25.70, 27.64, 28.60, 28.92, 31.34, 34.44, 35.32, 34.44, 46.85, 48.10, 48.42, 50.00, 50.24, 88.44, 91.53, 97.96, 108.65, 115.12, 131.70, 132.66, 133.45, 145.46, 149.72, 159.86, 220.30 ppm. EI-MS m/z: 471.28. Anal. Calcd. for $C_{30}H_{37}N_3O_2$: C, 76.40; H, 7.91; N, 8.91; O, 6.78. Found: C, 76.34; H, 7.88.

Physicochemical parameters evaluation

Some electronic parameters such as HOMO (Highest Occupied Molecular Orbital), LUMO (Lowest Unoccupied Molecular Orbital) energy, orbital coefficients distribution, molecular dipole moment and HBD (hydrogen bond donor groups) and HBA (hydrogen bond acceptor groups) and PSA (polar surface area) were evaluated using the SPARTAN'06 software [13].

Pharmacophore evaluation

The 3D pharmacophore model for the compounds 6 and 7 was determinate using LigandScout 4.08 software [14]

Theoretical evaluation of the interaction between compound 4 and kinase-2 protein (3FL5).

The interaction of compound 4 with both COX1-1 (2OYU) and COX-2 (3LN1) [11] was carried out using a DockingServer [15].

Results and Discussion

Several oxazolone analogs have prepared using some reagents such as $[(Ph_3P)Au(NCMe)]Sb_6$ complex [16], N,N'-terephthaloylbis-(*dl*-alanine) [17], resin [18], Ph_3P-CBr_4 adducts [19], palladium [20] and others. In this study, a steroid-oxazolone derivative was prepared using some strategies; the first stage was achieved via reaction of 2-nitroestrone with acetonitrile to form an amino-ethanol complex (Figure 1 and 2).

The ^{1}HNMR showed several signals for 2 at 0.90 ppm for methyl group bound to steroid nucleus; at 1.44 ppm for methyl bound to both hydroxyl and methylamine; at 1.20-1.34, 1.54-3.10, 6.56 and 8.42 ppm for steroid moiety; at 5.60 ppm for methylene group bound to both amino and hydroxyl groups; at 7.72 for both hydroxyl and amine groups. The ^{13}CNMR display some signals at 13.82 ppm for methyl group; at 24.90 for methyl bound to both hydroxyl and methylamine; at 21.70, 25.50-50.12 and 115.44-147.80 ppm for steroid moiety; at 76.62 ppm for methylene group bound to both amino and hydroxyl groups; at 219.70 ppm for ketone group. In addition, the mass spectrum from 2 showed a molecular ion (m/z) 358.18.

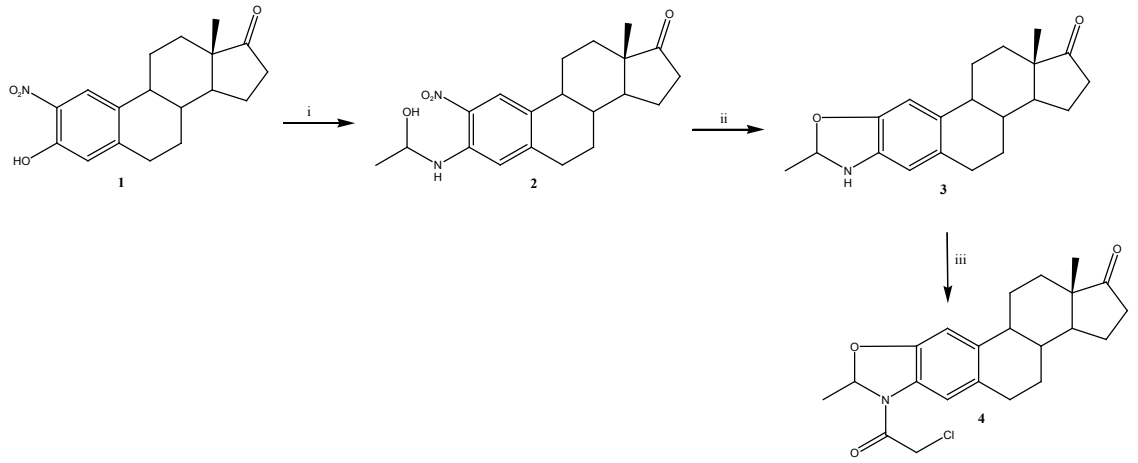

Reaction of 2-nitroestradiol with acetonitrile (i) to form a hydroxyethylamino-nitro-estrone (3). Then, an steroid oxazolone (3) via displacement of nitro group by hydroxyl in DMSO/K_2CO_3 (ii) presence of reacted with. Finally, 3 reacted with chloroacetyl chloride (iii) to form 4

Figure 1 – Preparation of a chloroacetyl-steroid-oxazolone derivative (4).

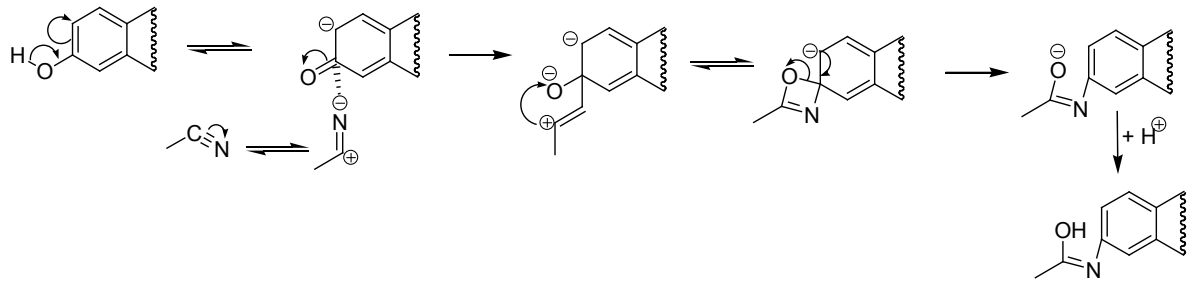

Figure 2 – Mechanism of reaction involved in the synthesis of hydroxyethylamino-nitro-estrone

The second stage was achieved by the synthesis of an ether-steroid derivative (3); it is important to mention that some reports have been reported for the preparation of ether derivatives via displacement of nitro group using methoxide as dipolar aprotic solvent [21, 22]. In this study, 3 was prepared using a previously method reported [12]; the reaction was carried out through intramolecular displacement from nitro group by the hydroxyl group of compound 2 in presence of DMSO/K_2CO_3 (Figure 1). The ^{1}HNMR showed several signals for 3 at 0.90 ppm for methyl group bound to steroid nucleus; at 1.18 ppm for methyl bound to oxazole ring; at 1.22-3.10 and 6.43-6.54 ppm for steroid moiety; at 6.24 ppm for oxazole ring; at 7.72 for both hydroxyl and amine groups. The ^{13}CNMR display some signals at 13.80 ppm for methyl group; at 19.91 for methyl bound to oxazole ring; at 21.82-50.40 and 107.22-144.00 ppm for steroid moiety; at 83.50 for oxazole ring; at 220.70 ppm for ketone group. Finally, the mass spectrum from 3 showed a molecular ion (m/z) 311.18.

On the other hand, a chloroamide-steroid derivative (4) was prepared; it is important to mention that there are many procedures for the formation of chloroamides which are known in the literature, for example the reaction of amine with trichloroisocyanuric Acid [23] or amide secondary with *N*-chlorobenzotriazole to form a chloroamide derivative [24]; in addition, have been prepared some chloroamide groups using chloroacetyl chloride [25]. The ^{1}HNMR showed several signals for 4 at 0.90 ppm for methyl group bound to steroid nucleus; at 1.40 ppm for methyl bound to oxazole ring; at 1.22-2.62 and 6.73-7.30 ppm for steroid moiety; at 3.92-4.00 ppm for methylene group of chloroamide; at 6.40 ppm for oxazole ring. The ^{13}CNMR display some signals at 13.80 ppm for methyl group; at 19.90 for methyl bound to oxazole ring; at 21.74-37.45, 46.87-50.22, 109.40-152.97 ppm for steroid moiety; at 42.42 ppm methylene group of chloroamide; at 88.84 for oxazole ring; at 160.82 ppm for amide group; at 220.30 ppm for ketone group. Addition-

ally, the mass spectrum from **4** showed a molecular ion (m/z) 387.16.

The following stage involves the synthesis of a propargylic-amide derivative (**5**). It is noteworthy that several propargylic-amide analogs have been prepared [26, 27]; however, some reagents are dangerous and are difficult to handle. Therefore in this study, **5** was prepared via addition 5-hexyn-1-ol to **4** in presence of Copper(II) chloride (Figure 2) using a previously method report [27]. The ^{1}HNMR showed several signals for **5** at 0.90 ppm for methyl group bound to steroid nucleus; at 1.40 ppm for methyl bound to oxazole ring; at 1.22-1.36, 1.55, 1.80-1.90, 2.10-2.20, 2.46-2.62 and 6.60-7.40 ppm for steroid moiety; at1.58-1.72, 2.26 and 3.62 ppm for arm bound to both alkyne and hydroxyl groups; at 1.94 ppm for hydroxyl group; at 6.40 ppm for oxazole ring. The ^{13}CNMR display some signals at 13.80 ppm for methyl bound to steroid nucleus; at 19.90 ppm for methyl bound to oxazole ring; at 17.62, 25.78, 30.04, 62.05, 109.50-135.40 and 152.82 ppm for arm bound to both alkyne and hydroxyl groups; at 21.74-25.71, 27.60-28.92 and 31.35-50.24 ppm for steroid moiety; at 73.96 and 90.12 ppm for both alkyne group; at 82.95 for oxazole ring; at 119.62 ppm for amide group; at 220.30 ppm for ketone group. Additionally, the mass spectrum from **5** showed a molecular ion (m/z) 435.24.

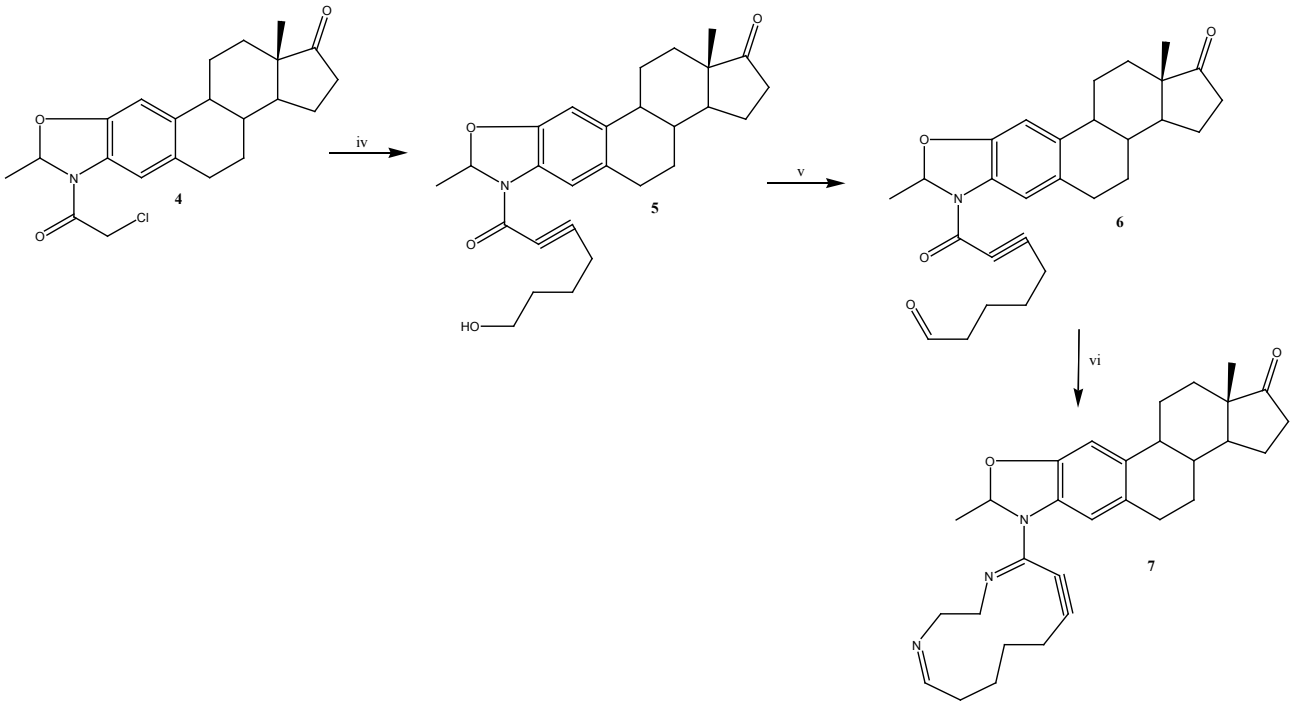

Reaction of chloroacetyl-steroid-oxazolone derivative (4) with 5-hexyn-1-ol to form hydroxyhept-2-ynoyl)-steroid-oxazolone (5) in presence of Copper(II) chloride (iv). Then, an oxazol-steroid-8-oxooctynal (6) was prepared via reaction of 5 with dimethyl sufuxide (v). Finally, 6 reacted with ethylenediamine to form 7

Figure 3 – Synthesis of 1,4-diazacyclododeca-4,12-dien-6-yn-5-yl-steroid-oxazolone (7).

In addition, 5 was reacted with dimethyl sulfoxide to form an aldehyde-oxazolone-steroid derivative using a previously method reported for synthesis of aldehyde groups [28]. The ^{1}HNMR showed several signals for 6 at 0.90 ppm for methyl group bound to steroid nucleus; at 1.40 ppm for methyl bound to oxazole ring; at 1.22-1.36, 1.54, 1.80-2.10, 21.3, 2.20-2.54, 2.62-2.63 and 6.60-7.40 ppm for steroid moiety; at 1.70-1.76, 2.12-2.14 and 2.56 ppm for arm bound to both alkyne and hydroxyl groups; at 1.94 ppm for hydroxyl group; at 6.40 ppm for oxazole ring; at 9.70 ppm for aldehyde group. The ^{13}CNMR display some signals at 13.80 ppm for methyl bound to steroid nucleus; at 19.90 ppm for methyl group bound to oxazole ring; at 18.15, 22.10, 25.76, 44.57 for arm bound to both aldehyde and alkyne group; at 21.70, 25.71, 27.62-37.42, 46.86-50.22, 109.52-135.40 and 152.82 ppm for steroid moiety; at 73.97 and 91.32 ppm for alkyne group; at 82.97 ppm for oxazole ring; at 208.44 ppm for aldehyde group; at 220.30 ppm for

ketone group. In addition, the mass spectrum from **6** showed a molecular ion (m/z) 447.24.

Finally, an 1,4diaza-cyclododeca-4,12-dien-6-yne ring was prepared via reaction of **6** with ethylenediamine to form imino groups of the 1,4-diazacyclododeca-4,12-dien-6-yn-5-yl-steroid-oxazolone (**7**). The ^{1}HNMR showed several signals for **7** at 0.88, 1.46, 2.30, 4.30-4.50 and 6.70 ppm for 1,4-diaza-cyclododeca-4,12-dien-6-yne ring; at 0.90 ppm for methyl group bound to steroid nucleus; at 1.58 ppm for methyl bound to oxazole ring; at 1.22-1.36, 1.55, 1.80-2.10, 2.46-3.10, 6.60 and 6.80 ppm for steroid moiety; at 6.88 ppm for oxazole ring. The ^{13}CNMR display some signals at 13.80 ppm for methyl bound to steroid nucleus; at 19.91 ppm for methyl bound to oxazole ring; at 19.42, 23.03, 28.60, 34.44 and 48.42-50.00 ppm for 1,4diaza-cyclododeca-4,12-dien-6-yne ring; at 21.70, 25.70-27.64, 28.92-31.34, 35.32-48.10. 50.24 and 108.65-145.46 ppm for steroid moiety; at 91.53 ppm for oxazole ring; at 149.72-159.86 ppm for imino group; at 220.30 ppm for ketone group. Finally, the mass spectrum from **7** showed a molecular ion (m/z) 471.28.

Physicochemical parameters of 2-7

There are studies which suggest some physicochemical parameters such as molar volume (M_V) and molar refractory (M_R) are chemical tools that correlate with different biological properties which may depend on the characteristics of each substituent involved in the chemical structure of a molecule. I this investigation, both M_V and M_R descriptors were determinate using a previously method reported [29]. The theoretical results showed (Table 1) that M_V and M_R were higher for 7 compared with 2-6. This phenomenon suggest that steric hindrance, conformational preferences, and internal rotation may be two factors which influence the biological activity exert by 7 on some biological model. However, other type of physiochemical factors such as hydrogen bond donor groups (HBD) and hydrogen bond acceptor groups (HBA), topological polar surface area (TPSA) has been used to predict the biological activity of some compounds in several theoretical models [30].

These physicochemical parameters (Table 1) were determinate using the Spartan 6.0 software; the theoretical data showed that the HBA value was <10 and the HBD value was <5 for compounds 2-7, this phenomenon suggest that these compounds may be well absorbed such happening with another type of compounds [31]. Other results showed that polar surface area (PSA) for 2-6 was < 100 Å values; it is noteworthy that some reports suggest that PSA < 140 Å values may condition the ability of some drugs to a good oral absorption and exhibit some biological activity [31].

Table 1 – Physicochemical parameters of compounds 2-7. The values were calculated using both ACDLabs and Spartan software

Parameters	2	3	4	5	6	7
Molar Refractivity (cm^3)	98.44	88.77	103.05	120.90	124.19	137.98
Molar Volume (cm^3)	279.40	269.80	307.50	359.50	375.80	371.50
Polarizability (cm^3)	39.02	35.19	40.85	47.93	49.23	54.70
Parachor (cm^3)	78.10	683.10	805.40	961.20	993.10	982.20
Index of refraction	1.62	1.57	1.58	1.58	1.57	1.66
Surface Tension (dyne/cm)	57.10	41.00	47.00	51.10	48.70	48.80
PSA $Å^2$	86.58	36.04	37.97	58.49	53.46	38.44
Density g/cm^3	1.28	1.15	1.26	1.21	1.19	1.26
HBD	2	1	0	1	0	0
HBA	6	3	4	5	5	4

Pharmacophore evaluation

This pharmacophore model can furnish a new insight to design novel molecules that can enhance or inhibit the function of the target and will be useful in drug discovery strategies. Therefore, in this study, LigandScout software [14] was used to develop a pharmacophore model of compounds 2 and 3. The results showed in Figures 4 and 5 indicated that there is a different type of functional groups involved in the compounds 2 to 7 that can interact via hydrophobic contacts or as hydrogen bond acceptors or as hydrogen bond donor with some biomolecules.

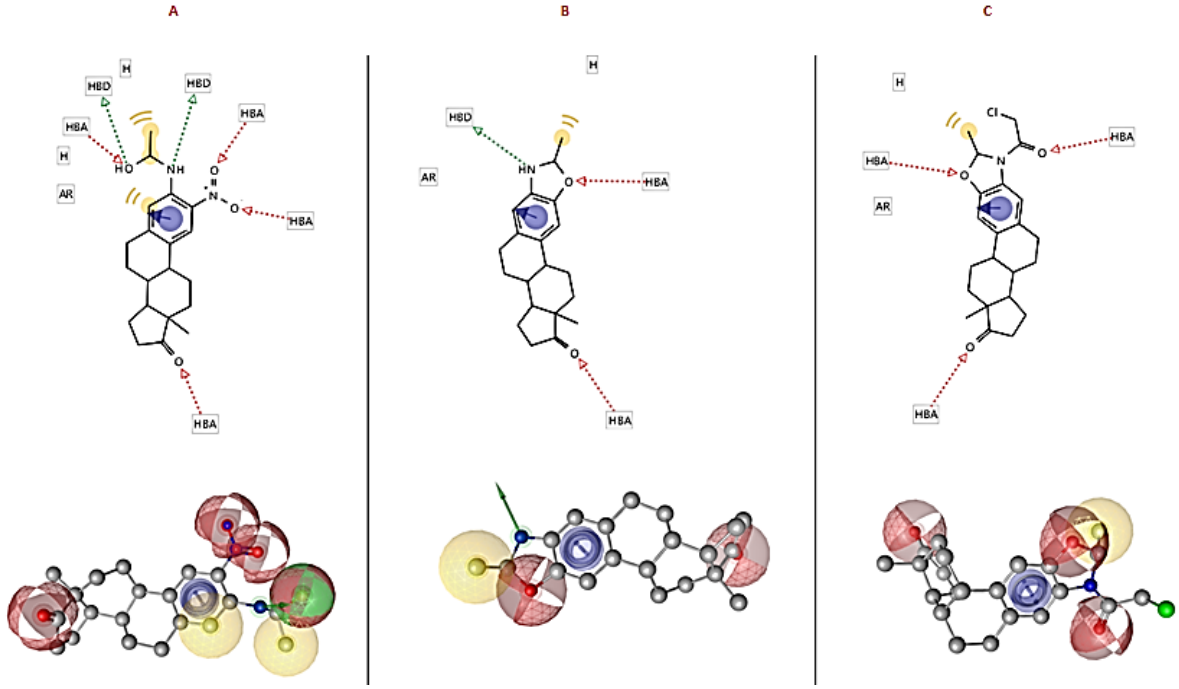

Figure 4 – Scheme represents a pharmacophore from both compounds **2** (A), **3** (B) and **4** (C) using the LigandScout software. The model involves a methyl group (yellow) hydrogen bond acceptors (HBA, red) and hydrogen bond donor (HBD, green)

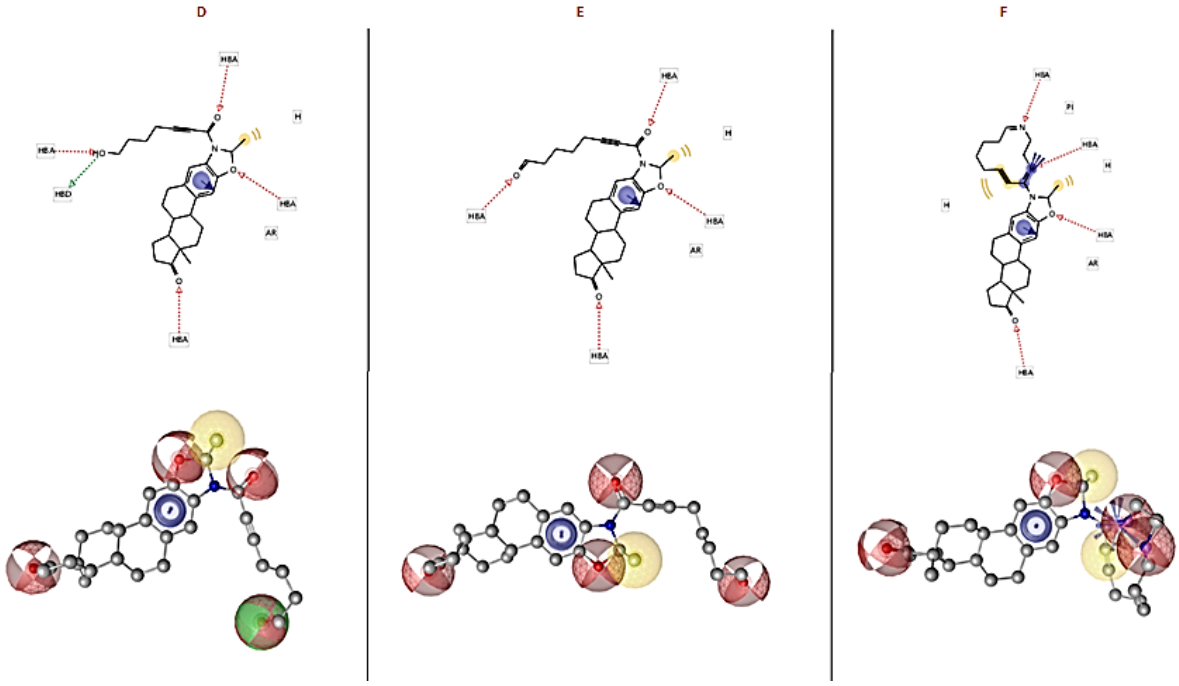

Figure 5 – Theorethical pharmacophore from both compounds **5** (D), **6** (E) and **7** (F) using the LigandScout software. The model involves a methyl group (yellow) hydrogen bond acceptors (HBA, red) and hydrogen bond donor (HBD, green).

Evaluation of interaction between compounds 2-7 with both COX1-1 and COX-2

Since several years ago, some theoretical models have been used to predict the interaction of some drugs with protein or enzymes [32]. Therefore, in this study was carried out a theoretical analysis on interaction of compounds **7** with both COX1-1 (2OYU) and COX-2 (3LN1) using a Docking model [15] using both indomethacin and Rofecoxib as controls.

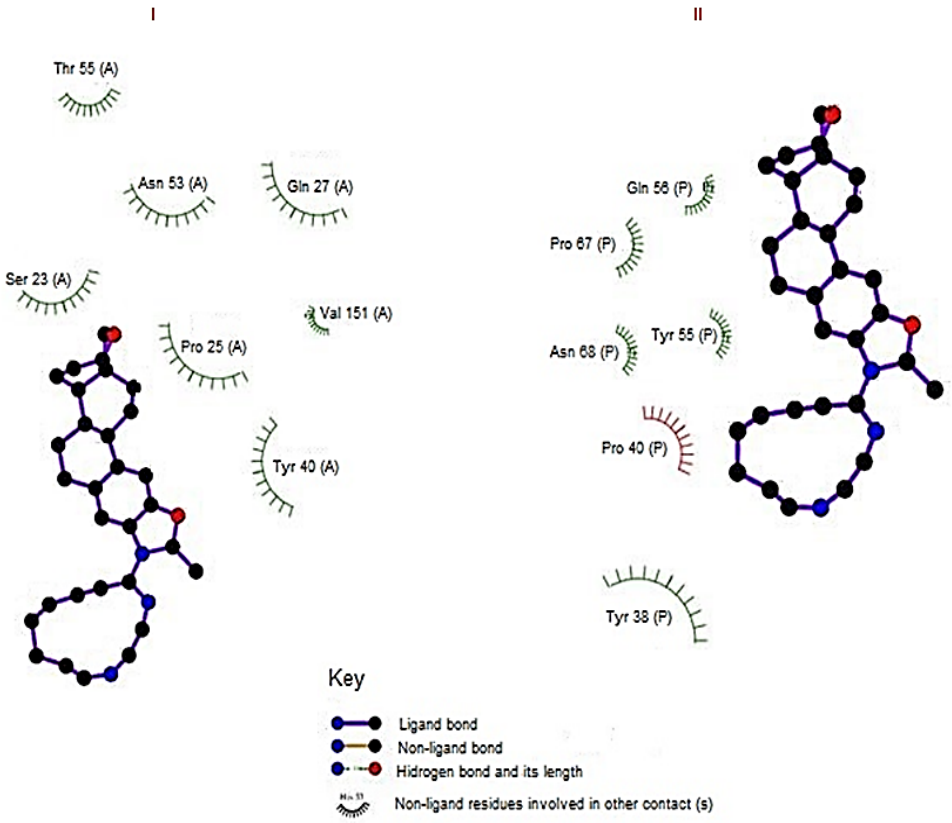

Figure 6 – The scheme shows the binding sites of compound **7** with some aminoacid residues involved on both COX 1 (2oyu [I]) and COX 2 (3LN1 [II]) enzymes.
The visualization was carried out using DockingServer software

The results showed the interaction of both indomethacin and compound **7** were only in two types of amino acid residues involved in the surface of the 2OYU protein, such as Tyr_{55}, Pro_{67}. Other theoretical data showed a similar interaction between both Rofecoxib and compound **7** with some Ser23, Pro25, GLn_{27}, Tyr_{40}, Asn_{53} amino acid residues of COX-2 (3LN1). All these data suggest that there are differences between the interaction of compound 7 with both COX 1 and COX 2 compared with the bound of indomethacin and rofecoxib with this type of enzymes.

Table 4 – Residue Aminoacids involved in the interaction between both steroid-oxazolone derivative (compound 7) and Indometacin with COX-1 enzyme (2oyu)

Steroid-oxazolone derivative	Tyr_{38} Pro_{40} Tyr_{55} Gln_{156} Pro_{67} Asn_{68}
Indometacin	Pro_{35} Arg_{54} Tyr_{55} Pro_{67}

Table 5 – Residue Aminoacids involved in the interaction between both steroid-oxazolone derivative (compound 7) and Rofecoxib with COX-2 enzyme (3LN1)

Compound	Aminoacid residues
Steroid-oxazolone derivative	Ser_{23} Pro_{25} Gln_{27} Tyr_{40} Asn_{53} Thr_{55} Val_{151}
Rofecoxib	Ser_{23} Pro_{25} Gln_{27} Tyr_{40} Asn_{53} Lys_{152}

Thermodynamic parameters

Analyzing the aforementioned data and other types of reports which suggest that the drug-protein interaction could involve other types of intramolecular interactions, in study a theoretical ass was carried out to evaluate some thermodynamic factors involved in the interaction of quinalizarin and the compound **7** with both 2OYU and 3LN1 proteins such as 1) free energy of binding which determinate the energy value that require a molecule to interact with a protein in a water environment. 2) Electrostatic energy that is the product of electrical charge and electrostatic potential, which are involved in the ligand-protein system; 3) total intermolecular energy and 4) Van der Waals (vdW) + hydrogen bond (Hbond) + desolvation energy (Desolv. Energy; which have an influence on the movement of water molecules into or out of the ligand-protein system) using a theoretical model [15].

The results showed that there are differences in the thermodynamic parameters of compound **7** compared to both indomethacin and rofecoxib. This phenomenon suggests that these differences could be translated as a higher inhibition of biological activity of COX 1 (2OYU) in the presence of compound **7** in comparison with indomethacin. In addition, a lower inhibition of COX 2 (3LN1) with the compound 7 compared with rofecoxib.

Table 6 – Thermodynamic parameters involve in the interaction of both steroid-oxazolone derivative and Indometacin with COX-1 enzyme (2oyu)

Compound	Est. Free Energy of Binding (kcal/mol)	Inhibition Constant, Ki (μM)	vdW + Hbond + desolv Energy (kcal/mol)	Electrostatic Energy (kcal/mol)	Total Intermol. Energy (kcal/mol)	Interact Surface
steroid-oxazolone derivative (4)	-6.47	18.01	-6.81	0.04	-6.77	628.614
Indometacin	-5.32	126.53	-6.24	-0.19	-6.43	576.698

Table 7 – Thermodynamic parameters involve in the interaction of both steroid-oxazolone derivative and Rofecoxib with COX-2 enzyme (3LN1)

Compound	Est. Free Energy of Binding (kcal/mol)	Inhibition Constant, Ki (μM)	vdW + Hbond + desolv Energy (kcal/mol)	Electrostatic Energy (kcal/mol)	Total Intermol. Energy (kcal/mol)	Interact Surface
steroid-oxazolone derivative (4)	-6.15	30.81	-6.36	0.09	-6.45	673.193
Rofecoxib	-3.78	1.69	-4.90	0.18	-4.73	557.621

Conclusions

These data suggest that the steroid-oxazolone derivative could be a good candidate as COX-inhibitor translated as a possible drug for treatment of pain.

References

1. Philippe J., Miller D. (2009) Selective and non-selective non-steroidal anti-inflammatory drugs and the risk of acute kidney injury. *Pharm Drug Saf.* Vol. 18, pp. 923-931.

2. Kearney P., Baigent C., Godwin J., Halls H., Emberson J, Patrono C. (2006) Do selective cyclooxygenase-2 inhibitors and traditional non-steroidal anti-inflammatory drugs increase the risk of atherothrombosis? Meta-analysis of randomised trials. *Bmj*. Vol. *332,* no. 7553, pp. 1302-1308.

3. Amadio P., Cummings D., Amadio P. (1993) Nonsteroidalanti-inflammatory drugs. Postgrad Med. Vol. 93, no. 4, pp. 73-88.

4. Simon L., Milis J. (1980) Non-steroidal anti-inflammatory drugs. *N Engl J Med.* Vol. 302, pp. 1237–1243.

5. Wallace C. (1998) The use of methotrexate in childhood rheu-matoid diseases. *Arthritis. Rheum.* Vol. 41, no. 3, pp. 381–391.

6. Halis S., Berna D., Yalçin K. (2007) Anti-inflammatory and side effects of cyclooxygenase inhibitors. *Pharmacol rep*. Vol. 59, no. 3, pp. 247-258.

7. Ahmadi A., Khalili M., Hajikhani R., Naserbakht M. (2011) New morpholine analogues of phencyclidine: Chemical synthesis and pain perception in rats. *Pharm Biochem Behavior.* Vol. *98*, no. 2, pp. 227-233.

8. Yogeeswari P., Menon N., Semwal A., Arjun M., Sriram D. (2011) Discovery of molecules for the treatment of neuropathic pain: Synthesis, antiallodynic and antihyperalgesic activities of 5-(4-nitrophenyl) furoic-2-acid hydrazones. *Eur j med Chem.* Vol. *46*, no.7, pp. 2964-2970.

9. Amir M., Kumar H., Khan S. (2008) Synthesis and pharmacological evaluation of pyrazoline derivatives as new anti-inflammatory and analgesic agents. *Bioorg Med Chem Lett.* Vol. *18*, no. 3, pp. 918-922.

10. Elisabetta T., Elisabetta B., Silvia D., Fulvio G., Maria N. R., Serena S., Cristina B., Carla G., Rosanna M. (2004) Design, Synthesis, and Preliminary Pharmacological Evaluation of 4-Aminopiperidine Derivatives as N-Type Calcium Channel Blockers Active on Pain and Neuropathic Pain. *J Med Chem.* Vol. *47,* no. 24, pp. 6070–6080.

11. Cleves A., Jain, A. (2015). Chemical and protein structural basis for biological crosstalk between PPARα and COX enzymes. *J Computer-aided Mol Des*. Vol. *29*, no. 2, pp.101-112.

12. Figueroa V. L., Diaz C. F., Rosas N. M., Mateu A. V., Montano T. E., Hau H. L., Alfonso J. A. (2019) Design and synthesis of two steroid derivatives from 2-nitroestrone and theoretical evaluation of their interaction with BRCA-1. *Asian J Green Chem.* Vol. *3*, no. 2, pp. 125-287

13. Zakharian T., Coon S. (2001) Evaluation of Spartan semi-empirical molecular modeling software for calculations of molecules on surfaces: CO adsorption on Ni (111). *Comput Chem.* Vol. *25, no*. 2, pp. 135-144.

14. Borišek J., Pintar S., Ogrizek M., Grdadolnik S. G., Hodnik V., Turk D., Novič M. (2018). Discovery of (phenylureido) piperidinyl benzamides as prospective inhibitors of bacterial autolysin E from Staphylococcus aureus. *J enz inh med chem. Vol. 33*, no. 1, pp. 1239-1247.

15. Lin Y. F., Cheng C. W., Shih C. S., Hwang J. K., Yu C. S., Lu C. H. (2016). MIB: metal ion-binding site prediction and docking server. *J chem inf mod.* Vol. *56, no.* 12, pp. 2287-2291.

16. Istrate F., Buzas A., Jurberg D. I., Odabachian Y., Gagosz F. (2008) Synthesis of functionalized oxazolones by a sequence of Cu (II)-and Au (I)-catalyzed transformations. *Org lett.* Vol. *10*, no. 5, pp. 925-928.

17. Cleaver C., Pratt B. (1995) Synthesis of 2, 2'-Bis-[5 (4H)-oxazolones]. *J Am Chem Soc.* Vol. *77*, no. 6, pp. 1544-1546.

18. Yamashita M., Sang H. L., Koch G., Zimmermann J., Clapham B., Janda K. (2005) Solid-phase synthesis of oxazolones and other heterocycles via Wang resin-bound diazocarbonyls. *Tetrahedron lett.* Vol. *46*, no. 33, pp. 5495-5498.

19. Mazurkiewicz R., Pierwocha A. (1996) 4-Phosphoranylidene-5 (4H)-oxazolones-A novel synthesis and properties. *Monatsh Chem.* Vol. *127*, no. 2, pp. 219-225.

[19] Huang H., He G., Zhu G., Zhu X., Qiu S., Zhu H. (2015) Palladium-Catalyzed Intramolecular Cyclization of Ynamides: Synthesis of 4-Halo-oxazolones. *J org chem.* Vol. *80,* no. 7, pp. 3480-3487.

20. Beck J. (1978) Nucleophilic displacement of aromatic nitro groups. *Tetrahedron*. Vol. 34, no. 14, pp. 2057-2068.

21 Takekoshi T., Wirth J., Heath D., Kochanowski J., Webber M. (1980) Polymer syntheses via aromatic nitro displacement reaction. *J Polymer Sci*. Vol. 18, no. 10, pp. 3069-3080.

22. Hiegel G., Hogenauer T., Lewis J. (2005) Preparation of N-Chloroamides Using Trichloroisocyanuric Acid *Syn Com*. Vol. 35, pp. 2099-2105.

23. Katritzky A., Majumder S., Jain R. (2003) Microwave assisted N-chlorination of secondary amides. *Arkivoc*. Vol. xii, pp. 74-79.

24. Harte A., Gunnlaugsson T. (2006) Synthesis of α-chloroamides in water. *Tetrahedron Lett*. Vol. 47, no. 35, pp. 6321-6324.

25. Hu Y., Xin X., Wan B. (2015) Cyclization reactions of propargylic amides: mild access to N-heterocycles. *Tetrahedron lett.* Vol. *56*, no. 1, pp. 32-52.

26. Xiao Y. B., Wen W. Z., Qian L., Bi J. L. (2018) Highly Enantioselective Synthesis of Propargyl Amides through Rh-Catalyzed Asymmetric Hydroalkynylation of Enamides: Scope, Mechanism, and Origin of Selectivity. *J Am Chem Soc.* Vol. 140, no. 1, pp. 506–514.

27. Figueroa V. L., Díaz C. F., García C. E., Pool G.E., Rosas N. M., López R. M., Vera E. I. (2018) Design and synthesis of two triazonine-carbaldehyde derivatives using several chemical tools. *J Saudi Chem Soc.* Vol. *22*, no.2, pp. 183-197.

28. Figueroa V. L., Diaz C. F., Lopez R. M., Garcia C. E. (2011) Synthesis of pregnenolone–danazol-ethylendiamine conjugate: relationship between descriptors log P, π, Rm, and Vm and its antibacterial activity in S. aureus and V. cholerae. *Med Chem Res.* Vol. *20*, no. 7, pp. 847-853.

29. Bandgar, B., Gawande, S., Bodade, R., Gawande, N., Khobragade, C. (2009). Synthesis and biological evaluation of a novel series of pyrazole chalcones as anti-inflammatory, antioxidant and antimicrobial agents. *Bioorg Med Chem*. Vol. *17*, no. 24, pp. 8168-8173.

30. Pajouhesh, H., Lenz, G. (2005). Medicinal chemical properties of successful central nervous system drugs. *NeuroRx*, Vol. *2*, no. 4, pp. 541-553.

31. Kitchen, D., Decornez, H., Furr, J., Bajorath, J. (2004). Docking and scoring in virtual screening for drug discovery: methods and applications. *Nature Rev Drug Discov*. Vol. *3*, no. 11, pp. 935.

IRSTI 31.25.17; 31.17.29

[1,2*]S. Turganbay, [3]S.B. Aidarova, G. [4]Turganbay,
[1]Ye. Tileuberdi, [5]Sheng-Li Chen

[1]Al-Farabi Kazakh National University, Almaty, Kazakhstan
[2]JSC "Scientific Center for anti-infectious drugs", Almaty, Kazakhstan
[3]Kazakh National Technical University, Almaty, Kazakhstan
[4]Kazakh National Agrarian University, Almaty, Kazakhstan
[5]China University of Petroleum-Beijing, Beijing, China
*e-mail: turganbay.s@gmail.com

Synthesis and characterization of sulfur nanoparticles with WSP/surfactants mixtures

Abstract: Sulfur nanoparticles display unique physical and chemical feature because of effects such as the quantum size effect, mini size effect, surface effect, and macro-quantum tunnel effect. Therefore, sulfur nanoparticles would present higher efficacies such as removal of heavy metals, radical-scavenging, antimicrobial activity, antioxidant and antitumor activities. They have been using as a fungicide product in agriculture and medicine; to obtain sulfur fertilizers and cosmetics industries, as well as in obtaining nanocomposite lithium batteries; to form stable carbon chains such as C_3S and C_5S for obtaining hybrid materials with useful properties for gas sensor and catalytic applications. This work presents the results of obtaining sulfur nanoparticles, which can be used in agriculture as a fungicide treatment. Sulfur nanoparticles were obtained by modifying the surface of sulfur by various water-soluble polyelectrolyte (WSP)/surfactant mixtures including NaCMC/CTAB, PDADMAC/SDBS, NaCMC/Triton X-100 (TX-100). The size and the structure of sulfur nanoparticles were determined by methods as LSA, XRD, SEM. It is shown that the nanoparticles have a sulfur monoclinic α-form, and their average size is in the range of 100-300 nm. The received products can be considered as perspective forms of application in agriculture and medicine.

Key words: sulfur nanoparticles, surfactant, aqueous surfactant solution, water-soluble polyelectrolytes adsorption, surface tension.

Introduction

Sulfur is the tenth most common element by mass in the universe and the fifth most common on Earth. Though sometimes found in pure, native form, sulfur on Earth usually occurs as sulfide and sulfate minerals. Chemical and, biologically active element, It displays three allotropic forms: orthorhombic, monoclinic and amorphous. The orthorhombic form is the most stable form of sulfur. it is widely used in many fields, such as the production of sulfuric acid, chemistry fiber, nitrogenous fertilizer, plastics, antimicrobial agents and rubber, pharmaceutical industry, and bioleaching processes, pulp and paper industries, and different other agrochemical industries [1-2]. The sulfur nanoparticles have many practical important applications such as synthesis of nanocomposites for lithium batteries [3-6], fungicides in agriculture [7], synthesis and modification of carbon nanostructures [8], synthesis of sulfur nanowires with carbon to form hybrid materials with useful properties for gas sensor and catalytic applications [9], in road construction, as a bitumen modifier [10], in the agricultural field, sulfur is used as a fungicide against the apple scab disease under colder conditions [11], The smaller of particle size, the larger surface area of sulfur particles, so there will be more efficiency in an application in medicine, cosmetics, agriculture, etc. Therefore, the synthesis of sulfur nanoparticles is currently an important issue.

Different methods were used for nanosize particle synthesis, among those: the microemulsion method is one of the very important methods to control the particle size. Nevertheless, microemulsion itself is a very complicated system, composed of oil, surfactant, co-surfactant and aqueous phases

with the specific compositions. The main disadvantages of the microemulsion method are the difficulties in process scale-up, separation and purification of the particles from the microemulsion, and finally, this method is consumed huge amounts of surfactants. Despite many exciting applications, there are only a few recent kinds of literature available on the synthesis of sulfur nanoparticles by different investigators [12-16] in both aqueous and microemulsion phase by different routes. Deshpande et al. [12] have synthesized sulfur nanoparticles from H_2S gas by using the biodegradable iron chelate catalyst in reverse microemulsion technique. They found a-sulfur or rhombic sulfur of average particle size 10 nm with a particle size range of 5-15 nm. They have also studied the antimicrobial activity of sulfur nanoparticles and shows it is very much effective, especially when the particle size is low. Guo et al. [13] have prepared sulfur nanoparticles from sodium polysulfide by acid catalysis in the reverse microemulsion technique. They found monoclinic or b-sulfur with an average particle size of around 20 nm. Xie et al. [14] have prepared nanosized sulfur particles from sublimed sulfur. They added aqueous cysteine solution dropwise on a saturated alcoholic sulfur solution with constant ultrasonic treatment and cysteine – nano-sulfur sol was obtained. S.Roy Choudhury et al. [15] get 20-50 nm particles of sulfur interaction sodium polysulfide and ammonium polysulfide with formic acid and further stabilization of the sulfur polyethyleneglycol-400. The same authors established the biological activity of the synthesized nanoparticles of sulfur. By the research of Rajib et al. [16], sulfur obtained by conducting the reaction of sodium thiosulfate interaction with various inorganic and organic acids. Subsequently, the same authors synthesized sulfur particles with particle sizes in the range of 30-60 and 200-300 nm, by modifying the sulfur with various surfactants.

However, despite the existence of different ways to get sulfur nanoparticles, they all have drawbacks. Namely: the multi-stage process, the use of various inorganic and organic acids, which requires multiple-treatment, significant harm to the human body when using poisonous gases, such as hydrogen sulfide.

In This study presents the method of obtaining sulfur nanoparticles by mechanical and ultrasonic grinding, Sulfur nanoparticles were obtained by modifying the surface of sulfur by various mixtures water-soluble polyelectrolytes (WSP)/surfactants including NaCMC/CTAB, PDADMAC/SDBS), NaCMC/TX-100, The size, surface tension at the water/air and the structure of sulfur nanoparticles were determined by methods as LSA, DCAT-21-Date physics, XRD, SEM.

Materials and methods

Crystalline sulfur production of LLP "Tengiz Shevroil" (Kazakhstan), cetyltrimethylammonium bromide (CTAB) with a purity of 99 % of company Loba Chemie Pvt. Ltd., (India), Triton X-100 (TX-100) and sodium dodecylbenzene sulfonate (SDBS) with a purity of 99% of company "Unilever Research Laboratory Port Sunlight (England), sodium carboxymethyl cellulose (NaCMC), polydiallyldimethylammonium chloride (PDADMAC) with 99% purity from Tianjin Heowns Biochem. LLC., (China). Were used as materials Bettersize-2000 (China), scanning electron microscope (SEM)-Auriga cross-beam, infrared spectroscopy, Colloid mill company Fritsch Pulverisettel (Germany). Ultra dispersant KQ-600GKDV (China) Surface tensiometer (DCAT-21, Date physics, Germany).

Synthesis of sulfur nanoparticles. Preparation of sulfur nanopowder was carried out in two stages: In the first stage, 10 g of crystalline sulfur was milled in a colloid mill Fritsch Pulverisettel (Germany) for 30 min. Size of the sulfur powder was 10-100 microns. In the second stage, the milled sulfur powders were dispersed into 100 ml of WSP/surfactants mixtures solution (where the concentration of mixtures NaCMC/CTAB and PDADMAC/SDBS was 1mM and the concentration of NaCMC/TX-100 was 0.1 mM) with an ultrasonic disperser KQ-600GKDV (China), Then the crushed sulfur was dried in the device Christ ALPHA 1-1 LD plus (Germany) [17].

The interfacial tension and critical concentration of WSP/surfactant mixtures at the water/air interface measured by the method of Vilgemi, using surface tensiometer (DCAT-21, Date physics, Germany) at room temperature (28 ±0.5 0C).

Characterization of sulfur nanoparticles. Crystal structure of sulfur nanoparticles was characterized by X-ray diffraction (XRD) using Philips (230 v, 65 KVA) X-ray diffractometer with the scanning rate of 0.0020 /s in the 2θ range from 100 to 500. Particle size measurement was carried out by laser size analyzing (LSA) using Bettersize-2000 laser particle size analyzer. The shape of sulfur nanoparticles was observed with a scanning electron microscope (SEM).

Results and discussion

Effect of WSP/surfactant mixtures concentration on the surface tension. The tensiometric plot of

CTAB, SDBS, and TX-100 shows a sharp decrease in surface tension with a slight increase in [CTAB, SDBS and TX-100] up to cac, then it approximately keeps constant giving 'first plateau' until critical saturation concentration csc. A further decrease in surface tension is observed up to cmc, beyond which they further stabilize, giving 'second plateau' due to the formation of free micelles in the solution [18-19]. The plot of CTAB (Figure 1 A-1), SDBS (Figure 2 B-1) and TX-100 (Figure 3 C-1) in pure water shows only one critical concentration (i.e., at cac), while in the presence of NaCMC, PDADMAC three critical concentrations (first at cac, second at csc and third at cmc) are observed. This indicates the influence of NaCMC, PDADMAC in the solution and theirs association with the cationic surfactant CTAB, anionic surfactant SDBS and nonionic surfactant TX-100. csc represents the critical saturation concentration of the surfactant (Figure 1 A-2, Figure 2 B-2, Figure 3 C-2) when all the binding sites on polyelectrolyte are saturated due to adsorption of CTAB, SDBS and TX-100 over polymer backbone. During this association process (at first plateau), the surface tension of the solution is almost constant as the added surfactant get associated with the water-soluble polyelectrolyte molecules in the solution and surfactant free molecules are not available to affect the surface properties of the solution. When all the binding sites on polyelectrolyte molecules are saturated with surfactant molecules, surface tension starts decreasing with increase in CTAB, SDBS and TX-100 concentration further till a certain concentration, termed as critical micelle concentration (cmc) is reached. At cmc, the micellization of polymer bound surfactant occurs resulting in the formation of insoluble WSP/surfactant mixtures. This suggests that the WSP/surfactant mixtures also undergoes a two-stage interaction process where the surfactant binds to the polyelectrolyte due to electrostatic attraction; thereafter, the micellization of polymer-bound surfactant molecules occurs as reported in the literature [20, 21]. As experimental results (Figure 1,2,3) show the minimum surface tension values (γCMC) for NaCMC(0.01%)/TX-100(0.1mM),; PDADMAC (0.01%)/SDBS(1 mM) and NaCMC(0.01%)/CTAB(1 mM) are 40.35, 45.7 and 42.8 Nm/m, respectively.

Effect of the concentration of WSP/ surfactants mixtures on the particle size of sulfur. It is well known that WSP/surfactant mixtures adsorbed on the surface of sulfur microcrystals, reduce the surface tension at the solid/liquid interface. This phenomenon is a good illustration of the Rehbinder effect**.** Theoretically, the WSP/surfactant mixtures adsorbed on the pores of sulfur microcrystals, facilitate their destruction. Firstly the WSP/surfactant mixtures adsorbed in the pores which creates a two-dimensional pressure. Secondly, it contributes to the weakening of intermolecular interactions, to reduce the formation of aggregates, therefore, increase the number of nanoparticles (Fig. 4). The Feature of WSP/surfactant mixtures are the presence of polar (hydrophilic) and non-polar (hydrophobic) groups. Simultaneous adsorption of non-polar groups on the surface of the solid phase and the interaction of polar groups with the hydrophilic medium determines the specific properties of surfactants.

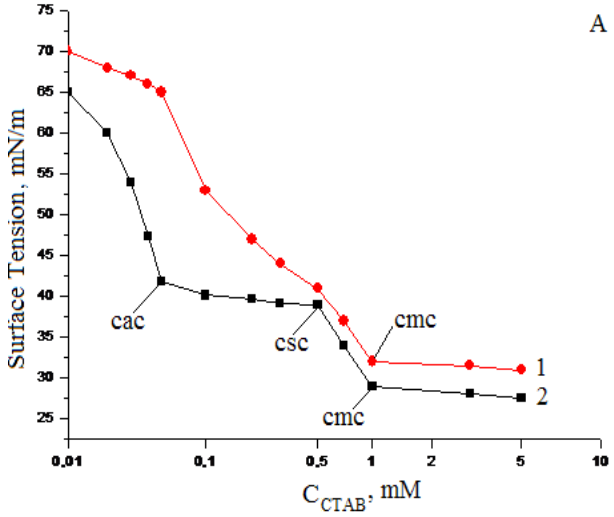

Figure 1 – Variation of surface tension (γ) with CTAB concentration in pure water (1), and 0.01 % NaCMC aqueous medium (2) at 25 ^{0}c

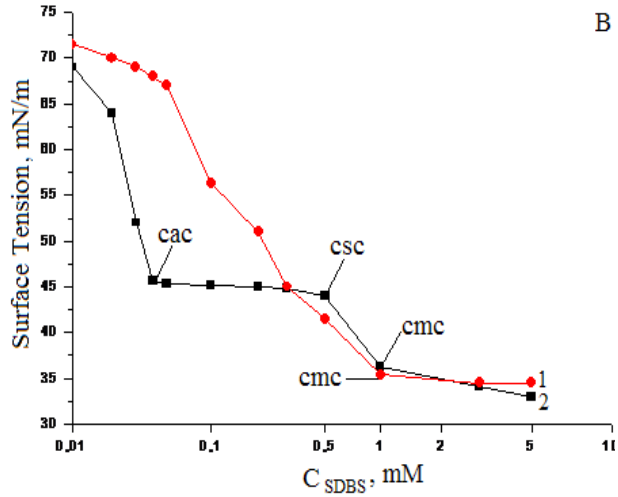

Figure 2 – Variation of surface tension (γ) with SDBS concentration in pure water (1), and 0.01 % PDADMAC aqueous medium (2) at 25 ^{0}c

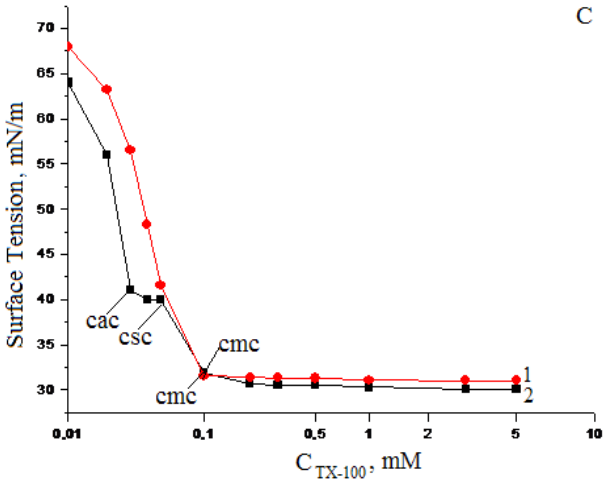

Figure 3 – Variation of surface tension (γ) with TX-100 concentration in pure water (1), and 0.01 % NaCMC aqueous medium (2) at 25 ^{0}c

However, the 300-500 nm of sulfur particles do not form a stable suspension. Apparently, this is a consequence of the predominance of hydrophobic interactions in the highly polar aqueous environment. Therefore, even with stirring sulfur aggregates are not destroyed. Mechanical effects (intense mixing) can lead to an imbalance of the adsorbed particles on the surface of colloidal stabilizers (modifiers). Thus destabilized particles are able to interact with each other at distance of intermolecular forces and may converge by the forces of gravity. Consequently, to obtain a stable suspension of sulfur, you should use the smallest particle size.

The last time in the industry is widely used by water-soluble polyelectrolyte/surfactant mixtures as additives. When we add WSP to a particular ionic surfactant solution, it has been observed that surface tension and contact angle values are reduced. This happens because the presence of WSP decreases the repulsion between the head groups. As the repulsion decrease, the cmc decrease, too. So the addition of WSP can give a more economical way of using the surfactants for decreasing the contact angle, particle size and altering the wetting property. [22-23]. WSP/surfactant composition influence to reduce sulfur particles through adsorption on the crystalline sulfur pores. In the study, 0.01% of the water-soluble polyelectrolyte solution was used. It is proved in the literature [19] that the better adsorb on the substance surface due to polyelectrolytes of this concentration allow reducing the surface tension of the water. In this reason, the use of WSO/ surfactant mixtures reduces sulfur particle size. this work was use mixtures (NaCMC (0.01%) /CTAB, PDADMAC (0.01%)/SDBS, NaCMC(0.01%)/ TX-100) Fig. 5 shows the Effect of the concentration of WSP/surfactant mixtures on the particle size of

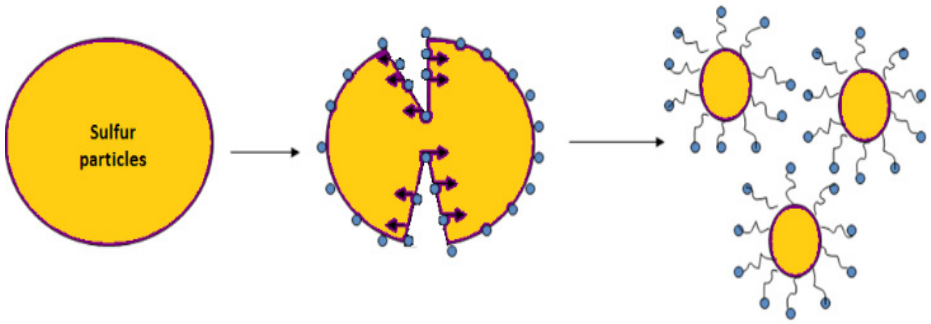

Figure 4 – Adsorption of WSP/surfactant mixtures solution on the pores of the microcrystals of sulfur

sulfur. Experimental results showed that with the increase of surfactant concentration, decrease sulfur particle size. At the CMC, there are minimum value of sulfur particle size at 0.035, 0.04, 0.05 mM, concentration of NaCMC/TX-100, PDADMAC/SDBS and NaCMC/CTAB respectively, sulfur particle sizes are in the range of 200-350 nm.

Figure 6 shows comparisons of particle size distribution among three of WSP/surfactant mixtures used in the study. NaCMC/TX-100, PDADMAC/ SDBS, and NaCMC/CTAB have a different size distribution, TX-100 having little sharp distribution than the other two WSP/surfactant mixtures but the change is not very significant.

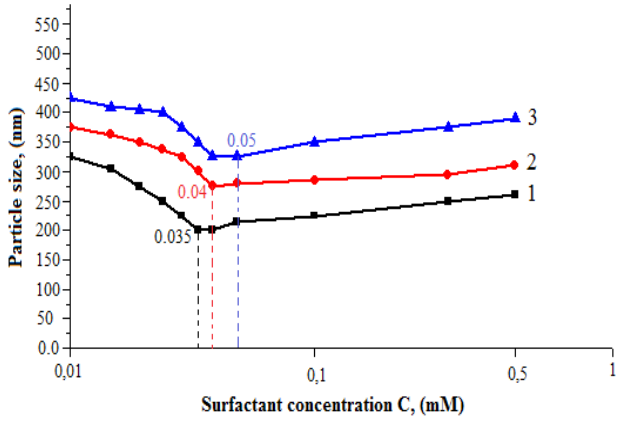

1- NaCMC(0.01%)/TX-100;2-PDADMAC(0.01%)/SDBS,
3- NaCMC (0.01%)/ CTAB

Figure 5 – Effect of concentration
of WSP/ surfactant mixtures on the sulfur particle size

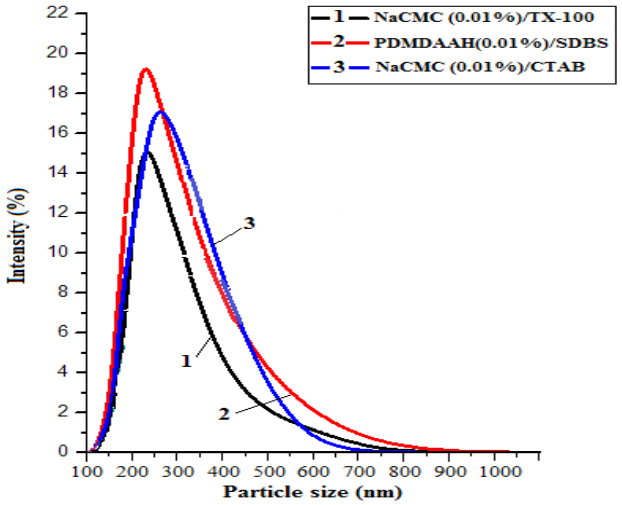

Figure 6 – Differential curves
of sulfur particles in of mixtures WSP / surfactants

XRD and SEM analysis of the Sulfur particles. Determination of particle diameter (D) was done by the XRD analysis using Debye-Scherrer formula,

$$D = \frac{\kappa\lambda}{\beta cos\theta}$$

Where D crystallite size, *k* – Scherrer constant usually taken as 0.89, λ – wavelength of the X-ray radiation (0.154056 nm for Cu Kα), and α is the full width at the half maximum of the diffraction peak measured at 2θ the position and intensities of the diffraction peaks of all samples were compared with standard α-sulfur particle diffraction pattern (24).

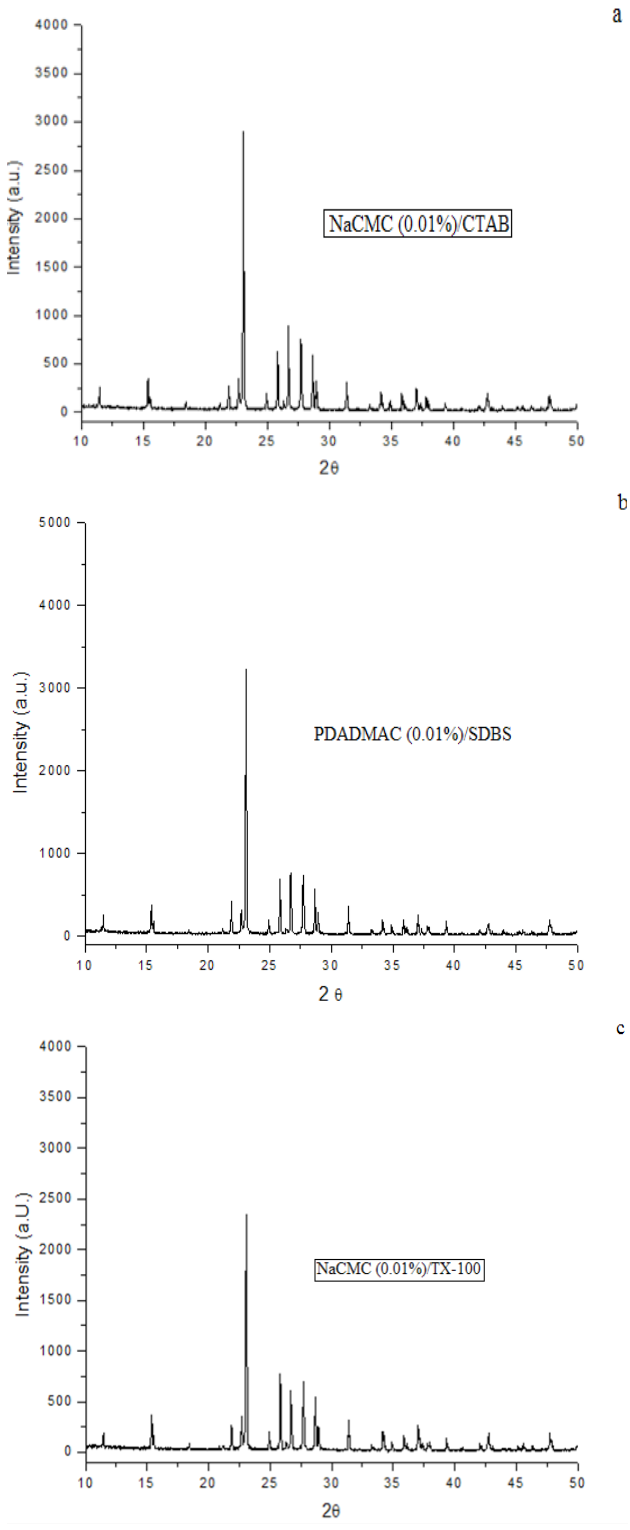

Figure 7 – XRD pattern of sulfur nanoparticles:
surfactant and mixture WSP/surfactant media

The XRD analysis of sulfur nanoparticles synthesized in WSP/surfactant mixtures are shown in Figure 5, which are a,b and c, the XRD pattern of sulfur particles indifferent in the presence of WSP/surfactant mixtures media, respectively. The positions and intensities of the diffraction peaks have the same means with the literature values for orthorhombic or a-phase sulfur on S_8 structure (74-1465 from JCPDS PDF Number). The XRD samples are prepared by successive washing by fresh water, so it was got an only pure sulfur peak.

Analysis by scanning electron microscope (SEM). Figs. 8 A-B show the SEM images of sulfur particles synthesize by mixtures of WSP/Surfactant (NaCMC/CTAB, PDADMAC/SDBS) (A, B images) have had uni-α-form, too. From the figure, it is clear that the sulfur particles are the almost spherical shape and uniform size.

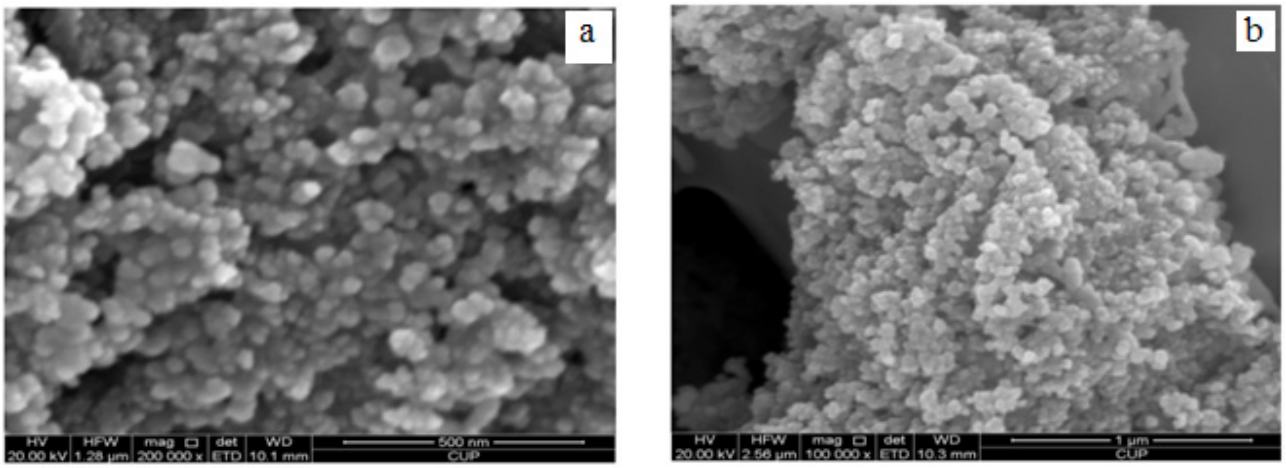

a– NaCMC/CTAB, b-PDMDAAX/SDBS

Figure 8 – SEM micrographs of sulfur nanoparticles

Conclusions

Thus, the experimental results showed the minimum surface tension values (γCMC) for NaCMC(0.01%)/TX-100(0.1mM),; PDADMAC (0.01%)/SDBS(1 mM) and NaCMC(0.01%)/CTAB(1 mM) are 40.35, 45.7 and 42.8 Nm/m, respectively. The use of mixtures NaCMC/CTAB, PDADMAC/SDBS and NaCMC/TX-100 as modifiers lead to a lot reduction in the size of sulfur particles were obtained. There is the minimum value of the size of sulfur particle at concentration of 0.035, 0.04 and 0.05 mM of NaCMC/TX-100, PDADMAC/SDBS and NaCMC/CTAB with sulfur particle sizes in the range of 200-350 nm. The size, crystal structure and morphology of sulfur nanoparticles were determined by methods of laser size analyzing (LSA), X-ray diffraction (XRD) and scanning electron microscope (SEM). It was found that the nanoparticles had a sulfur monoclinic α-form structures, and their average size was in the range of 100-300 nm.

References

1. J.A. Ober (2003) *Materials Flow of Sulfur: US Geological Survey Open-File Report*, 02-298.

2. X. Yu, J. Xie, J. Yang, K. Wang, (2004) *J. Power Sources,* P.132 181.

3. X. Yu, J. Xie, J. Yang, K. Wang, (2004) *J. Power Sources*, P.132 181.

4. W. Zheng, Y.W. Liu, X.G. Hu, C.F. Zhang, (2006) *Electrochim. Acta*, 51, P.1330.

5. Z. Yong, Z. Wei, Z. Ping, W. Lizhen, X. Tongchi, H. Xinguo, Y. Zhenxing, J. (2007) Wuhan Univ. Technol. – Mater. Sci. Ed., 22 234.

6. T. Kobayashi, Y. Imade, D. Shishihara, K. Homma, M. Nagao, R. Watanabe, T. Yokoi, A. Yamada, R. Kanno, T. Tatsumi (2008) *J. Power Sources,* 182, P.621.

7. Z. Yong, Z. Wei, Z. Ping, W. Lizhen, X. Tongchi, H. Xinguo, Y. Zhenxing, J. (2007) Wuhan Univ. Technol. – Mater. Sci. Ed., 22, P.234.

8. W. Zheng, Y.W. Liu, X.G. Hu, C.F. Zhang (2006) *Electrochim. Acta*, 51, P.1330.

9. P. Santiago, E. Carvajal, D.M. Mendoza, L. Rendon (2006) *Microsc. Microanal*., 12, P.690.

10. Tileuberdi Y., Akkazyn Y.A., Ongarbayev Y.K., Imanbayev Y.I., Mansurov Z.A. (2018) *Materials Science and Engineering*, Vol. 323, Issue 1, Article number 012004. doi:10.1088/1757-899X/323/1/012004.

11. M.A. Ellis, D.C. Ferree, R.C. Funt, L.V. Madden (1998) *Plant Dis.,* 82, P.428.

12. A.S. Deshpande, R.B. Khomane, B.K. Vaidya, R.M. Joshi, A.S. Harle, B.D. Kulkarni (2008) *Nanoscale Res. Lett*., 3, P.221.

13. Y. Guo, J. Zhao, S. Yang, K. Yu, Z. Wang, H. Zhang (2006) *Powder Technol*., 162, P.83.

14. X.Y. Xie, W.J. Zheng, Y. Bai, J. Liu (2009) *Mater. Lett*., 63, P.1374.

15. R.G. Chaudhuri, S. Paria (2009) *J. Colloid Interface Sci*., 337, P.555.

16. Rajib Ghosh Chaudhuri, Santanu Paria (2010) *J. Colloid Interface Sci*., 343, P.439-446.

17. Turganbay Seitzhan, S. B. Aidarova, Neila Bekturganova, Saltanat S. Kumargalieva (2013) *Adv. Mater. Res*., V. 785–786, P. 475.

18. Anis A. Ansari,M. Kamil, Kabir-ud-Din (2013) *Journal of Petroleum Science Research*, Volume 2, Issue 1, P.264.

19. C. Wang and K. C. Tam (2002), *Langmuir*, 18, P. 6484-6490.

20. T. Chakraborty, I. Chakraborty and S. Ghosh (2006), *Langmuir*, 22, P. 9905-9913.

21. N. Sardar, M. Kamil and Kabir-ud-Din (2012), *Ind. Eng.Chem. Res*., 51, P. 1227−1235.

22. Fridrihsberg R.A. (2010) Course of Colloid Chemistry, Moscow. P. 315.

23. S. Turganbay, S.B.Aidarova, N.E. Bekturganova, Chen ShengLi (2012), *Eurasian Chemico-Technological Journal*, 14(4), P.313-319

24. Joint Commission on Powder Diffraction Standards. Powder diffraction file, Inorganic phase. International center for diffraction data. PA, USA. JCPDS No. 08247, p. 410

IRSTI 31.21.15: 31.21.29

[1]A.A. Omarova, [1,*]L.R. Sassykova, [2]S. Sendilvelan, [1]M.I. Tulepov

[1]Faculty of Chemistry and Chemical Technology, al-Farabi Kazakh National University,
71, al-Farabi ave., 050040, Almaty, Kazakhstan
[2]Department of Mechanical Engineering, Dr. M.G.R. Educational and Research Institute,
Chennai 600095, India
*e-mail: larissa.rav@mail.ru

Processing of model n-alcanes and diesel fraction on the catalyst La-Zn-Mn / Al_2O_3 + ZSM

Abstract: Catalytic cracking is one of the most common processes in the oil refining industry. It contributes to a significant deepening of the oil refining degree and it is used for the production of high-octane gasolines and diesel fuels from heavy oil fractions, as well as for the production of petrochemical synthesis products. One of the promising methods for the regulation of catalytic properties is the introduction of modifying additives into the catalytic composition. In this work the catalysts on the base of Al_2O_3, ZSM catalyst modified by introduction of additives of manganese, lanthanum and zinc have been prepared and studied during the hydrogen-free conversion of hexane, tetradecane and the diesel fraction. The structure and state of the catalyst's active centers have been studied using a complex of physico-chemical methods (TEM, XPA, TPD). It has been found that catalysts are characterized by the presence of both acid (Bronsted and Lews) and M^{0-} or Mn^{+}-metal centers. The structure of acid centers can include $MnSiO_3$, La_5Si, $Mn_{15}Si_{26}$, $LaMn_2Si_2$, $La\ Al_{11}O_{18}$, $La_2Si_2O_7$, La_3Si_2, La_3Si_2, functioning as Lews acid sites. The degree of hexane and tetradecane conversion, the composition of the compound form is determined by the length of the hydrocarbon chain and the conditions of the process.

Key words: catalytic cracking, modified zeolites, C6-alkanes, C14-alkanes, high-octane gasoline, diesel fraction

Introduction

With the rapid growth of the car park, gasoline consumption is increasing every year. Modern automobile gasoline is one of the most qualified and expensive energy carriers. To obtain them, a complex set of technological processes for oil refining is used, as well as various additives and additives that ensure compliance with modern requirements for the composition and quality of this type of motor fuel [1-5]. Catalytic cracking is one of the large-scale processes, after catalytic reforming, that provide deep oil refining and largely determines the technical and economic indicators of modern refineries of the fuel profile. Catalytic cracking is the fastest growing oil refining process. It contributes to a significant deepening of the oil refining degree and it is used for the production of high-octane gasolines and diesel fuels from heavy oil fractions, as well as for the production of petrochemical synthesis products. Typically, the catalytic cracking is carried out in the vapor phase at the temperature of 450º-520ºC and the contact time of the feedstock with the catalyst for a few seconds. Aluminum silicates, both natural and synthetic (zeolites), are used as catalysts for cracking [6-8]. The paraffins are the main component of many oil fractions, their cracking has a high activation energy on catalysts, hence, proceeds with a significant rate only at elevated temperatures. The determinations of the primary cracking products and the simple low molecular paraffins are difficult because of the olefins form rapid secondary transformations. The important factor affecting the degree of conversion, the direction of the alkane cracking and transformation is the length of its hydrocarbon chain. Nanoscale catalysts based on high-silica zeolites are used in oil refining and petrochemical processes, their activity is mainly determined by unique acid-base properties. One of the possible ways to regulate the catalytic properties is the introduction of modifying additives into the catalyst composition [9-13].

In this article, we studied the regularities of the conversion of model C_6 and C_{14}-alkanes and diesel fraction without hydrogen using the Al_2O_3 + ZSM as catalyst, modified by the addition of manganese, lanthanum and zinc additives.

Materials and methods

The catalyst was synthesized by the impregnation method [14-17] of Al_2O_3+ZSM composition with water-soluble salts of lanthanum, zinc, and manganese. The ratio of Al_2O_3: ZSM is 7:3, the zeolite modulus is 35.5. The zeolite crystallinity is 92-93%. The catalyst was tested during the processing of C_6 and C_{14} paraffins in a flow-through plant in an inert atmosphere (argon) in the temperature range 300-500ºC, pressure = 0.1 MPa, feed rate 1.5 h^{-1}.

The analysis of the starting and forming compounds was carried out by means of GLC. A complex of physicochemical methods was used to study the structure and state of the surface of catalysts: TEM, BET, IR spectroscopy using ammonia as a probe molecule [18, 19].

The surface of the Al_2O_3 + ZSM composition is 338.3 cm^2/g, the pore volume = 0.39 ml/g, the pores with $d_{average}$≈1.0 nm and $d_{average}$≈6.5-7.5 nm predominate. The surface of La-Zn-Mn / Al_2O_3 is 264.5 m^2/g, there are two types of pores with $d_{average}$≈1.5-2.5 nm and 6.0 nm. The total pore volume is ≈224.23 ml/g.

Results and discussion

In the Table 1 the degree of hexane conversion (T=300-500ºC) during its non-hydrogen processing and the yields of the main products formed are shown. As can be seen from these data, with an increase in temperature in the range of 320- 500ºC, the degree of conversion of C_6H_{12} over La-Zn-Mn/Al_2O_3+ZSM significantly increases – from 29.1 to 96.9%. Under these conditions, an increase in the yield of light hydrocarbons and a decrease in the amount of the liquid phase are observed: from 66.7% to 89.3% and 33.3% to 10.7%, respectively. At 320ºC the liquid part of the final mixture after reaction contains 77.6% of naphthenic hydrocarbons C_4-C_{14}, 13.5% of iso-alkanes C_4-C_6, 2.2% of C_4-C_{10} olefins, 3.7% of aromatic hydrocarbons, 2.9% of naphthene hydrocarbons and 0.1% of benzene. With an increase in temperature to 500ºC, the yield of C_4-C_6 paraffins (up to 4%), C_4-C_6 olefins (up to 0.2%), naphthenic hydrocarbons (up to 1.9%), the concentration of aromatic compounds (up to 66.6%) and benzene (up to 14.1%), the maximum yield of C_4-C_{10} iso-alkanes is observed at 350-400 ºC and is 20.1-20.8%.

The molecular weight of the initial alkane significantly affects the qualitative changes in the composition of the resulting compounds that occur with increasing temperature. To identify the behavior of heavier n-alkanes in the process of non-hydrogen processing, the cracking of tetradecane on a La-Zn-Mn/Al_2O_3+ZSM catalyst was investigated. It was found that the conversion of tetradecane varied little with an increase in the studied temperature range – from 86.5 to 87.6% (Table 2). Under these conditions, the yield of the liquid-phase products decreases from 80.0 to 57.5% but the yield of the gas-phase products grows from 20.0 to 42.7%.

Table 1 – The effect of temperature on the process of hydrogen-free conversion of hexane on the catalyst La-Zn-Mn/Al_2O_3 + ZSM at P=0.1MPa and V=1.5h^{-1}

Yield of components, %	Process temperature, ºC				
	320	350	400	450	500
Composition of a gas phase, %					
Paraffins C_1-C_4	75.9	76.9	76.5	82.2	89.2
Olefins C_2-C_7	1.9	1.1	0.6	0.4	0.3
Isoparaffins C_4-C_7	21.3	21.1	21.5	11.1	2.1
Naphthenic hydrocarbons C_5-C_7	0.3	0,3	0.2	0.1	0.07
Aromatic hydrocarbons C_6-C_7	0.08	0.1	0.1	1.2	2.8
Hydrogen	0.4	0.5	1.0	5.0	5.6
Yield of a gas phase	66.7	80.0	82.7	86.7	89.3
Yield of a liquid phase	33.3	20.0	17.3	13.3	10.7

Continuation of table 1

Conversion	29.1	50.1	82.2	86.1	96.9
Composition of a liquid phase, %					
∑ Paraffins C_4-C_6	77.6	60.7	20.6	15.2	4.0
∑ Iso-alkanes C_4-C_6	13.5	20.8	20.1	18.1	13.1
∑ Olefins C_4-C_6	2.2	0.9	0.6	0.6	0.2
∑ Aromatic hydrocarbons	3.7	14.4	54.0	57.8	66.6
Benzene	0.1	0.4	1.9	5.6	14.1
∑ Naphthenic hydrocarbons	2.9	2.8	2.7	2.6	1.9
Octane number (research method)	39.9	55.1	85.2	92.3	101.6
Octane number (motor method)	49.3	57.9	75.9	79.8	85.4

Table 2 – The impact of temperature on the process of hydrogen-free transformation of tetradecane on the catalyst La-Zn-Mn / Al_2O_3 + ZSM at P=0.1MPa, V=1.5h^{-1}

Yield of components, %	Process temperature, ºC			
	320	350	400	450
Composition of the gas phase, %				
Paraffins C_1-C_4	57.7	74.8	75.7	89.7
Olefins C_2-$_C$7	17.8	1.6	1.6	0.1
Isoparaffins C_4-C_7	22.3	19.2	15.9	3.8
Naphthenic hydrocarbons C_5-$_C$7	0.7	0.4	0.4	0.02
Aromatic hydrocarbons C_6 -C_7	0.4	0.4	2.3	1.3
Hydrogen	1.0	3.5	4.0	5.1
Yield of a gas phase	20.0	29.3	44.0	42.7
Yield of a liquid phase	80.0	70.7	56.0	57.3
Conversion	86.5	85.0	86.1	87.6
Composition of the liquid phase, %				
∑ Parafins C_4-$_{C1}$4	23.7	27.0	17.3	12.8
∑ Iso-alkanes C_4-C_{14}	19.9	22.5	19.5	12.1
∑ Olefins C_4-C_{10}	13.1	9.3	1.7	0.5
∑ Aromatic hydrocarbons	21.6	29.7	52.3	61.9
Benzene	0.8	1.6	5.3	11.4
∑ Naphthenic hydrocarbons	20.9	11.0	3.9	1.3
Octane number (research method)	76.0	80.2	88.9	93.4
Octane number (motor method)	62.0	65.3	73.9	78.5

From the data presented in Table 2, it is seen that the amount of light C_1-C_4 -alkanes formed in the gas phase at 350ºC is 57.7%, C_4-C_7 iso-alkanes – 22.3%, C_2-C_{10}-olefins – 17.8 %. There is an insignificant amount of aromatic and naphthenic hydrocarbons. Under these conditions, 23.7% of C_4-C_{14} paraffins, 19.9% of C_4-C_{10} iso-alkanes, 13.1% of C_4-C_{10} olefins, 21.6% of aromatic hydrocarbons, 20.9% of naphthene hydrocarbons and 0.8% benzene are in the liquid part of the final product mixture. With an increase in temperature up to 500ºC, the aromatization direction of transformations of tetradecane and fragments of its cracking is enhanced: the amount of aromatic hydrocarbons and benzene formed grows to 61.9 and 11.4%, respectively. The content of C_4-C_{14} paraffins, C_4-C_{14} iso-

alkanes and C_5-C_{10} olefins decreases to 12.8, 12.1 and 0.5%, respectively.

The dependence of the behavior of La-Zn-Mn/Al_2O_3 + ZSM catalyst on temperature during the non-hydrogen processing of alkanes is probably related to the restructuring of the structure and the state of the active sites of the catalyst. Thus, it was established that when the hydrogen-free treatment of hexane and tetradecane on this catalyst their molecular weight significantly affects the qualitative changes in the composition of the resulting compounds, which occur with an increase in temperature from 320 to 500ºC, especially the yield of C_4-C_n -alkanes. When processing hexane, their amounts changed from 77.6 to 4.0%, and in the case of tetradecane their yields varied within the limits of 23.7-12.8%. The amount of C_4-C_{10}-olefins formed during the cracking of tetradecane is 13.1-0.5%. In the case of hexane, their yield is lower – 2.2-0.2%. The maximum yield of aromatic compounds in the processing of hexane is higher than for tetradecane: 66.6 and 61.9%.

In this work conversion of the diesel fraction was also researched (Table 3). It was found that the yield of a liquid phase decreases from 53.3 at 350ºC to 27.0 at 450ºC. The yield of hydrocarbons of petrol fraction increases in these conditions from 28.0 to 62.0%, and the octane number changes from 79.8 to 74.6 (on motor method) and from 97.0 to 109.7 according to research method. When processing diesel fraction in the process of the hydrogen-free transformation a significant amount of hydrogen is formed. So at 450 ºC, in a gas phase, along with light C_3-C_4 hydrocarbons (with the n- and iso- structures), contains to 9.5% of hydrogen.

It should be noted that olefinic hydrocarbons in the catalytic cracking process are primarily subjected to the reactions of cleavage of the C-C bond, isomerization of the double bond, skeletal isomerization, hydrogen transfer, disproportionation, cyclization and polymerization [20-23].

The structure and state of the La-Zn-Mn/Al_2O_3 + ZSM catalyst active sites were studied using TEM (Figure) and IR spectroscopy. TEM and XPA studies of the dispersity, structure, and states of the La-Zn-Mn/Al_2O_3 + ZSM active centers show a significant inhomogeneity of its surface, which is associated with the formation of surface structures of heteronuclear nanoscale particles that are different in structure.

Table 3 - Effect of temperature on the process of diesel fraction hydrogen-free transformation at P=0.1MPa, V=1.5h^{-1}

Yield of components, %	Process temperature, ºC		
	350	400	450
Composition of the gas phase,%,			
Paraffins	63.9	74.1	85.0
Olefins	1.9	1.8	1.1
Iso-paraffins	30.5	17.6	3.3
Naphthenic hydrocarbons	0.2	0.05	-
Aromatic hydrocarbons	0.2	0.2	0.2
Hydrogen	3.0	6.0	9.5
Yield of a gas phase	46.7	56.0	73.0
Yield of a liquid phase	53.3	44.0	27.0
Hydrocarbon composition of gasoline fraction			
∑ Parafins C_4-C_{14}	5.0	3.1	2.9
∑ Iso-alkanes C_4-C_{14}	1.1	1.2	8.8
∑ Olefins C_4-C_{10}	32.7	24.5	25.6
∑Aromatic hydrocarbons	8.5	5.2	1.5
Aromatic hydrocarbons	52.4	63.9	59.2
Octane number (research method)	97.0	101.0	109.7
Octane number (motor method)	79.2	82.2	74.6
Yield of a liquid phase	28.0	45.8	62.0

It was found that on the surface of the La-Zn-Mn/Al_2O_3 + ZSM catalyst the nonuniformly distributed aggregates of large dense particles with cut features with d ≈ 150.0-300.0 nm, identified as a complex mixture of $LaMn_2Si_2$, $LaMnO_3$,15, $LaSi_2$, ZnO and β-MnO_2 are present. Also there are the small formations with d~7.0-10.0 nm, which include Mn_2O_3, Mn_3O_4, $La_2Si_2O_7$, La $Al_{11}O_{18}$ and Mn $(OH)_2$. Microdiffraction studies showed that extensive clusters of particles with d ~ 3.0-4.0 nm consist of La_2O_3, Mn_2O_3, La $Al_{11}O_{18}$ La_3Si_2 and ZnO. There were revealed the small accumulations of particles consisting of oxidized and reduced forms of lanthanum – La_2O_3, LaO and La0 – with d ~ 3.0 nm; structures with d ~ 5.0-7.0 nm, formed by La_2O_3, La_5Si, $Mn_{15}Si_{26}$ and single particles $MnSiO_3$ (d ~ 10.0 -20.0 nm).

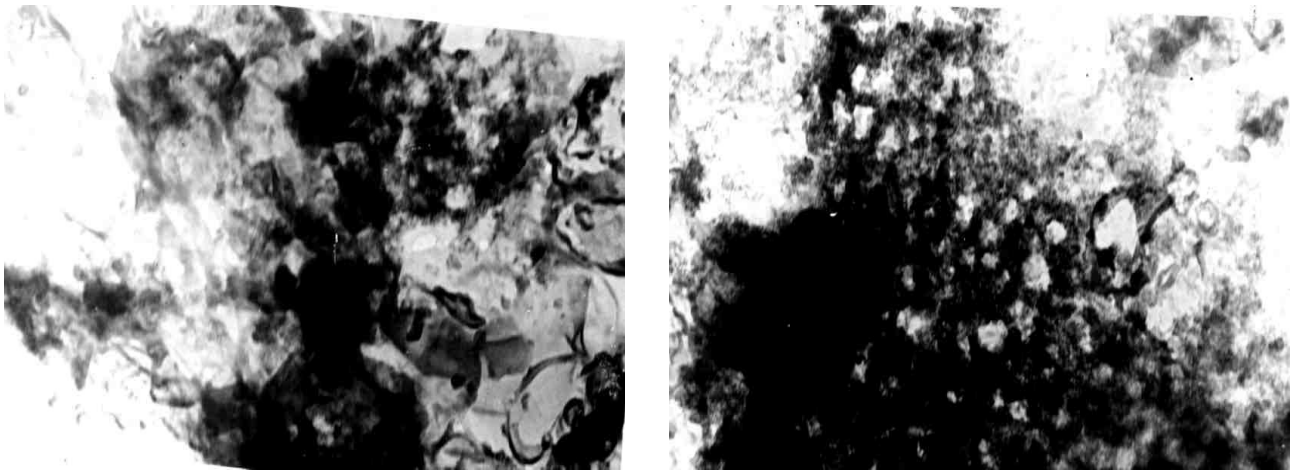

Figure 1 – Electron micrographs of La-Zn-Mn/Al_2O_3 + ZSM catalyst (zoom 80,000)

The results of electron microscopy indicate the presence of strong interaction in the La-Zn-Mn/Al_2O_3 + ZSM system: La, Zn and Mn are introduced into the Al_2O_3 crystal lattice and the zeolite. According to data in refs. [20, 22-25], the structures of $MnSiO_3$, La_5Si, $Mn_{15}Si_{26}$, $LaMn_2Si_2$, La $Al_{11}O_{18}$, $La_2Si_2O_7$, La_3Si_2, La_3Si_2 can function as Lews acid centers.

The TEM data are in good agreement with the IR spectroscopic studies of the La-Zn-Mn/Al_2O_3+ZSM catalyst using ammonia as a molecular probe. In the IR spectra of ammonia adsorbed on the surface of La-Zn-Mn/Al_2O_3 + ZSM-catalyst, written at 250°C, there were found peaks at 3,500; 3,300; 3,200 and 1,630 cm^{-1}. These peaks indicate the presence of Lewis acid sites, and peaks at 1,570 and 850 cm^{-1} are characteristic for Brönsted acid sites. The shift to the low-frequency region up to 1,650; 1, 400 and 3,400 cm^{-1} (that is, the strengthening of the NH_3 bond is the active center), 362 and 1,200 cm^{-1} were found.

Conclusion

In the work the laws governing the transformation of model C_6, C_{14} – alkanes and the diesel fraction in the absence of hydrogen on the Al_2O_3 + ZSM catalyst modified by the addition of manganese, lanthanum and zinc have been studied. A considerable increase of the conversion degree of hexane is noted with increasing temperature in the range of 320-500°C, the degree of conversion of C_6H_{12} increases significantly – from 29.1 to 96.9%. Under these conditions, an increase in the yield of light hydrocarbons and a decrease in the amount of the liquid phase are observed. While in a case of the tetradecane transformations, it was found that an increase in temperature in the same temperature range slightly changes the hydrocarbon conversion (from 86.5 to 87.6%). As the temperature rises to 500°C, the aromatization direction of the transformations of tetradecane and its cracking fragments increases: the amount of aromatic hydrocarbons and benzene formed rises to 61.9 and 11.4%, respectively.

Thus, it was found that in the hydrogen-free processing of hexane and tetradecane on the La-Zn-Mn/Al_2O_3 + ZSM catalyst, their molecular weight significantly affects the qualitative changes in the composition of the formed compounds, which occur with increasing temperature from 320 to 500°C, especially on the yield of C_4- C_n-alkanes. The structure and composition of the products formed during the processing of the La-Zn-Mn/ Al_2O_3 + ZSM catalyst by the C_6 and C_{14} n-alkanes indicates the develop-

ment of several directions of paraffins transformation on the catalysts. At the same time, several reactions occur: cracking and dehydrogenation with the formation of intermediate activated complexes with a reduced content of carbon atoms and adsorbed states of olefins, isomerization, dehydrocyclization, alkylation. Depending on the nature of the active center of the catalyst, different directions of transformation develop with the participation of intermediate activated complexes.

References

1. Maxwell I.E., Stork W.H.J., (2001) Chapter 17 Hydrocarbon processing with zeolites, *Studies in Surface Science and Catalysis*, 137, 747-819.

2. Derouane E., Vanderveken D.J., (1988) *Applied Catalysis*, 45, 15.

3. Sharipov R.A., Sidorov G.M., Zinnatullin R.R., Dmitriev Y.C. (2015) *Modern problems of science and education*, 1(1).

4. Sassykova L.R., (2018) Technology of heterolytic and homolytic oil refining processes: *Educational manual, Qazaq University, Almaty*, ISBN 978-601-04-3497-4.

5. Scott A., (2002) *J. Chemical Week*, 164(21), 24.

6. O'Connor P. (2007) Chapter 15 Catalytic cracking: The Future of an Evolving Process, *Studies in Surface Science and Catalysis*, 166, 227-251.

7. Wada K., Tada K., Itayama N., Kondo T., Mitsudo T. (2004) *Journal of Catalysis*, 228(2), 374-385.

8. Sassykova L.R. (2017) *Chemical and biochemical engineering quarterly*, 31, 4, 447-453.

9. Dai L., Hashimoto Y., Tominaga H., Tatsumi T. (1997) *Catalysis Letters*, 45, 107-112.

10. Choudhary V.R., Mayadevi S., Akolekar D.B. (1993) *Journal of Catalysis*, 144(1), 16-29.

11. Tashmukhambetova Zh.Kh., Zhakirova N.K., Sassykova L.R., Kadirbekov K.A., Aubakirov Y.A., Zhumakanova A.S. (2017) *Orient. J. Chem.*, 33(6), 2803-2809.

12. Moretti G. (1991) *J. Surface and Interface analysis*, 17(10), 745-750.

13. Viswanadham N., Muralidhar G., Prasada Rao T.S.R. (2004) *Journal of Molecular Catalysis A: Chemical*, 223(1–2), 269-274.

14. Abul-Hamayel M. A. (2002) *Chemical engineering & technology*, 25(1), 65-70.

15. Itoh H., Hidalgo C.V., Hattori T., Niwa M., Murakami Y.J. (1984) *Journal of Catalysis*, 85(2), 521-526.

16. Jacoby M. (2002) *Chemical & Engineering News*, 70(37), 30.

17. Lassinantti M. (2001) *Micropores and Mesopores Materials*, p.25-63.

18. Stocker M. (2005) *Microporous and Mesoporous Materials*, 82, 257–292.

19. Rigutto S.M., Veen R., Laurent H. (2007) *Studies in Surface Science and Catalysis*, 168, 855-913.

20. Tuktin B.T., Nurgaliyev N.N., Tenizbayeva A.S., Shapovalov A.A. (2017) *Orient J Chem*, 33(4), 1799-1804.

21. Brueva T.R., Mishin I.V., Kapustin G.I. (2001) *Thermochimica Acta*, 379,15-23.

22. Vosmerikov A.V., Echevsky G.V., Korobitsyna L.L. (2004) *Eurasian Chemico-Technological Journal*, 6(3), 201-206.

23. Zhang Y., Zhou Y., Tang M., Liu X., Duan Y. (2012) *Chemical Engineering Journal*, 181-182, 530- 537.

24. Yang G., Wang Y., Zhou D.H., Zhuang J.Q., Liu X.C., Han X.W., Bao X.H. (2003) *J. Chem. Phys.*, 119, 9765-9770.

25. Wagner C.D., Moulder J.F., Davis L.E., Riggs W.M. (1992) *Handbook of X-ray photoelectron Spectroscopy*, Perkin–Elmer Corp., Minnesota, USA.

IRSTI 31.23.99

[1]Y.S. Ikhsanov, [2]A.I. Zhussupova, [2]D.T. Kasymova, [3]S.A. Ross, [2]G.E. Zhusupova

[1]Center of Physico-chemical Methods of Research and Analysis, Almaty, Kazakhstan
[2]Al-Farabi Kazakh National University, Almaty, Kazakhstan
[3]University of Mississippi

Study of the hexane fraction isolated from the substance obtained from the roots *Limonium Gmelinii* by GC-MS

Abstract: Current paper presents the results of chemical study of the non-polar fraction obtained from the substance isolated from the roots of *Limonium gmelinii* (Willd.). *Limonium gmelinii* is a perennial wild-growing plant with a flowering period in June-September. It is found in all regions of Kazakhstan, western and eastern Siberia, European part of Russia, Central Asia, Southeastern Europe, Western China and Mongolia. Roots of *Limonium gmelinii* are introduced into the medicine and State Pharmacopoeia of the Republic of Kazakhstan. In this work, we obtained a substance using ultrasound to intensify the extraction process, which is effective, both from the economic and ecological side. *Limonium gmelinii* plants were harvested in Almaty region in 2018. Extracts were obtained by solvent extraction of a dry substance isolated from the roots of the studied plants with hexane, and studied by chromatography – mass spectrometry on a gas chromatograph with a mass-selective detector. In non-polar extract obtained from such substance, 27 individual compounds were identified, most of them are represented by higher fat-soluble hydrocarbons that are a part of natural waxes and resins; particularly high content of tetradecane, pentadecane, hexadecane, genicosane, octadecane, eicosane and their isomers was noted. In addition, the presence of a quinoline derivative in the form of 1,2-dihydro-2,2,4-trimethyl-quinoline was observed. For comparison, non-polar extract directly from the roots of *Limonium gmelinii* comprised 15 compounds belonging to the classes of hydrocarbons and esters of higher carboxylic acids. Dominating are hexadecanoic acid, ethyl ester, ethyl oleate, linoleic acid ethyl ester. In addition, a number of hydrocarbons, such as heptadecane, octadecane and tetradecane, and a quinoline derivative of 1,2-dihydro-2,2,4-trimethyl quinolone as well as phenol 2,4-bis (1,1-dimethylethyl) have been identified.

Key words: *Limonium gmelinii*, ultrasonic extraction, non-polar fraction, GC-MS, chemical composition.

Introduction

Limonium is a genus of plants that includes more than 300 different species distributed in many regions of the planet, including Central Asia, Southern Europe, North Africa and Middle East. On the territory of CIS, 35 species of the genus were described. Out of 18 *Limonium* species in Kazakhstan, the most industrially significant and productive is *Limonium* (*L.*) *gmelinii* (Willd.), which has wide ecological amplitude and is easily adapted to the environment, normalizing the maintenance of calcium and sodium salts in the soil.

L. gmelinii is a perennial wild-growing plant with a height of 30-80 cm. Roots are thick, nodular, and dark-brown, with thin bark, placed tightly to wood. Stem is truncated, with a little, usually paired branches. Leaves are numerous, green or blue-green, redden at ruptures. Flower stalks are few, apical and axillary. Flowers are in small 1-4 flower clusters, assembled in sufficiently short dense spikes, forming corymbose or pyramidal inflorescences. Spikes are 4.5-6 mm long; the cap is 4-4.5 mm long, at the base and up to the middle densely and reasonably long omitted by veins. Limb is fade white or faded purple, 5-10 notched. Petals are blue-violet, rarely white. Seeds are oblong-ovate, 2 mm in length, 0.6 mm in width, dark-purple-brown. Blooms in June-September, bears fruits in August-September. Area of distribution: all regions of Kazakhstan, western and eastern Siberia, European part of Russia, Central Asia, Southeastern Europe, Western China and Mongolia. Roots of *L. gmelinii* were introduced into the medicine and into the State Pharmacopoeia of the Republic of Kazakhstan, harmonized with the European Pharmacopoeia [8; 9].

On the basis of the plant roots of the *L.gmelinii* species, we obtained and patented a substance in the form of a complex of biologically active compounds, which has antiinflammatory, antioxidant and wound healing effects [10-13].

Considering the possibilities of optimizing the technology for obtaining the substance of our interest, the process of its extraction from the roots of *L.gmelinii* was intensified using ultrasound by varying its power and time of extraction. The amplitude of the ultrasound pulse is 400-1600 watts, pulse duration is 30 minutes. Ultrasonic dispersion was performed using an Elmasonic S450H ultrasonic bath (Elma Schmidbauer GmbH, Germany) at an ultrasound frequency of 37 kHz. The improved technological scheme for substance isolation from plant raw material allowed to increase its yield up to 45-50%. Phytochemical analysis of the substance was conducted as well [14-17].

Materials and methods

The substance was obtained according to the following procedure: 200 g of crushed roots are filled with 1200 ml of 50% aqueous alcohol and extraction is carried out by ultrasonic dispersion with the following electrophysical characteristics: ultrasonic pulse amplitude – 400 V, frequency 37 kHz, pulse duration – 20 min, temperature 35 °C. Ultrasonic dispersion was performed using Elmasonic S 450 (Elma Schmidbauer GmbH, Germany), working volume 45 L. Extraction time 4 hours at room temperature. The extract is filtered and concentrated to dryness on a rotary evaporator. The obtained substance is extracted with hexane in order to isolate from it the non-polar fraction, the composition of which was studied on a gas chromatograph with a mass-selective detector model Agilent 7890N/5973N (CTC Analytics / Leap Technologies, USA). At the same time, the volume of the gas phase to be taken is equal to 1 μl, the sample introduction temperature is 250 °C without dividing the flow. Separation was performed using a DB-35 MS chromatographic capillary column with a length of 30 m, an inner diameter of 0.25 mm and a film thickness of 0.25 μm at a constant carrier gas (helium) rate of 1 ml/min. The temperature of chromatography was programmed from 40 °C to 200 °C with a heating rate of 10 °C/min.

The software Agilent MSD ChemStation (version 1701EA) was used to control the gas chromatography system, record and process the obtained results and data. Data processing included determination of retention times, peak areas, as well as processing of spectral information obtained using a mass spectrometric detector. The Wiley 7th edition and NIST'02 libraries were used to decipher the mass spectra obtained (the total number of spectra in the libraries is more than 550 thousand).

The results of a comparative study of non-polar fractions obtained from the roots of the plant *L.gmelinii* and from the substance isolated from them during the intensification of the extraction process with ultrasound are presented in Tables 1 and 2.

Results and discussion

As a result of studying the hexane fraction of a substance obtained from the roots of plants of the species *L. gmelinii* (50% aqueous alcohol and ultrasound), 27 compounds were identified, most of which were classified as hydrocarbons (Table 1).

Table 1 – Research data of a hexane fraction obtained from a substance isolated from *L. gmelinii* roots by GC-MS

No.	Retention time	Name of compound	Content %
1	6.54	undecane	0.64
2	8.05	dodecane	1.08
3	8.92	2,7,10-trimethyl-dodecane	0.83
4	9.52	tridecane	3.38
5	10.35	2,3-dimethyldodecane	0.48
6	10.42	2,6,10-trimethyl-dodecane	0.50
7	10.91	tetradecane	7.48
8	10.99	1-tetradecene	0.43
9	11.54	2,6,10-trimethyl-tetradecane	1.14

Continuation of table 1

10	11.82	7-hexyl-tridecane	1.00
11	11.99	octyl-cyclohexane	0.55
12	12.23	pentadecane	10.28
13	12.91	1-tetradecanol	2.03
14	12.97	2-methyl-pentadecane	0.79
15	13.10	3-methyl-pentadecane	0.93
16	13.33	n-nonylcyclohexane	0.98
17	13.49	hexadecane	10.77
18	13.88	1,2-dihydro-2,2,4-trimethyl-quinoline,	3.47
19	14.49	2,6,10,14-tetramethyl-pentadecane	4.50
20	14.68	heptadecane	10.67
21	15.47	3-methyl-heptabecane	1.11
22	15.69	2,6,10,14-tetramethyl-hexadecane	3.57
23	15.81	octadecane	10.99
24	18.48	eicosane	7.34
25	19.82	phenanthrene	2.97
26	20.47	heneicosane	6.96
27	23.22	9-hexyl-heptadecane	5.12
Total			100.00

Typical for non-polar plant extracts is the dominance of hydrocarbons in their composition. In particular, a high content of tetradecane, pentadecane, hexadecane, genicosane, octadecane and eicosane was detected. Their total share is 96.52%, with the bulk of them being higher hydrocarbons, such as hexadecane, heptadecane, octadecane. 1,2-dihydro-2,2,4-trimethyl-quinoline, which is a quinoline derivative, is also identified.

Since plants of *L. gmelinii* are distributed mainly in arid zones, long-chain hydrocarbons are typical metabolites for such plants, which are mainly found in the composition of wax-like and resinous compositions on the outer integument, which act as barriers to the drying out and penetration of microorganisms into plants [18-23].

A comparative analysis of the above hexane extract with hexane extract obtained from the roots of the plant *L. gmelinii* was carried out. As a result, 14 compounds were identified, mainly belonging to the class of hydrocarbons, as well as to esters of higher fatty acids (Table 2).

Table 2 – Research data of *L. gmelinii* roots by GC-MS

No.	Retention time	Name of compound	Content %
1	6.53	undecane	0.94
2	8.05	dodecane	2.66
3	9.52	tridecane	4.07
4	10.91	tetradecane	4.15
5	10.99	7-tetradecene, (z)	0.89
6	12.23	9-methylheptadecane	3.22
7	13.49	heptadecane	7.61
8	13.83	phenol 2,4-bis(1,1-dimethylethyl)	1.72
9	13.88	1,2-dihydro-2,2,4-trimethyl quinoline	4.17

Continuation of table 1

10	15.69	tetracosane	3.43
11	15.81	octadecane	5.26
12	19.78	hexadecanoic acid, ethyl ester	24.51
13	25.40	ethyl oleate	11.16
14	25.78	linoleic acid ethyl ester	26.19
Total			100.00

In contrast to the non-polar fraction obtained from the substance isolated from the roots of the plant *Limonium gmelinii*, in the non-polar total extract directly from the roots the hydrocarbon content is 32.23%, which is 3 times less than in the non-polar fraction from the substance. At the same time, heptadecane, octadecane and tetradecane are also the dominant hydrocarbons, which belong to higher fat-soluble hydrocarbons. In addition to hydrocarbons in the roots of *L. gmelinii*, fatty acid esters were identified as hexadecanoic acid, ethyl ester, ethyl oleate, linoleic acid ethyl ester, which together account for 61.86% of the total mass of the identified compounds. Absence of these compounds in the hexane fraction of the substance is explained by the nature of the initially taken extractant in the isolation of the substance from the raw material with 50% aqueous alcohol, which does not dissolve esters of higher fatty acids.

A quinoline derivative in the form of 1,2-dihydro-2,2,4-trimethyl quinoline, different from the quinoline derivative found directly in the roots, was also found in a non-polar extract obtained from a substance isolated from the roots of plants of the species *L. gmelinii*. In addition, phenol 2,4-bis(1,1-dimethylethyl) was identified in the roots in an amount equal to 1.72%.

Conclusion

As a result of the study, the technological scheme for isolating a substance from the roots of plants of the *Limonium gmelinii* species was improved; It has been established that fat-soluble hydrocarbons dominate in the non-polar fraction of the substance obtained from the roots of *Limonium gmelinii* plants, while esters of higher carboxylic acids dominate in the analogous fraction of the roots.

Acknowledgment

This work was carried out within the framework of the grant financing program of the SC MES RK AR05134034 “Development and creation of high-performance gels based on pharmacopoeial wild plants of Kazakhstan and their integrated research.”

References

1 Palov M. (1997). Jenciklopedija lekapctvennyh pactenij. *MCP*, pp.130.

2 Kukenov M. (1996). Lekapctvennye pactenija Kazahctana i ih icpol’zovanie. *Fylym*, pp.344 p.

3 Sokolov P. (1985). Pactitel’nye pecupcy CCCP. *L. Nauka*, vol.1, pp. 293-297.

4 Komarov V.L.(1952). Flopa CCCP. *AN CCCP*, vol. 28, pp. 411-467.

5 Mihajlova V. (1968). Dubil’nye pactenija flopy Kazahctana i ih ocvoenie. *Nauka*, pp. 326.

6 Pavlov N. (1961).Flopa Kazahctana. *Nauka*, vol. 7, pp. 79-80.

7 Aljukina L.(1977). Flavonoidonocnye i tanidonocnye pactenija Kazahctana. *Nauka*, pp. 152.

8 Gocudapctvennaja fapmakopeja Pecpubliki Kazahctan (2008). *Zhibek zholy*, vol.1, pp.592

9 European Pharmacopoeia (2001). *EDQM*, pp. 1705

10 Zhucupova G. (2009) Lekapctvennye cpedctva, poluchennye na ocnove pactenij vida Limonium gmelinii. *Vectnik medicinckogo univepciteta*. No 1, pp.105-112.

11 Korulkina L., Shults E., Zhusupova G., Abilov Zh., Erzhanov K., and Chaudri M. (2004), Biologically active compounds from Limonium Gmelinii AND L. Popovii. I. *Chemistry of Natural Compounds*, vol. 40, pp. 465-468

12. Zhusupova G., Abilkaeva S. (2006), Flavanes from Limonium gmelinii. II. *Chemistry of Natural Compounds*, vol. 42, pp. 112-113

13 Korulkina L., Zhucupova G, Shul′ts E., Erzhanov K. (2004), Fatty-acid composition of two Limonium plant species. *Chemistry of Natural Compounds*, vol. 40, pp. 417-419

14. Mojtaba H., Davoud S., Bolourian S. (2014) Optimization of ultrasonic-assisted extraction of phenolic compounds from bovine pennyroyal (*Phlomidoschema parviflorum*) leaves using response surface methodology. *Industrial Crops and Products*, vol.57, pp.195-202.

15. Saliha S., Önder A., Esra I. (2013). Optimisation of ultrasonic-assisted extraction of antioxidant compounds from *Artemisia absinthium* using response surface methodology. *Food Chemistry*, vol.141, pp.1361-1368.

16. Önder A., Esra I., Saliha S., Demir C. (2013) Optimization of ultrasonic-assisted extraction of antioxidant compounds from blackberry leaves using response surface methodology. *Industrial Crops and Products*, vol. 44, pp. 558–565

17. Ruizhan C., Yuan L., Zhiqiang L., Shizhe L., Simin Y., Xinlong L. (2012). Optimization of ultrasonic extraction process of polysaccharides from Ornithogalum Caudatum Ait and evaluation of its biological activities. *Ultrasonics Sonochemistry*, vol. 19, pp. 1160–1168

18 Akhani H., Malekmohammadi M., Mahdavi P., Gharibiyan A., Chase M. (2013). Phylogenetics of the Irano-Turanian taxa of Limonium (Plumbaginaceae) based on ITS nrDNA sequences and leaf anatomy provides evidence for species delimitation and relationships of lineages. *Bot. J. Linn. Soc*., vol.171, pp.519-550.

19 Gancedoa N., Medeirosa D., Milaneze-Gutierreb M., Mello J. (2018). Morpho-anatomical characters of Limonium brasiliense leaves Revista. *Brasileira de Farmacognosia*, vol.28, pp.513-519

20 Lin L., Chou C. (2000). Flavonoids and phenolics from Limonium sinense. *Planta Medica*, vol.-66, pp.382-383.

21 Komekbay Zh., Halmenova Z., Umbetova A., Bisenbay A.(2018). Phytochemical analysis and development of production of biologically active complex on the basis of raw Melissa officinalis l. *News of NAS RK. Series of chemistry and technology*, vol. 427, pp.53 – 58

22 Umbetova A, Slan G., Omarova A., Burasheva G., Abidkulova K.(2018). The study of chemical composition of *Atraphaxis virgata* from the almaty region. *News of NAS RK. Series of chemistry and technology*, vol.- 428, pp.52 – 55

23 Utegenova L., Nurlybekova A., Aisa H, Jenis J. (2018) Liposoluble constituents of fritillaria pallidiflora. *News of NAS RK. Series of chemistry and technology*, vol. 432, pp.156 – 162

IRSTI 31.23.99

[1,2]O.M. Nassar, [3,4*]M.H. El-Sayed, [5]I.A. Elsehemy

[1]Department of Home Economics, Northern Border University, Kingdom of Saudi Arabia
[2]Nutrition and Food Sciences Department, Faculty of Home Economics, Minufiya University, Minufiya, Egypt
[3]Department of Biology, Faculty of Science and Arts, Northern Border University, Kingdom of Saudi Arabia.
[4]Department of Botany and Microbiology, Faculty of Science, Al-Azhar University, Cairo, Egypt
[5]Department of Natural and Microbial Products Chemistry, National Research Centre, Cairo, Egypt
*e-mail: m_helal2007rm@yahoo.com

Estimation of total phenolic contents and antioxidant capacities in some green and black tea of Saudi Arabia markets and evaluation of their antibacterial activity

Abstract: Tea is the most commonly consumed beverage in the world after water and considered a good antioxidant nutrient against free radical reactions. Teas are classified into more than one type depending on the manufacturing process. Green and black tea leaves are rich in phenolic compounds that are known for their antioxidant activity, having a beneficial effect on human health. The objective of this study was to determine phenolic content, antioxidant capacities as well as the antibacterial activity of green and black tea for the most popular brands in Saudi Arabia, Lipton and Rabea. The results showed that the content of polyphenols was higher for green brands 524.10 ± 11.8 and 553.75 ± 14.0 mg/g than black brands 468.70 ± 10.5 and 466.25 ± 6.8 mg/g for Lipton and Rabea types respectively. Moreover, it was found that all tea types exhibited high antioxidant activity, but green tea brands were higher 93.94 and 94.08 % than black brands 93.64 and 93.32 % for Lipton and Rabea brands respectively. Test of antibacterial activity showed that green tea was more effective in inhibiting the growth of the test organisms than black tea, where it showed antibacterial activity with a mean diameter of inhibition zone ranged from 9.0 ± 0.22 to13.0 ± 0.24 mm in comparison with black tea 9.0 ± 0.20 to 11.0 ± 0.10 mm. The present study indicated that no significant differences were noted in total phenolic contents and antioxidant activities for black and green tea. but Rabea green tea exhibited stronger antibacterial activity than black tea brands. To our knowledge, no studies have so far been done to compare these properties of two commercial black and green teas available in the markets of Saudi Arabia.

Key words: green, black tea, total phenolic content, radical scavenging activity, Saudi Arabia.

Introduction

In the last decades, lots of epidemiological studies were focused on bioactive phytochemicals such as phenolic compounds due to their beneficial effect on human health. It has been suggested that an initial cause of most chronic diseases is a free radical attack on biomolecules; thus, consumption of foods rich in phenolic compounds that are capable of the scavenging of reactive species may be a mechanism of protection recommending those foods for maximum health benefits [1; 2]. Historically, tea has important roles not only as ancient health therapy but also as a subject of the visual and literary arts. Tea was painted, drawn and figured on textiles and ceramics. Its shape, color, perfection and social interactions were described in many Odes [3; 4]. Tea is the most widely consumed drink in the world after water. It has been cultivated and consumed for more than 2000 years. Tea comes from the leaves of two classes of *Camellia sinensis* plant: assamica and sinensis, which originate in China and Southeast Asia [5; 6]. Teas are classified into three major types depending on the manufacturing process. Non-fermented green tea is produced by drying and steaming the fresh leaves to inactivate the polyphenol oxidase and thus, oxidation does not occur. Semi-fermented oolong tea is produced when the fresh leaves are subjected to a partial fermentation stage before drying. Fermented black and red (Pu-Erh) teas undergo a post-harvest fermentation stage before drying and steaming. However, the manufacturing process of black and red teas

is not identical, since the fermentation of black tea is due to oxidation catalyzed by polyphenol oxidase, while the fermentation of red tea is attained by using microorganisms [7; 8]. The percentage of each type of tea produced and consumed in the world is 78% black, 20% green and 2% oolong tea [9]. Among the different types of tea, green tea is now preferred as it has much more positive health benefits in comparison to other natural products [10]. Tea has a complex structure, which contains polyphenols, amino acids, proteins, alkaloids, minerals, carbohydrates, volatile compounds and trace elements [11]. Due to the presence of polyphenols, many scientific studies have proved the health benefits of tea such as anticarcinogenic, anti-oxidant, anti-aging, anti-mutagenic, anti-viral, anti-bacterial, and anti-inflammatory properties [12; 13]. The antimicrobial effect of tea was first demonstrated almost a century ago, in 1906, in the laboratory by McNaught, who showed that brewed black tea killed *Salmonella typhi* and *Brucella melitensis*. Thus, he recommended that the water bottles of troops should be filled with tea in order to prevent outbreaks of infections due to these agents. The precise antimicrobial spectrum of tea is difficult to be defined due to variation in definitions of 'susceptible' and 'resistant' as well as due to variation in the methods of testing, that have been used [14]. Tea polyphenols are also known for their antibacterial activity. In general, antibacterial activity decreases when the extent of tea fermentation is increased, implying stronger activity in green tea than black tea [15; 16]. Green tea catechins, particularly EGCG and ECG, have antibacterial activity against both Gram-positive and Gram-negative bacteria [17-19]. There are many types of tea (local and exotic) commonly consumed in Saudi Arabia. Most of these teas are traded and consumed without knowing their positive health benefits. So, comparing these teas with its chemical and biological activities is greatly required. Thus, the purpose of our research was to compare the total phenolic content, antioxidant capacities and antibacterial activity of two popular black and green tea brands from local Saudi markets by using several different methods. According to our knowledge, this is the first study to compare these characteristics of the most common green tea brands available in the Saudi markets.

Materials and methods

Tea samples. Camellia sinensis green teas (Lipton and Rabea), and black teas (Lipton and Rabea) were purchased from some supermarkets of Rafha governorate at the Northern Border region in Kingdom of Saudi Arabia. The tea samples were stored in a cool dry place before analysis.

Chemicals. 1,1-diphenyl-2-picrylhydrazyl (DPPH) used as the source of free radicals and Folin-Ciocalteu's phenol reagent used for estimation of total phenolic content were purchased from Sigma-Aldrich Chemical Co. (Pool, UK).

Samples and extract preparation. Two different brands of commercial black and green tea, purchased from the local markets (Lipton classic and Rabea tea), were used in this study. Tea samples were extracted using the hot water method [20]. Teas (25 g) were extracted with 250 ml of hot water three times, with continuous swirling at 120 rpm in an orbital shaker, for 1 h each time. The boiling water was allowed to cool throughout the extraction process to mimic tea brewing. After filtration under suction through Whatman No. 1 filter paper, the residues were re-extracted again with 250 ml of hot water. The water in the extracts was removed using a freeze dryer. Dried extracts were kept at -20°C in a freezer for further analysis.

Folin-ciocalteu assay. Total phenolic content (TPC) of extracts was determined using the Folin-Ciocalteu method [21; 22]. Samples (300 µl, in triplicate) were introduced test tubes wrapped in aluminum foil followed by addition of 1.5 ml of FC reagent (10 times dilution) and 1.2 ml of sodium carbonate solution (7.5% w/v). The tubes were allowed to stand in the dark for 30 min before absorbance was measured at 765 nm. TPC was expressed as gallic acid equivalent (GAE) in mg/g of sample. The calibration equation for gallic acid was $y = 0.0111x + 0.0148$ ($R2 = 0.9998$).

DPPH radical scavenging assay. Antioxidant activity was measured using the DPPH radical scavenging assay [22; 23]. Different dilutions of the extracts (1 ml) were added to 2 ml of DPPH (5.9 mg/100 ml methanol) in test tubes wrapped in aluminum foil. Absorbance (A) was measured at 517 nm after 30 min incubation in the dark. All measurements were made with distilled water as a blank. The scavenging ability (%) of the samples was calculated as $(A_{control} - A_{sample})/A_{control} \times 100)$ and calculated as IC_{50}, the concentration of sample needed scavenge DPPH free radicals by 50%. IC50 was expressed as ascorbic acid equivalent antioxidant capacity (AEAC) using the equation: AEAC (mg AA/g sample) = $IC_{50}(AA)/IC_{50}(sample) \times 10^5$. The IC_{50} of AA used for calculation of AEAC was 0.00387 mg/ml.

Disc-diffusion method. Antibacterial activity of extracts and fractions of green and black teas were

tested against Gram-positive *Bacillus subtilis* ATCC 6633 and *Staphylococcus aureus* ATCC 6538, and against Gram-negative *Pseudomonas aeruginosa* ATCC 9027 and *Escherichia coli* ATCC 7839. Antibacterial activity was measured using the disc-diffusion method [24]. Inoculums (100 µl) were spread evenly onto 20 ml Mueller-Hinton agar set in 90-mm Petri dishes using a sterile cotton swab. Sterilized paper discs (6-mm diameter) were impregnated with plant samples (2 mg per disc) using a micropipette and firmly placed onto the inoculated agar ensuring even distribution to avoid overlapping of zones. Streptomycin susceptibility discs (10 µg) were used as positive controls. After incubation overnight at 37ºC, the minimum inhibitory dose (MID) or lowest concentration of extract or fraction in mg/disc required to show a zone of inhibition was recorded [25; 26].

Statistical analysis. The data were statistically analyzed using Microsoft Excel 2019. Results with $p < 0.05$ were considered statistically significant. All experiments were performed in triplicate and the values were expressed as mean ± SD. The differences between the samples were assessed using single factor analysis of variance (ANOVA).

Results and discussion

Tea is consumed more than any other beverage worldwide [27]. It is a hot water infusion of the dried, young leaves and/or buds of the evergreen *Camellia sinensis* plant [28; 29]. In 2012, 4.884 million tons of tea was produced and consumed globally [30]. The chemical composition of tea is complex and not completely understood. The detailed investigations which have been made were done mainly to understand how tea gets its characteristic flavor and appearance. In the present study, hot water extract of two popular black and green tea brands from local Saudi markets (Lipton and Rabea tea) were prepared for estimation of total phenolic content, antioxidant capacities and antibacterial activity. Hot water was used for extraction since it is the traditional way of brewing tea and previous studies have shown it to be an efficient way of extracting tea [31; 32]. Studies have shown that water temperature is an important factor when extracting tea. Significantly higher yields of hot water than cold water extraction of green tea and stronger radical scavenging activity of oolong tea extracted with hot water of increasing temperature have been reported [33; 34]. For green, oolong, and black teas, extraction with water at 100°C for 3 min yielded higher total flavanol content than extraction with water at 60 and 80°C [35].

Total phenolic content (TPC). Polyphenols are a class of chemical constituents with one or more hydroxyl groups associated to the aromatic arene (phenyl) ring. Consequently, they are considered as one of the most potent antioxidative compounds that contribute to the antioxidant activity [36]. Hence, it is important to quantify polyphenol content and to estimate its contribution to antioxidant activity. Total phenolic contents of black teas (Lipton and Rabea) and green teas (Lipton and Rabea) brands were expressed as gallic acid equivalent. The results showed that the content of polyphenols was higher for green brands 524.10 ± 11.8 and 553.75 ± 14.0 mg/g than black brands 468.70 ± 10.5 and 466.25 ± 6.8 mg/g for Lipton and Rabea brands respectively (Table 1).

Table 1 – Total phenolic content (TPC) of extracts of *Camellia sinensis* teas

No	Type	Brand (County)	TPC[a] (mg GAE/g)
1	Black	Lipton (United Arab Emirates)	468.70 ± 10.5
		Rabea (Saudi Arabia)	466.25 ± 6.8
2	Green	Lipton (United Arab Emirates)	524.10 ± 11.8
		Rabea (Saudi Arabia)	553.75 ± 14.0
Note: [a]TPC (total phenolic content) represented by means ± SD (n = 3).			

Our results showed that the concentration of total phenol content was high in both brands especially in the green teas, this result may be referred to the high antioxidant activity of tea catechins, which are mainly found in green tea. The concentration of TPC obtained in this study is slightly lower than TPC obtained in the previous study concerned with the comparison of TPC activity of two popular green tea beverages available in the local market of Saudi Arabia recorded high phenolic content for the two green brands [37].

DPPH radical scavenging activity. DPPH assay is used to evaluate the free radical scavenging activity of hydrogen donating antioxidants in many plant extracts. DPPH is a stable free radical with a dark violet color. This method is based on the principle that DPPH accepts a hydrogen atom from the antioxidant, resulting in the reduction of DPPH to DPPH2, the violet color changes to yellow with a consequent decrease in absorbance at 517 nm. The efficiency of the antioxidant compound is measured by its ability to change color. The percentage of inhibition caused by green tea brands was higher 93.94 and 94.08 % than black brands 93.64 and 93.32 % for Lipton and Rabea brands respectively (Figure 1).

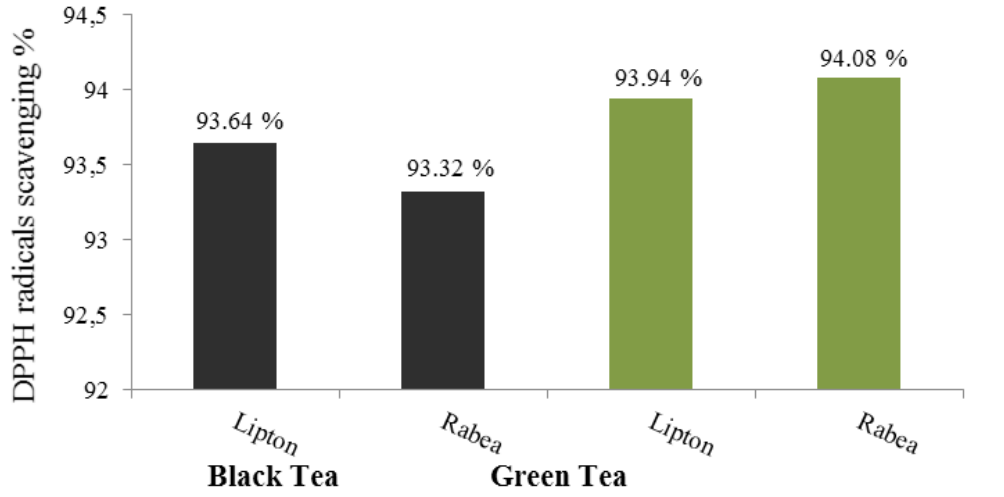

Figure 1 – Radical scavenging activity by black and green (Lipton and Rabea) teas
The value expressed as means ± SD (n = 3).
Compression of means was made using unpaired t-test (P > 0.05)

Results demonstrate that black and green of the two brands have the ability to scavenge free radicals. Therefore, both have the same high antioxidant activity. The presence of chlorophyll and pheophitin in green tea extract could explain the higher DPPH scavenging activity in these samples (Figure 1). The main green tea catechins are Epicatechin (EC), epigallocatechin (EGC), epicatechin gallate (ECG) and epigallocatechin gallate (EGCG) [38]. In general, Epigallocatechin gallate is the most powerful catechins in tea and it is responsible for the majority of the biological activity of green tea. It is well known that green tea has greater total catechins than black tea due to the fermentation process; catechins in the black tea are reduced as they are converted to the flavins and thearubigins [39]. Moreover, our results showed that the two brands have the ability to scavenge free radicals. Studies conducted by Omar et al. [37] and Gramza et al. [40], indicated that the analysis of DPPH free radicals scavenging ability by green tea showed higher radicals scavenging efficiency than black tea extract.

Antibacterial properties. Antibacterial activity of hot water extracts of black and green teas are recorded in Table 2 and represented in Figure 2.

The results obtained showed that green tea was more effective in inhibiting the growth of the test organisms than black tea, where it was showed antibacterial activity with mean diameter of inhibition zone ranged from 9.0 ± 0.22 to 13.0 ± 0.24 mm in comparison with black tea 9.0 ± 0.20 to 11.0 ± 0.10 mm. Furthermore, it was found that green Rabea brand was the most active one where it was active against all of the bacterial test organisms, while the weakest one was in case of black Rabea brand where it exhibited activity against *B. subtilis* ATCC 6633 with inhibition zone diameter 9.0 ± 0.20 mm and non-active against the other test organisms. The inhibition of tea extracts against *P. aeruginosa* and *E. coli* has been reported [16; 18] although an earlier study has explicitly reported that tea extracts are not effective against *P. aeruginosa* and *E. coli* [19]. The disparity in findings could be due to different strains of bacteria used, and to the different concentrations and

types of extracts investigated. Gram negative bacteria are less susceptible to antibiotics as their outer membrane of lipoproteins and lipopolysaccharides is able to regulate the access of antibacterial agents into the underlying structures [41]. Several studies have shown that catechins from green and black teas, particularly EGCG and ECG, inhibited the growth of many bacterial species [17].

Table 2 – Antibacterial activity of extracts of *Camellia sinensis* teas using the disc-diffusion method

Type	Brand (County)	Inhibition zone diameter (mm)			
		Gram positive		Gram negative	
		B. subtilis ATCC 6633	*S. aureus* ATCC 6538	*P. aeruginosa* ATCC 9027	*E. coli* ATCC 7839
Black	Lipton (United Arab Emirates)	11.0 ± 0.10	0.0	0.0	0.0
	Rabea (Saudi Arabia)	9.0 ± 0.20	0.0	0.0	0.0
Green	Lipton (United Arab Emirates)	13.0 ± 0.24	0.0	0.0	12.0 ± 0.15
	Rabea (Saudi Arabia)	13.0 ± 0.15	9.0 ± 0.22	11.0 ± 0.10	9.0 ± 0.25

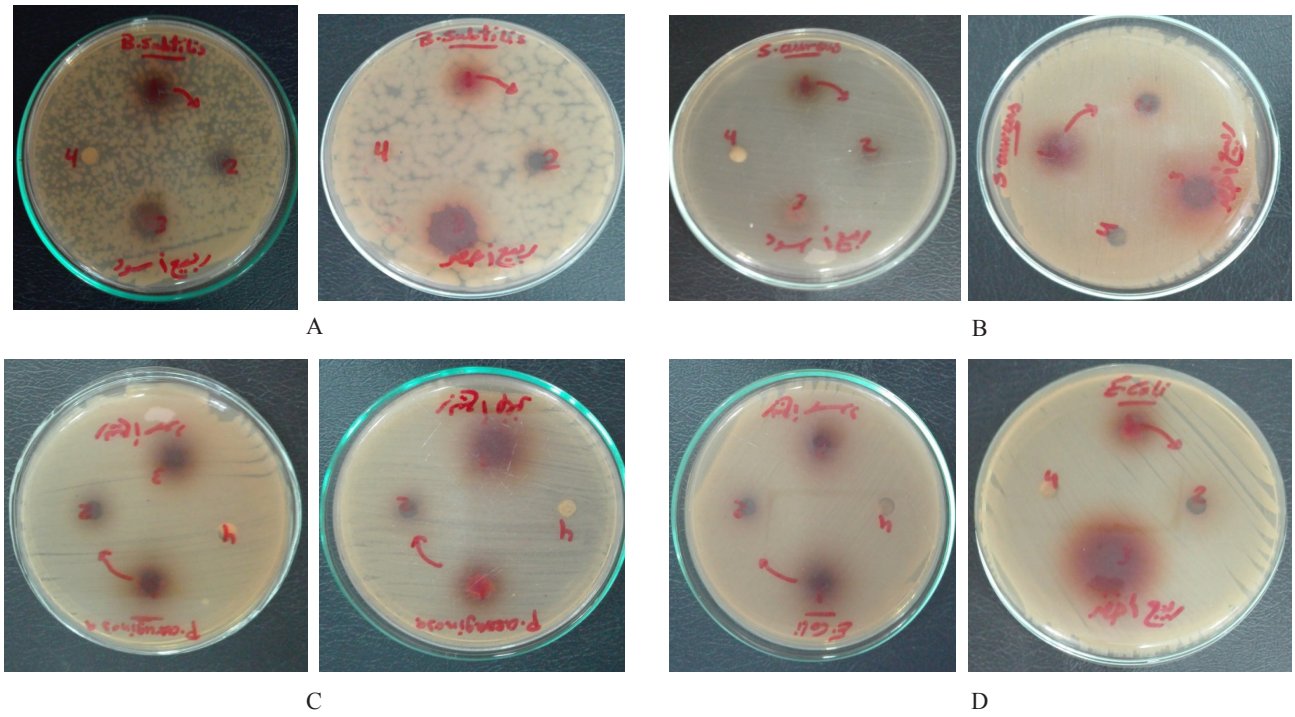

Figure 2 – Antibacterial activity of black and green teas (Lipton and Rabea) against (A): *B. subtilis,* (B): *S. aureus*, (C) *P. aeruginosa* and (D): *E. coli*.

Contrary to findings from this study, earlier studies have reported that black teas inhibited the growth of Gram positive bacteria [18; 42]. Extracts of green tea have been reported to be more effective in inhibiting bacterial growth than black tea [15]. In general, antibacterial activity decreased when the extent of tea fermentation increased [16; 19].

Conclusion

Our research work showed that green and black tea of the most popular brands in Saudi Arabia, Lipton and Rabea showed similar activity in their total phenolic contents (524.10 ± 11.8 to 553.75 ± 14.0 and 466.25 ± 6.8 to 468.70 ± 10.5 mg GAE/g) and

antioxidant activity (93.64 to 93.32% and 93.94 to 94.08%). However, green tea exhibited stronger antibacterial activity against all tested strains (0.0 to 13.0 mm) than black tea which was active against only one strain (0.0 to 11.0 mm). Continued researches are needed to further the current knowledge on the health-promoting effects of this popular beverage using different supplements by different mechanisms.

Acknowledgement

Olfat M. Nassar, Mohamed H. El-Sayed and Islam Abd Elmageed Elsehemy gratefully acknowledge the approval and support of this research study by the grant No. 7279-SAR-2017-1-8-F from Deanship of Scientific Research, Northern Border University, Arar, KSA.

References

1. Pellegrini N., Serafini M., Colombi B., Del Río D., Salvatore S., Bianchi M., Brighenti F. (2003) Total antioxidant capacity of plant foods, beverages, and oils consumed in Italy assessed by three different in vitro assays. *J. Nutr.,* vol. 133, no. 9, pp. 2812-2819.

2. Pérez-Jiménez J., Arranz S., Tabernero M., Diaz-Rubio M.E., Serrano J., Goñi I., Saura-Calixto F. (2008) Update methodology to determine antioxidant capacity in plant foods, oils and beverages: extraction, measurement and expression of results. *Food Res. Int.,* vol. 41, no. 3, pp. 274-285.

3. Marchand F., Desharnais J. (2014) Tea: History, Terroirs, Varieties: Kevin Gascoyne, François Marchand, Jasmin Desharnais, Hugo Americi editors. 2ed edition. Firefly Books. pp. 41-47.

4. Panda H. (2016) The Complete Book on Cultivation and Manufacture of Tea. 2ed revised edition. Asia Pacific Business Press Inc. pp. 321-325.

5. Quan T., Hang V., Ha H., Glang L. (2007) Total polyphenols, total catechin content and DPPH free radical scavenger activity of several types of Vietnam commercial green tea. *Sci. Technol. Devel.,* vol. 10, no. 1, pp. 5-11.

6. Rabiul I., Gias Uddin M., Mahfuzur R., Yousuf A. (2013) Short communication: caffeine and total polyphenol contents of market tea cultivated and processed in Bangladesh. *Malaysian J. of Nut.,* vol. 19, no. 1, pp. 143-147.

7. Cabrera C., Artacho R., Gimenez R. (2006) Beneficial effects of green tea: A Review. *J. Am. Coll. Nutr.,* vol. 25, no. 1, pp. 79-99.

8. McKay L., Blumberg B. (2002) The role of tea in human health: An update. *J. Am. Coll. Nutr.,* vol. 21, no. 1, pp. 1-13.

9. Chan W., Lim Y., Chew L. (2007) Antioxidant activity of *Camellia sinensis* leaves and tea from a lowland plantation in Malaysia. *Food Chem.,* vol. 102, no. 1, pp. 1214-1222.

10. Kusmita L., Puspitaningrum I., Limantara L. (2015) Identification, isolation and antioxidant activity of pheophytin from green tea (*Camellia sinensis* (L.) Kuntze). *Procedia Chem.,* vol. 14, no. 1, pp. 232-238.

11. Reto M., Figueira E., Filipe M., Almeida M. (2007). Chemical composition of green tea (*Camellia sinensis*) infusions commercialized in Portugal. Plan. *Foods Hum. Nut.,* vol. 62, no. 1, pp. 139-144.

12. Sangsrichan S., Ting R. (2010) Antioxidation and radical scavenging activities and tyrosinase inhibition of fresh tea leaves, *Camellia sinensis*. *Sci. J. Ubon Ratchathani Univ.,* vol. 1, no. 1, pp. 76-81.

13. De la Luz Cádiz-Gurrea M., Fernández-Arroyo S., Segura-Carretero A. (2014) Pine bark and green tea concentrated extracts: antioxidant activity and comprehensive characterization of bioactive compounds by HPLC-ESIQTOF-MS. *Int. J. Molec. Sci.,* vol. 15, no. 1, pp. 20382-20402.

14. Eugenia Ch Y. (2012) Recent patents on antibacterial, antifungal and antiviral properties of tea. *Recent Pat. on Anti-Inf. Drug Disc.,* vol. 7, no. 1, pp. 60-65.

15. Tiwari R., Bharti S., Kaur H., Dikshit R., Hoondal G. (2005). Synergistic antimicrobial activity of tea and antibiotics. *Indian J. Med. Res.,* vol. 122, no. 1, pp. 80-84.

16. Almajano M.P., Carbó R., Jiménez J.A., Gordon M.H. (2008) Antioxidant and antimicrobial activities of tea infusions. *Food Chem.,* vol. 108, no. 1, pp. 55-63.

17. Hamilton-Miller J. (1995) Antimicrobial properties of tea (*Camellia sinensis* L.). *Antimicrob. Agents Chemother.,* vol. 39, no. 1, pp. 2375-2377.

18. Bancirova M. (2010) Comparison of the antioxidant capacity and the anti-microbial activity of black and green tea. *Food Res. Int.,* vol. 43, no. 1, pp. 1379-82.

19. Toda M., Okubo S., Hiyoshi R., Shimamura T. (1989) The bactericidal activity of tea and coffee. *Lett. Appl. Microbiol.,* vol. 8, no. 1, pp. 123-125.

20. Chan W., Lim Y., Chong L., Tan L., Wong K. (2010) Antioxidant properties of tropical and temperate herbal teas. *J. Food Compos. Anal.,* vol. 23, no. 1, pp. 185-9.

21. Kähkönen P., Hopia I., Vuorela J., Rauha P., Pihlaja K., Kujala S, et al. (1999) Antioxidant activity of plant extracts containing phenolic compounds. *J. Agric. Food Chem.,* vol. 47, no. 1, pp. 3954-62.

22. Wong S., Lim Y., Abdullah N., Nordin F. (2011) Antiproliferative and phytochemical analyses of leaf extracts of ten Apocynaceae species. *Phcog. Res.,* vol. 3, no. 1, pp. 100-106.

23. Miliauskas G., Venskutonis P.R., van Beek T.A. (2004) Screening of radical scavenging activity of some medicinal and aromatic plant extracts. *Food Chem.,* vol. 85, no. 1, pp. 231-237.

24. Chung Y., Chung Y., Ngeow F., Goh H., Imiyabir Z. (2004) Antimicrobial activities of Malaysian plant species. *Pharm. Biol.,* vol. 42, no. 1, pp. 292-300.

25. Mackeen M., Ali M., El-Sharkawy H., Manap Y., Salleh M., Lajis H, et al. (1997) Antimicrobial and cytotoxic properties of some Malaysian traditional vegetables (ulam). *Pharm. Biol.,* vol. 35, no. 1, pp. 174-178.

26. Chan W., Ng P., Tan V., Low Y. (2011) Antioxidant and antibacterial properties of *Alpinia galanga*, *Curcuma longa* and *Etlingera elatior* (Zingiberaceae). *Phcog. J.,* vol. 3, no. 1, pp. 54-61.

27. Ho C., Lin K., Shahidi F. (2008) Tea and tea products: chemistry and health-promoting properties. Boca Raton: CRC Press. pp. 215-219.

28. Chu C., Juneja, R. (1997) General chemical composition of green tea and its infusion. Chemistry and applications of green tea. Boca Raton: CRC Press. pp. 13-22.

29. Saberi H. (2010) Tea: a global history. London: Reaktion Books. pp. 94-95.

30. Shannon E., Jaiswal K., Abu-Ghannam N. (2017). Polyphenolic content and antioxidant capacity of white, green, black, and herbal teas: a kinetic study. *Food Res.,* vol. 2, no. 1, pp. 1-11.

31. Farhoosh R., Golmovahhed G.A., Khodaparast M.H. (2007) Antioxidant activity of various extracts of old tea leaves and black tea wastes (*Camellia sinensis* L.). *Food Chem.,* vol. 100, no. 1, pp. 231-236.

32. Nkubana A., He Q. (2008) A comparative study of antioxidant activity between black tea from Rwandan highlands with green and oolong teas from China. *Int. J. Food Saf. Nutr. Public Health,* vol. 1, no. 1, pp. 159-66.

33. Su X., Duan J., Jiang Y., Shi J., Kakuda Y. (2006) Effects of soaking conditions on the antioxidant potentials of oolong tea. *J. Food Compos. Anal.,* vol. 19, no. 4, pp. 348-353.

34. Lin D., Liu H., Mau L. (2008) Effect of different brewing methods on antioxidant properties of steaming green tea. *LWT – Food Sci. Technol.,* vol. 41, no. 9, pp. 1616-1623.

35. Horžić D., Komes D., Belscak A., Ganic K.K., Ivekovic D., Karlovic D. (2009) The composition of polyphenols and methylxanthines in teas and herbal infusions. *Food Chem.,* vol. 115, no. 2, pp. 441-448.

36. Andjelković M., Van Camp J., De Meulenaer B., Depaemelaere G., Socaciu C., Verloo M., Verhe R. (2006) Iron-chelation properties of phenolic acids bearing catechol and galloyl groups. *Food Chem.,* vol. 98, no. 1, pp. 23-31.

37. Omar U., Shorbaji A., Arrait E., Al Agha T., Al-Marzouki H., Al Doghaither H., Al-Ghafari A. (2016) Comparative study of the antioxidant activity of two popular green tea beverages available in the local market of Saudi Arabia. *Nat. Sci.,* vol. 8, no. 1, pp. 227-234.

38. Sabouri S., Geng J., Corredig M. (2015) Tea polyphenols association to caseinate-stabilized oil-water interfaces. *Food Hydrocoll.,* vol. 51, no. 1, pp. 95-100.

39. Carloni P., Tiano L., Padella L., Bacchetti T., Customu C., Kay A., Damiani E. (2013) Antioxidant activity of white, green and black tea obtained from the same tea cultivar. *Food Res. Int.,* vol. 53, no. 1, pp. 900-908.

40. Gramza A., Pawlak-Lemanska K., Korczak J., Wasowicz E., Rudzinska M. (2005) Tea extracts as free radical scavengers. *Polish J. Environ. St.,* vol. 14, no. 1, pp. 861–867.

41. Unten L., Koketsu M., Kim M. (1997) Anti-discoloring activity of green tea polyphenols on β-carotene. *J. Agric. Food Chem.,* vol. 45, no. 6, pp. 2009-2012.

42. Chopra I., Greenwood D. (2001) Antibacterial agents: Basis of action. In: Battista J, editor. Encyclopedia of Life Sciences. Hoboken, New Jersey: Wiley; p. 1-8.

IRSTI 31.23.99; 31.23.01

[1] M. Gharibi.Tehrani, [1] A.H. Elhamirad, [2]* E. Azarpazhooh,
[1] A. Pedramnia, [2] P. Sharayei

[1] Department of Food Science & Technology, Sabzevar Branch, Islamic Azad University, Sabzevar, Iran
[2] Agricultural Engineering Research Department, Khorasan Razavi Agricultural and
Natural Resources Research and Education Center, AREEO, Mashhad, Iran
* e-mail:Azarpazhooh@gmail.com

Natural valuable compound extraction from onion by-products using a pulsed electric field

Abstract: Onion by-products, a waste generated from fruit processing industry, is a potential source of phenolic compounds that are known for their anti-oxidative properties. The influence of pulsed electric field (PEF) treatment on the bioactive compounds from onion by-products at different pulse voltage (PV); 2000, 4000, 6000Vand number of pulse (NP); 40, 50, 60 has been investigated. Response surface methodology, based on a Face-Centered Experimental Design (FCED) was used to determine optimal PEF treatment and optimize extraction yield, antioxidant strength, total phenolic compound (TPC),and quercetin content. The experimental data were fitted to a second-order polynomial equation and also profiled into the corresponding 3-D contour plots. Optimal extraction conditions were as follows:PV were 4102.97 V and and NP 51.43. Under these conditions, TPC, DPPH, FRAP,Quercetin and extraction yield were 48.912 ± 6 mg/kg, 50.366 ± 1 %, 465.414 ± 5 µmFe2/l, 31.761 ± 0.5 mg/100g and 88.107 ± 1% ; respectively and matching well with the predicted value. The results demonstrated that PEF could be a very effective method for continuous extraction of natural compounds.

Key words: antioxidant, phenolic, quercetin, extract, onion, optimal.

Introduction

Onion (*Allium cepa L.*) has been used as a food and as a treatment for many diseases since ancient history. Allium family plants are major sources of many phenolic and flavonoid compounds in the diet [1;2]. Flavonoids in food and other phenolic compounds, such as quercetin flavonols, kaempferol, and myricetin, have antioxidant activities and antibacterial [3].

Considering abundant quantities of onions annually are disposed of as waste from the process in plant protein products, and as an important nutritional source for the production of natural additives with antioxidant and antimicrobial properties, also can lead to problems such as wasting this national capital and disposing of these wastes. Besides, the agricultural by-products in food processing are increased; one of the applications of these materials is the extraction of flavonoids from fruits and vegetables such as apples, onions, and citrus fruits, which have antioxidant activities [4], especially, onion by-products that are quercetin-rich antioxidant and as retrieval raw materials. [5]. Extraction with conventional methods, including soaking, maceration, boiling, grinding, soxhlet extraction and etc [6;7], have limitations like long processing time, low EY, high solvent consumption and thermal degradation of thermo-unstable active compounds [8] To prevail over the defects of conventional extraction processes mentioned above, several novel techniques have been researched, including UAE[1], PEF-assisted extraction, MAE[2], SFE[3], and etc [9;10]. The advantages of developed methods were substantiated by comparing with conventional extraction techniques, such as soxhlet and maceration methods [11]. PEF process is a technique of green extraction, which has created increased interest in recent years due to its economic efficiency in foodstuff. The basis of the PEF technique is extracting intracellular materials from a plant for the application of electrical energy using an electric field and the formation of a pore in the cell membrane, which was called electroporation [12]. The external electric field creates a membrane transition potential that is larger

[1] – ultrasound-assisted extraction
[2] – microwave assisted extraction
[3] – supercritical fluid extraction

than the natural potential of the cell, and when the overall membrane potential reaches a critical level, the membrane ruptures, which is reversible and irreversible. The extraction process of intracellular materials from the plant can be used only in the irreversible rupture that facilitates the release of water and transfer of heat or osmosis material from permeability phenomenon. One of the most important achievements of this method was to accelerated the extraction process and speed, increased efficiency, environmentally-friendly, save energy, preservation material qualification properties [13], also extracted valuable compounds from softened plant material [14] The results of the researchers demonstrated that PEF-assisted extraction was increased the of polyphenol extracts (67-75%) in Chardonnay grape [15]. It also raised the antioxidant activity and the TPC of the extract of grape wastes [16].

Extraction of polyphenols in orange peel using the PEF showed that this technique can be used as a mild extraction process to improve the process of extraction of polyphenols from fresh orange peel, also increased the antioxidant capacity of the extract, and reduced the time of extraction without the need for organic solvents [17]. PEF was used to extract polyphenols from plant wastes such as anthocyanidins from red grape pulp, flavonols from onion by-products and phenolic acid from potato peel and polyphenols from apple pulp [18].

The aim of this study was to investigate the use of PEF process for extraction bioactive compounds from yellow onion by-product and determine the independence valuables such as the PV and the NP required achieving maximum cell degradation and ease of mass transfer for more extraction, also, Response Surface Methodology(RSM) and the FCED were used to optimize and comprise of total phenolic compound, strength of antioxidant, quercetin content and EY the onion by-products extracts with Conventional solid-liquid extraction.

Materials and methods

Raw materials

Onion by-products (*Allium cepa L.*), as an unacceptable production, were manually gathered from Fruit Bazar, Mashhad, Iran in the month of July of 2017. The samples were stored in cold storage at 4° C for further analysis.

Chemical and Reagents

All chemicals and reagents used in this study, were analytical grade consisting of 2,4,6 tris(2-pyridyl)-s-triazine(TPTZ), Folin-Ciocalteu(FC), gallic acid, DPPH & quercetin were provided from Sigma-Aldrich (St. Louis, MO),chemical and organic solvents were purchased from Merck (Darmstadt, Germany).

Extraction procedures

Conventional solid-liquid extraction

Extraction of onion by-products with ethanol was performed. Samples of onion wastes (1-10 v/wt) were mixed with 70% ethanol at temperatures (25, 30 and 35 °C), and times (12, 18 and 24 hours) by magnetic stirrer with a circumference of about 230 rpm. The extracted extracts were separated using Whatman filter paper No. 1 and vacuum pump from plant solids. Then, in order to remove the solvent, the extracts were obtained in a rotary machine, EI141 vapor Rotary, (Buchi, Switzerland) under vacuum distillation. The extracts transferred to glass plates and heated to 45 °C in constant temperature until they reached constant weight. Then, plates were closed and covered with aluminum foil and stored in a freezer at -18 ° C for analysis [19].

PEF-assisted extraction

The PEF processing of onion by-products was conducted using an apparatus (constructed by Sib Food.Tech, Germany). This system created electricity flow 20KV, logarithmic pulses and a power supply electric pulses (220-240V, at the frequency of 50Hz), Transmitted electricity to a power supply, There, a linear flow of electrical energy was transmitted to a capacitor series and the energy stored in the capacitors was pulled out by the two electrodes with the pulse key.

Before the extraction procedure, for carrying out extraction, 200 g sample of onion by-product was weighed and the mixture consisting of water and ethanol was subjected to PEF for different PV (2000, 4000, 6000 V) and the NP (40, 50, 60).when the extraction process was completed, the treatments were filtered with Whatman filter paper No 1, (Whatman International Ltd, UK) and placed at room temperature for 48 hours, until the solvent was removed, concentrated and the concentrate was dried. Finally, the dried samples were prepared for analysis.

Statistical analysis

Experimental design

In order to study the effect of extraction process on antioxidant activity of onion by-products, FCED Response Surface Methodology RSM and a design Expert Software Version 8.0.7.1(Minneapolis, USA)

was used to determine the effect of two independent parameters in extraction using a PEF [PV (X_i) and NP (X_j)] at three levels (-1, 0, +1), five replicates at the central points on the EY %, TPC;mg gallic acid equivalents per kg, FRAP;µmol Fe $^{2+}$/g, DPPH %. The coded and actual levels of each of the variables are given in Table 1.

Table 1 - Valuable codes, actual value and independence variables used in FCED

Independence variables	Valuable Codes	Actual values
PV	-1, 0, +1	2000, 4000, 6000 V
NP	-1, 0, +1	40, 50, 60

Modeling of variables

The statistical significance of the regression equations was performed by variance analysis (ANOVA) to obtain the response. In order to evaluate the validity of fitted models accuracy, lack of fit, CV, R-square, R-square (adj), model and P-coefficients were used to Design Expert Software. To illustrate the relationship between each of the dependent variables in the regression model with independent variables, their graphs were plotted by this software. Various responses were the conclusion of various interactions of independent variables; the second order polynomial regression equation was fitted to the experimental data of all responses, (Eq.1) [20].

$$Y=\beta_0+\sum_{j=1}^{k} \beta_j X_j+\sum_{j=1}^{k} \beta_{jj} X_{jj}+\sum_{i=1}^{j1-} \sum_{j=2}^{k} \beta_{ij} X_i X_j+\varepsilon \quad (1)$$

Y: predicted response, β_0: constant, βi: linear coefficient, βjj: interaction coefficients, Xi and Xj: independent variables, ε: noise or error

Measurement of TPC

TPC of onion extracts was measured by the Folin–Ciocalteu method [21]. TPC Data were presented as mg gallic acid equivalents per kilogram dry weight. For the analysis, sample solution of 100 µl was mixed (100 mg of the sample in 10 ml of methanol), and then 2.5 ml reagent of Folin-Ciocalteu was added and was remained at room temperature, for 8 min to react. Then, 1.5 ml of sodium carbonate (20% w/v) was stirred to the aqueous phase and kept in a dark place at room temperature for 30 min. the absorbance of the sample was calculated at 765 nm in conformity with the following formula (Eq.2). Water and reagent mixtures were used as a blank. Standard gallic acid solutions were prepared in methanol at concentrations ranging from 0.04 to 0.4 mg/ml (Eq.2).

$$Y=1.0776X+0.2644X+0.0099 \quad (2)$$

X: absorbance in 765 nm

$$P = \frac{Y}{W} * 1000$$

P: TPC (mg gallic acid per Kg)
Y: TPC (mg gallic acid per ml)
W**:** Sample Weight (g)

Determination of antioxidant capacity

Antioxidant capacity was measured by DPPH free radical scavenging capacity [22] and FRAP [23].

DPPH free radical scavenging assay

The DPPH free radical-scavenging activity of onion by-products extracts was evaluated by Ersus and Urdagol [22]. The solution of 0.006% DPPH free radical reagent in methanol was prepared. The test tubes were stored in a dark place for 30 min. Finally, Discolorations were measured at an absorbance of 512 nm by using a UV-1601 spectrophotometer (Shimadzu, Kyoto, Japan) in the following formula (Eq.3). All of the analyses were done in triplicate.

$$\%DPPH = \frac{A\ count - Asample}{Acount} * 100 \quad (3)$$

A_{count}: Absorbance of control
A_{sample}: Absorbance of sample

Determination of FRAP assay

FRAP was determined using 2, 4, 6-tripyridyl-s-triazine (TPTZ) by the method of Benzie and Strain 1996 [23]. This method is according to the reduction of the ferric tripyridyltriazine complex to its ferrous, colored form in the presence of antioxidants. The stock solutions were consist of, 300 mM acetate buffer (pH3.6), 10mM TPTZ solution in 40Mm HCl, and 20 mM $FeCl_3 \cdot 6H_2O$ solution. The analysis solutions were made freshly by stirring 25 ml of acetate buffer, 2.5 ml of TPTZ solution, and 2.5 ml of $FeCl_3 \cdot 6H_2O$ solution. The mixed solution was incubated at 37°C for 30 min and was referred to as FRAP solution and then, Sample (150 µl) along with 3 ml of FRAP solution remained for 30 min in the dark place. Readings of the colored product (ferrous-tripyridyltriazine complex) were then taken at 593 nm. The1mmol/l FeSO4 was used as the standard solution. For the construction of the calibration curve, five concentrations of $FeSO_4.7H_2O$ (1000, 750, 500, 250, and 125

μmol/l) were used and the absorbance was taken as a sample solution. The data were expressed as μmFe^{3+} that reduced to Fe^{2+} form per l.

Determination of EY

The EY of samples was measured to the following formula (Eq.4)

$$EY\ \% = \frac{W1 - W2}{W1} * 100 \qquad (4)$$

EY: Extraction Yield

W_1: the initial weight of the onion by-product before extraction

W_2: the weight of the onion by-product after extraction

Quercetin content

Quercetin content was carried out by the method of Chang et al. [24] with slight changes. The stock solutions were provided by 0.5 ml quercetin solution that was provided in 0.1 ml methanol. quercetin standard solutions were made, by using different dilutions (5-200μg/ml methanol). Then, 0.6 ml $FeCl_3$ solution was added to 0.6 ml solution of quercetin standard. The solution was placed at room temperature for 60 min and was referred to as quercetin solution [25]. To prepare the sample, 1.10 g of extract of onion by-products were mixed to 4 cc ethanol solution, 1200 of μm methanol, 160 μm $ALCL_3$ (10%), 160 μm potassium acetate 1 molar and 2080 of μm distilled water, Finally, kept at room temperature for 40 min and absorbance of the sample was calculated at 415 nm according to the following formula (Eq.5).

$$Q = \left(A - 0.0596/89.663\right) * 100000 \qquad (5)$$

$$A = \left(Asample - Acount\right)$$

Q: quercetin content (mg/100g)

$A_{Count:}$ absorbance value of control

$A_{Sample:}$ absorbance value of sample

Results and discussion

Model fitting

The effect of two independent variables consists of the PV and NP in the PEF assisted extraction process on the dependent variables including determining the EY %, DPPH %, FRAP μmol Fe /l, TPC, mg/kg and quercetin mg/100g was evaluated. FCED was performed with five central points. In order to determine the experimental model for prediction of the response, polynomial equations including linear, two factorials, quadratic term, and third term, fitted on the data obtained from the Response Surface Methodology (RSM). Then, these models were statistically analyzed. It should be noted that the statistical model of adequate, is a model that lack of fit was not significant and has the highest R^2 and Adj R^2. The responses of the dependent variables derived from the experimental and predicted experiments through the Response Surface Methodology (RSM) are presented in Table 2. The observations in this Table are shown a very good correlation between the results obtained by the experimental method and the predicted values by the statistical method. Also, this model was used to evaluate the linear, quadratic, third terms effects of independent variables on dependent variables. Analysis of variance and regression were used to assay the correspondence of the proposed models and statistical analysis of the significant variables of the model.

Investigating the effect of independent variables on qualitative and quantitative properties of onion extract

Determination of EY

An empirical model was obtained for predicting responses, polynomial relationships including linear, two factorial, quadratic term, that were fitted to the data obtained from these responses (Table 2). Also, it was shown that the linear model was the best model for interpreting the effect of variables (PV, NP) on the EY. According to the analysis of variance, independent variables were PV and NP in the linear and quadratic model, that had significant statistical differences ($P < 0.05$). In the regression model, the R-square (0.710) was high and lack of fit was not significant ($P < 0.05$). These values provide an appropriate mathematical model. The relationship between extraction efficiency and experimental variables was presented .in Fig 1. The most EY content was achieved in the highest NM and PV. The combination of the two independent variables (NM, PV) can be expected to enhance the EY (Fig1). Also, the NP was increased (40 to 50V), and EY was increased with slight gradient and it's following, with more increasing of NP (50 to 60), the EY increased sharply. The highest EY (92.66%) was at PV of 6000V and NP of 40 Which it was probably due to the destruction of the internal structure and the electrical decomposition of the cells and their greater permeability [4;26]. As a consequence, the increase of the NP resulted in enhancement of the degradation coefficient of the treatments and extracted intracellular compounds from damaged cells. Researchers demonstrated that the EY of effective compounds from papaya seeds increased with elevation of the NP, which was in agreement with this research [27].

Table 2 – Analysis of variance for the predicted linear, quadratic models for properties of onion extract in PEF assisted extraction process

Source	d.f	TPC(mg/kg)		DPPH (%)		FRAP(μmFe/l)		Quercetin(mg/100g)		EY (%)	
		Coefficient	Sum of squares	Coefficient	Sum of squares	Coefficient	Sum of squares	Coefficient	Sum of squares	Coefficient	Sum of squares
Model linear	5	-25 4.278*	947.18	-.176.08*	495.74	-2235.431*	80186.54	11.438*	892.81	21.700**	266.97
X_i	1	-3.996*	383.36	0.012ns	7.91	-0.039*	38187.49	0.014*	578.01	0.012**	151.65
X_j	1	12.501 ns	38.30	7.718ns	55.94	111.790ns	3299.88	ns	ns	1.098ns	49.38
Quadratic											
X_{ii}	1	ns	ns	-1.621ns	116.25	ns	ns	-2.467ns	34.81	ns	ns
X_{jj}	1	0.127*	525.52	-0.074*	151.76	-1.094*	38699.16	ns	ns	ns	ns
Interaction											
X_{ij}	1	ns	ns	ns	ns	ns	ns	ns	ns	-2.030*	65.95
Residual	7		537.91		205.05		45678.25		842.87		108.64
Lack of fit	3	ns	271.22	ns	138.52	ns	10707.88	ns	33.60	ns	67.44
Pure error	4		266.69		66.53		34970.38		782.54		41.20
Total	12		1485.09		700.79		1.259		1735.68		375.61
Std.Dev		7.73		5.06		71.24		9.18		3.47	
Mean		40.06		41.74		407.89		26.74		86.70	
CV (%)		19.30		12.13		17.47		34.34		4.01	
R^2		0.637		0.707		0.637		0.514		0.710	
Adj R^2		0.517		0.561		0.516		0.417		0.614	
Predicted R^2		0.344		0.052		0.400		0.310		0.334	

Subscripts: i: PV, j: NP
ns: no significant effect at level<0.05.
Std.Dev: Standard Deviation
*$P<0.05$.
**$P<0.01$.
***$P<0.001$.

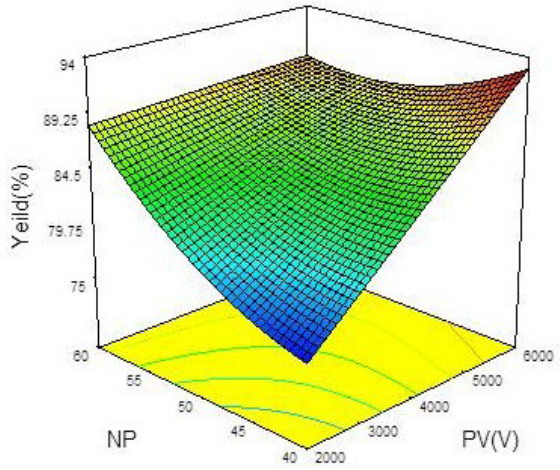

Figure 1 – Response surface plot of the EY of onion extraction as a function of PV and NP

Effects of PV and NP on TPC extraction

The analysis of variance of onion extract compounds by PEF in Table 2 was indicated. It can be considered that the linear coefficient of the NP, the quadratic term of PV and the interaction term coefficient were not significant ($P>0.05$). In order to obtain an empirical model for predicting the response, linear and polynomial relations of the second order fitted on the provided data from the analysis. In this response, the coefficient of R^2 of the predicted models (0.637) and *P*-Value for lack of fit for achieved model, was 0.595, which declared that it had no significant effect ($P>0.05$). These values presented an appropriate mathematical model. Fig 2, illustrated the NP was an effective factor in the efficiency and selectivity of the extraction technique. The PV parameter on the TPC was a significant effect ($P<0.05$), so that, the TPC decreased with the promotion of the PV from 2000 to 6000V. In conformity with Fig 2, the TPC extraction increased with the elevating the NP from 40 to 50 that caused to damage to the cell membrane and ultimately, extracted more TPC. While with a further increasing NP until 60, the TPC extraction was decreased. As it can be described, Increasing PV and NP (50 to 60) were reduced TPC extraction that Due to the decomposition effect of high PV on TPC. These results presented similar behavior with the issues of Bobinaie et al. [28] which depicted that expansion of the field intensity from 1 to 5 kV/m caused in a significant increase in TPC extraction ($P<0.05$), as well as, a slight decrease in the amount of phenolic compounds in the blueberry fruit and its by-products, when there was the highest flow intensity (5 kV/cm). In fact, they showed that the more intensity above 1 kV / cm for fresh blueberry fruit did not increase the release of TPC in the juice. Also, Toepfi et al. [29] exposed that the high electric field intensity above 300-500 V/cm for texture of many fruits and vegetables, reduced amount of yield and damaged to the tissues [21], also increased the electric pulse field intensity that the created irreversible damages to the cell membrane and it's following caused irreversible permeability and more extraction of TPC into solvent [26].

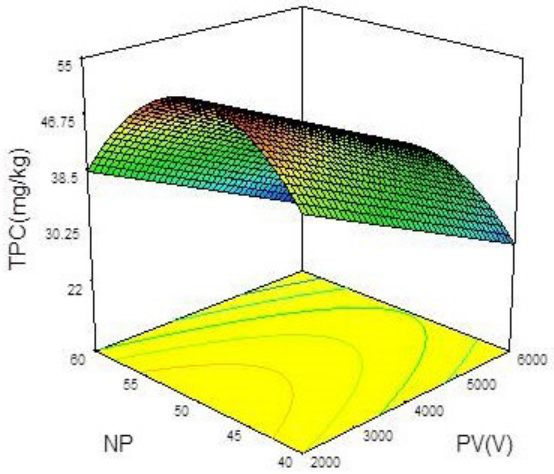

Figure 2 – Response surface plot of the total phenolic compound (TPC) of onion extract as a function of PV and NP

Effects of PV and NP on antioxidant activity DPPH radical-scavenging capacity

The antioxidant activity evaluation is dependent on the ability of DPPH as a stable free radical to bleach in the presence of antioxidants. Therefore, the less value of DPPH exhibited the high ability of the extract to inhibit free radicals activities [30]. The results of Table 2 declared that in the linear model and the interaction term, independent variables (PV and NP) had not a significant effect on DPPH radical-scavenging capacity ($P>0.05$). In the second order, the independent variable of NP demonstrated a clear significant effect on DPPH radical-scavenging capacity ($P<0.05$). In the regression model, R^2 (0.770) was highly significant. Based on response surface Fig 3, the increase in PV from 2000 to 4000 V, resulted in an increase in DPPH (38.71%). While the further increase in PV up to 6000 V, caused a decrease in DPPH (27.63%). By increasing the NP from 40 to 50, DPPH value, raised (50.98%), and then, extending the NP, until 60, could lead to declining the DPPH value (35.72%). According to researches by

Anagnostopoulou et al. [31]. There was a direct relationship between TPC and antioxidant activity. In this study, The NP of 40 and the PV of 4000 V had the highest TPC, antioxidant strength of the extract (Fig 3) due to increase the permeability and release of TPC, and therefore the DPPH radical-scavenging strength. Rocco et al; Csepregi et al. [32;33] stated that there was a high correlation between the TPC content and antioxidant activity of the extract, that it was in agreement with this research. The information of Table 2 indicated that the model fitted to the data obtained for independent variables, in the study condition, exactly and with high accuracy, the ability to fit the data. The high CV, R^2 and Adj R^2 confirmed model has *adequate fit* to the observed data.

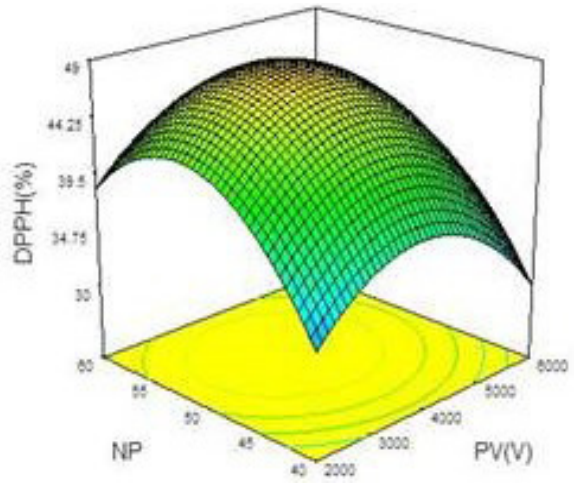

Figure 3 – Response surface plot of the DPPH of onion extract as a function of PV and NP

Ferric reducing/antioxidant power criterion

Reduction of Fe^{+3} is often used as an indicator of electron reduction capability, which is an important mechanism in the antioxidant action of phenolic compounds [34]. The antioxidant capacity of onion extract was determined by the antioxidant ability. In these extracts, the reduction of the Fe^{+3} to Fe^{+2} by the FRAP reagent was observed. The results of Table 2 showed that in the linear term, PV and in quadratic term NP were significant (*P<0.05*). In the interaction term, independent variables (PV, NP) were not significant (*P>0.05*). it can be seen in Fig 4 when the PV go to increase (2000 to 6000 V), the FRAP started to decrease, while FRAP initially increased and then decreased as the NP raised from 40 to 50, due to the thermal decomposition of the antioxidant compounds of susceptible [35;36]. Since the PV (4000 V) and the NP (50) were, the highest FRAP content, was 549.15 µM $Fe^{+2/l,}$ whereas the PV (6000 V) and the NP (40) were, the lowest FRAP content was purposed 252.15 µM $Fe^{+2/l.}$ In the regression model, lack of fit was significant (*P*<0.05) and its CV was (17/47), which confirmed the power of this model.

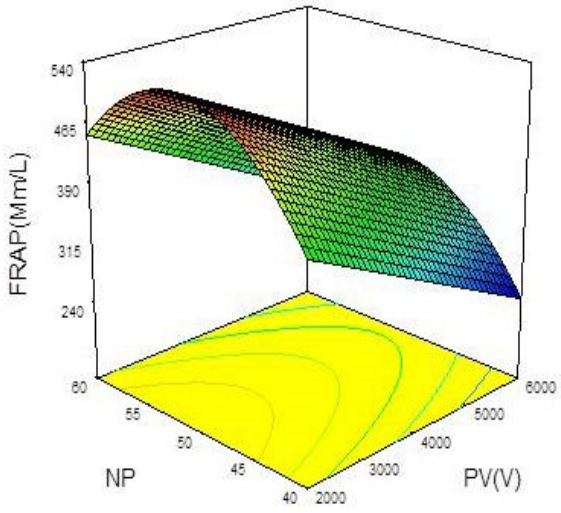

Figure 4 – Response surface plot of the FRAP of onion extract as a function of PV and NP

Effects of PV and NP on Quercetin content

The analysis of variance Table 2 illustrated that in linear coefficient, only, PV on the quercetin extraction was significant (*P<0.05*). While in the quadratic term, the interaction effect, the independent variables (PV, NP) did not have a significant effect on the quercetin content (*P>0.05*). Regression model had a relatively suitable R-square (R^2 = 0.514). Based on the sum of squares, the independent variable in the quadratic term was PV. As it can be shown in Fig 5, the PV parameter had the greatest effect on quercetin content and caused a significant increase (*P<0.05*) in quercetin extraction. Since quercetin is a heat-resistant flavonoid compound [37], therefore, when the PV increased to 4000 V, the solubility and was enhanced. The results of other researchers on *Inga edulis* plant leave were in agreement with this study [38]. Also, considering the significance of the second order term the PV parameter, exhibited that by increasing the PV to 4000 V and the NP to 50, the highest quercetin extraction content (47.88 mg/100 g) was obtained. As the PV exceeds up to 4000 V, quercetin content decreased sharply.

This effect can be attributed to the increase in PV and hence the thermal degradation of this composi-

tion. The results of this study coincided with earlier researchers [39]. Regarding the evaluation of the proposed model in Table 2 for the quercetin content, it was clear that the predicted relationship between the R^2 and the Adj R^2 were proportional and significant (*P<0.01*).

The lack of fit was not significant (*P>0.05*) and its CV was (34/34), which confirmed the strength of this model.

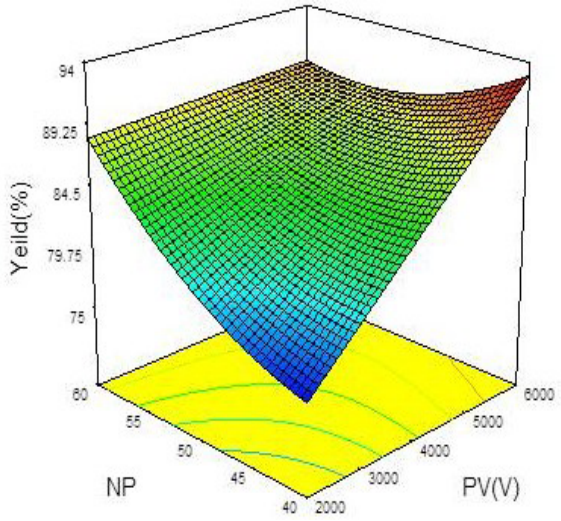

Figure 5 – Response surface plot of the Quercetin conten onion extract as a function of PV and NP

Optimization comparison PEF-assisted extraction with conventional extraction

Considering the best extraction condition of onion extract by PEF treatment that was based on the study of the PV from 2000 to 6000V and the NP from 40 to 60, the extraction process was optimized for all response variables in order to determine the maximum of EY, TPC and antioxidant strength. Characteristics of phenolic antioxidants found out by PEF process and under optimal condition were compared with conventional extraction (Table 3). The results Table 3 showed that to achieve the above objectives, the PV and NP should be 4102.97 V and 51.43 respectively. Under these terms, the quercetin content, DPPH, EY, TPC and FRAP were 31.76 mg / 100 g, 50.36%, 88.10%, 48.91 mg/kg, 465.41μmFe^{2+}/l, sequentially. To evaluate the accuracy of the optimized process, the proposed treatment was produced under the same conditions as the other treatment, and the results of TPC content, DPPH, FRAP, Quercetin content compared with the predicted results by model. There was no significant difference (*P>0.05*) between actual and empirical observations. (Table 3). Also, the desirability was achieved at 628% (Fig 6). PEF method gave a higher amount of the TPC, DPPH, FRAP, Quercetin content and EY than the conventional extraction method. PEF is more effective than the conventional method in maximizing characteristics of antioxidant compounds. Thus, this method can cause an increase in mass transfer.

Table 3 - Actual and predicted values of the response variables at optimal conditions for PEF and conventional methods

Characteristics	Extraction Method		
	PEF		Conventional
	Predicted values	Actual values	Actual values
TPC (mg/kg)	46.881[a]	48.912[a] ±6	21.234[b]±3
DPPH (%)	49.544[a]	50.366[a,a] ±1	26.544[b]±1
FRAP (μmFe^{2+}/l)	460.322[a]	465.414[a] ±5	398.112[b]±0.2
Quercetin (mg/100g)	30.666[a]	31.761[a] ±0.5	18.566[b]±0.1
EY (%)	87.110[a]	88.107[a] ±1	62.097[b]±2

Mean ± standard deviation

Conclusion

In this research, the quality properties of onion extract evaluated by PEF assisted extraction. The novel method of PEF was a rapid process and was known as one of the best environmentally friendly extraction methods due to low solvent consumption, low environmental pollution. This process had a positive effect on the antioxidant activity of the extract. The response surface analysis of the FCED contains two independent variables: PV and NP were performed as effective and important parameters on the extrac-

tion of antioxidant compounds of onion extract by PEF process. The results showed that the Response Surface Methodology (RSM) can be used to evaluate the EY. Both of the PV and NP was increased the antioxidant activity of the treatments.

Also, in the linear term, the PV in some cases, such as EY, TPC, Quercetin and FRAP and in the second order the NP has been affected on the TPC, FRAP, and DPPH. The proposed models in this research explained R^2 and Adj R^2. Also, the lack of fit was not significant and the low CV relatively indicated that the model was suitable for predicting the parameters. Additionally, optimization of PV and NP can produce high and adequate extract value by PEF assisted extraction, using this regression model, Enhanced antioxidant power, TPC and EY along with acceptable quercetin content showed the superiority of this new extraction technique to the conventional method. Therefore, we can predict and correct the required conditions by using the PEF assisted extraction method.

Acknowledgment

The authors are appreciated from the Agricultural Engineering Research Department, Khorasan Razavi Agricultural and Natural Research and Education, AREEO Mashhad, Iran, due to financial support throughout the research.

Abbreviation

CV Coefficient of Variation
DPPH 2, 2-diphenyl-1-picrylhydrazyl
EY Extraction Yield
FCED Face Centered Experimental Design
FRAP Ferric Reducing-Antioxidant Power
NP Number of Pulse
PEF Pulsed Electric Field
PV Pulse Voltage
TPC Total Phenolic Compounds

References

1. Hertog, Michael GL, Peter CH Hollman, Martijn B. (1992), *Journal of agricultural, and food chemistry*, 40, no. 12, P. 2379-83.

2. Tepe, Bektas, Dimitra Daferera, Atalay Sokmen, Munevver Sokmen, and Moschos, Polissiou (2005), *J Food chemistry,* 90, no. 3, P. 333-40.

3. Shon, Mi-Yae, Sang-Do Choi, Goon-Gjung Kahng, Sang-Hae Nam, Nak-Ju, Sung (2004), *J Food and Chemical Toxicology,* 42, no. 4, P. 659-66.

4. Ko, Min-Jung, Chan-Ick Cheigh, Sang-Woo Cho, and Myong-Soo Chung (2011), *Journal of Food Engineering,* 102, no. 4, P. 327-33.

5. Turner, Charlotta, Pernilla Turner, Gunilla Jacobson, Knut Almgren, Monica Waldebäck, Per Sjöberg, Eva Nordberg Karlsson, and Karin E, Markides (2006), *J Green Chemistry,* 8, no. 11, P. 949-59.

6. Vergara-Salinas, José R, Jara Pérez-Jiménez, Josep Lluís Torres, Eduardo Agosin, José R, Pérez-Correa (2012), *Journal of agricultural and food chemistry*, 60, no. 44, P. 10920-29.

7. Yang, Bao, Yueming Jiang, John Shi, Feng Chen, and Muhammad (2011), *J Food Research International Ashraf*, 44, no. 7, P. 1837-42.

8. Chan, Chung-Hung, Rozita Yusoff, Gek-Cheng Ngoh, and Fabian Wai-Lee (2011), *Journal of Chromatography*, 1218, no. 37, P. 6213-25.

9. Azmir, Jannatul, ISM Zaidul, Rahman, MM., Sharif, KM., Mohamed, A., Sahena, F., Jahurul, MHA., et al. (2013), *Journal of Food Engineering*, 117, no. 4 426-36.

10. Wang, Lijun, Curtis L (2006), *Trends in Food Science,* 17, no. 6: 300-12.

11. Smith, Roger M (2003), *Journal of chromatography A*, 1000, no. 1-2, P. 3-27.

12. Barbosa-Cánovas, Gustavo V, Usha R Pothakamury, M Marcela Gongora-Nieto, and Barry G Swanson (1999) Preservation of Foods with Pulsed Electric Fields, Elsevier.

13. Barbosa-Cánovas, Gustavo V, María S Tapia, and M Pilar Cano (2004), Novel Food Processing Technologies. CRC press.

14. Donsì, Francesco, Giovanna Ferrari, and Gianpiero, Pataro. (2010), *J Food Engineering Reviews,* 2, no. 2, P. 109-30.

15. Grimi, Nabil, Nikolai I Lebovka, Eugene Vorobiev, and Jean Vaxelaire (2009), *J Food Biophysics,* 4, no. 3, P. 191-98.

16. Corramles, M, S Toepfl, P Butz, D Knorr, B, Tausche. (2008), *J Innovative Food Science and Emerging Technologies,* 9, P. 85-91.

17. Luengo, Elisa, Ignacio Álvarez, Javier, Raso (2013), *J Innovative Food Science and Emerging Technologies,* 17 79-84.

18. Wijngaard, H., Hossain, M. B., Rai, D. K., & Brunton, N. (2012), *J Food Research International,* 46(2), P. 505–513.

19. Rouhani, Sh, Valizadeh, N and Salimi, Sh. (2009), *Progress in color colorants and coatings,* 2, no 2, P. 103-113.

20. Azarpazhooh, Elham, Hosahalli S (2012), *J Food and bioprocess technology*, 5, no. 5 1486-501.

21. Singleton, Vernon L, Rudolf Orthofer, and Rosa M Lamuela-Raventós (1999), In Methods in Enzymology, Elsevier, " Analysis of Total Phenols and Other Oxidation Substrates and Antioxidants by Means of Folin-Ciocalteu Reagent", P.152-78.

22. Ersus, S., Yurdagel, U. (2007), *Food Engineering,* 80, P.805-812.

23. Benzie, Iris FF, and Strain, J. (1999), In Methods in Enzymology, "Ferric Reducing/Antioxidant Power Assay: Direct Measure of Total Antioxidant Activity of Biological Fluids and Modified Version for Simultaneous Measurement of Total Antioxidant Power and Ascorbic Acid Concentration", Elsevier, P. 15-27.

24. Chang, Chia-Chi, Ming-Hua Yang, Hwei-Mei Wen, Jiing-Chuan, Chern. (2002), *Journal of food and drug analysis,* 10, no. 3.

25. Chandra, Suman, Shabana Khan, Bharathi Avula, Hemant Lata, Min Hye Yang, Mahmoud A ElSohly, Ikhlas A, Khan. (2014), Evidence-Based Complementary and Alternative Medicine. "Assessment of Total Phenolic and Flavonoid Content, Antioxidant Properties, and Yield of Aeroponically and Conventionally Grown Leafy Vegetables and Fruit Crops: A Comparative Study.".

26. Lebovka, NI, MI Bazhal, and E, Vorobiev. (2002), *Journal of Food Engineering,* 54, no. 4, P. 337-46.

27. Bobinaitė, Ramunė, Gianpiero Pataro, Nerijus Lamanauskas, Saulius Šatkauskas, Pranas Viškelis, Giovanna, Ferrari. (2015), *Journal of food science and technology*, 52, no. 9, P. 5898-905.

28. Toepfl, S, V Heinz, D, Knorr. (2007), *Chemical engineering and processing: Process Intensification,* 46, no. 6, P. 537-46.

29. Amarowicz, R, RB Pegg, P Rahimi-Moghaddam, B Barl, and JA, Weil. (2004), *Food chemistry,* 84, no. 4, P. 551-62.

30. Anagnostopoulou, Maria A, Panagiotis Kefalas, Vassilios P Papageorgiou, Andreana N Assimopoulou, and Dimitrios, Boskou. (2006), *Food chemistry*, 94, no. 1, P. 19-25.

31. Csepregi, Kristóf, Susanne Neugart, Monika Schreiner, and Éva, Hideg. (2016), *Molecules*, 21, no. 2, P. 208.

32. Rocco, A., Fanali, C., Dugo, L. and Mondello L. (2014), *Electrophoresis*, 35(11), P. 1701-1708.

33. Nabavi, S.M, Ebrahimzadeh, M.A., Nabavi, S.F., Hamidinia, A. and Bekhradnia, A.R., (2008), *Pharmacologyonline*, no.2, P. 560-567.

34. Ahmadian-Kouchaksaraie, Zahra, Razieh Niazmand, Masoud Najaf-Najafi. (2016), *Innovative food science and emerging technologies*, no. 36, P. 234-44.

35. Vergara-Salinas, José R, Jara Pérez-Jiménez, Josep Lluís Torres, Eduardo Agosin, José R, Pérez-Correa. (2012), *Journal of agricultural and food chemistry,* 60, no. 44, P. 10920-29.

36. Everaldo Moreira, José Maria Barbosa Filho, Ticiano Gomes do Nascimento, and Rui Oliveira, Macêdo. (2002), *Thermochimica Acta*, 392, P. 79-84.

37. Silva, EM, JNS Souza, H Rogez, Jean-François Rees, and Yvan, Larondelle. (2007), *Food Chemistry*, 101, no. 3, P. 1012-18.

38. Aoyama, Sakiko, Yukiko, Yamamoto. (2007), *Food science and technology research*, 13, no. 1, P. 67-72.

IRSTI 31.21.29

A.B. Niyazbekova, T.A. Shakirov

Zhangir khan West Kazakhstan agrarian-technology University, Uralsk, Kazakhstan
e-mail: abnyazbekova@mail.ru, shakirov_1985@mail.ru

Study of the effectiveness of mixed organo-inorganic inhibitors

Abstract: The relevance of the study lies in the fact that industrial production requires inhibitors with a high degree of protection, low cost of production and meet the requirements for chemical reagents. Individual organic or inorganic inhibitors used in production do not always meet the above requirements. The mutual influence of mixtures of various inhibitors was considered by V.P. Barannik. Using the concepts developed in the theory of catalysis for mixed catalysts, he established that the action of inhibitor mixtures in many respects resembles the action of catalyst mixtures. For mixtures of inhibitors, the effects of mutual amplification are established — synergism of the protective action, additivity, and the effect of mutual weakening — antagonism of the protective action. Strengthening the protective action of an organic corrosion inhibitor is possible by creating a composition of this inhibitor with other substances that enhance its action or by introducing into the molecule of this organic substance functional groups with heteroatoms different in charge (for example, N, O, P). The study and creation of mixed organo-inorganic compositions of inhibitors, mutually reinforcing the action of each other and capable of forming self-organizing surface layers is a promising and little-studied area. For research as main components of the inhibiting compositions taken: sodium dihydrogen phosphate, sodium hydrogen phosphate, sodium orthophosphate, sodium dihydrogendiphosphate, diphosphate sodium, sodium cyclotriphosphate and sodium cyclohexaphosphate, urea, thiourea, diethylamine hydrochloric acid, monoethanolamine, triethanolamine. The research was conducted according to the methods of state standards. The research methods were gravimetry, photocolorimetry, potentiometry. Experimentally determined quantitative indicators of the corrosion process: the rate of the corrosion process, degree of protection, depth indicator, braking coefficient. Analysis of the experimental data allows us to establish the laws of change in the quantitative indicators of the corrosion process and the stability of the resulting protective film on the metal surface. The experimental data obtained correlate well with the calculated data of the thermodynamic parameters of the corrosion process. Based on the research conducted, the chemical process and the mechanism of the interaction of the inhibitor with the surface of the metal plate were established. The evaluation of the stability of the resulting film was carried out on a scale of corrosion resistance in relation to steel St-3. On the basis of the obtained data, it was established that the anticorrosion efficiency depends on the nature of the organic and inorganic component and the ratios of the components of the systems. Mathematical and static data processing was carried out by Student's method with a confidence interval of 0.95. The regularities established during the work expand and complement the existing ideas about the protective effect of two-component organic-inorganic systems. The results will significantly contribute to the creation of effective, environmentally friendly and cost-effective inhibitors of steel corrosion.
Key words: corrosion, inhibitor, phosphate, degree of protection, depth indicator.

Introduction

In the largest countries of the world, the production of metal corrosion inhibitors is represented by a wide range of chemical products; however, for the industrial production of a certain product, the cost of production and its compliance with the requirements for chemicals are an important factor [1, 2, 3].

At present, the modification of the surface of metals with inhibitors, containing in its composition compounds capable of forming self-organizing surface layers, is promising and is a little studied area.

Studying the effectiveness of such systems, consisting of mixed corrosion inhibitors and determining the nature of their interaction is important.

The works of A.Gabitov shown [4] that it is possible to create high-performance environmentally friendly corrosion inhibitors of carbon steels are the most studied compounds, aromatic and aliphatic amines. Unfortunately, the reagents used do not always provide a sufficiently high protective effect.

For most organic inhibitors characterized by an increase in their concentration to a certain amount of increase in the effectiveness of the protective action, and then the effectiveness does not change. In inorganic anode inhibitors at low concentrations there is an increase in the corrosion rate and only when a certain concentration is reached there is a sharp decrease in the corrosion rate due to the passivation of the metal surface.

Of the inorganic inhibitors, phosphoric acid and its salts are the most promising for corrosion suppression, but their inhibitory properties are manifested only at fairly high concentrations.

A promising direction of creation of new effective metal corrosion inhibitors for aqueous media is the use of sodium phosphates, which in condensed form are in the waste of phosphorus production – the liquid phase of poor phosphorus sludge, the so-called "cottrel milk".

The inhibitory effect of sodium polyphosphate may be due to the ability of polyphosphates to prevent the reduction of oxygen on the surface of iron, thereby facilitating the adsorption of dissolved oxygen, which leads to the passivation of the metal.

Currently, there are two ways to obtain inhibitors: the first way - the creation of individual inhibitory compounds by chemical synthesis using the knowledge of the mechanism of action of inhibitors and the relationship of protective action with the structure of molecules; the second way - to obtain combined inhibitors, especially on the basis of waste chemical and petrochemical industries.

The first way is characterized by high cost and complexity of obtaining individual compounds. These disadvantages are deprived of the second way, however, in this case, for the purposeful creation of combined inhibitors, it is necessary to know the patterns of mutual influence of their components with a joint action on the corrosion process.

Even in the conditions of one field at different sites, this figure may vary significantly. This may be due to the solubility (dispersibility) of the inhibitor in formation fluids, its low degree of compatibility with formation waters, incorrect selection of the reagent for specific conditions. Usually in practice, this problem is solved by increasing the dosage of the reagent, which also does not always give the desired effect.

Therefore, it is necessary to create new inhibitor compositions that could provide a high protective effect in a wide range of conditions of use or improve the quality of existing formulations.

The mutual influence of mixtures of different inhibitors was first studied in detail by V.Barannik [5]. Using the concepts developed in the theory of catalysis for mixed catalysts, he found that the action of inhibitor mixtures is largely similar to the action of catalyst mixtures [6]. For mixtures of inhibitors, the effects of mutual reinforcement were established – synergism of the protective action, additivity and the effect of mutual weakening – antagonism of the protective action.

Strengthening the protective action of an organic corrosion inhibitor can, in principle, be achieved in two ways: creating a composition of this inhibitor with other substances that enhance its action and introducing into the molecule of this organic substance functional groups with heteroatoms differing in charge (for example, N, O, P). In the first case, they usually speak of intermolecular synergism, in the second case, intramolecular [7, 8].

The essence of this effect is that one or two functional groups with a heteroatom are introduced into the inhibitor molecule, which differ in size and sign of charge from the one available in the molecule. In this case, one group can behave like a cation, the other – like anion. Examples of such inhibitors may be substances containing -NH_2 and -OH, -NH_2 and -SH, -NH_2 and -COOH groups. When molecules of such a substance are adsorbed on a metal, some of them are adsorbed by one group (for example, by an amino group), and some by another (for example, by a hydroxy group). This leads to a decrease in repulsive forces between molecules on the metal surface and contributes to the formation of a more dense inhibitor film.

Materials and methods

To assess the effectiveness of the inhibitory effect of mixed organo-inorganic compositions, the study was conducted at a concentration of 0.01 mol/dm^3 at a ratio of reagents in the mixture: 1:3, 1:1 and 3:1. As the main elements inhibiting compositions taken: sodium dihydrogen phosphate, sodium hydrogen phosphate, sodium orthophosphate, sodium dihydrogendiphosphate, diphosphate sodium, sodium cyclotriphosphate and sodium cyclohexaphosphate, urea,

thiourea, diethylamine hydrochloric acid, monoethanolamine, triethanolamine. Corrosion tests were carried out according to the methods of state standards on steel St-3 composition [9, 10, 11]. The duration of the experiments ranged from 24-480 hours. The following research methods were used: gravimetry, photocolorimetry, potentiometry. Studies were carried out in comparison with control samples of individual inorganic and organic inhibitors.

Quantitative indicators of corrosion processes were calculated by the formulas; the evaluation of measurement uncertainty was carried out according to an algorithm using Student's coefficient [12, 13].

Results and Discussion

In the study of the sodium dihydrophosphate system in a mixture with organic components (Figure 1), it was found that in two-component NaH_2PO_4 systems with urea, thiourea, diethylamine, with a 3:1 ratio of components, changes in the corrosion rate are insignificant. The system NaH_2PO_4-urea shows increased protective effect (Z = 79.92%).

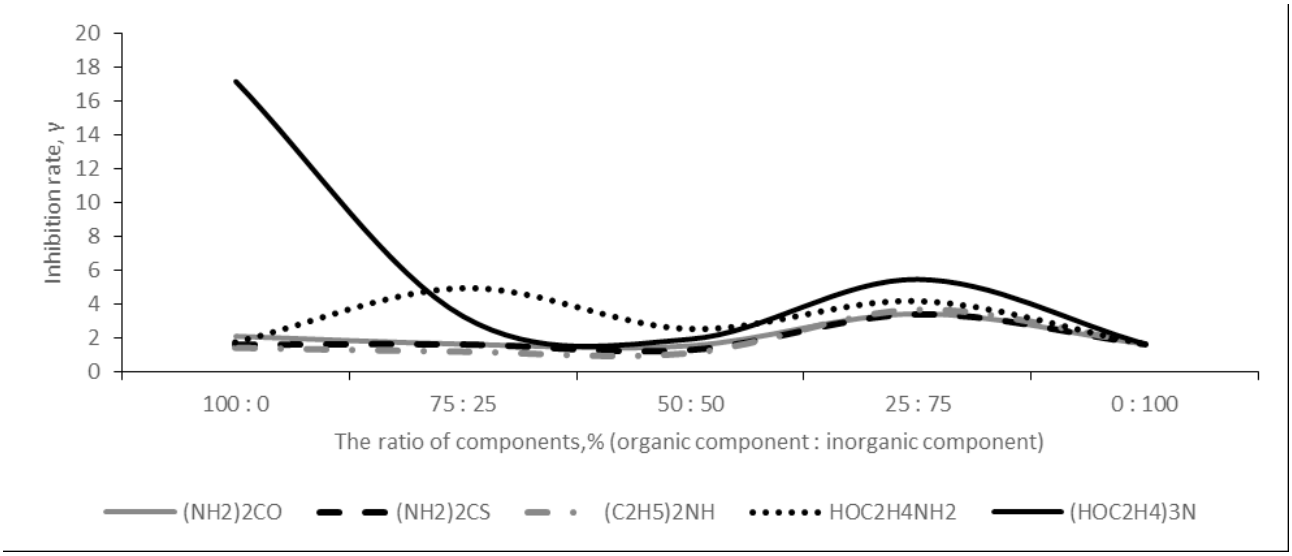

Figure 1 - Inhibition of St-3 steel corrosion in systems with sodium dihydrophosphate NaH_2PO_4 (C_m = 0.01 mol/dm^3)

Observations have shown that in systems with a ratio of 1:1 component in the presence of organic additives, the protective effect is similar in all systems. For systems with a 1:3 ratios, an increase in the protective effect of 3.5 times was observed, in contrast to a one-component system containing only an inorganic inhibitor.

Studies have shown that in stationary conditions, the addition of an organic component to NaH_2PO_4 leads to a decrease in the corrosion rate, steel compared to the control sample by 2-3 times.

In the Na_2HPO_4 systems with organic components (Figure 2), according to the results of gravimetric tests, it was revealed that in clean environments there is a high rate of the corrosion process and, accordingly, a low inhibition coefficient. Comparison of changes in the rates of corrosion processes of a system with a pure inorganic inhibitor and systems with a ratio of 3:1 components showed similar values of the corrosion rate constants and inhibition coefficients. In the system Na_2HPO_4 - triethanolamine, the protective effect was reduced by a factor of 1.5 from 94.61 to 65.08, and in systems with a 1:1 ratio of components, the protective effect did not change compared to a pure phosphate inhibitor. In the Na_2HPO_4 - $(HOC_2H_4)_3N$ system with a 1:3 ratio of components, a sharp increase in the protective effect is observed, as evidenced by comparing the values of inhibition coefficients in this system (79.33) and in the system containing pure Na_2HPO_4 (4.67).

The increase of the protective effect in the system of triethanolamine, apparently due to participation of the lone pairs on the nitrogen atom in the molecule of triethanolamine, that binds the hydrogen atom in the hydrogen phosphate in the donor-acceptor mechanism with the formation of neutral salts. And unlike pure triethanolamine, it is more easily sorbed on the formed phosphate film covering the surface of the

metal, than increases the protective effect of the entire system:

$$HPO_4^{2-} + :N(C_2H_4OH)_3 \rightarrow [H:N(C_2H_4OH)_3]^+ + PO_4^{3-}$$

In the system under consideration, the inhibitor Na_3PO_4 and its mixtures with organic components experimental data show that in a single-component system containing only Na_3PO_4, high inhibitory properties with a degree of protection of 97,46% are manifested. The data in the Na_3PO_4-diethylamine system in a 1:3 ratio shows a 5-fold decrease in the protective effect. In systems with other organic components with the same ratio, an increase in the protective effect up to 98,24% is observed in the presence of both urea and triethanolamine.

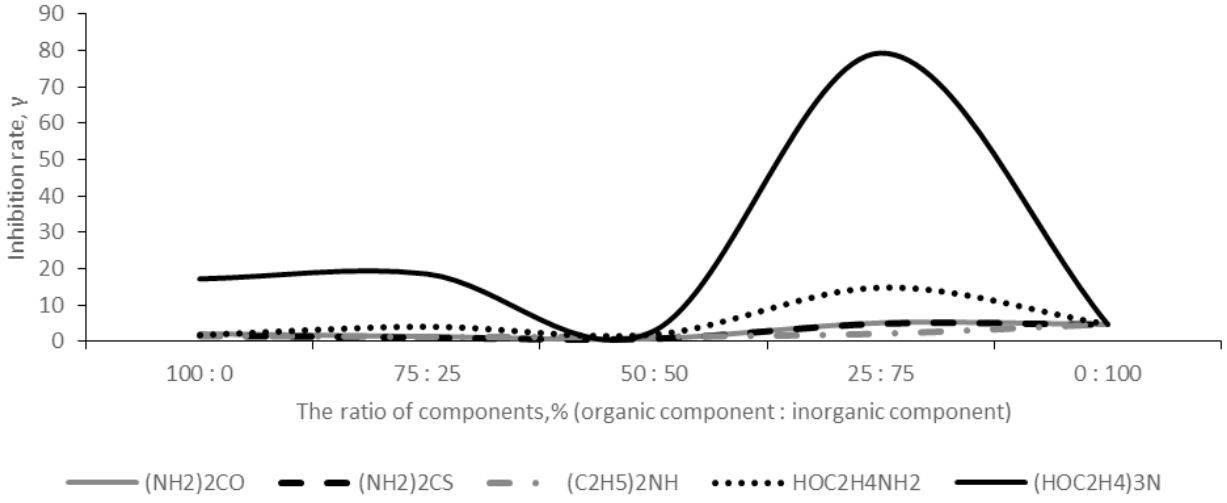

Figure 2 - Inhibition of St-3 steel corrosion in systems with sodium hydroorthophosphate Na_2HPO_4 (C_m = 0.01 mol/dm^3)

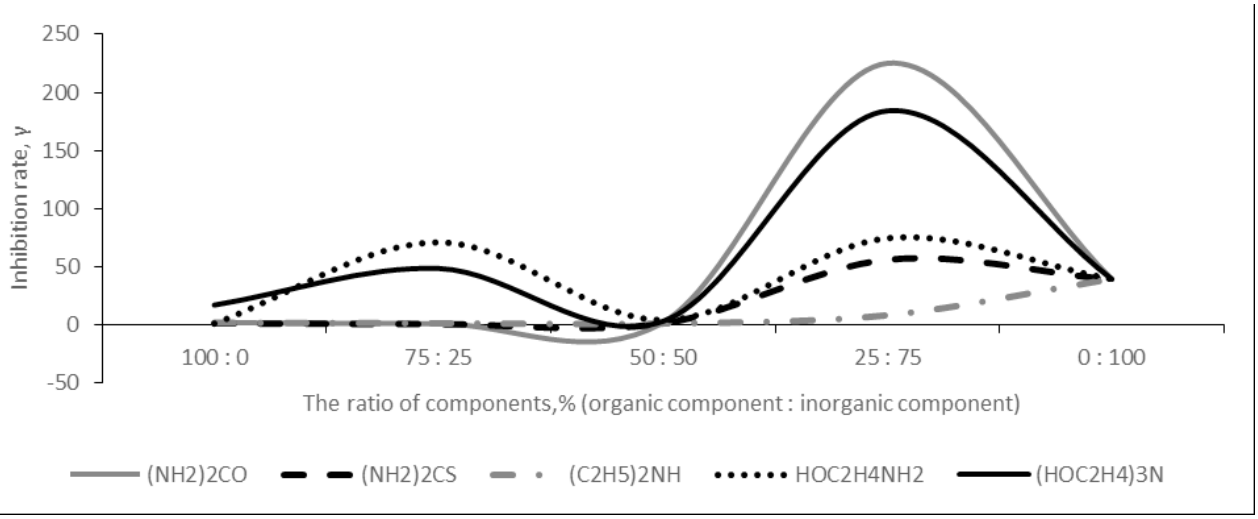

Figure 3 - Inhibition of St-3 steel corrosion in systems with sodium orthophosphate Na_3PO_4 (C_m = 0.01 mol/dm^3)

With a 1:1 ratio of components, the protective effect is not significant for all systems. In systems with a 3:1 ratio, the protective effect is increased in the following sequence:

urea > triethanolamine > monoethanolamine.

The test results of two-component dihydrodiphosphate inhibitory systems with control samples

showed that in all systems of this series, at all ratios of the components, the inhibition coefficient is low and does not exceed 4.

Sodium diphosphate systems with organic substances are also considered according to the main indicators characterizing the course of the corrosion process. Analysis of the data obtained makes it possible to assert that pure diphosphate systems have the least protective ability (Figure 4). The addition of a small amount of the organic component causes a multiple increase in the protective effect of the inhibitor, which can be shown by the example of the diphosphate system with triethanolamine, the protective effect of which is 94.18%.

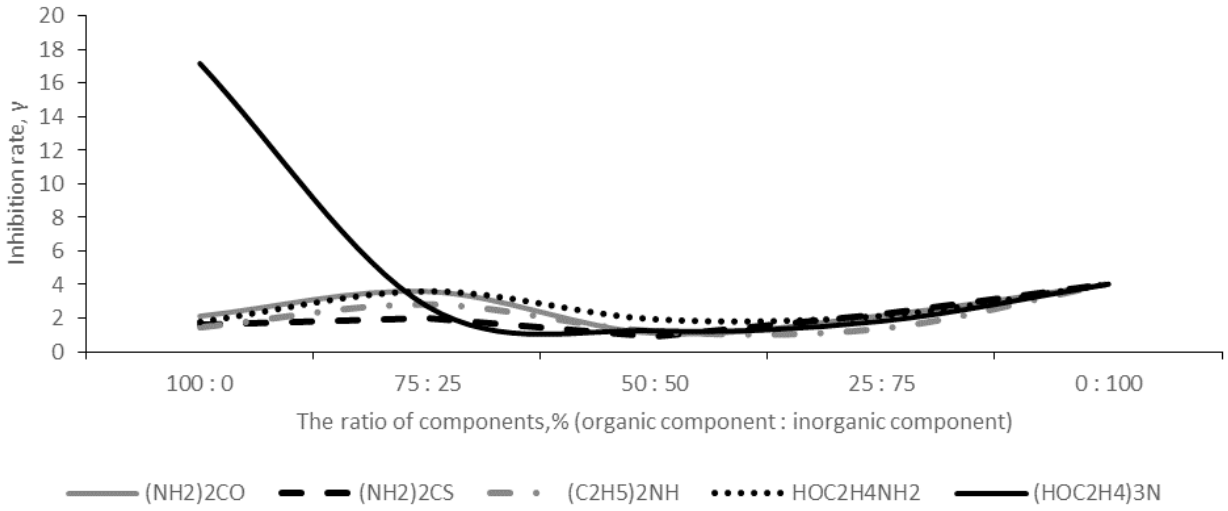

Figure 4 - Inhibition of St-3 steel corrosion in systems with sodium dihydrodiphosphate $Na_2H_2P_2O_7$ (C_m = 0.01 mol/dm^3)

The degree of change of the protective effect in two-component systems is influenced by both the nature of organic matter and the ratio of components. Thiourea was the best supplement in this series. The least strongly protective effect of pure diphosphate is triethanolamine (Figure 5).

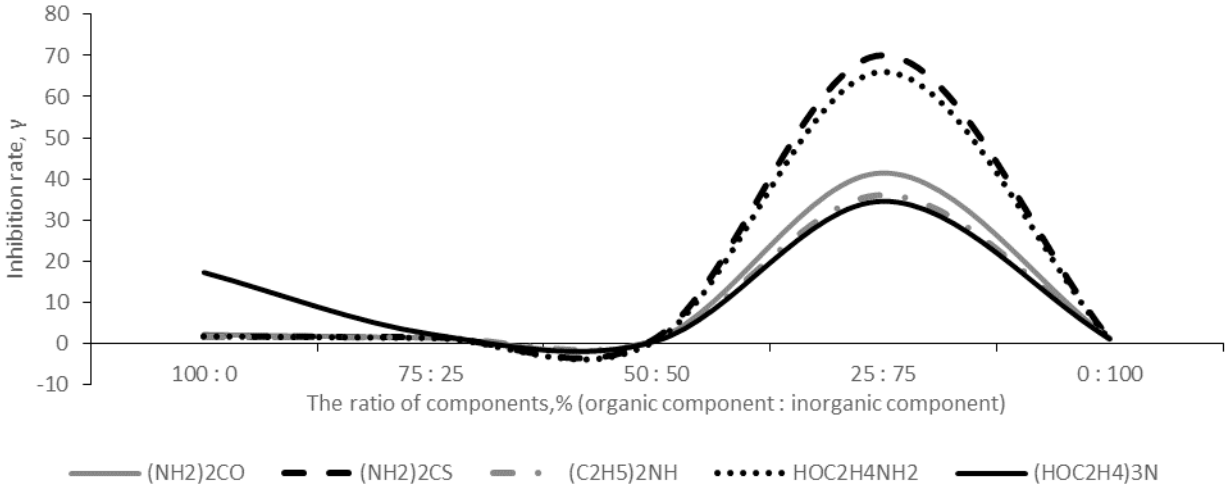

Figure 5 - Inhibition of St-3 steel corrosion in systems with sodium diphosphate $Na_4P_2O_7$ (C_m = 0.01 mol/dm^3)

Trimetaphosphate systems have also been investigated for inhibitory abilities both in pure form and as mixtures (Figure 6). In all cases, with the exception of pure triethanolamine, the protective effect is relatively low and γ does not exceed 5.

The environment with pure trimetaphosphate compared with the system with triethanolamine 2,2 times lower in inhibiting properties. In systems with trimetaphosphate, the degree of protection is also influenced by the ratio and nature of organic components. The change in the protective properties in a two-component system at different ratios shows an equivalent relationship, but the absolute values differ by an average of 2 times.

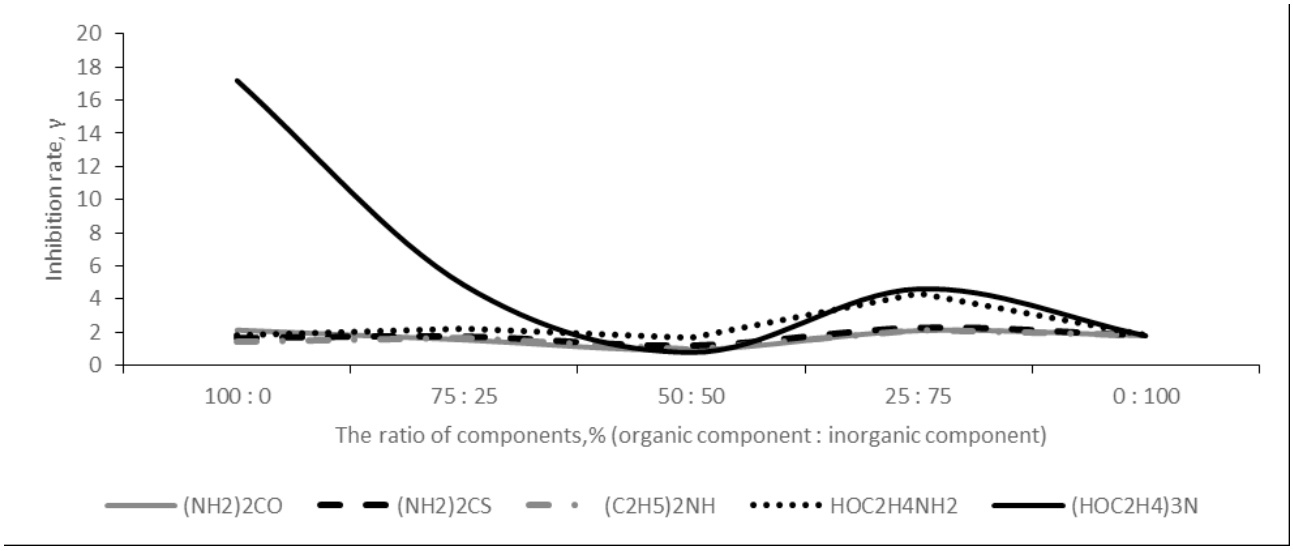

Figure 6 - Inhibition of St-3 steel corrosion in systems with sodium cyclotriphosphate $Na_3P_3O_9$ (C_m = 0.01 mol/dm^3)

Pure one-component cyclohexaphosphate system does not exhibit high inhibitory properties (Figure 7). A system containing a purely organic component, triethanolamine, exhibits a protective effect of 94.18%. Two-component hexaphosphate systems showed moderately viable but insignificant absolute values of the protective coefficient (not higher than 4).

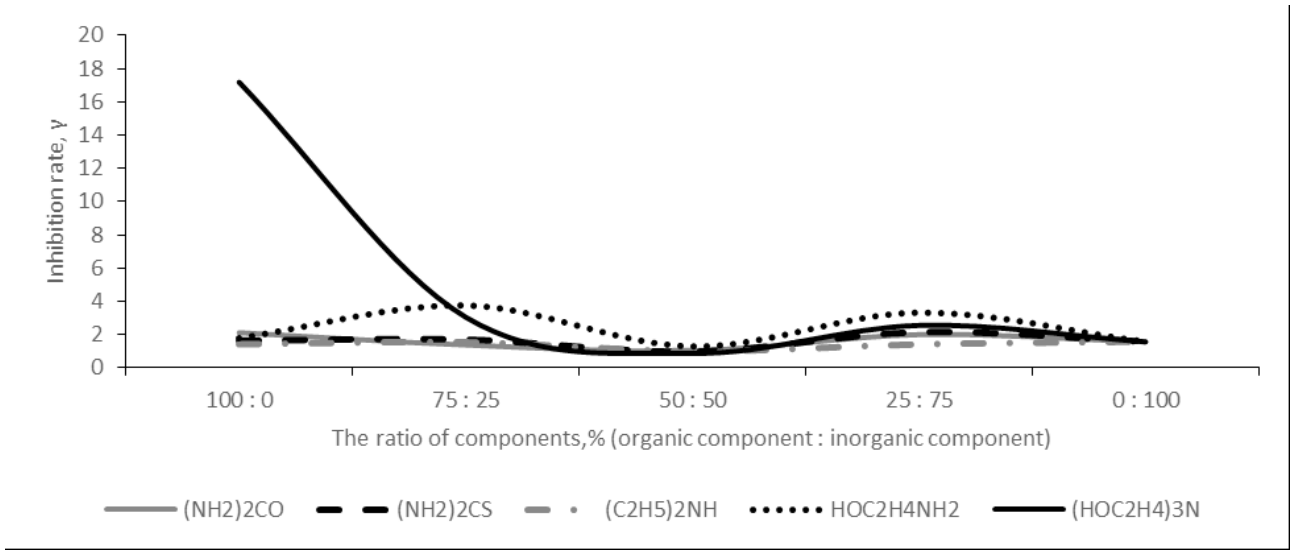

Figure 7 - Inhibition of St-3 steel corrosion in systems with sodium cyclohexaphosphate $Na_3P_3O_9$ (C_m = 0.01 mol/dm^3)

During the experiment, 118 systems (13 single-component and 105 two-component) were investigated and the dependence of their anti-corrosive effectiveness on the nature of the organic and inorganic components, as well as their ratios. It has been established that, in pure form, sodium orthophosphate and triethanolamine have the most pronounced protective properties, and fully substituted inorganic phosphates with the introduction of a small additive of organic component are most effective.

Of all the systems, antagonism is most pronounced in the sodium hydrophosphate-diethylamine system (Figure 8).

The type of interaction in the considered compositions depends on the ratio of components. A significant decrease in the protective effect, with respect to pure substances, is observed for all systems with a component ratio of 1:1.

The effectiveness of the protective effect of all considered systems also depends on the pH of the solution and the total mineralization. With an increase in the pH of the medium and the overall mineralization, the protective effect increases.

On the basis of the experimental data obtained, it was found that the most practically significant protective effect is 14 two-component (Table 1).

According to the research results, metal resistance was evaluated by a scale of corrosion resistance in relation to the systems under consideration, based on the deep corrosion index [14, 15].

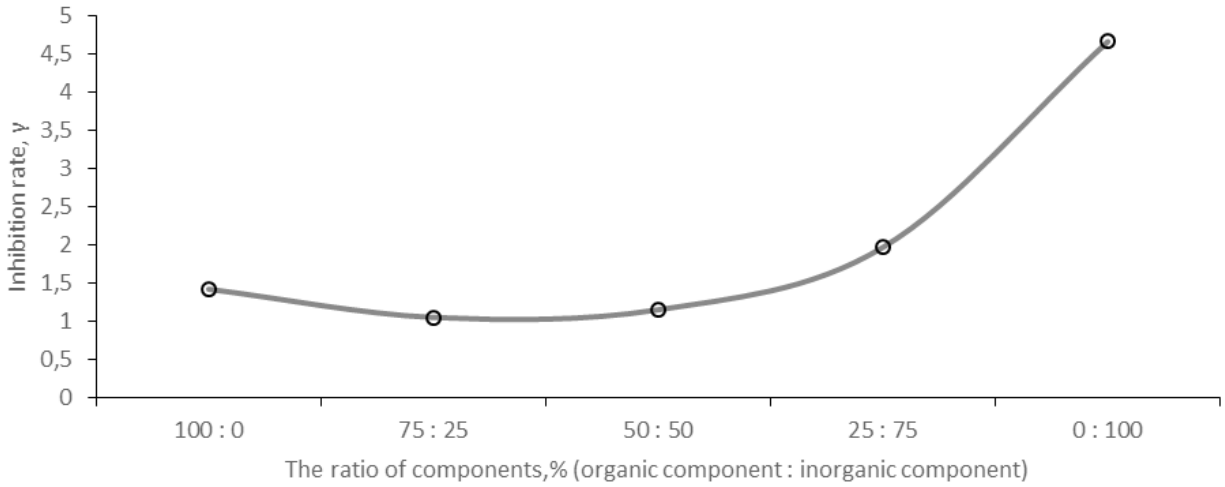

Figure 8 - Antagonism in the system sodium hydrophosphate - diethylamine (C_m = 0.01 mol/dm^3)

Table 1 – The most effective systems in terms of corrosion resistance of steel St-3

№	System (ratio)	pH	Corrosion rate, mg/ m^2·hour	Degree of protection, Z%	Inhibitory effect, γ
Completely resistant (point - 0)					
1	$Na_3PO_4 + (NH_2)_2CO$ (1 : 3)	9,09	0.51± 0,05	99.56	225.17
2	$Na_3PO_4 + (HOC_2H_4)_3N$ (1 : 3)	8,21	0.60 ± 0,02	99.46	184.24
Extremely resistant (point - 1)					
3	$Na_4P_2O_7 + (NH_2)_2CO$ (1 : 3)	7,13	2.9 ± 0,1	97.59	41.43
4	$Na_3PO_4 + (NH_2)_2CS$ (1 : 3)	9,39	2.1 ± 0,1	98.24	56.67
5	$Na_4P_2O_7 + (NH_2)_2CS$ (1 : 3)	9,63	1.7 ± 0,1	98.57	70.00
6	$Na_4P_2O_7 + (C_2H_5)_2NH$ (1 : 3)	9,53	3.3 ± 0,1	97.23	36.04
7	$Na_3PO_4 + HOC_2H_4NH_2$ (1 : 3)	9,42	1.60 ± 0,06	98.66	74.38

Continuation of table 1

8	$Na_4P_2O_7 + HOC_2H_4NH_2$ (1 : 3)	5,53	1.8 ± 0,1	98.49	66.11
9	$Na_2HPO_4 + (HOC_2H_4)_3N$ (1 : 3)	9,01	1.5 ± 0,1	98.74	79.33
10	$Na_4P_2O_7 + (HOC_2H_4)_3N$ (1 : 3)	5,41	3.4 ± 0,3	97.1	34.54
11	$Na_3PO_4 + HOC_2H_4NH_2$ (3 : 1)	10,83	1.70 ± 0,05	98.59	70.92
12	$Na_3PO_4 + (HOC_2H_4)_3N$ (3 : 1)	10,83	2.4 ± 0,1	97.95	48.71
Extremely resistant (point - 2)					
13	$Na_2HPO_4 + HOC_2H_4NH_2$ (1 : 3)	3,71	8.0 ± 0,6	93.28	14.88
14	$Na_2HPO_4 + (HOC_2H_4)_3N$ (3 : 1)	9,38	6.4 ± 5,4	94.61	18.56

Conclusion

Thus, of all the studied systems, 14 two-component systems are - very resistant (point 0-2). The relatively low protective effect of two-component systems containing cyclic phosphates is apparently due to the fact that this type of phosphate in a dilute aqueous solution is subject to significant hydrolytic cleavage [16, 17, 18] with the formation of a large amount of acid salts of ortho- and diphosphoric acids, which leads to increasing the pH of the solution and a corresponding decrease in the effectiveness of the inhibiting compositions.

On the basis of the experimental data obtained, it was established that the anticorrosive efficiency depends on the nature of the organic and inorganic component, and the proportions of the systems.

The regularities established during the work expand and complement the existing ideas about the protective effect of two-component organic-inorganic systems. The results will significantly contribute to the creation of effective, environmentally friendly and economically viable steel corrosion inhibitors.

References

1. E. McCafferty, (20100, Introduction to Corrosion Science, Springer, New York.

2. J. Vosta and J. Eliasek, (1971), *Corros. Sci*., 11, P.223

3. N.P. Zhuk. (1976), Course in the Theory of Corrosion and Protection of Metals, Moscow, Metallurgy, 8 p.

4. G.G. Ulig., R.U. Revi. (1985) Corrosion and the fight against it. Introduction to corrosion science and technology: Per. From the English / Ed. A.M. Sukhotin. - L .: Chemistry, 1989, Trans. Ed., USA, 456 p.

5. Bregman J.I. (1966), Inhibitors of corrosion, Moscow: Chemistry, 312 p.

6. S.M. Reshetnikov. (1986), Inhibitors of acid corrosion of metals, L.: Chemistry, 116 p.

7. Vladimirskaya T.N., Chepelevetskii M.L. (1989), *Chemistry and Technology of Condensed Phosphates,* p.158-162.

8. Niyazbekova A.B., Akatyev N.V., Sulekeshova G.K., Shakirov T.A. (2013), Chromatographic study of systems cyclotri-, cyclotetra- and cyclohexaphosphate with two and trivalent cations of p- and d-elements. Technology «Materials of the vi international research and practice conference», Munich, Germany

9. Kuanysheva G.S., Makasheva G.R., Kamalova G., Niyazbekova A.B. (1999), *Bull. of KazGU,* №1 (13), p.71-73.

10. Corbridje D.E.C. The structural of chemistry of phosphates (1971), *Bull. soc. fr. miner. et. cristallog,* Vol. 94, No. 1, P. 271–299.

11. Zhdanov U.F. (1979), Chemistry and technology of polyformings, Moscow: Khimiya, 240 p.

12. Lazerov A.B., Kubasova L.B., Chudinova N.N. (1982), Receipts and researches and phosphates of alkaline metals, Vol, 18, No. 9, P. 127–131.

13. André Durif. (2005), *Solid State Sciences*, Vol. 7, Iss. 6, P. 760–766.

14. Pearson R. (1974), *Successes of chemistry,* Vol. 15, No. 7, P. 1259–1271.

15. Tananayev I.B., Lavrov A.B., Chudinova N.N. (1988), *Research of phosphates*, Vol. 33, No. 5, P. 2041–2048.

16. Narayana N., María Rao, Gómez-García R., Kornberg A. (2009), *An- nual Review of Biochemistry*, Vol. 78, P. 605–647.

17. Karapetov M.Kh., Drakin C.I. (1981), General and Inorganic Chemistry, Moscow: Khimiya, 428 p.

18. Genichiro Kura. (1987), *Polyhedron,* Vol. 6, Iss. 3, P. 531–533.

IRSTI 31.25.19

[1,2*]El-Sayed Negim, [3]L. Bekbayeva, [1]A. Nabiyeva,
[3]G. Yeligbayeva, [4]G. Eshmaiel

[1]School of Chemical Engineering, Kazakh-British Technical University, 106 Walikhanov Street, Almaty, 050010, Kazakhstan
[2]National Research Centre, Polymer & Pigment Department, 33 El Bohouth St., Dokki, Giza 12622, Egypt
[3]Institute of Chemical and Biological Technologies, Satbayev University, 22 Satpayev Street, 050013 Almaty, Kazakhstan
[4]School of Energy, Construction and Environment, Faculty of Engineering, Environment & Computing,
Sir John Laing Building, JL138, Coventry University, Coventry, CV1 2HF
*Corresponding author: elashmawi5@yahoo.com

Utilization of copolymer based on poly (vinyl alcohol) and 2-ethylhexyl acrylate as admixture for cement pastes

Abstract: In this study, three composition ratios of [polyvinyl alcohol (PVA)- 2-ethylhexyl acrylate (2-EHA)] were prepared by grafting polymerization techniques in aqueous solution using ammonium persulfate as free radical initiator. The ratio of PVA/2-EHA in the grafted copolymers was variable: 1/ 8, 1/ 6 and 1/ 4, respectively. The obtained grafted copolymers were characterized by different techniques including FTIR, ^{1}H NMR, TGA and DSC. The copolymers were mixed with cement to study the physico-mechanical properties of cement pastes including W/C ratios, setting time, workability, water absorption as well as compressive strength were investigated. The results showed that the addition of grafted copolymers to cement pastes affected the physicomechanical properties. As the content of 2-EHA in the grafted copolymers increased, the water of consistency decreased, whereas the setting times (initial & final) were shortened. The compressive strength of the cement pastes was increased at all ages of hydration while water absorption decreased with increasing 2-EHA.
Key words: PVA, 2-EHA, copolymer, admixture, cement, workability.

Introduction

Admixtures are ingredients in concrete that mixed with water, cement, and aggregates to produce concrete with high workability, durability, and compressive strength. Admixture can be classified by their function, including air-entraining, water-reducing, plasticizers, accelerating, retarding, hydration-control and miscellaneous admixtures [1-3]

PVA is one of the major polymers used in the industry because of its excellent chemical resistance and physical properties [4]. PVA has been widely used in a broad range of applications in different industries such as for textile sizing, adhesives, protective colloids for emulsion polymerization and plasticizer for cement [5]. Styrene/methacrylate copolymer has been prepared by emulsion polymerization in presence of PVA as surfactant. The obtained polymer was mixed with cement to study physical and mechanical properties of cement pastes and mortars [6, 7]. The results showed that the emulsion copolymers in presence of PVA obviously improved most of the specific characteristics of the cement pastes [6]. The addition of PVA to cement pastes, significantly improved flexural strength, permeable pore volume and water absorption as well as water/ cement ratio [8]. Negim et al., [9] have incorporated a modified PVA by blending with carbamide as a chemical admixture to cement pastes.

Singh and Sarita [10] reported that PVA increased the strength and decreased the porosity due to the interaction of PVA with cement. On the other hand, Negim et al have prepared acrylate copolymers including poly(2-hydroxy ethyl acrylate-co-styrene) [11], poly(2-hydroxy ethyl acrylate-co-butyl acrylate) [12], poly(methyl cellulose-co-poly(acrylic acid)[13], poly(acrylic acid-co-styrene)[14], poly(2-hydroxyethyl acrylate-co-vinyl ether of ethylene glycol) [15], poly(methoxypolyoxyethylene-g-poly-maleic anhydride) [16], poly(acrylic acid-co-butyl methacrylate) [17], poly(2-hydroxy ethyl acrylate-co-2-hydroxyethyl methacrylate)[18] and poly (methyl methacrylate-co-ethylhexyl acrylate-co-methacrylic acid) [19]. The effect of acrylic copolymers on prop-

erties of cement pastes was investigated. The addition of acrylic copolymers to cement pastes improved the properties of cement pastes such as compressive strength, water absorption, setting time as well as workability.

This article describes the preparation of acrylic copolymer based on polyvinyl alcohol (PVA) and 2-ethylhexyl acrylate (2-EHA) by grafting polymerization. The effect of variable ratios of PVA/2-EHA on the physico-mechanical properties of cement pastes was studied.

Materials and methods

Materials

Polyvinyl alcohol (PVA), 2-ethylhexyl acrylate (2-EHA) and ammonium persulfate (APS) were obtained from Sigma Aldrich, USA. All these chemicals were of pure grade and used as received.

The raw materials used in the present study are Portland cement clinker (PCC) and raw gypsum (G). Each of those raw materials was separately ground in a steel ball mill until the surface area of respectively 3650 and 2800 cm^2/g was achieved. The chemical composition of the raw materials is shown in Table 1. The mineralogical composition of the PCC sample is C_3S, 58.79 %; β- C_2S, 17.68 %; C_3A, 8.08 %; C_4AF, 9.72 %. The Portland Cement (PC) was prepared by mixing 96 % PCC and 4 % G (by weight) in a porcelain ball mill for one hour using 3 balls to ensure complete homogeneity of the cement. The Blaine surface area of the cement sample was 3350 cm^2/g [20].

Table 1 – The Chemical Composition of the Raw Materials (M0), Mass %

Oxides Materials	SiO_2	Al_2O_3	Fe_2O_3	CaO	MgO	SO_3	Na_2O	K_2O	L.O.I
PCC	21.48	6.03	4.22	64.29	0.68	0.39	0.21	0.11	1.32
G	0.58	0.14	0.11	30.08	0.13	45.36	0.07	0.09	22.16

Synthesis of the P(PVA-g-2-EHA)

Graft polymerization was carried out in a 250 mL three- necked flask equipped with a thermometer, reflux condenser, and stirrer. PVA was dissolved in distilled water and stirred continuously at a constant temperature of 60 °C. After the PVA was fully dissolved, the temperature of the system was strictly maintained at a required value. Freshly prepared ammonium persulphate APS solution was added followed by dropwise addition of 2-EHA. The reaction was conducted for two hours with stirring continued for another 20 min at room temperature. The grafting polymerization was prepared with various ratios of PVA /2-EHA (1/8, M1; 1/6, M2 and 1/4, M3). The obtained copolymer were reprecipitated several times from ethanol to diethyl ether and dried in vacuum desiccators at 30 °C until a constant weight was achieved and poly 2-ethylhexyl acrylate dissolved.

The graft yield (G%), the grafting efficiency (GE%) and the amount of homopolymer (H%) formed were calculated according to the following equations:

Graft yield (G%)=$[(W_1 - W_0)/W_0]\times100$

Homopolymer (H%)=$[(W_2 - W_1)/W_3]\times100$

Grafting efficiency (GE%)=$(W_1/W_2)\times100$

Where W_0, W_1 are the weights of initial matrix and grafted matrix i.e. weight of the product after extraction, respectively. W_2 is the crude product before extraction and W_3 is the weight of monomer [21]. The grafting efficiency of the copolymer was 91.5% for M1, 89.9% for M2 and 83.8% for M3.

Characterization

Chemical composition of the prepared copolymer was verified by FTIR and ^1H NMR spectra, which was recorded on a Bruker Tensor 37 FTIR spectrometer and ^1H NMR (Bruker Avance 300 and 400, Switzerland).

The prepared grafted copolymers were added to the mixing water and then added gradually to 300 g of the dry cement in order to determine the water of consistency and setting time of the cement using Vicat apparatus [21, 22]. The determined water of consistency premixed with the copolymers (M1, M2 and M3) was added to 500 g of the dry cement. The resulting cement pastes were directly moulded into one-inch cube stainless steel moulds. The moulds were manually agitated for 2 minutes and then on a vibrator for another 2 minutes to assure the complete removal of air bubbles and voids and to produce

suitable pastes. The moulds were kept in a humidity chamber at 100 % R. H and a constant room temperature overnight, then demoulded and cured under water till the time of testing (1, 3, 7 and 28 days) for total porosity and compressive strength [23]. The compressive strength test was carried out using a hydraulic testing machine of Type LPM 600 M1 SE-IDNER (Germany) having full capacity of 600 KN. The loading was applied perpendicular to the direction of the upper surface of the cubes. The total porosity, ξ of each sample at any interval was calculated from the following equation [24]:

$$\xi = 0.99 \text{ X We X dp / (1 + Wt)}$$

where 0.99 is the specific volume of the free water, We is the evaporable water content, dp is the bulk density, g/cm^3 and Wt is the total water content which is equal to the sum of evaporable water (We) and combined water (Wn) contents. The bulk density (dp) was determined from the following equation: dp = W1 / W1-W2 g/cm^3, where W1 is the saturated surface dry weight in air (g) and W2 is the submerged weight in water (g).

Results and discussion

The grafting polymerization in presence of APS including initiation, propagation and termination steps is shown in Scheme 1.

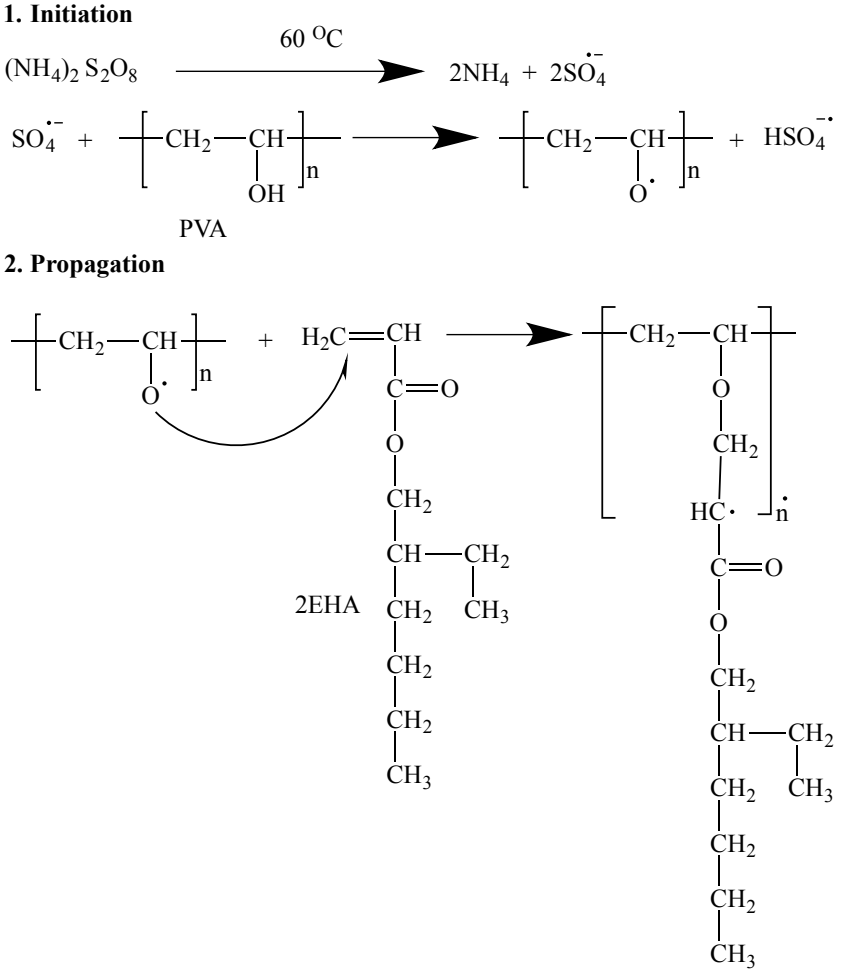

3. Termination

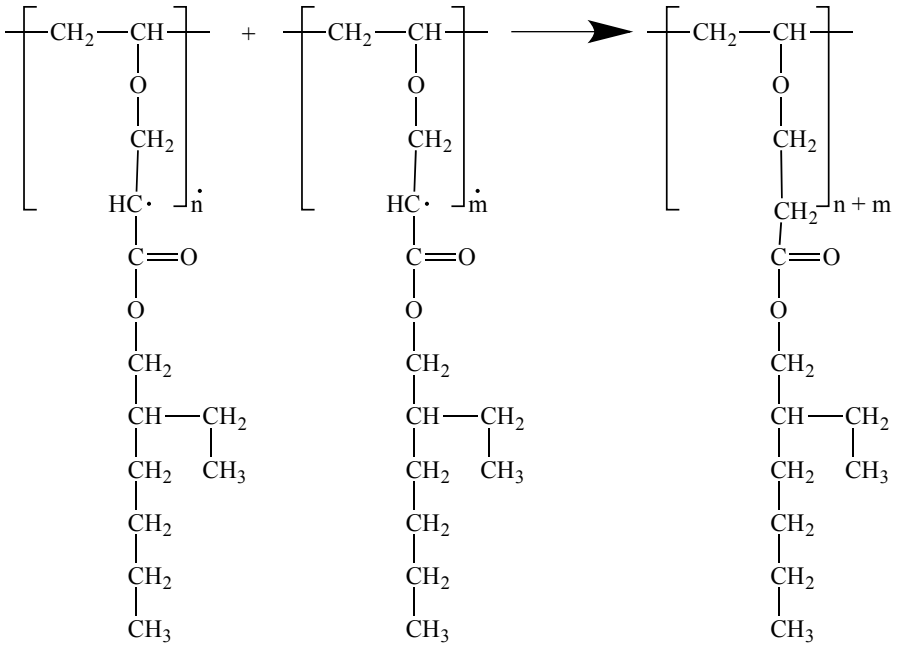

Scheme 1 – Mechanism of grafting polymerization of 2-EHA onto PVA

FTIR spectra

Evidence of grafting formation is provided by FTIR spectroscopy. From the FTIR spectrum of PVA (Fig. 1a), it is obvious that PVA shows a broad peak at 3300 cm^{-1} for the –OH group, and one peak at 1087 cm^{-1} attributed to –C-O- groups as in the study reported in ref. [25]. FTIR spectrum of the grafted copolymer is shown in Fig. 1b. It can be observed C–H broad alkyl stretching band (n = 2850-3000 cm^{-1}). 1460 cm^{-1} and 1380 cm^{-1} suggest the bending vibration of C–H. The C-O stretching at approximately 1159 cm^{-1}, is attributed to the ether (C-O). The peak at 1732 cm^{-1} represents the C=O stretching band and the peak at 1150 cm-1 is attributed to C-O-C are distinguished.

^{1}H NMR spectrum

The ^{1}H NMR spectrum of grafted copolymer dissolved in chloroform is shown in Fig. 2. The assignment peaks of the proton species in PVA and its grafted with 2-EHA. The typical peaks for grafted copolymer are indicated in Fig. 2 appeared at δ = 0.87-0.89, 1.27-1.4, 1.66, 1.88, 2.3, 3.32, 3.74 and 4.48 ppm correspond to the protons bonded to C1, C2, C3, C4, C5, C6, C7 and C8 respectively [25-31].

Thermal properties

The thermal behaviour of pure PVA and P(PVA-g-2-EHA) was evaluated with TGA, DTG in air at a heating rate of 10°C/min and DSC at the same heating rate under nitrogen atmosphere. The TGA thermograms for the pure PVA and P(PVA-g-2-EHA) are given in Fig. 3. TGA measurements of pure PVA and grafted PVA with 2-EHA in different compositions indicate that thermal degradation temperature is higher than 400 °C as shown in Table 2. TGA curves also indicate that, the pure PVA follows five step degradation process as shown in Fig. 3 and Table 2. The first weight losses occur between 30 and 200 °C, which corresponds to the removal of water. The second, third, fourth and fifth weight loss occurs between 200 to 900 °C correspond to completely decomposition with loss of CO_2. Fig. 3 and Table 2 show the lost weight % of grafted copolymer M1. One stage decomposition was observed between 29 and 910 °C, while decomposition of grafted copolymer M2 was observed in 2 steps. The first step ranging between 29 and 317°C, and the second step of degradation occurs between 317 and 907 °C. The rate of degradation in the second step is slightly faster than that in the first step.

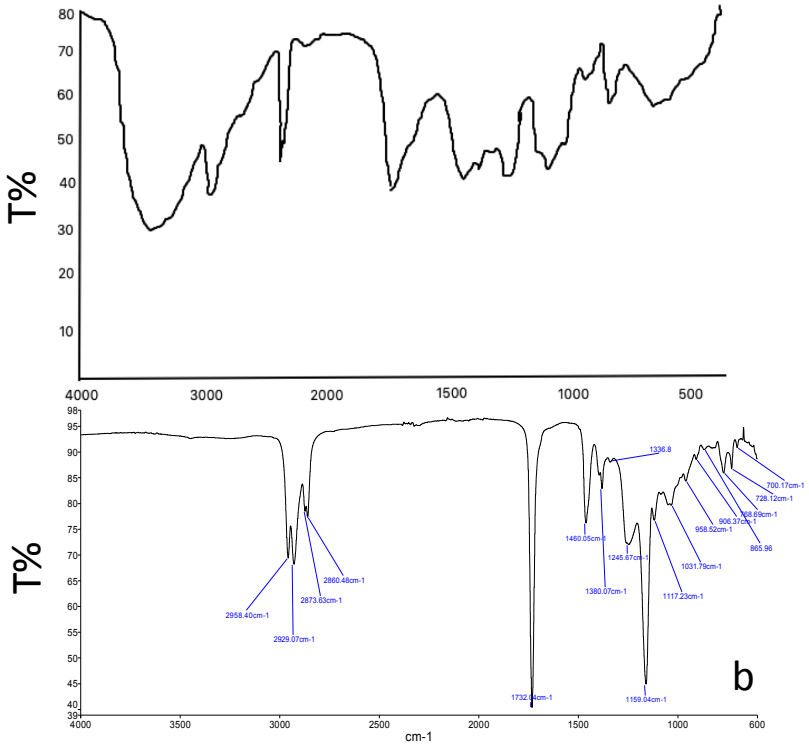

Figure 1 – FTIR spectra of (a) PVA and (b) P(PVA-g-2-EHA)

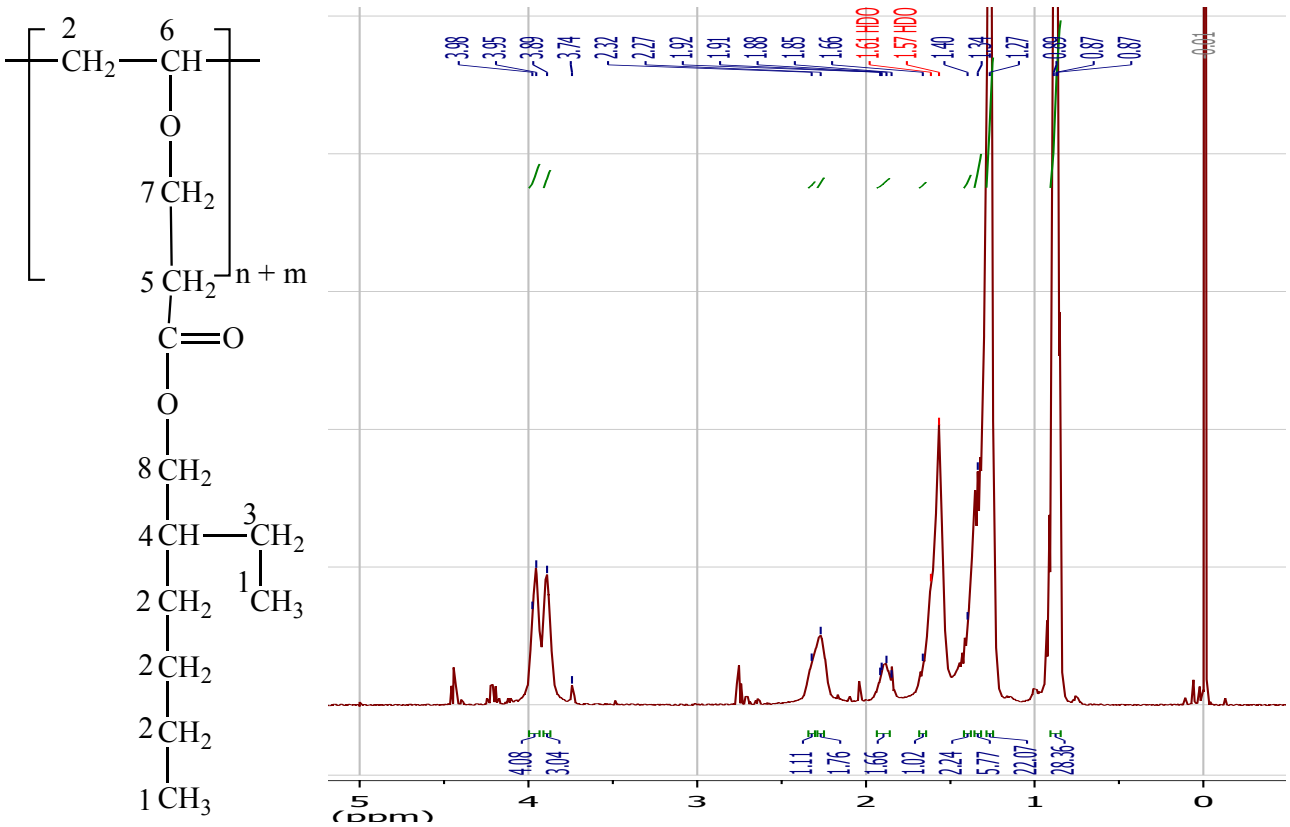

Figure 2 – ^{1}H NMR spectra of P(PVA-g-2-EHA)

Three weight losses were observed in grafted copolymer M3 as shown in Fig. 3 and Table 2. The first weight loss was observed in the range 29 – 176 °C in step 1 of degradation, which corresponds to the loss of water. Upon heating PVA above the decomposition temperature the polymer begins a rapid chain-stripping elimination of water [26, 27]. The second weight loss was observed in between 176 and 333 °C in step 2 of degradation. The third weight lost was between 333 and 905 °C and it was much shorter than the first. The maximum polymer degradation temperature (PDT_{max}) (28, 29) corresponds to the temperature at which the maximum rate of weight loss occurred and appeared 460 °C for pure PVA blend and at 425 ° C for pure grafted copolymers M1, M2 and M3 [30, 31].

Glass transition temperatures (T_g) of pure PVA and grafted polymer with different ratios of 2-EHA were calculated from the corresponding typical DSC traces as given in Fig. 4 and Table 2. The T_g value for pure PVA is 70 ºC as shown in Table 2. From the data present in the DSC curves, it can be seen that, the increase of 2-EHA content from 20 to 40% shifts the glass transition to higher temperatures. M1 has higher T_g value due to the higher 2-EHA content. No data was observed from the second heating cycle for all the formulation.

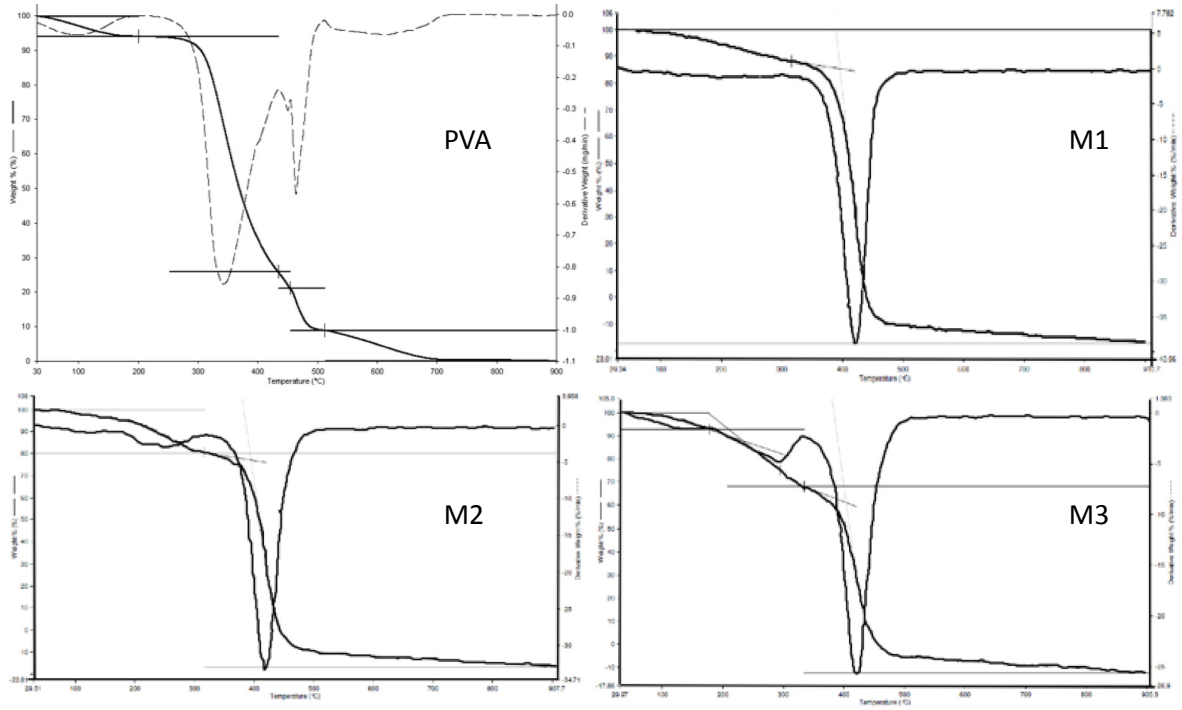

Figure 3 – TGA thermograms of PVA and P(PVA-g-2-EHA) (M1-M3)

Table 2 – Thermal properties of PVA and PVA-g-2-EHA

Polymer Ratio %	T_g (°C)[a]	Temperature (°C) for decomposition [b]	Weight loss [b] (%)	Residual [b] (%)	PDT(°C) [b]
PVA	70	30-200 200-433 433-454 454-511 511-900	5.9 68.1 4.875 12.15 8.81	94.01 25.9 21.031 8.87 0.006	460
M1	60.74	29.34-910	100	0.0	425
M2	46.9	29-317 317-907	19.5 80	80.5 0.0	425

Continuation of table 2

M3	45.2	29-176 176-333 333-905	7.2 24.6 68	92.7 68.1 0.0	425

[a] Determined from DSC curves

[b] Determined from the derivative of TGA.

Application of Graft Copolymer for Cement

Water/ Cement Ratio

The results W/C ratios of pure cement (M0) and various cement pastes mixed with grafted copolymers (M1-M3) are shown in Fig. 4. It is clear that the W/C ratio of cement pastes decreases from 0.312 to 0.29 with addition of the grafted copolymers. However, W/C ratios increased with decreasing 2-EHA content in the grafted copolymers. These W/C ratios of cement maybe change according to kind of polymers, and concentrations of polymer during the mixing of cement with polymers (1, 31).

Setting time

The setting time (initial & final) of cement pastes premixed with grafted copolymers are given in Fig. 6. The setting time of cement pastes is extended when mixed with grafted copolymers. However, the initial and final setting time of cement pastes shorten with increasing the content of 2-EHA in the grafted copolymers. For example, initial and final setting time of M1 is lower than those of M2 and M3. This attributed to the evaporation of water from the surface of the cement pastes mixed with (M1) is less than those of cement pastes mixed with M1 and M2 [32, 33].

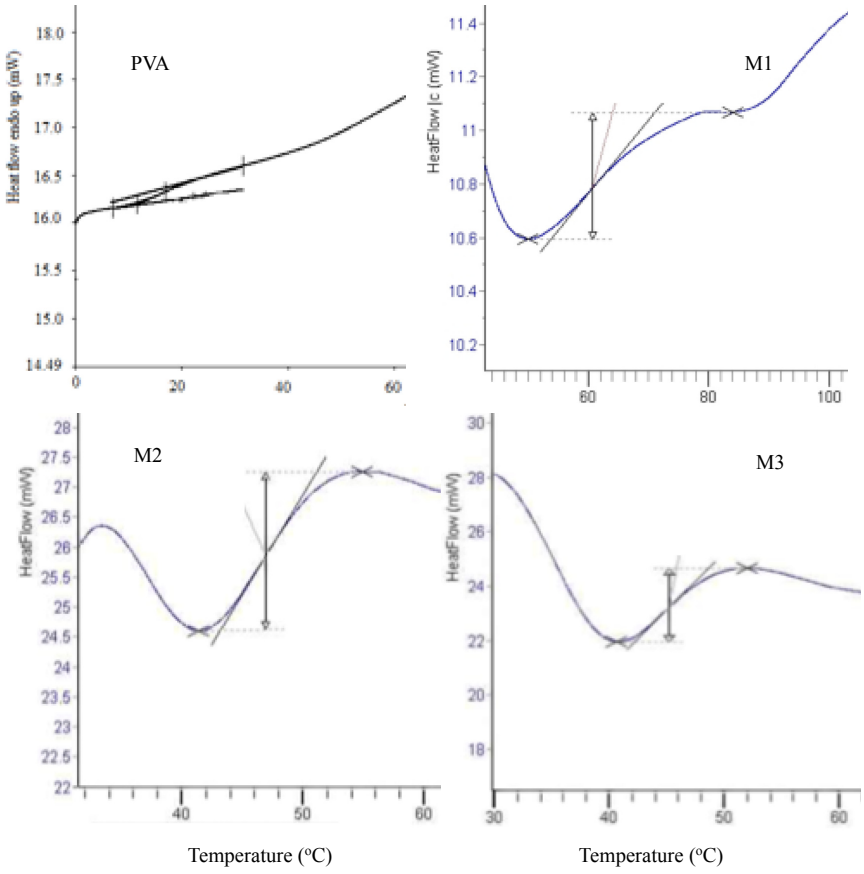

Figure 4 – DSC thermograms of PVA and P(PVA-g-2-EHA) (M1-M3)

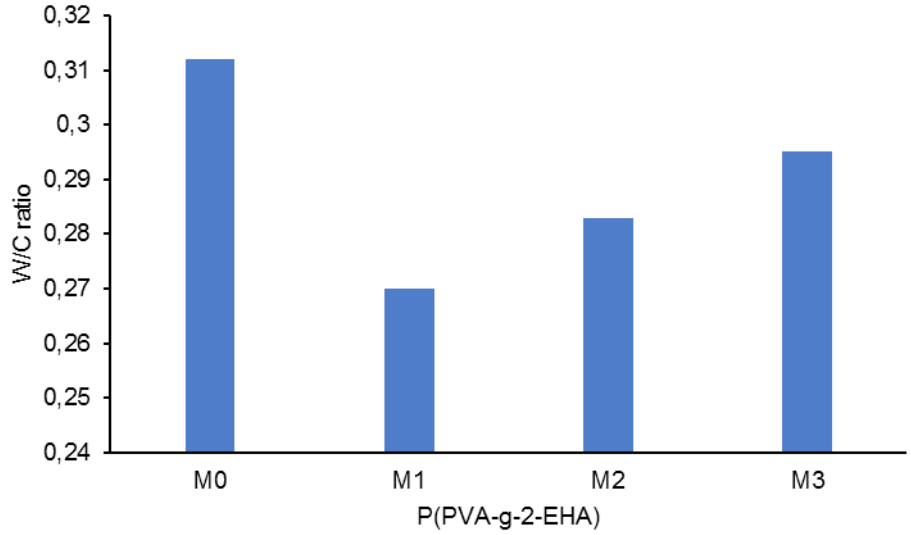

Figure 5 – Effect of P(PVA-g-2-EHA) content on the W/C ratios of cement pastes

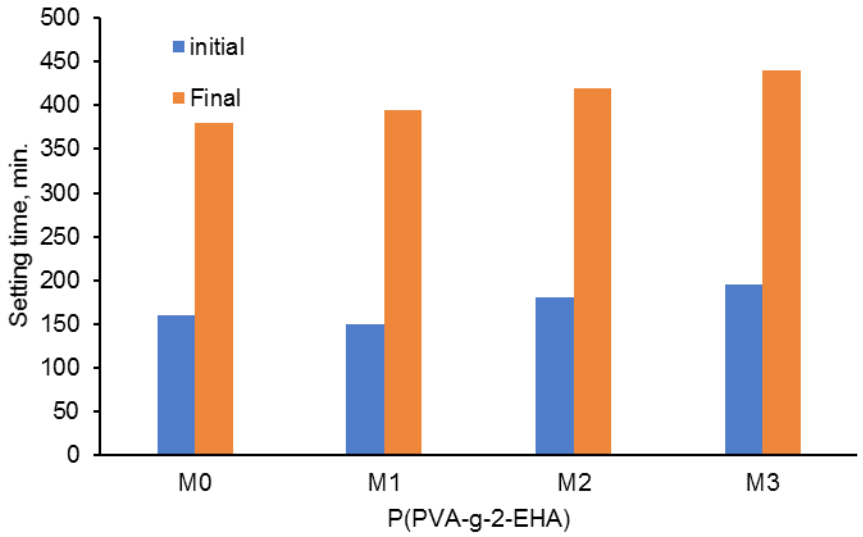

Figure 6 – Effect of P(PVA-g-2-EHA) content on the setting time of cement pastes.

Workability

The results of the cement pastes workability are presented graphically in Fig. 7. The results showed that cement paste had an initial workability of 135 mm; however, there was an increase in workability measurement with the addition of grafted copolymers. This increase in workability was attributed to surface active of the grafted copolymers [34]. Fig. 7 shows an increase in flow of mortar with increasing the content of 2-EHA in the grafted copolymers.

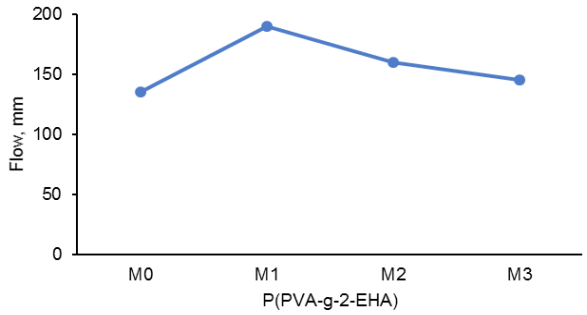

Figure 7 – Effect of P(PVA-g-2-EHA) content on the flow of cement paste

Water absorption

Generally, the contact of cement with water, cement paste absorbs water because of its porous microstructure. The lower the water absorption, the lower the permeable pore volume [34].

The effect of grafted copolymers with different content of 2-EHA on water absorption of hardened cement paste is shown graphically in Fig. 8. It can be seen that water absorption decreased with addition grafted copolymers to cement pastes. This indicates that the addition of polymer results in reduction of the porosity of the pastes [33, 34]. However, the water absorption of cement pastes mixed with grafted polymers decreased with increasing of 2-EHA in the grafted copolymers.

Compressive strength

The effects of grafted copolymers on the compressive strength of cement pastes are represented as a function of curing time in Fig. 9. As shown from Fig. 9, the compressive strength of cement pastes increased with addition of grafted copolymers to cement pastes at nearly all-curing periods. Furthermore, an increasing in the 2-EHA content in the grafted copolymers increased the compressive strength of the cement pastes. Cement pastes mixed with 40% 2-EHA (M1) gave highest strength with 78.7 MPa while cement pastes mixed with 20% 2-EHA (M3) gave lowest strength with 71.9 MPa. This is attributed to the agglutinant action of grafted copolymers with grains of cement and led to improve the mechanical properties of cement pastes (35).

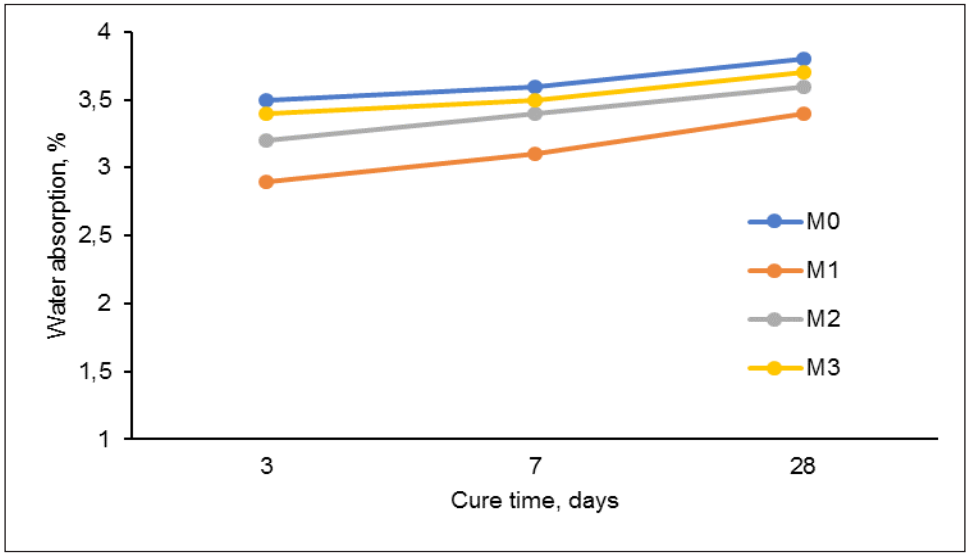

Figure 8 – Effect of P(PVA-g-2-EHA) content on water absorption of cement pastes.

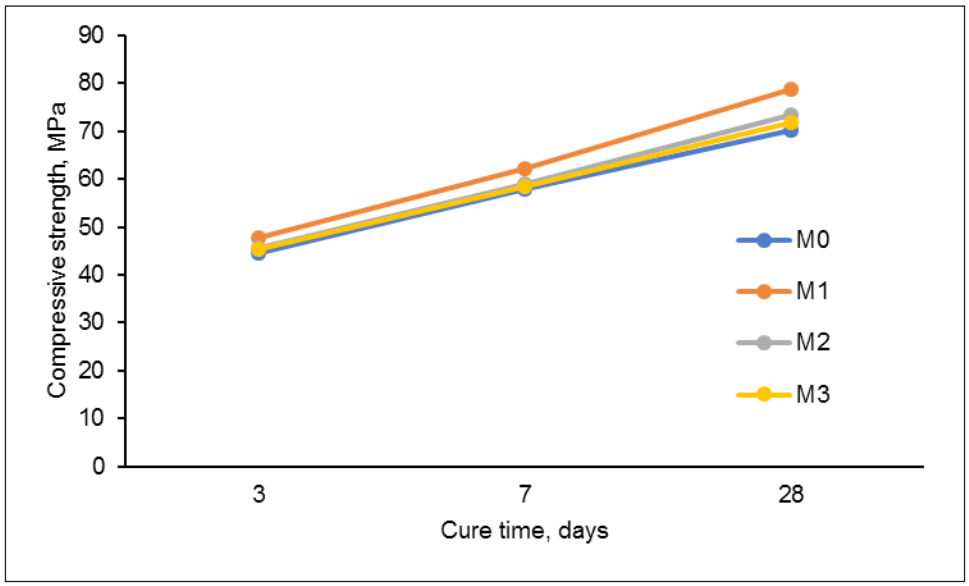

Figure 9 – The effect of P(PVA-g-2-EHA) on the compressive strength of cement pastes

Conclusions

Grafted copolymers of polyvinyl alcohol (PVA) with 2-Ethylhexyl acrylate (2-EHA) in three different ratios, of 1:8, 1:6 and 1:4 were prepared and characterized in relation to FT-IR, ^{1}H NMR, TGA and DSC. From thermal analysis, it is shown that, the degradation profiles of grafted copolymers obtained from aqueous dispersion were influenced by the ratios of 2-EHA in the grafted copolymers. The rate of degradation for the grafted polymers is thermally stable formulation depending upon the 2-EHA loading from 30 to 900 °C. Transition glass temperature (T_g) was determined from DSC. The value of T_g shifted from 45 °C to 60 °C with increasing the content of 2-EHA in grafted polymers and indicated that the grafted copolymers are miscible.

Mixing of cement pastes with water and the grafted polymer P(PVA-g-2-EHA) evidently improves the properties of cement pastes. The W/ C-ratio decreases, i.e., the grafted polymer acts as a water reducing agent when mixed with the cement pastes. Setting time of cement pastes increased with decreasing the content of 2-EHA. The workability of cement pastes also enhances and seems to be higher than that of the pure Portland cement pastes. Water absorption of the hardened cement pastes premixed with the grafted copolymers decreased, while compressive strength increased compared with those of the reference cement pastes. As the ratio of 2-EHA in the grafted polymer increased, the properties of the cement pastes also improved.

References

1. Hewlett P.C. (1998). Lea,s chemistry of cement and concrete. 4th Edn., Wiley and Sons Inc., New York, Toronto.

2. El-Hosiny, F.I., Gad E.A.M. (1995) Effect of some superplasticizers on the mechanical and physicochemical properties of blended cement pastes. *Journal of Applied Polymer Science*, vol. 56, no. 2, pp.153-159.

3. Ohama Y. (1995) Handbook of Polymer-Modified Concrete and Mortars. Park Ridge, New Jersey, USA.

4. Tubbs R.K. (1966) sequence distribution of partially hydrolyzed poly(vinyl acetate). *J. Polym. Sci. Part A-1: Polym. Chem*., vol. 4, pp. 623-629.

5. Jones J.I. (1973) Polyvinyl alcohol: Properties and application. *British Polymer Journal*, vol. 5, pp. 493-494.

6. El-Sayed Negim, Mahyuddin Ramli, Bahruddin Saad, Lyazzat Bekbayeva, Muhammad Idiris Saleh (2011) Effects of Surfactants on the Properties of Styrene/Methacrylate –type Superplasticizer in Cement Paste. *J. Polymer-Plastics Technology and Engineering*, vol. 50, no. 941, pp. 946, 2011.

7. El-Sayed Negim, Lyazzat Bekbayeva, Irmukhametova G.S., Ainur Kuzhantayeva, Dilara Sultanova, Aziza Suleimenova, Yeligbayeva G., Mun G.A. (2017) Utilization of styrene copolymer lattices (DBSS/PVA) as chemical admixture for mortar. *International Journal of Biology and Chemistry*, vol. 9, no. 2, pp. 27-31.

8. Allahverdi A., Kianpur K., Moghbeli M.R. (2010) Effect of polyvinyl alcohol on flexural strength and some important physical properties of Portland cement paste. *Iran. J. Mater. Sci. Eng*., vol. 7, no. 1, pp. 1–6.

9. Negim E.S.M, Yeligbayeva G.Zh., Niyazbekova R., Rakhmetullayeva R., Mamutova A.A., Iskakov R., Sakhy M., Mun G.A. (2015) Studying physico-mechanical properties of cement pastes in presences of blend polymer as chemical admixtures. *International Journal of Basic and Applied Sciences*, vol. 4, no. 3, pp. 297-302.

10. Singh N.B., Sarita R. (2001) Effect of polyvinyl alcohol on the hydration of cement with rice husk ash. *Cement and Concrete Research*, vol. 31, pp. 239-243.

11. Negim E.S.M., Khatib J.M., Yeligbayeva G.Zh., Rakhmetullayeva R., Urkimbaeva P.I., Sakhy M., Shilibekov S., Mun G.A. (2013) Synthesis, characterization and application of hydrophilic copolymers on physico-mechanical properties of cement pastes. *World Applied Sciences Journal*, vol. 25, no. 7, pp.1044-1052.

12. El-Sayed Negim, Khatib J.M., Sakhy M., Shilibekov S., Shanshabayev N., Jakiyayev B. (2014) The Effect of pH on Physico-Mechanical Properties of Cement Pastes Containing Poly (Acrylate) Latexes –Chemical Admixtures. *World Applied Sciences Journal*, vol. 29, no. 6, pp.796-804.

13. EL-Sayed Negim, Niyazbekova Rimma, Lyazzat Bekbayeva, Utelbayeva Akmaral, Bengin M. Herki, Nursultanov Merey, Iskakov Rinat, Gulzhakhan Yeligbayeva. (2017) Effect of Methyl cellulose/poly(acrylic acid) Blends on Physico-Mechanical Properties of Portland Cement Pastes. *Oriental Journal of Chemistry*, vol. 33, no. 1, pp. 450-457.

14. El-Sayed Negim, Mahyuddin Ramli, Saber E. Mansour, Bahruddin Saad, and Muhammad Idiris Saleh. (2010) Utilization of hydrophilic copolymers as superplasticizers for cement pastes Part I: Poly[acrylic acid-co-styrene]. *Middle-East Journal of Scientific Research*, vol. 6, no. 2, pp. 99-107.

15. El-Sayed Negim, Jamal Khatib, Mahyuddin Ramli, Bahruddin Saad, Muhammad Idiris Saleh. (2010) Synthesis and Characterization of Hydrophilic Copolymers as Superplasticizers for Cement Pastes. *J. World Applied Sciences*, vol. 10, no. 6, pp. 685-694.

16. El-Sayed Negim, Mahyuddin Ramli, Saber E. Mansour, Bahruddin Saad, and Muhammad Idiris. (2010) Synthesis, Characterization, and Cement Application of maleic anhydride water-soluble grafted polymer. *J. World Applied Science*, vol. 10, no. 4, pp. 443-450.

17. El-Sayed Negim, Jamal M. Khatib, Nurlan O. Inkarbekov. (2013) Effect of Acrylate Copolymers on the Rheological Properties of Portland Cement Mortar Pastes, Part III. *World Applied Sciences Journal*, vol. 23, no. 4, pp. 549-553.

18. El-Sayed Negim, Jamal Khatib, Khalid Al Mutairi, Rakhmetullayeva Raikhan and Mun A. Grigoriy. (2012) The effect of molar ratios of the monomers on the physic-mechanical properties of ordinary Portland cement. *Middle- East Journal of Scientific Research*, vol. 11, no. 8, pp.1131-1139.

19. Negim E.S.M, Aisha A.M.B., Yessimkanova U., Kurmanbekova A., Tyazhina K., Urkimbaeva P.I., Rakhmetullayeva R.K., Shatabayeva E., Irmukhametova G., Mun G.A., Yeligbayeva G.Zh., Khatib J.M. (2015) The effect of terpolymer admixtures on physico-mechanical properties of cement pastes. *International Journal of Basic and Applied Sciences*, vol. 4, no. 1, pp. 10-18.

20. ASTM-Standards, C204-82. (1993) Standards test method for fineness of hydraulic cement by air-permeability apparatus.

21. Bhattacharya A, Misra B. N. (2004) Grafting: a versatile means to modify polymers techniques, factories and applications. *Prog. polym. sci*. 29: 767-814

22. ASTM-Standards, C187-86. (1993) Standard test method for normal consistency of hydraulic cement, pp.148-150.

23. ASTM-Standards, C191-92, (1993). Standard test method for setting time of hydraulic cement by Vicat apparatus, pp. 866-868.

24. ASTM-Standards, C170-90, (1993) Standard test method for compressive strength of dimentional strones, pp. 828-830.

25. El-Didamony H., Haggag M.Y., Abo-El-Enein S.A. (1978) Studies on expansive cement II. Hydration kinetics, surface properties and micro-structure. *Cem. Concr. Res.*, vol. 8, no. 3, pp. 351-358.

26. Herman S.M., Carolina M.S., Adriana N.S., Alexandra A.P.M. (2008) FTIR spectroscopy characterization of poly(vinyl alcohol) hydrogel with different hydrolysis degree and chemically crosslinked with glutaraldehyde. Material Science and Engineering: C, vol 28, no. 4, pp 539-548.

27. Milestone, N.B. (1979) Hydration of tricalcium silicate in the presence of lignosulfonates, glucose and sodium gluconate. *J. Am. Cer. Soc.*, vol. 62, pp. 321-324.

28. Lei L., Plank J. (2012) A concept for a polycarboxylate superplasticizer possessing enhanced clay tolerance. *Cem. Concr. Res*., vol. 42, no. 10, pp.1299–1306.

29. Kim J.H., Robertson R.E. (1998) Effects of polyvinyl alcohol on aggregate-paste bond strength and the interfacial transition zone. *Adv. Cem. Based Mater*., vol. 8, no. 2, pp. 66–76

30. Tomida M., Nakato T., Kuramochi M., Shibata M., Matsunami S., Kakuchi T. (1996) Novel method for synthesizing poly(succinimide) and its copolymeric derivatives by acid-catalysed polycondensation of L-aspartic acid. *Polymer* 1996, vol. 37, no. 19, pp. 4435-4437..

31. Rixom R., & Mailvaganam, N. (1999). Chemical Admixtures for Concrete, 3rd ed, E & FN Spon.

32. Walters D.G. (1990). A comparison of latex-modified Portland cement mortars. *ACI Materials J.*, vol. 87, no. 4, pp. 371-377.

33. Aïtcin P.C., Jolicoeur C., MacGregor J.G. (1994). Superplasticizer: How they work and Why they occasionally don't. Concrete International, vol. 16, no. 5 pp. 45-52.

34. Singh R.K., Rai U.S. (2005) Effect of polyacrylamide on the different properties of cement and mortar. *J. Mater. Sci. Eng.,* vol. 392, pp. 42-50.

35. Ohama Y. (1987) Principle of latex modification and some typical properties of latex modified mortar and concrete. *J. ACI Mater.*, vol. 86, pp. 511-518.

36. Shaker F.A. (1977) Durability of styrene butadiene latex modified concrete. *J. Cem. Con. Research*, vol. 27, no. 5, pp. 711-720.

37. Lea H., Neville K. (1967) Handbook of Epoxy Resins, Me Grew. Hill, New York